The University Of Sheffield.

Investigation of siRNA as a Treatment for Cushing's Disease

Ahmed Abdulaziz S Alzahrani

A thesis submitted in partial fulfilment of the requirements for the degree of
Doctor of Philosophy

The University of Sheffield
Faculty of Medicine, Dentistry and Health
Department of Oncology and Metabolism

February, 2021

Summary

Background: Cushing's disease results from a pituitary corticotroph adenoma that secretes adrenocorticotrophic hormone (ACTH). High levels of ACTH stimulate the synthesis of excess cortisol from the adrenals, the effects of which include hypertension, diabetes, depression, and weight gain. If left untreated, Cushing's disease carries a 50% five-year mortality rate. At present, there is no suitable medical therapeutic and transsphenoidal surgery, which is the first line treatment, has a high rate of recurrence.

RNA-interference is a cellular mechanism that enables gene silencing at the level of mRNA. It can also be used to reduce gene expression by employing small interfering (si)RNAs that target the specific gene of interest.

The proopiomelanocortin (POMC) peptide is encoded by the POMC gene and is processed to release ACTH as well as other hormones.

Aims: The first aim of the current project was to test the hypothesis that POMC-targeting siRNAs could be an effective medical therapy for Cushing's disease; post-transcriptional knock-down of POMC expression could reduce ACTH secretion and thereby cortisol production. Current challenges to using siRNAs as a medical therapy include the lack of targeted delivery to the required cell type. The second aim of this project was investigate if the corticotroph-specific corticotrophin-releasing hormone receptor 1 (CRHR1) could be used as a means of specific delivery of POMC siRNAs if they were conjugated that to an anti-CRHR1 antibody.

Methods: A murine AtT-20 cell line, an ACTH hypersecreting *in vitro* model of Cushing's disease, was used to assess how effective POMC-targeted siRNAs could be at decreasing ACTH secretion. Following transfection of AtT20 cells with POMC siRNAs, the ACTH concentration in the culture medium was measured by immunoassay. Activation of the innate immune system by POMC siRNAs was analysed by measuring for interferon (IFN)-α, IFN-β, interleukin (IL)-1β, IL-6, and tumour-necrosis factor (TNF)-α by ELISA. Analysis of CRHR1 expression in AtT20 cells and in a CHO FlpIN-CRHR1 cell line was undertaken using RT-PCR, cAMP-stimulation in response to CRH, and indirect fluorescence-activated cell sorting (FACS).

Results: Three POMC-specific siRNAs affected a reduction in the secretion of ACTH following transfection of AtT20 cells; the concentration of ACTH in the culture medium was 15.6% (8,868 pg/ml), 18.1% (10,717 pg/ml), and 10.6% (6,037 pg/ml), respectively, of that secreted from untreated AtT20 cells (56,978 pg/ml). ACTH levels were reduced statistically significantly when compared to untreated cells (One-way ANOVA, $P < 0.0001$). None of the POMC siRNAs appeared to trigger the innate immune response in AtT20 cells; the secretion of IFN-α, IFN-β, IL-1β, IL-6, and TNF-α was not detected. The cell surface expression of CRHR1 on AtT20 cells was detected, but was at too low a level for effective detection by the available anti-CRHR1 antibodies. A CHO-FlpIN-CRHR1 cell line was isolated and shown to express the receptor by indirect FACS using a receptor-specific mouse antibody.

Conclusions: siRNAs targeting POMC reduced ACTH secretion from AtT20 cells. The POMC siRNAs did not appear to be immunostimulatory. The cell surface expression of CRHR1 AtT20 cells was confirmed. This receptor might be useful as a target for the specific delivery of POMC siRNAs to corticotrophs if they are conjugated to a specific anti-CRHR1 antibody or to CRH peptide.

Declaration

I hereby declare that this thesis has been written by myself and has not been accepted previously in any publication for a higher degree. The work reported in this thesis was performed by myself, except where specifically acknowledged in the text. All information sources have been specifically acknowledged by means of references.

Ahmed Abdulaziz S Azahrani

February 2021

Acknowledgements

First of all, I would like to thank ALLAH almighty for all his blessings, for providing me with what it takes to pursue a PhD degree, and for all the continued magnificent blessings throughout my life.

I would also like to express my appreciation to the Ministry of Health of Saudi Arabia and the Saudi Cultural Bureau in London, UK, for all their help and assistance.

I would like to express my utmost gratitude to my supervisors, Dr Helen Kemp and Professor John Newell-Price, for their kind unwavering support and insightful guidance throughout my PhD research study. Their consistent constructive and tailored directives have enriched my learning outcome and boosted my confidence as a scientist, which unequivocally has set me up for better career opportunities.

I would also like to convey my special thanks to Professor Richard Ross whose thought-provoking comments and suggestions during the many laboratory meetings have proven invaluable to the progress of this research work. The support and friendship of laboratory members, Dr Ian Wilkinson, Mrs Susan Justice, Ms Julie Porter, Mrs Susan Clark, Dr Alfituri Alhaslok, Ms Elizabeth Foulkes, and Mr Jacob Whatmore have also contributed greatly to my progress.

My years of study were made possible by the loving support of my parents in Saudi Arabia and my darling wife and children who have loyally supported me during my stay in the UK.

Table of Contents

List of Figures

List of Tables

List of Abbreviations

Abbreviation	Full Word
ACTH	Adrenocorticotropic hormone
AIP	Aryl hydrocarbon receptor-interacting protein
AIMAH	ACTH-independent macronodular adrenal hyperplasia
AGO2	Argonaute 2
AMD	Age-related macular degeneration
ApoB	Apolipoprotein B
AT	Antithrombin
LPH	Lipotropin
BIPSS	Bilateral inferior petrosal sinus sampling
CAH	Congenital adrenal hyperplasia
CD	Cushing's disease
CLIP	Corticotropin-like intermediate lobe peptide
CPP	Cell-penetrating peptides
CRH	Corticotrophin-releasing hormone
CRHR1	Corticotrophin-releasing hormone receptor type 1
cAMP	Cyclic AMP
CNV	Chloroidal neovascularization
CT	Computerised tomography
DNA	Deoxyribonucleic acid
dsRBD	dsRNA-binding domain
dsRNA	Double-stranded RNA
DUF283	A domain of unknown function
EGFR	Epidermal growth factor receptor
FAP	Familial amyloidotic polyneuropathy
GalNAc	N-acetylgalactosamine.
HBV	Hepatitis B virus
HPA	Hypothalamic-pituitary-adrenal axis
HSP47	Heat-shock protein 47
IFN	Interferon
IRF3	Interferon regulatory factor 3
KSP	Kinesin spindle protein
LDDST	Low-dose dexamethasone suppression test
LNA	Locked nucleic acid
MC2R	Melanocortin 2 receptor
MEN1	Multiple endocrine neoplasia type 1
miRNA	Micro RNA
MRI	Magnetic resonance imaging
mRNA	Messenger ribose nucleic acid
MSH	Melanocyte-stimulating hormone
MyD88	Myeloid differentiation primary response 88
NFκB	Nuclear factor kappa light chain enhancer of activated B cells
NR0B1	Nuclear receptor subfamily 0 group B member 1
NRT	Non- reverse transcriptase control
NR3C1	Nuclear receptor subfamily 3 group C member 1
OMe	2-O-Methyl
ONDST	Overnight dexamethasone suppression test
PA	Pituitary adenomas
PAZ	Piwi-Argonaute-Zwille
PCSK9	Proprotein convertase subtilisin/kexin type 9
PEG	Polyethylene glycol
PIWI	P-element-induced wimpy testis
POMC	Proopiomelanocortin
PPNAD	Primary pigmented nodular adrenal disease
PS	Phosphorothioate
RISC	RNA-induced silencing complex

RRM2	Ribonucleotide reductase subunit M2
RNA	Ribonucleic acid
RNAi	RNA interference
RSV	Respiratory syncytial virus
siRNA	Short interfering RNA
SNALPs	Stable nucleic acid lipid particles
TLR	Toll-like receptor
TP53	Tumour protein p53
TRPV1	Transient receptor potential cation channel subfamily V member 1
TTR	Transthyretin
UFC	Urinary free cortisol
UNA	Unlocked nucleic acids
UTR	Untranslated region
USP8	Ubiquitin-specific peptidase 8
VEGF	Vascular endothelial growth factor

List of Permissions

The following copyrighted material was used with the listed permissions.

Publisher	Figure
OpenStax, Rice University, Houston, Texas, USA.	**Figure 1.2**: Anatomy and physiology of the hypothalamus and pituitary.
Oxford University Press, Oxford, UK	**Figure 1.4**: Clinical complications associated with Cushing's syndrome. **Figure 1.6:** Treatment algorithm for Cushing's disease.
Elsevier Limited, Cambridge, UK	**Figure 1.5:** Diagnosis of Cushing's syndrome. **Figure 1.11:** Induction of the immune response by siRNA. **Figure 1.13c**: The principle of liposome-mediated siRNA delivery. **Figure 1.14:** siRNA-conjugates as delivery systems.
Svoboda, P. Author of paper	**Figure 1.8: The domains of the Dicer enzyme.**
The American Society of Gene and Cell Therapy, Waukesha, Wisconsin, USA.	**Figure 1.7:** RNAi regulation of gene expression. **Figure 1.10b:** A schematic representation of the important features of siRNA structure and of siRNA binding to its target mRNA. **Figure 1.12:** Chemical modifications of siRNA.
MDPI, Basel, Switzerland	**Figure 1.9**: The domains of the Argonaute 2 protein. **Figure 3.13**: Tolerance for mismatches between an siRNA and its target.
Springer Nature Limited, Berlin, Germany	**Figure 1.10a**: A schematic representation of the important features of siRNA structure and of siRNA binding to its target mRNA.
Aston University, Birmingham, UK	**Figure 1.13a:** The principle of liposome-mediated siRNA delivery.
commons.wikimedia.org.	**Figure 1.13b:** The principle of liposome-mediated siRNA delivery.
InvivoGen Europe, Toulouse, France	**Figure 3.18:** Polyinosinic-polycytidylic acid induction of the innate immune response.
Bentham Science Publishers, Sharjah, United Arab Emirates	**Figure 4.1:** Schematic diagram of the corticotropin-releasing hormone receptor type 1.
University of Munich, Munich, Germany	**Figure 4.2:** Corticotropin-releasing hormone receptor type 1 signalling pathways.

List of Publications

Alzahrani A, Foulkes E, Porter JA, Kemp EH, Newell-Price J. Anti-POMC siRNA reduces ACTH secretion in a cell culture model of Cushing's disease. Society for Endocrinology British Endocrine Societies Meeting 2018, Glasgow, UK. **Endocrine Abstracts** 2018;59:P125.

Whatmore J, Alzahrani A, Porter J, Kemp EH, Newell-Price J. Antisense oligonucleotides as a novel medical therapy for Cushing's disease. Society for Endocrinology British Endocrine Societies Meeting 2019, Brighton, UK. **Endocrine Abstracts** 2019;65:P270.

Chapter 1

Introduction

1 Introduction

1.1 Overview

Dr Harvey Williams Cushing was one of the foremost neurosurgeons in America. He discovered Cushing's disease in 1912 and described this in his work entitled 'The pituitary and its disorders' (Cushing, 1912). Observable symptoms in his 22-year-old female patient were hypertension, truncal obesity, severe abdominal striae, erythrocytosis, and buffalo hump. Twenty years later, he linked the symptoms to the presence of a basophilic pituitary adenoma (Cushing, 1932). The clinical features of Cushing's disease are known now to result from excessive secretion of cortisol by the adrenal glands due to the over-production of adrenocorticotropic hormone (ACTH) from the anterior pituitary because of a pituitary adenoma.

This introduction will include a description of the hypothalamic-pituitary-adrenal (HPA) axis, the clinical features of Cushing's disease, and the current regimens for its treatment. A discussion of the concept of RNA interference (RNAi) and its application as a medical therapy will be included also. Finally, the use of short interfering (si)RNA as a potential treatment for Cushing's disease, specifically by silencing expression of the ACTH-encoding *POMC* gene, will be discussed.

1.2 The hypothalamic-pituitary-adrenal axis

The HPA axis refers to a set of hormonal interactions between three endocrine glands: the hypothalamus, the pituitary gland, and the adrenals (Figure 1.1) (Reeder et al., 2004). Overall, this hormonal communication acts to regulate the stress response by controlling glucocorticoid release from the adrenal glands. Under stress, activation of the HPA axis results in corticotrophin-releasing hormone (CRH) secretion from the hypothalamus. Binding of CRH to its receptor CRHR1 (Hemley et al., 2007), found mainly on corticotroph cells in the pituitary, causes expression of the *POMC* gene, which encodes proopiomelanocortin (POMC). Subsequently, the POMC peptide undergoes enzymatic cleavage releasing ACTH, which is then secreted from the cells. Via the circulation, ACTH reaches the adrenal cortex where upon it interacts with the melanocortin-2 receptor (MC2R), promoting the synthesis of glucocorticoids such as cortisol (Reeder et al., 2004; Bicknell et al., 2008). Rising glucocorticoid levels then feedback in a negative loop to suppress the secretion of CRH and ACTH (Figure 1.1).

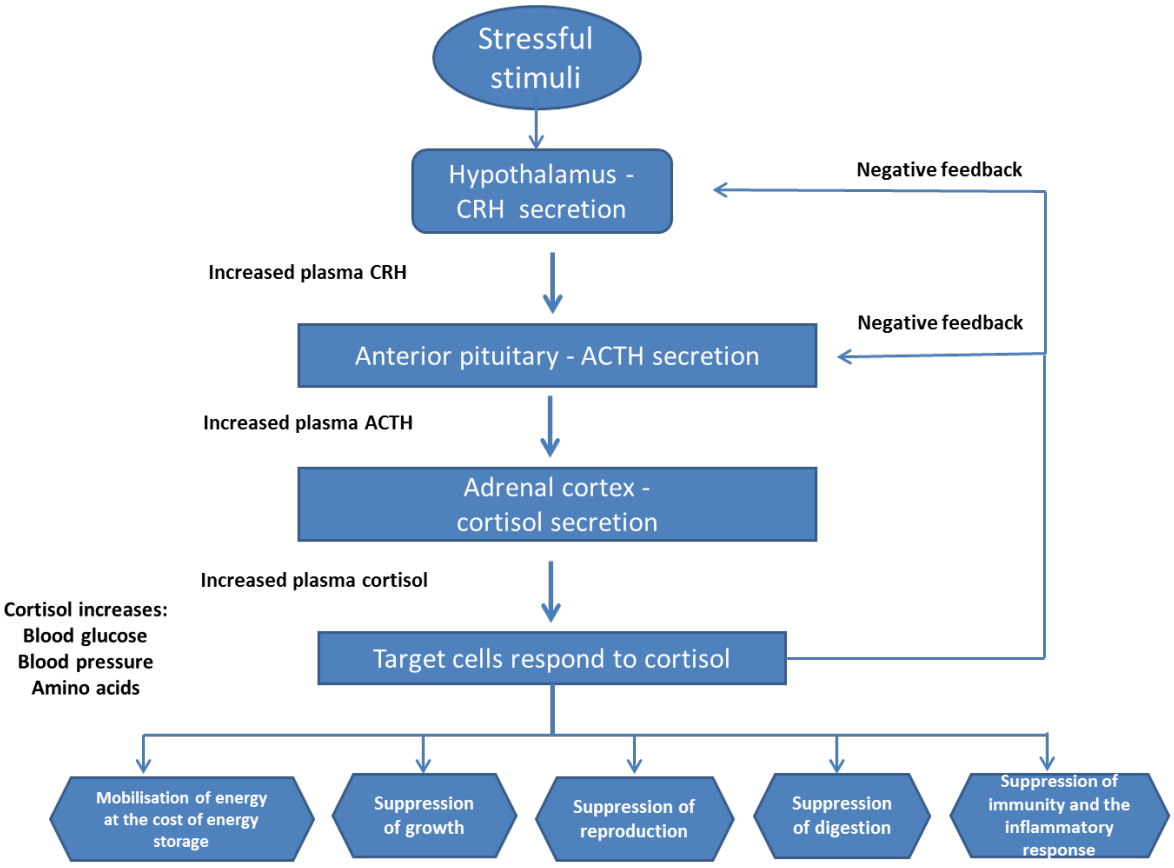

Figure 1.1: The hypothalamic-pituitary-adrenal axis.

The hypothalamic-pituitary-adrenal axis comprises a complex set of direct influences, feedback mechanisms, and hormonal interactions between three endocrine glands: the hypothalamus, the pituitary gland, and the adrenals. This hormonal communication acts to regulate the stress response by controlling glucocorticoid (cortisol) release from the adrenal glands. ACTH, adrenocorticotropic hormone; CRH, corticotrophin-releasing hormone.

The result of this hormonal interplay is to maintain a physiological concentration of blood glucocorticoids (Miller and O'Callaghan, 2002; Reeder et al., 2004).

The proper functioning of the HPA axis is critical for an effective response to stress. Disruption to the pathway can have devastating consequences for the individual (Miller and O'Callaghan, 2002). In Addison's disease where insufficient glucocorticoids are produced, lifelong hormone replacement is necessary (Howlett et al., 1986; Miller and O'Callaghan, 2002). Conversely, Cushing's syndrome occurs where there are excessive glucocorticoids (Howlett et al., 1986; Miller and O'Callaghan, 2002). This disease will be discussed in more detail in later sections. The components of the HPA axis are described in more detail in the following sections.

1.2.1 The hypothalamus

The hypothalamus controls important aspects of parenting and attachment behaviours, circadian rhythms, thirst, sleep, fatigue, body temperature, and hunger. It is found at the base of the forebrain below the thalamus (Figure 1.2). One of the most important functions of the hypothalamus is to link the nervous and endocrine systems, which it does via the pituitary gland (Figure 1.2). Hormones such as oxytocin and vasopressin are released into the posterior pituitary from magnocellular neurosecretory cells in the paraventricular nucleus and supraoptic nucleus (Coote, 2005). The parvocellular neurosecretory cells of the paraventricular nucleus are responsible for the release of hormones such as CRH, which enter the anterior pituitary and act to stimulate or inhibit the secretion of pituitary hormones (Coote, 2005).

1.2.2 The pituitary gland

The pituitary gland regulates body homeostasis during development and stress. It plays an intermediary role for physiological signal exchanges between the hypothalamus and peripheral organs. The pituitary gland is localised in a small bone cavity known as the *sella turcica* (Figure 1.2), which is covered by a dural fold named the *diaphragm sellae*. The pituitary gland contains two functionally distinct lobes; the anterior and posterior pituitary (Amar and Weiss, 2003; Coote, 2005).

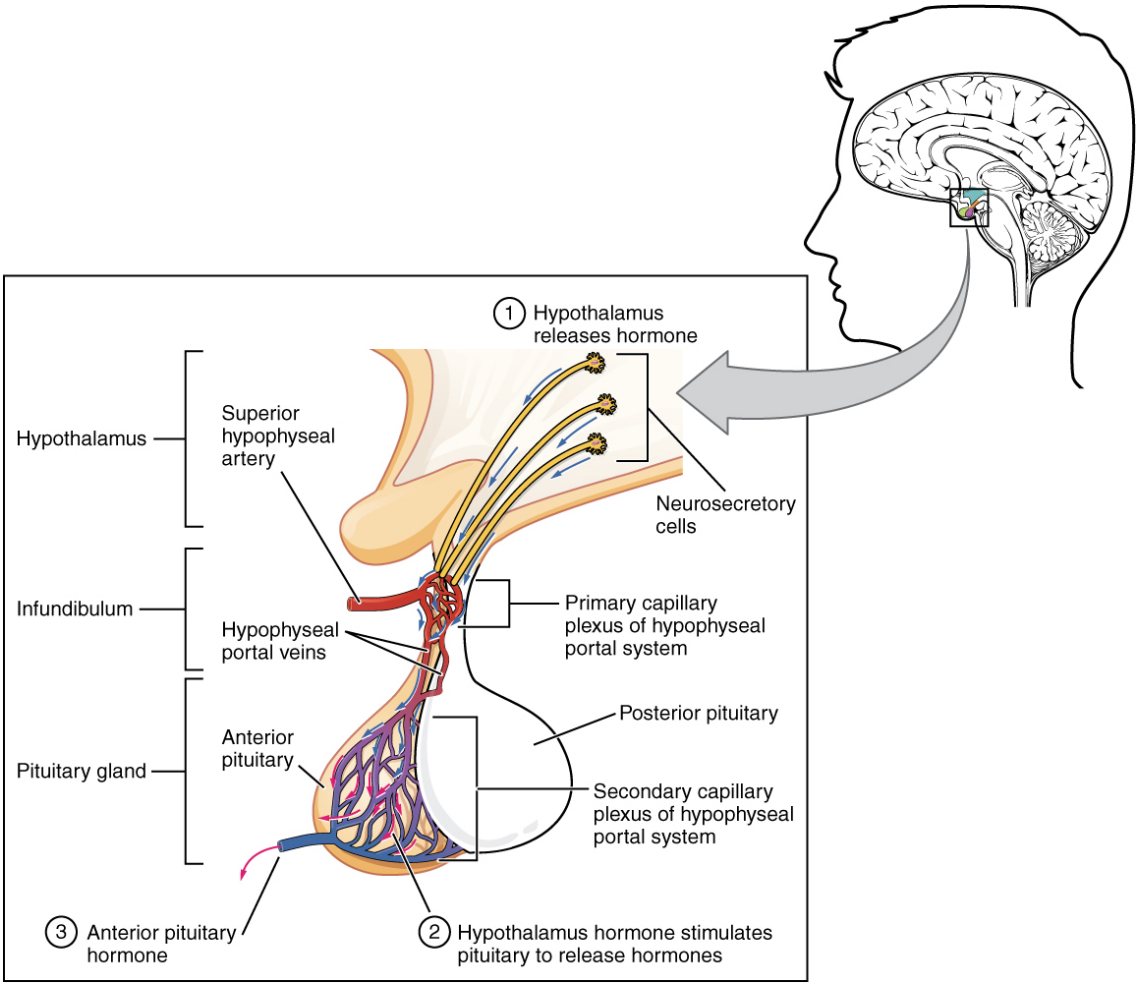

Figure 1.2: Anatomy and physiology of the hypothalamus and pituitary gland.

Hormones of the hypothalamus such as corticotrophin-releasing hormone are secreted into a portal venous system. This stimulates the hormonal secretion of the anterior pituitary gland including adrenocorticotropic hormone (ACTH). Hormones of the posterior pituitary gland such as oxytocin are directly secreted from the hypothalamus. The image, from http://philschatz.com/anatomy-book/contents/m46699.html, was used with kind permission from David Harris, Editor-in-Chief at OpenStax (Rice University, Houston, Texas, USA).

The posterior pituitary consists of the neural lobe, which is behind the anterior pituitary, and the infundibular stalk, which connects the gland to the hypothalamus (Figure 1.2). In detail, the posterior pituitary consists mainly of the axons of magnocellular neurosecretory cells extending from the paraventricular and supraoptic nuclei areas of the hypothalamus. These axons store and release oxytocin and vasopressin, which are synthesised in the hypothalamus.

The anterior pituitary consists of distal, intermediate, and tuberal lobes, and is vascularised by branches of the superior hypophyseal artery via the hypophyseal portal system (Figure 1.2). Several physiological processes including stress, growth, reproduction, and lactation are controlled by the anterior pituitary through the action of its secreted hormones. Briefly, growth hormone-releasing hormone, dopamine, gonadotropin-releasing hormone, thyrotropin-releasing hormone, and CRH, which are released by the parvocellular neurosecretory cells in the hypothalamus act upon, via specific receptors, the appropriate endocrine cells of the anterior pituitary. In turn, the five types of endocrine cells respond by expressing and secreting their respective hormones; somatotrophs (growth hormone), lactotrophs (prolactin), gonadotrophs (follicle-stimulating hormone and lutenising hormone), thyrotrophs (thyroid-stimulating hormone), and corticotrophs (ACTH).

1.2.2.1 The corticotrophin-releasing hormone receptor

The human CRHR1 is a G protein-coupled receptor encoded by the CRHR1 gene at locus 17q21.31. The full-length gene transcript has 14 exons and encodes 444 amino acids, but the final protein is 415 amino acids as exon 6 is excised (Hillhouse and Grammatopoulos, 2006). The receptor consists of seven transmembrane hydrophobic α-helices, a carboxy-terminal intracellular domain, and a G protein-coupling domain between transmembrane domains five and six. It is activated by conformational changes induced by the binding of its ligand CRH on the surface of corticotroph cells in the anterior pituitary. On CRH-binding, CRHR1 is coupled to a stimulatory G protein, which activates the adenylyl cyclase-cyclic AMP (cAMP) signalling pathway (Hillhouse and Grammatopoulos, 2006). In turn, this leads to an increase in intracellular cAMP levels, which enhances POMC transcription and ACTH secretion. Following prolonged stimulation of CRHR1 by CRH, the receptor is endocytosed and the cAMP signalling continues after internalisation (dos Santos Claro et al., 2019). The downstream effects

of the activation of CRHR1 include synthesis and secretion of ACTH (Aguilera et al., 1986).

1.2.2.2 Adrenocorticotrophic hormone

Encoded by the *POMC* gene, ACTH is a linear 39-amino acid peptide with species differences in the carboxy-terminal (Schwyzer, 1977; Ghaddhab et al., 2017). The first 24 amino acids adopt a helical structure and are biologically important. Residues four and 10 assume a β-turn conformation (Hruby et al., 1993). The hormone is responsible for regulating the production and release of adrenal steroid hormones (Jenks, 2009). Upon release from corticotrophic cells, ACTH interacts with MC2R on the parenchymal cells of the adrenocortical zona fasiculata (Spiga and Lightman, 2015). This activates steroidogenesis via increasing levels of intracellular cAMP and the uptake cholesterol into the cell (Simpson and Waterman, 1988; Smith and Vale, 2006). Cholesterol is translocated into the mitochondria where it is converted to corticosterone. Adrenocorticotrophic hormone also upregulates the expression of mitochondrial enzymes responsible for corticosterone synthesis including P450 side-chain enzyme (CYP11A), 11-β-hydroxylase (CYP11B1), aldosterone synthase (CYP11B2), 17-α-hydroxylase (CYP17), and 21-hydroxylase (CYP21) (Ney et al., 1967; Garren et al., 1971; Gill, 1972; Elias and Clark, 2000).

Release of ACTH from the anterior pituitary gland is at its peak just before awakening in the morning and levels decline throughout the day. Appropriately, raised blood cortisol levels are detected in the hypothalamus such that the release of CRH is downregulated (Gallo-Payet, 2016). This in turn downregulates the expression and secretion of ACTH into the bloodstream (Gallo-Payet, 2016).

1.2.2.3 Proopiomelanocortin

The *POMC* gene that encodes ACTH consists of three exons interspersed by two introns (Figure 1.3) (Drouin et al., 1989; de Souza et al., 2005; Millington, 2007). In humans, it is located on chromosome 2p23.3 (Chang et al., 1980). The mouse *pomc* gene is located on chromosome 12 and has a similar structure to the human *POMC* gene (Uhler et al., 1983). Transcription of the gene, mRNA splicing, and addition of a poly-A tail results in the formation of pro-POMC mRNA. On translation into pro-POMC peptide, exon 1 remains untranslated and exon 2 encodes the pre-

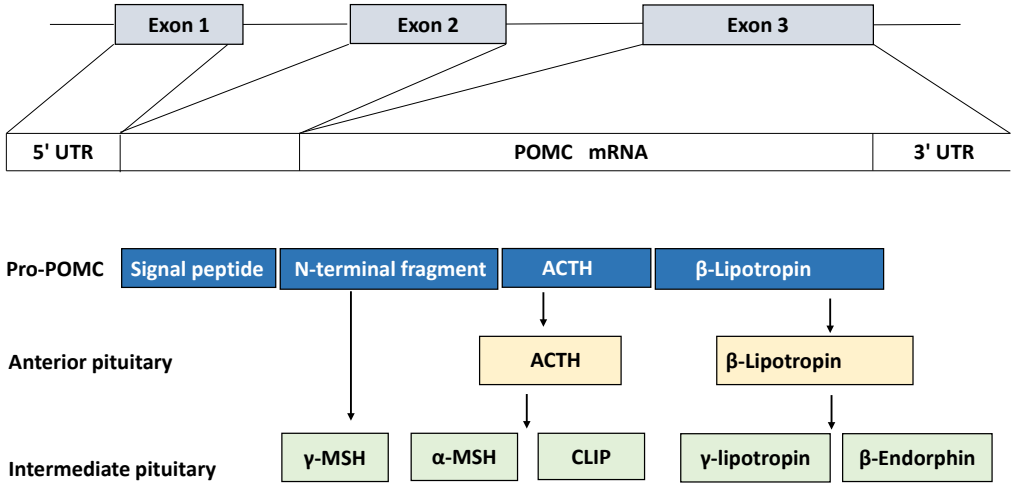

Figure 1.3: Overview of the *POMC* gene structure and posttranslational modification of proopiomelanocortin.

The mammalian *POMC* gene is made up of three exons of which exons 2 and 3 are translated into the 285-amino acid pro-POMC precursor which has a 26-amino acid signal sequence that directs the peptide to the secretory system of the cell. The POMC molecule is then cleaved into several peptide hormones. ACTH, adrenocorticotropic hormone; CLIP, corticotropin-like intermediate lobe peptide; β-LPH, β-lipotropin; γ-LPH, γ-lipotropin; α-MSH, α-melanocyte-stimulating hormone; γ-MSH, γ-melanocyte-stimulating hormone; POMC, proopiomelanocortin; UTR, untranslated region.

POMC signal peptide, needed for transport through the secretory pathway of the cell plus, as well as a short length of the amino-terminal of pro-POMC. Exon 3 encodes all of the POMC peptide hormones (Jenks, 2009).

Once the 285-amino acid pro-POMC polypeptide (Figure 1.3) enters the secretory pathyway, the signal peptide sequence is cleaved and the remaining peptide is processed into several peptides by cell-specific enzymes (Allen et al., 1988; Cool et al., 1997). Pituitary corticotrophs express pro-peptide convertase PC1 that cleaves POMC to generate the amino-terminal peptide, joining peptide, ACTH, β-lipotrophin and β-endorphin (Figure 1.3) (Seidah et al., 1992; Zhou et al., 1993). Melanotrophs express PC1, PC2, carboxypeptidase E, N-acetylating and amidating enzymes, and these act to produce α-MSH and β-endorphin (Figure 1.3) (Seidah et al., 1992; Evans et al., 1994; Paquet et al., 1996; Millington et al., 2007). After cleavage, the peptide hormones are packaged into large, dense core vesicles and, in response to appropriate stimuli, the peptides are released from cells by exocytosis.

A variety of functions are carried out by the POMC peptide hormones. Pituitary ACTH stimulates the MCR2 in the adrenal gland, ultimately regulating steroid hormone production (Alwani et al., 2011). α-MSH, which is derived from ACTH 1-13 (Figure 1.3), is produced from the intermediate lobe in rodents and the vestigial lobe in humans (Van der Neut et al., 1988; Trifanescu et al., 2011). It acts locally in the skin to control melanogenesis and thermoregulation via melanocortin receptors MC1R and MC5R. In addition, α-MSH from neurons in the arcuate nucleus influences appetite and sexual behaviour (Wessells et al., 2000). γ-MSH is a product of the amino-terminal fragment of POMC and has a more limited spectrum of biological activities; its receptor is MC3R. Corticotrophin-like immediate protein (CLIP) is thought not to circulate in humans or have a biological role (Cowley et al., 2001). β-lipotrophin lies at the carboxy-terminus of POMC and is cleaved to γ-lipotrophin and β-endorphin. The endorphins are endogenous opioid peptides that have actions on the brain and are involved in the regulation of behaviour, and the onset of obesity, diabetes, and psychiatric diseases (Goldfarb et al., 1991; Dalayeun et al., 1993).

In humans, corticotroph cells in the anterior pituitary, the arcuate nucleus of the hypothalamus, and melanocytes are the main sites where *POMC* is expressed, although its mRNA has been detected in other tissues (Autelitano et al., 1989; Raffin-

Sanson et al., 2003). The tissue-specific expression of POMC can be explained to some extent by different methylation patterns of the promoter and by the activity of different transcription factors (Newell-Price, 2003; Jenks, 2009). The active promoter in corticotrophs of the anterior pituitary is situated at the 5' region upstream of exon 1 (Figure 1.3). Transcription from this site gives an mRNA transcript of 1150 nucleotides. A second promoter further upstream towards exon 1 yields a transcript of 1350 nucleotides. A small amount of this longer mRNA can be detected in the anterior pituitary as well as being the transcript in non-pituitary ACTH-secreting tumours. Transcription of *POMC,* in other tissues takes place from a third promoter that is located in intron B (Figure 1.3). The transcript is 800 nucleotides. The peptide translated from this transcript lacks the signal peptide so cannot be secreted and its function remains obscure (Newell-Price, 2003; Raffin-Sanson et al., 2003).

The promoter that produces the 1150-nucleotide transcript is the most well-studied (Newell-Price, 2003). It contains several response elements that are activated by specific transcription factors (Jenks, 2009). Transcription factors involved in activation of *POMC* expression are Tpit, Pitx, NeuroD1, and Nur77 (Lamonerie et al., 1996; Phillips et al., 1997; Lamolet et al., 2001). Having many transcription factors allows the expression of POMC to be controlled tightly, and the variation of transcription factors expressed in different tissues contributes to *POMC* tissue-specific expression (Jenks, 2009).

1.2.3 The adrenal glands

The adrenal glands are highly vascularised retroperitoneal endocrine structures situated above the kidneys. Their blood supply is from the renal and phrenic arteries and the aorta. They consist of two distinct endocrine organs; the inner adrenal medulla and the outer adrenal cortex (Davies et al., 2005; Siebert et al., 2017). The adrenal medulla is made up of chromaffin cells originating from ectoderm of the neural crest and consists of 30% of the adrenal gland. It is supplied with corticosteroid enriched blood from the cortex and regulates the conversion of norepinephrine to epinephrine (Davies et al., 2005). The majority of medullary cells secrete epinephrine, while a small fraction secretes norepinephrine. The adrenal cortex consists of the outer zona glomerulosa, the zona fasiculata, and the inner zona reticularis. Glucocorticoids such as cortisol are secreted from the zona fasiculata. Mineralocorticoids such as

aldosterone are secreted from the zona glomerulosa and androgens are secreted from zona reticularis (Miller and O'Callaghan, 2002; Davies et al., 2005).

1.2.3.1 Glucocorticoids

Glucocorticoids are a group of steroid hormones that regulate metabolic, immune, cardiovascular and behavioural processes (Sapolsky et al., 2000). Cortisol is the predominant glucocorticoid. They mediate their effects by ligating to ubiquitously distributed cytosolic intracellular receptors called glucocorticoid receptors. The glucocorticoid receptor is a 94-kDa protein. It is inactive in cells because it is bound to various heat shock proteins that dissociate upon glucocorticoid binding. Ligand-binding induces a conformational change on the receptor and enhances its translocation into the nucleus where it forms a homodimer and binds specific DNA motifs called glucocorticoid responsive elements in the promoter of glucocorticoid responsive genes where it regulates gene expression (Pratt, 1993).

Cortisol acts on the HPA axis to instigate negative feedback on its own synthesis, by the trans-repression of hypothalamic CRH and anterior pituitary ACTH (Zhang et al., 2016). Cortisol binds to the glucocorticoid receptor NR3C1, on cell surfaces in the hypothalamus and anterior pituitary, to form a NR3C1/cortisol complex. The complex translocates from the cell cytoplasm to the nucleus where it inhibits transcription of the genes encoding POMC and CRH by binding to their glucocorticoid response elements (Smith and Vale, 2006). In this way, the HPA axis is tightly controlled. However, changes in the feedback mechanism result in excessive serum and urinary cortisol, which is the basis of Cushing's syndrome. The disease is discussed in the next sections.

1.3 Cushing's syndrome

1.3.1 Epidemiology and aetiology

Cushing's syndrome results from prolonged and excessive amounts of blood cortisol. If left untreated, the disease has an associated five-year 50% mortality rate due cardiovascular complications, psychiatric disturbances, and infections (Castinetti et al., 2012; Steffensen et al., 2010). It has an estimated incidence of 0·2–5·0 per million individuals per year with a prevalence in various populations of 39–79 per million (Lacroix et al., 2015). The median disease onset-age is 41 years and it is more common in females than males with a ratio of 3:1 (Lacroix et al., 2015). The most common cause of Cushing's syndrome is exposure to steroids used in medical treatments and is referred to as exogenous or iatrogenic. So-called endogenous Cushing's syndrome can be classified as ACTH-dependent, in 80% of cases, or ACTH-independent, in 20% of cases (Lacroix et al., 2015).

1.3.1.1 ACTH-dependent pituitary Cushing's syndrome

In 80% of ACTH-dependent cases of Cushing's syndrome, the disease is caused by a slow-growing benign pituitary adenoma that is usually less than 10 mm and that produces high levels of ACTH. This is referred to as Cushing's disease, first described by Harvey Cushing in 1912 (Cushing, 1912; Gicquel et al., 1992; Woo et al., 2005; Bertagna et al., 2009; Castinetti et al., 2012). Corticotroph tumours are sporadic with very few cases described in hereditary endocrine syndromes (Albani et al., 2018), and the genes implicated in their formation are given in Table 1.1. Recent advances have identified mutations in the ubiquitin-specific peptidase 8 (USP8) gene in 23-60% of corticotroph tumours (Ma et al., 2015; Reincke et al., 2015; Losa et al., 2019; Wanichi et al., 2019). These mutations are specific to corticotroph tumours and result in an increase in *e*pidermal growth factor receptor (EGFR) and *POMC* gene expression (Fukuoka et al., 2011; Hayashi et al., 2016). However, the tumours generally retain some negative feedback response to excessive levels of glucocorticoids.

Table 1.1: Mutations associated with Cushing's disease

Gene	Mutation	Mutation type	Disease	Reference
MEN1	-	Deletion	Paediatric familial/syndromic CD	Stratakis et al., 2010
	p.R415X	Nonsense	Paediatric familial/syndromic CD	Stratakis et al., 2010
	p.R460X	Nonsense	MEN1 with CD	Matsuzaki et al., 2004
NR3C1	p.1559N	Missense	CD	Karl et al., 1996
AIP	c.696G>C/p.P232P	Silence	CD	Georgitsi et al., 2007
	c.308A>G /p.K103R	Missense	Recurrent CD	Stratakis et al., 2010
TP53	p.L145R	Missense	Atypical PA causing CD	Kawashima et al., 2009
NROB1	g.259_260insAGCG	Insertion	ACTH-secreting PA and X-linked adrenal hypoplasia congenita	De Menis et al., 2005
USP8	p.5718C	Missense	CD	Reincke et al., 2015
	p.P720R	Missense	CD	Reincke et al., 2015
	p.5718del	Deletion	CD	Perez-Rivas et al., 2015
	p.5718P	Missense	CD	Ma et al., 2015
	p.P720Q	Missense	CD	Ma et al., 2015
DICER1	c.3046delA/p.S1016VfsX1065	Frameshift	Pituitary blastoma presenting with CD	Sahakitrungruang et al., 2014
	c.5538>T/p.E1813V>>	Missense		
CYP21A2	p.V281L	Missense	CD with CAH	Haase et al., 2011
	-	Splicing	ACTH-producing PA	Haase et al., 2011
	-	Deletion	ACTH-producing PA	Boronat et al., 2004
GNAS	p.R179G	Missense	Corticotroph adenomas	Williamson et al.,1995
	p.Q227R	Missense	Corticotroph adenomas	Riminucci et al., 2002
	p.Q227H	Missense	Corticotroph adenomas	Riminucci et al., 2002
	p.R2201H	Missense	CD	Riminucci et al., 2002

MEN1, menin 1; NR3C1, nuclear receptor subfamily 3 group C member 1; AIP, aryl hydrocarbon receptor-interacting protein; TP53, tumour protein p53; NR0B1, nuclear receptor subfamily 0 group B member 1; USP8, ubiquitin-specific peptidase 8; DICER1, Dicer 1, ribonuclease III; CYP21A2, cytochrome P450 family 21 subfamily A member 2; GNAS, GNAS complex locus; CD, Cushing's disease; MEN1, multiple endocrine neoplasia type I; PA, pituitary adenomas; ACTH adrenocorticotropic hormone; CAH, congenital adrenal hyperplasia; -, not mentioned.

1.3.1.2 ACTH-dependent ectopic Cushing's syndrome

The remaining 20% of ACTH-dependent cases are due to ectopic secretion of ACTH from tumours in other parts of the body, usually the lungs (Newell-Price et al., 2003). Mostly, in such cases, there is no negative feedback response from high levels of cortisol (Kirk et al., 2000). In a recent study, it has been suggested that the proportion of Cushing's syndrome patients with ectopic ACTH secretion is higher than previously reported (Wengander et al., 2019). Half of the cases were caused by Cushing's disease, 25% by ectopic ACTH-secreting tumours, and the remaining 25% by adrenal disease. It has also been argued that the proportion of adrenal causes are rising due to the increase in detection of cortical-secreting adrenal incidentalomas that are associated with mild hypercortisolism (Hirsch et al., 2018).

1.3.1.3 ACTH-independent Cushing's syndrome

Cases of ACTH-independent endogenous Cushing's syndrome are mainly due to benign, in 60% of cases, or malignant, in 40% of cases, adrenal tumours (Castinetti et al., 2012) that cause high levels of cortisol secretion. Rare adrenal causes are due to macronodular adrenal hyperplasia, McCune Albright syndrome, and primary pigmented nodular adrenal disease.

1.3.2 Clinical features of Cushing's syndrome

Excessive levels of cortisol result in the clinical features of Cushing's syndrome, which may include plethoric facial appearance, truncal and facial fat deposition, muscle atrophy, skin thinning, and easy bruising (Nieman et al., 2008). Cushing described the symptoms of his patient, Minnie G, as: 'The moon shaped plethoric face, accompanied by a buffalo hump, wasted limbs and purple striae are classical, and are due to the catabolic effects of excess and prolonged glucocorticoids' (Figure 1.4) (Cushing, 1932). Features vary and are difficult to diagnose at early or cyclical stages of the disease, thus diagnosis my take between 2-4 years (Feelders et al., 2012). High levels of cortisol can also be associated with cardiovascular disease risk factors such as diabetes, dyslipidemia, hypertension, and obesity. Other conditions associated with chronic high levels of cortisol are osteoporosis, thromboembolism, and psychological and cognitive disturbances (Feelders et al., 2010; Van der Pas et al., 2012). One of the most common and initial symptoms in patients with Cushing's disease is visceral

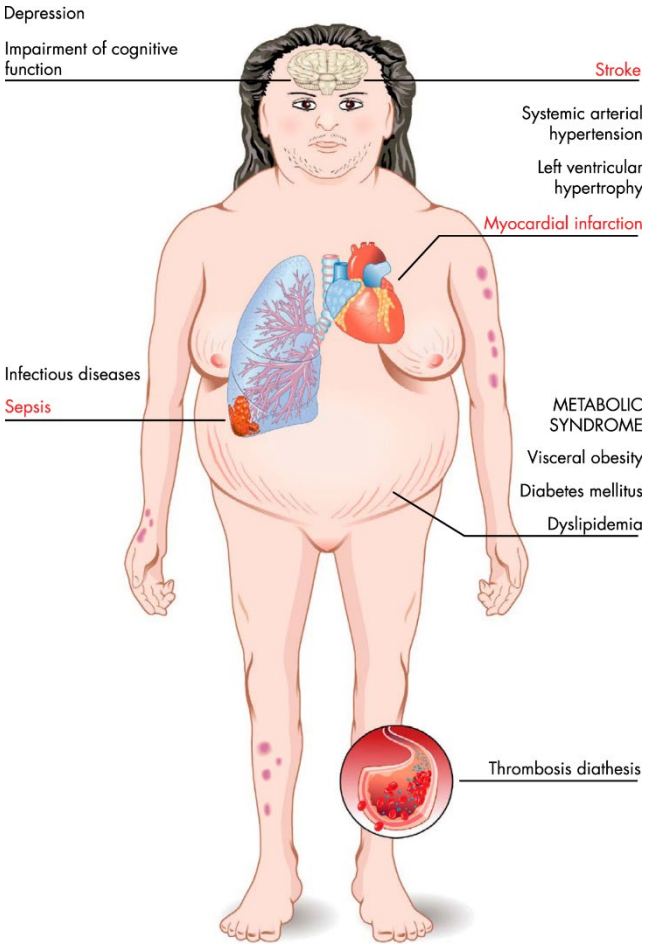

Figure 1.4: Clinical complications associated with Cushing's syndrome.

Excessive levels of cortisol result in the clinical features of Cushing's syndrome, which may include plethoric facial appearance, truncal and facial fat deposition, muscle atrophy, skin thinning and easy bruising. Comorbidities and clinical complications such as myocardial infarction, sepsis, and stroke are associated with excessive mortality. The image, from a paper by Pivonello et al. (2015), was used with kind permission from Oxford University Press (Oxford, UK).

fat deposition (Bertagna et al., 2009). These abnormal fat distributions that develop in the face (moon face) and dorsalcervical fat pads (buffalo hump) give rise to the observations described by Cushing (Cushing, 1932). In addition to obesity, skin thinning, muscle and bone wasting, and wide purple striae are often observed due to the protein wasting effect of cortisol (Ross and Linch, 1982, Ohmori et al., 2003).

1.3.3 Diagnosis of Cushing's syndrome

There are three main tests that are used to establish the diagnosis of Cushing's syndrome in what is a two-step analysis (Figure 1.5) (Daniel and Newell-Price, 2017). The low-dose dexamethasone suppression test is the most widely used test for Cushing's syndrome (Lindholm et al., 2004). Secondly, the late night salivary and serum cortisol test. In normal individuals, the levels of serum cortisol are lowest at midnight and this is associated with the level found in the saliva. The upper value of cortisol at midnight is 3.8 nmol/L, and thus, values above that are regarded as positive for hypercortisolism (Elamin et al., 2008). Serum cortisol greater than 206 nmol/L at midnight may suggest Cushing's syndrome. Finally, the 24-h urinary free cortisol test can indicate renal impairment in Cushing's syndrome. High performance liquid chromatography gives a normal range of cortisol above 1379 nmol/L per 24 h while radioimmunoassay gives a normal range of above 2483 nmol/L per 24 h. Though these tests are simple and cost effective, it must be noted that they should be performed under controlled conditions by avoiding stressful conditions. This is because serum cortisol levels are not accurately represented by the activity of the HPA axis when under stress. Serum cortisol levels are also affected in women with high oestrogen levels or those taking oral contraceptive due to increased cortisol-binding globulin levels (Bansal et al., 2015).

1.3.4 Differential diagnosis of Cushing's syndrome

Following the confirmation of Cushing's syndrome, the levels of ACTH are measured to indicate the possible cause (Figure 1.5) (Daniel and Newell-Price, 2017). Values lower than 5 pg/mL indicate that the adrenals are the primary cause of Cushing's syndrome. If concentrations are above 15 pg/mL then Cushing's syndrome can be ascribed to a pathology that is ACTH-dependent, including the possibility of Cushing's disease, which can then be further investigated by the following tests and analysis.

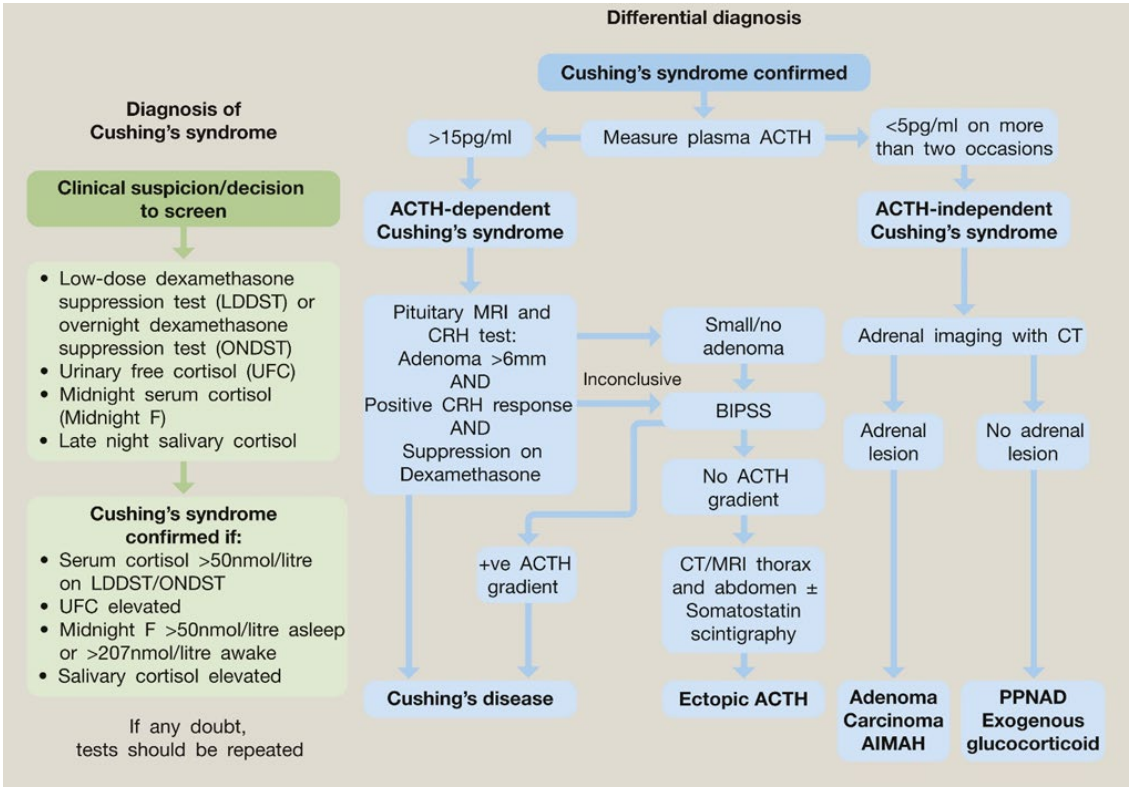

Figure 1.5: Diagnosis of Cushing's syndrome.

The diagnosis and differential diagnosis of Cushing's syndrome are outlined. ACTH, adrenocorticotrophic hormone; AIMAH, ACTH-independent macronodular adrenal hyperplasia; BIPSS, bilateral inferior petrosal sinus sampling; CRH, corticotrophin-releasing hormone; PPNAD, primary pigmented nodular adrenal disease, LDDST, low-dose dexamethasone suppression test; ONDST, overnight dexamethasone suppression test; UFC, urinary free cortisol; MRI, magnetic resonance imaging; CT, computerised tomography. The image, from a paper by Daniel and Newell-Price (2017), was used with kind permission from Elsevier Limited (Cambridge, UK).

The CRH-stimulation test can be used for the differential diagnosis of ACTH-dependent Cushing's syndrome. However, it may not always differentiate between Cushing's disease and ectopic ACTH secretion (Loriaux et al., 1986; Reimondo et al., 2003). An inferior petrosal sinus stimulation test measures ACTH levels in peripheral blood vessels and in both sides of the inferior petrosal sinus following stimulation by CRH and is the best way to differentiate between pituitary and non-pituitary ACTH (Scott et al., 1999; Deipolyi et al., 2012). Finally, sella magnetic resonance imaging is used to confirm the presence of a pituitary tumour prior to surgery. It has the highest level of accuracy with a predictive value of about 86% when compared with other tests such as inferior petrosal sinus sampling or a positron emission tomography scan (Wind et al., 2013).

1.3.5 Treatment and management of Cushing's disease

Once Cushing's disease has been diagnosed, the goal for its treatment are normalisation of cortisol secretion, reversal of clinical symptoms, recovery of clinical complications, and long-term disease control without recurrence (Newell-Price et al., 2006; Biller et al., 2008; Pivonello et al., 2008). The treatment algorithm is depicted in (Figure 1.6).

1.3.5.1 Pituitary and adrenal surgery

Pituitary surgery is the first line treatment of Cushing's disease. The surgical approach may be transcranial or transsphenoidal. Pituitary transcranial surgery is used on rare occasions when transsphenoidal surgery is not an option due to the location, size and expansion of the pituitary tumour (Pivonello et al., 2015). Endoscopic transsphenoidal surgery has advantages over microscopic transsphenoidal surgery including; greater extent of resection, improved safety, less invasive, and potentially better results (Cappabianca and de Divitiis, 2004).

Adrenal surgery is a secondary approach after failed pituitary surgery for Cushing's disease (Ding et al., 2014). It may be regarded as unilateral adrenalectomy if one of the adrenal glands is removed or as bilateral adrenalectomy when it involves the removal of both adrenal glands. Unilateral adrenalectomy is aimed at preserving endogenous cortisol production and is usually followed by conventional radiotherapy.

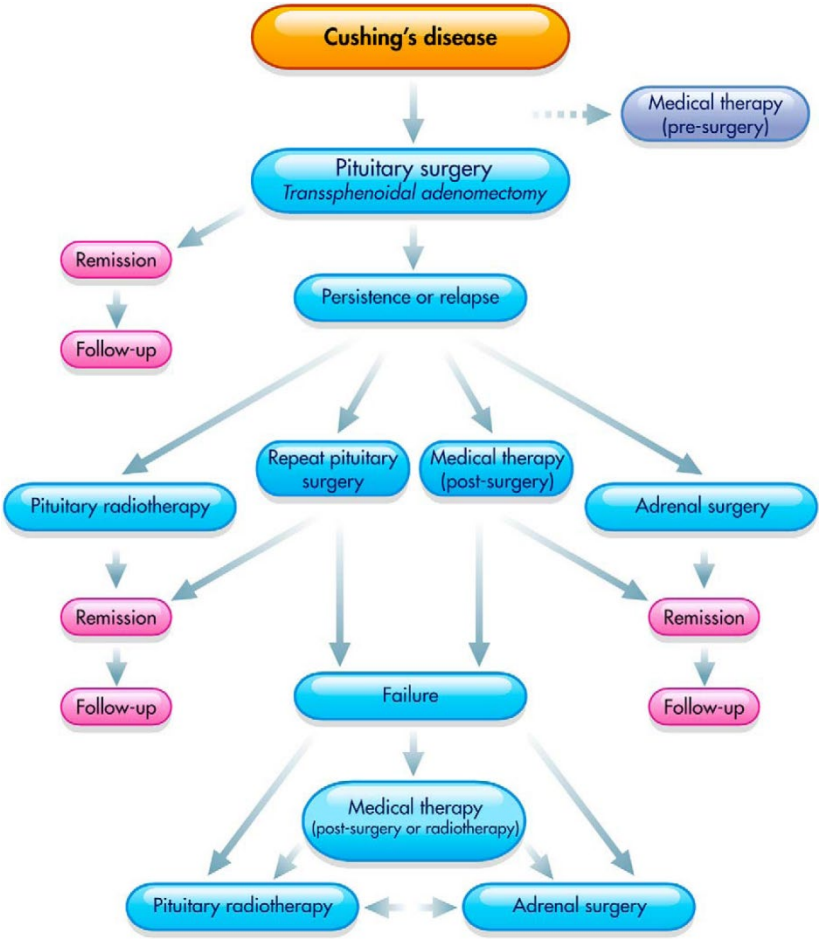

Figure 1.6: Treatment algorithm for Cushing's disease.

The treatment algorithm for Cushing's disease is outlined. Usually, surgeries are considered as the first-line treatment while medical therapy is considered if there is a relapse of the clinical symptoms after surgery. The image, from a paper by Pivonello et al. (2015), was used with kind permission from Oxford University Press (Oxford, UK).

Bilateral adrenalectomy is usually aimed at complete suppression of cortisol synthesis to give rapid relief from clinical symptoms.

1.3.5.2 Radiotherapy

Between 1940 and 1980, pituitary radiotherapy was used initially as the first-line treatment of Cushing's disease. However, it is now used only when surgical attempts have failed, especially when the pituitary tumour is aggressive and/ or invasive (Bertagna et al, 2009; Juszczak et al., 2013). Radiation doses are usually 45-50 Gray units (Minniti and Brada, 2007; Pivonello et al., 2015). It can be delivered as a single treatment at a dosage of 18-24 Gray units or as a fractionated treatment at a dosage of 45-50 Gray units (Starke et al., 2010; Loeffler and Shih, 2011).

1.3.5.3 Medical treatments

Medical therapies are considered a secondary line of treatment for Cushing's disease. It can be used either before surgery, after surgery, before and after pituitary radiotherapy, and as a first-line treatment. It is used before surgery in patients with severe Cushing's disease to control the excess levels of cortisol. Drugs used for the treatment of Cushing's disease can be classified into three categories; adrenal-directed drugs, pituitary-directed drugs, and glucocorticoid receptor-directed drugs (Vieira et al., 2014).

Drugs directed at the adrenals are effective in suppressing hypercortisolemia, but they fail to treat the underlying cause of the increase in blood cortisol and, thus, are used temporarily to rapidly correct complications that may have arisen in the patient (Pivonello et al., 2015). The European Union has approved ketoconazole, an antifungal imidazole derivative, and metyrapone, a pyridine derivative as two adrenal directed drugs for the treatment of Cushing's syndrome. Other drugs in this category include aminoglutethimide, mitotane, and etomidate (Pivonello et al., 2015). Ketoconazole functions secondarily as an inhibitor of cortisol synthesis. One adverse effect that can arise from the continuous use of ketoconazole is hepatotoxicity, which may cause fatal hepatitis. Metyrapone interferes with cortisol production by inhibiting 11-β-hydroxylase which catalyses the final stage of corticol synthesis (Chart and Sheppard, 1958).

Pituitary-directed drugs have the advantage of acting at the site responsible for Cushing's disease, the pituitary tumour. Amongst this group of drugs, the dopamine agonist cabergoline and the somatostatin analog pasireotide result in disease remission in a consistent subgroup of patients with Cushing's disease (Fleseriu 2014). However, so far, there has been little success reported of these drugs for treating Cushing's disease in large population clinical trials (Fleseriu, 2012; Tritos and Biller, 2014). Pituitary-directed drugs are divided into two groups; neuromodulatory drugs and nuclear receptor ligands. Neuromodulatory drugs influence the HPA axis directly. They were proposed to have an active role in the treatment of Cushing's disease, but there is little evidence of their clinical benefit (Miller and Crapo, 1993). Metergoline, cyproheptadine, kentanserine, and ritanserine inhibit the secretion of CRH and arginine vasopressin from the hypothalamus, thus preventing the synthesis and secretion of ACTH (Suda et al., 1983). In the case of nuclear receptor ligands, retinoic acid, and peroxisome proliferator-activated receptor-γ agonists are the most common that have potential in treating Cushing's disease. In rodents and canine models, retinoic acid has been demonstrated as a possible treatment for Cushing's disease as it can reduce corticotrophic tumour size, ACTH secretion, adrenal hyperplasia, and inhibit cell proliferation. It mediates these effects by antagonising transcription factors that are involved in the positive regulation of the *POMC* gene such as activator protein-1 and the Nur transcription factors. Mild adverse effects were observed including transitory mouth and conjunctival dryness, headache, worsening leukocytosis, arthralgias, diarrhoea, and abdominal discomfort (Páez-Pereda et al., 2001; Castillo et al., 2006; Pivonello et al., 2015).

Drugs directed at the glucocorticoid receptor are also referred to as glucocorticoid antagonists. Inhibiting the effects of glucocorticoids can rapidly reduce the effects of hypercortisolism and, therefore, can be used as a treatment modality for Cushing's disease. Mifepristone is a type 2 glucocorticoid receptor ligand with a very high affinity of three to 10-fold higher than dexamethasone and cortisol, respectively (Sartor and Cutler, 1996). It was introduced for treating Cushing's syndrome in 1985. Later on, it was considered a treatment for Cushing's disease, and was found to be effective in 38-75% of patients (Castinetti et al., 2009). The activity of mifepristone affects both the central and peripheral nervous systems. Mifepristone can be taken orally at a dose of between 300-1200 mg per day. It is rapid in therapeutic action and has a long half-

life of 24-90 h. Mifepristone alters the negative feedback effect of glucocorticoid on CRH and ACTH secretion (Johannsen and Allolio, 2007; Pivonello et al., 2015). It can also indirectly activate the mineralocorticoid pathway, which may result in hypertension, hypokalemia, alkalosis, and edema.

1.3.5.4 Combination therapy

Cushing's disease can be treated by the combination of various drugs to reduce adverse effects that occur from monotherapy as small doses of the different combinations can be given (Thoren et al., 1985). Studies have been performed in which patients were given a combination of low doses of metyrapone, ketoconazole, and mitotane. A rapid reduction in the level of urinary cortisol and a rapid improvement in clinical symptoms was observed. However, adverse effects were also observed; hypokalemia was found in 100% of patients, acute adrenal insufficiency in 36.4%, an increase in liver enzymes in 18-82%, dizziness and confusion in 9%, and nausea and vomiting in 64% (Kamenický et al., 2011).

1.4 RNA interference

RNA interference (RNAi) is a natural biological process that uses short sequences of double-stranded RNA (dsRNA) to prevent gene expression (Bosher and Labouesse, 2000; Younis et al., 2014). The term RNAi was coined by Fire and colleagues when they observed sequence-specific gene silencing in *Caenorhabditis elegans* in response to the introduction of dsRNA into cells (Fire et al., 1998; Tabara et al., 1998; Fire, 1999). Since then, RNAi has been shown in many eukaryotic cells, although the mechanism is more complex in higher organisms (Aigner, 2006). RNAi is believed to have evolved as a cellular mechanism to counter the effects of viral gene transcription and transposon activity. However, it is also forms part of endogenous gene regulation, for example, in certain developmental pathways (Grishok et al., 2001; Meister and Tuschl, 2004). In addition, exploiting the RNAi mechanism for gene silencing also provides a powerful research tool and potential for the development of novel therapeutics (Hannon and Rossi, 2004).

1.4.1 Mechanism and components of the RNAi pathway

RNAi occurs naturally in the cell in response to the presence of dsRNA. Briefly, during RNAi, the enzyme Dicer processes dsRNA and pre-micro(mi)RNA into small interfering (si)RNAs and miRNAs, respectively (Figure 1.7). These then combine with a RNA-induced silencing complex (RISC) resulting in the degradation of the target mRNA or the inhibition of mRNA translation (Hannon, 2002; Agrawal et al., 2003; Watson et al., 2005; Pecot et al., 2011).

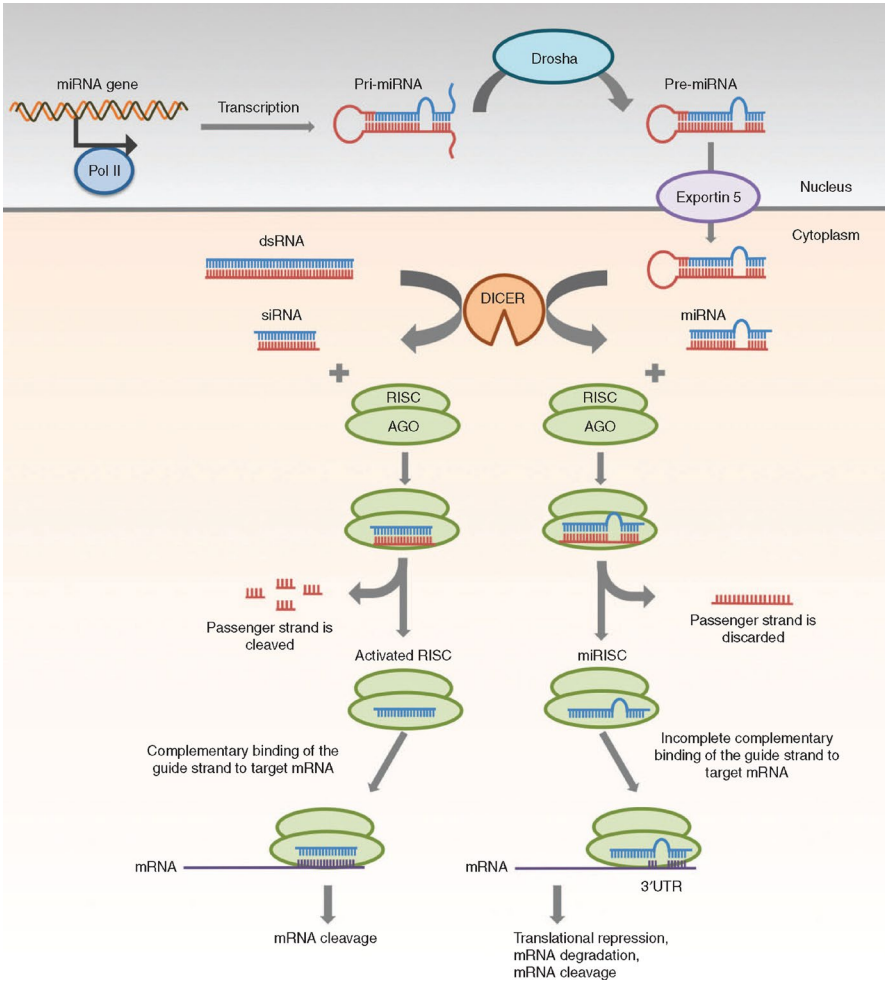

Figure 1.7: RNAi regulation of gene expression.

For double-stranded (ds)RNA is processed by Dicer into short-interfering (si)RNA which is loaded into the RNA-induced silencing complex (RISC). AGO2, which is a component of RISC, cleaves the passenger strand of siRNA. The guide strand then guides the active RISC to the target messenger (m)RNA. The full complementary binding between the guide strand of siRNA and the target mRNA leads to the cleavage of the mRNA. For micro (mi)RNA, transcription of the miRNA gene is carried out by RNA polymerase II in the nucleus to give primary (pri)-miRNA, which is then cleaved by Drosha to form precursor (pre)-miRNA. The pre-miRNA is transported by exportin-5 to the cytoplasm where it is processed by Dicer into miRNA. The miRNA is loaded into the RISC where the passenger strand is discarded, and the RISC is guided by the remaining guide strand to the target mRNA through partially complementary binding. The target mRNA is inhibited via translational repression, degradation or cleavage. The image, from a paper by Lam et al. (2015), is used with kind permission from the American Society of Gene and Cell Therapy (Waukesha, WI, USA).

1.4.1.1 Micro RNAs

In addition to siRNAs that are derived from exogenous (e.g., viral RNA) or endogenous (e.g., aberrant gene transcripts) dsRNA, micro RNAs (miRNAs) are also substrates for the RNAi pathway (Figure 1.7). They are small non-coding RNAs of about 22 nucleotides derived from RNA hairpins known as primary miRNAs (Catto et al., 2011). They act as endogenous mediators of RNAi that target the 3'-untranslated region (UTR) of mRNA to regulate gene expression. Initially, the RNase III, Drosha, cleaves primary miRNAs into precursor (pre)-miRNAs that are shorter transcripts of approximately 70 nucleotides with a two-nucleotide overhang at the 3'-end. Pre-miRNAs are then transported across the nuclear membrane by exportin-5 into the cytosol where they are cleaved by Dicer into mature miRNAs (Lund et al., 2004; López-Fraga et al., 2009). The 5'-end of a miRNA contains the targeting region that binds to the complementary sequence of the 3'-UTR in the target mRNA. The miRNA-mRNA complex then recruits a RISC to degrade the target mRNA or inhibit its translation (Bartel, 2009; Catto et al., 2011).

1.4.1.2 Dicer

Dicer is a member of the ribonuclease (RNase) III family of nucleases that digests dsRNA into small siRNA and pre-miRNA into miRNA (Figure 1.7). The enzyme was detected first in Drosophila extracts where it was shown to digest dsRNA into short fragments of 22 nucleotides with 3' overhangs of two or three nucleotides (Bernstein et al., 2001). It has distinct domains including an amino-terminal DEAD-box helicase domain, a domain of unknown function (DUF283), a Piwi-Argonaute-Zwille (PAZ) domain, two catalytic RNase III domains, and a dsRNA-binding domain (dsRBD) at the carboxy-terminal (Figure 1.8) (Murchison et al., 2005; Svoboda, 2014). The dsRBD recognises duplex RNA structures, and the PAZ domain binds protruding 3'-overhangs in dsRNAs or pre-miRNAs. The DEAD-box helicase domain is thought to catalyse the unwinding of dsRNA (Hilbert et al., 2009), whilst the two RNase III domains each cleave one strand of the RNA duplex. Dicer activity eventually produces short siRNAs or miRNAs, with a two-nucleotide 3'-overhang, which are then loaded onto a RISC for further processing (Figure 1.7).

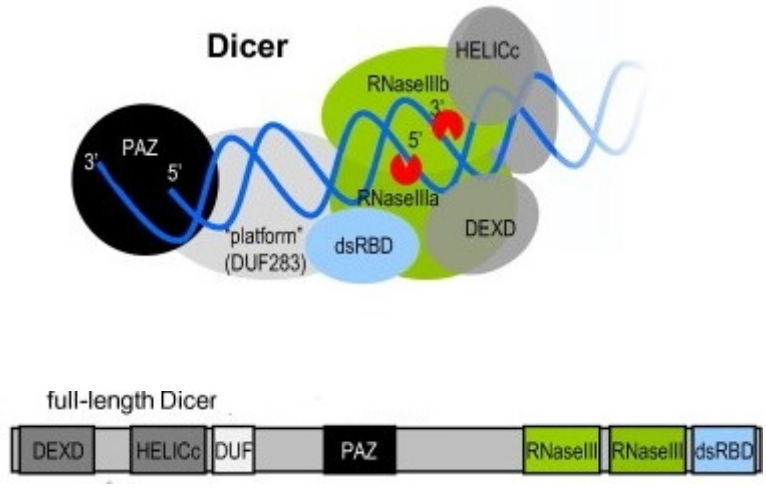

Figure 1.8: The domains of the Dicer enzyme.

Dicer has distinct domains including an amino-terminal DEAD-box helicase domain (DEXD-HELICc), a domain of unknown function (DUF283), a Piwi, Argonaute, and Zwille (PAZ) domain, two catalytic RNase III domains, and a dsRNA-binding domain (dsRBD) at the carboxy-terminal. The image, from a paper by Svoboda (2014), is used with kind permission from the author.

1.4.1.3 RNA-induced silencing complex

RNA-induced silencing complex (RISC) is an RNA-directed sequence specific nuclease responsible for the cleavage or degradation of target mRNA (Figure 1.7). It was defined in an experiment when certain endogenous genes of Drosophila S2 cells were observed to be silenced after transfection with dsRNA. In an attempt to trace the reason for the loss of phenotypic function, cellular extracts were treated with calcium-dependent nucleases that can degrade both DNA and RNA or with DNase I. Loss of phenotypic function was only observed in nuclease-treated samples whilst DNase I had no effect on phenotypic function. This suggested that RNA played a major role in the activity of the nuclease (Hammond et al., 2000). Partial purification of the nuclease from crude extracts revealed that 25-nucleotide RNA species co-fractionated with the nuclease suggesting that they functioned as a sequence recognition guide for the nuclease to target mRNA.

Later characterisation of the nuclease revealed a 500-kDa ribonucleoprotein complex that included a member of the Argonaute family of proteins termed Argonaute 2 (AGO2) (Hammond et al., 2001). Studies of the 130-kDa AGO2 protein have revealed it consists of four domains (Figure 1.9) (Elkayam et al., 2012; Schirle and Macrae, 2012). The amino-terminal domain comprises two motifs, at amino acid residues 44–48 and 134–166, that are needed for full catalytic activity of AGO2. The PAZ domain is required for anchoring the 3′-end of guide RNAs whilst the middle (MID) domain binds the 5′-phosphate of guide RNAs. The P-element-induced wimpy testis (PIWI) domain is critical for the slicing activity of AGO2. Other components of the RISC that have been identified include vasa intronic gene and dFMR proteins, p68 RNA helicase, ribosomal proteins L5 and L11, and 5S ribosomal RNA (Ishizuka et al., 2002).

Once siRNAs are loaded into the RISC, AGO2 cleaves the passenger strand of siRNA (Figure 1.7). The guide strand then guides the active RISC to the target mRNA. The full complementary binding between the guide strand of siRNA and the target mRNA leads to the cleavage of the mRNA. For miRNA, the molecules are loaded into the RISC where the passenger strand is discarded (Figure 1.7). The RISC is guided by the remaining guide strand to the target mRNA through partial complementary binding. The target mRNA is then inhibited via translational repression, degradation or cleavage.

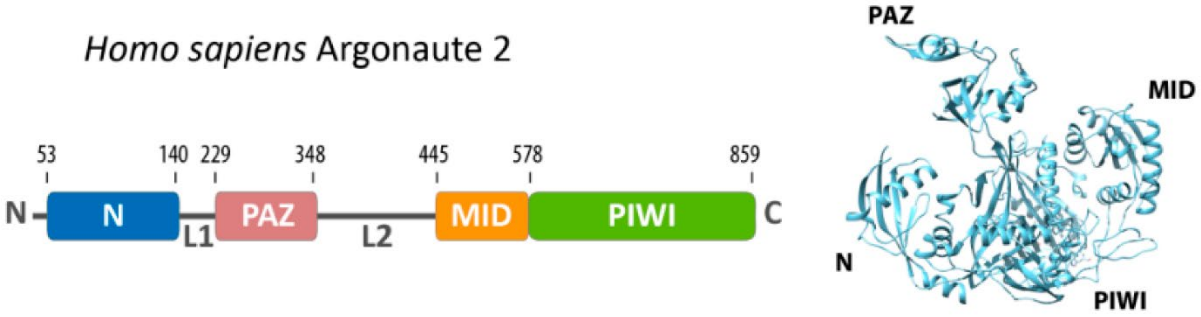

Figure 1.9: The domains of the Argonaute 2 protein.

The amino-terminal domain comprises two motifs, at amino acid residues 44–48 and 134–166, that are needed for catalytic activity of AGO2. The PAZ domain is required for the anchoring of the 3′-end of guide RNAs whilst the middle (MID) domain binds the 5′-phosphate of guide RNAs. The P-element-induced wimpy testis (PIWI) domain is critical for the slicing activity of AGO2. The image, from a paper by Willkomm et al. (2015), is used with kind permission from MDPI (Basel, Switzerland).

1.5 RNAi as a tool for therapeutic gene silencing

Exploiting the gene silencing RNAi mechanism as a research tool or for novel therapeutics using exogenous dsRNA initially proved difficult (Hannon and Rossi, 2004). In mammalian cells, instead of obtaining a gene silencing effect, the introduction of dsRNA induced immune responses and the global shut down of protein expression (Hannon and Rossi, 2004; López-Fraga et al., 2009), a response akin to dsRNA virus infection. A solution to this problem was the discovery that exogenous smaller-sized siRNAs could bypass the activation of the immune response.

1.5.1 Short interfering RNA

Short interfering RNAs are exogenous dsRNA molecules, usually 21-22 nucleotides in length. Their generic structure is shown in Figure 1.10. They are characterised by 5'-phosphate and 3'-hydroxyl termini, a 19-nucleotide base pair central region, and 3'-dinucleotide or 3'-trinucleotide overhangs. The passenger or sense strand of the siRNA matches the mRNA of interest in terms of sequence. The guide or antisense strand is completely complementary to the target mRNA. In addition, siRNA molecules have a seed region that is at the first 2–8 bases of the antisense strand and a cleavage site at bases 8–10 of the antisense strand.

Exogenous siRNAs elicit gene silencing as shown in Figure 1.7. The siRNA interacts with and activates the RISC. The AGO2 endonuclease cleaves the passenger strand of the siRNA while the guide strand continues to be associated with the RISC. The antisense strand then guides the activated RISC to its target mRNA for cleavage by AGO2. As the guide strand only binds to mRNA that is fully complementary to it, siRNA results in specific gene silencing (Hannon, 2002). siRNAs are highly efficient and can cause silencing effects on numerous identical mRNA transcripts because the guide strand-RISC complex remains active after mRNA cleavage (Hutvágner and Zamore, 2002).

(a)

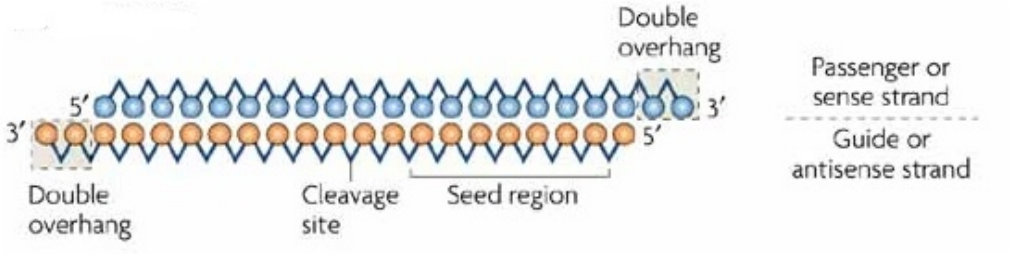

(b)

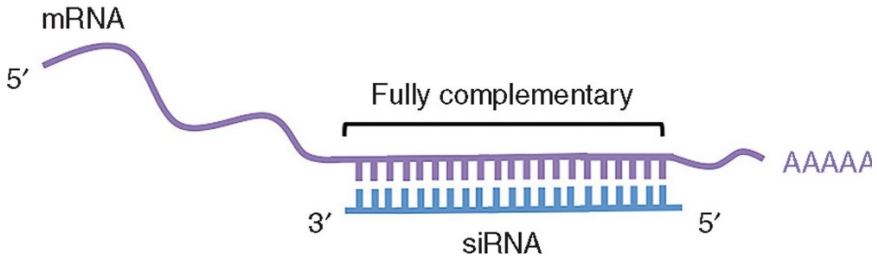

Figure 1.10: A schematic representation of the important features of siRNA structure and of siRNA binding to its target mRNA.

(a) Short interfering RNAs (siRNAs) are double-stranded RNA of 21-22 nucleotides. They are characterised by 5'-phosphate and 3'-hydroxyl termini, a 19-nucleotide base pair central region, and 3'-dinucleotide or 3'-trinucleotide overhangs. The passenger or sense strand of the siRNA matches the mRNA of interest in terms of sequence. The guide or antisense strand is completely complementary to the target mRNA. In addition, siRNA molecules have a seed region that is at the first 2–8 bases of the antisense strand and a cleavage site at bases 8–10 of the antisense strand. The image, from a paper by Fougerolles et al. (2007), is used with kind permission from Springer Nature Limited (Berlin, Germany). **(b)** The guide stand is shown binding to its target mRNA. The image, from a paper by Lam et al. (2015), is used with kind permission from the American Society of Gene and Cell Therapy (Waukesha, WI, USA).

1.5.2 Design of effective siRNAs for *in vivo* use

The appropriate design of siRNAs is crucial to overcome the challenges they present in terms of efficacy, stability, immunogenicity, and undesirable off-target effects when used in vivo (Soutschek et al., 2004; De Paula et al., 2007). Indeed, these issues have been obstacles for the development of siRNAs into commercially available drugs (Richard-Pargmann and Voller, 2008; Olejniczak et al., 2010). Several important factors to be considered in the design of effective therapeutic siRNAs are given in Table 1.2, and these are discussed in the next sections.

1.5.2.1 Sequence and nucleotide considerations

Appropriate sequence and nucleotide selection of the required siRNA are important to provide the best efficacy and avoid unwanted off-target effects. Helpful guidelines for the design of effective gene silencing siRNAs can be found in the computer programs developed by Ambion (www.ambion.com). Obviously, sequences should be chosen to avoid those that have significant homology with other genes. It is also usual to select a sequence 50-100 base pairs downstream of the ATG start codon, while the 5'- or 3'-untranslated regions and the regions near the ATG start codon should be avoided. This is because siRNA or RISC complex-binding may be prevented by untranslated region-binding proteins or translation initiation complexes, respectively (Elbashir et al., 2001; Holen et al., 2002; Schwarz et al., 2002).

Ideally, the GC base pair content of the siRNA sequence should be kept between 30% and 64% (Birmingham et al., 2007), and stretches of nucleotides that are rich in GCs, specifically greater than nine nucleotides, appear to adversely affect gene silencing (Ui-Tei et al., 2008). siRNA molecules should normally be 21-22 nucleotides long, to circumvent immunological effects, and also include a 3'-overhang of two or three U residues (Figure 1.10).

In addition to the above considerations, studies have shown that the thermodynamic stability of the two ends of the siRNA molecule contribute to the selection of the strand that will be loaded into the RISC complex (Figure 1.7) (Khvorova et al., 2003; Schwarz et al., 2003). The strand with the least stable 5'-end is the one that is selected so this parameter should always be considered and applied to the guide strand of the siRNA. Furthermore, the 5′-nucleotide is also significant for proper loading of the siRNA by

Table 1.2: Design of effective siRNAs

siRNA parameter	Strategy	Reference
Sequence/strand selection for better activity	Guide strand selected with a relatively unstable 5'-end. Guide strand selected with a U or A at position one at the 5'-end.	Petri and Meister, 2013; Lam et al., 2015
Nucleotide content for better activity	Content of G and C ideally between 30–64%. Avoid G/C stretches of more than nine nucleotides.	Birmingham et al., 2007
Avoidance of off-target effects	Use lowest siRNA concentration possible. Use pool of different siRNAs to the same mRNA. Avoid miRNA seed sequences.	Grimm et al., 2006; Jackson et al., 2006; Kozomara and Griffiths-Jones, 2011
Avoidance of immune responses	Avoid sequences rich in uracil (U). Avoid sequences that contain: 5'-GUCCUUCAA-3'; 5'-UGUGU-3'; 5'-UGU-3'; 5'-UGGC-3'.	Judge et al., 2005; Fedorov et al., 2006; Goodchild et al., 2009

AGO2 into the RISC complex (Figure 1.7). The strand with a U or an A residue at position one at the 5′-end of the siRNA is preferred by AGO proteins. Consequently, it is preferable to incorporate a U or an A at the 5′-end of the guide strand. The passenger strand should always include a G and a C residue at the 5′-end to avoid it being selected inadvertently by the RNAi machinery (Petri and Meister, 2013; Lam et al., 2015).

1.5.2.2 Reducing off-target effects

Even though designed to target a specific mRNA, siRNAs can produce off-target effects by binding to unrelated mRNAs and leading to the downregulation of their expression. It is therefore necessary, in the design of siRNAs, to eliminate any off-target effects as the consequences of inappropriate targeting can include cell death (Fedorov et al., 2006). A micro (mi)RNA-like action is the commonest type of off-target effect by siRNA (Saxenaa et al., 2003; Scacheri et al., 2004; Jackson et al., 2006; Jackson and Linsley, 2010). This occurs when the 5'-end of the siRNA antisense strand complements the 3'-untranslated sequence of mRNAs, which is akin to the targeting action of miRNAs (Doench et al., 2003). As a consequence, the siRNA behaves like a miRNA and leads to the inactivation of several different mRNA molecules that encode different proteins (Snove and Holen, 2004; Lin et al., 2005). A second form of off-target effect happens when the cell's RNAi machinery becomes overloaded (Jackson and Linsley, 2010). On introduction into cells, siRNAs are in competition with endogenous miRNAs for components of the RNAi pathway. Consequently, normal gene expression that requires the action of miRNAs can be affected adversely resulting in off-target effects (Grimm et al., 2006).

One strategy to reduce off-target effects has been to employ the lowest siRNA concentrations possible that are still effective in gene silencing but are less likely to saturate the RNAi machinery or act like miRNAs (Grimm et al., 2006; Jackson et al., 2006). In addition, the pooling of several siRNAs that target the same mRNA can be used to accomplish effective gene silencing with each siRNA in the pool at a lower concentration than if used alone (Jackson and Linsley, 2010). In order to avoid off-target effects due to miRNA-like action, it is wise to design the required siRNA with as little complementarity as possible between the siRNA 5'-end seed region and the 3'-untranslated region of the mRNA (Kozomara and Griffiths-Jones, 2011). Furthermore,

it is also helpful in reducing this type of off-target effect if any duplex that does form between the siRNA seed region and the 3'-end of the mRNA has low thermodynamic stability (Ui-Tei et al., 2008; Naito and Ui-Tei, 2013).

An additional method to eliminate off-target effects is by chemically modifying the siRNA molecule. This is discussed in Section 1.5.2.4.

1.5.2.3 Avoiding immune response effects

The development of siRNAs was undertaken to avoid the triggering of the immune response, via activation of the interferon (IFN) pathway (Figure 1.11), that was observed when cells were transfected with dsRNAs of over 30 nucleotides (Gantier and Williams, 2007). Despite this advance, siRNAs have been shown to activate the innate immune response (Judge et al., 2005; Robbins et al., 2009), which is a major drawback for their therapeutic use.

Short-interfering RNAs may stimulate IFN-α and IFN-β synthesis independent of their sequences via the signaling pathways of dsRNA-dependent protein kinase R (PKR), retinoic acid-inducible gene 1 protein (RIG-1), and melanoma differentiation-associated protein 5 (MDA5) that are present in the cytoplasm of certain cell types (Figure 1.11) (Kleinman et al., 2008). In addition, sequence-independent activation of the toll-like receptor (TLR)-3, which is expressed in the endosomes and on the cell surface of certain cell populations, can also result in a type 1 IFN production (Figure 1.11) (Kleinman et al., 2008).

Furthermore, siRNAs can activate the immune response in a sequence-dependent manner via the TLR-7 and TLR-8 receptors present in the endosomes, respectively, of dendritic cells and monocytes (Figure 1.11) (Heil et al., 2004). Induction of IFN-α and IFN-β occurs through the actions of myeloid differentiation primary response 88 (MyD88). Activation of MyD88 can also induce expression of nuclear factor kappa light chain enhancer of activated B cells (NFκB), which activates the expression of pro-inflammatory cytokines such as tumour necrosis factor-α (TNF-α), interleukin (IL)-1 and IL-6 (Figure 1.11) (McMillan and Khairuddin (2012).

Sequences that have been reported to cause immune activation include 5'-GUCCUUCAA-3', 5'-UGUGU-3, 5'-UGU-3', and 5'-UGGC-3' (Table 1.2) (Judge et al.,

2005; Fedorov et al., 2006). Moreover, the activation of both TLR-7 and TLR-8 is correlated with sequences that are rich in uracil (Goodchild et al., 2009). It may well not be possible to design the required siRNAs without the presence of U molecules so as to reduce the immune response. In such cases, immune activation via TLR-7 and TLR-8 could be avoided by using delivery vehicles that do not rely upon endosomal delivery of the siRNA or by chemically modifying the stimulatory nucleotides of the siRNA (Bramsen et al., 2013). Overall, it is necessary to test siRNAs for any immune responses that they might induce.

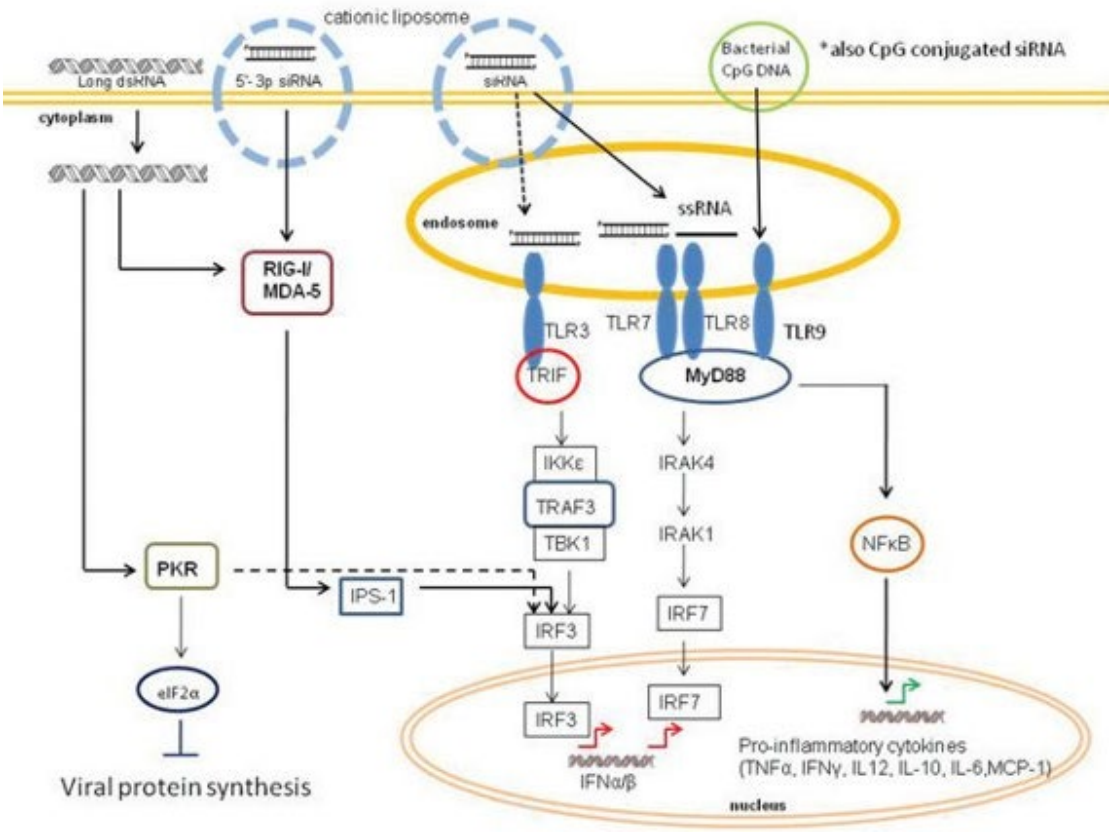

Figure 1.11: Induction of the immune response by siRNA.

siRNAs can trigger innate immunity through transcription of type I interferons (IFN) via the cytoplasmic double-stranded RNA-dependent protein kinase (PKR) and retinoic acid–inducible gene 1 protein (RIG-1) pathways. Activation of cell-surface or endosomal toll-like receptor (TLR)-3 can also result in type 1 interferon production. Induction of IFN-α and IFN-β can also occur through the actions of myeloid differentiation primary response 88 (MyD88) when activated by recognition of siRNAs by TLR-7 or TLR-8. Activation of MyD88 also induces nuclear factor kappa light chain enhancer of activated B cells (NFκB) which activates the expression of pro-inflammatory cytokines. eIF2-α, eukaryotic translation initiation factor 2-α; IKK, IκB kinase complex; IPS-1, IFN-β promoter stimulator 1; IRF, interferon regulatory factor; MDA5, melanoma differentiation-associated protein 5; TBK1, TANK-binding kinase 1; TRAF3, TNF receptor-associated factor; TRIF (TICAM-1), toll-IL-1 receptor-containing adaptor molecule-1. The image, from a paper by McMillan and Khairuddin (2012), is used with kind permission from Elsevier Limited (Cambridge, UK).

1.5.2.4 Chemical modifications

Chemical modifications of siRNA molecules have been developed to address their vulnerability to nucleases in the serum that result in poor stability and therefore short half-lives (Layzer et al., 2004). Such modifications can also help to reduce off-target and immune effects (Watts et al., 2008). Certain siRNA sites are important in interaction with the RISC and AGO proteins, so are less available for chemical modification. These include the central positions, the 5′-phosphate, and the 5′-proximal part of the guide strand (Wang et al., 2008; Lima et al., 2009). More useful sites for chemical modification are the 3′-overhang and 3′-proximal part of the guide strand, as well as the passenger strand (Bramsen et al., 2009). The main types of modifications that have been used with siRNA are detailed below.

Backbone modifications of the phosphorothioate (PS) type have been used frequently to increase the resistance of nucleic acids to nuclease degradation (Figure 1.12a). (Campbell et al., 1990). The modification also enhances the binding of plasma proteins, which reduces clearance of nucleic acids by kidney filtration and excretion in the urine (Eckstein, 2014). This modification has been shown to increase the *in vivo* stability of siRNA, but also led to higher toxic effects and less activity in terms of silencing gene expression (Braasch et al., 2004; Choung et al., 2006). These downsides have been overcome by controlling the stereochemistry of the PS-modification (Jahns et al., 2015). Boranophosphate modifications of siRNA (Figure 1.12a) have also been reported as having a lesser toxic effect than PS-modifications (Hall et al., 2004).

Modifications of the ribose 2-OH group are frequently used. These include 2′-O-methyl (2′-O-Me), 2′-fluoro (2′-F) and 2′-methoxyethyl (2′-O-MOE) substitutions (Figure 1.12b), which are effective in enhancing siRNA stability. A combination of 2′-F and 2′-O-Me substitutions has been reported to be the best way to retain silencing potency and reduce nuclease degradation compared with using just one modification type (Allerson et al., 2005; Jackson et al., 2006). However, substitutions with 2′-O-MOE groups have been seen to be less well-tolerated with regard to the activity of the siRNA (Prakash et al. 2005; Bramsen et al., 2009). A further advantage of modifications of the ribose 2-OH group is reduced immunogenicity of the siRNA (Judge et al., 2006). Indeed, 2′-O-Me or 2′-F modifications can prevent an immune response while the

activity of the siRNA remains (Cekaite et al., 2007). Alternating 2′-O-Me substitutions of the passenger strand has been reported to have a similar effect (Hamm et al., 2010).

Locked nucleic acid (LNA) contains a methylene bridge between the 2′-O and the 4′-C of the sugar (Figure 1.12c). This makes a “locked” ring conformation that is stable and which increases siRNA resistance to nuclease attack (Veedu and Wengel, 2010). LNA-modifications can lead to a reduction in the efficacy of siRNA (Grunweller et al., 2003; Elmén et al., 2005), but have shown to reduce immunogenicity (Hornung et al., 2005) and off-target effects (Elmén et al., 2005). Unlocked nucleic acids (UNA) are acyclic derivatives of RNA that lack the C2′ and C3′-bond of the RNA ribose ring (Figure 1.12c). A single UNA-modification in the passenger or guide strand enables effective gene silencing along with better stability of the siRNA (Laursen et al., 2010). In addition, UNA-modifications in the guide-strand seed-region can prevent miRNA-like off-target effects (Vaish et al., 2011).

Although, overall, chemical modifications of siRNA can improve their stability and reduce adverse immune and off-target effects, inadequate delivery is still a major issue for the clinical use of siRNAs. The different methods that have been developed to improve siRNA delivery are discussed in the next section.

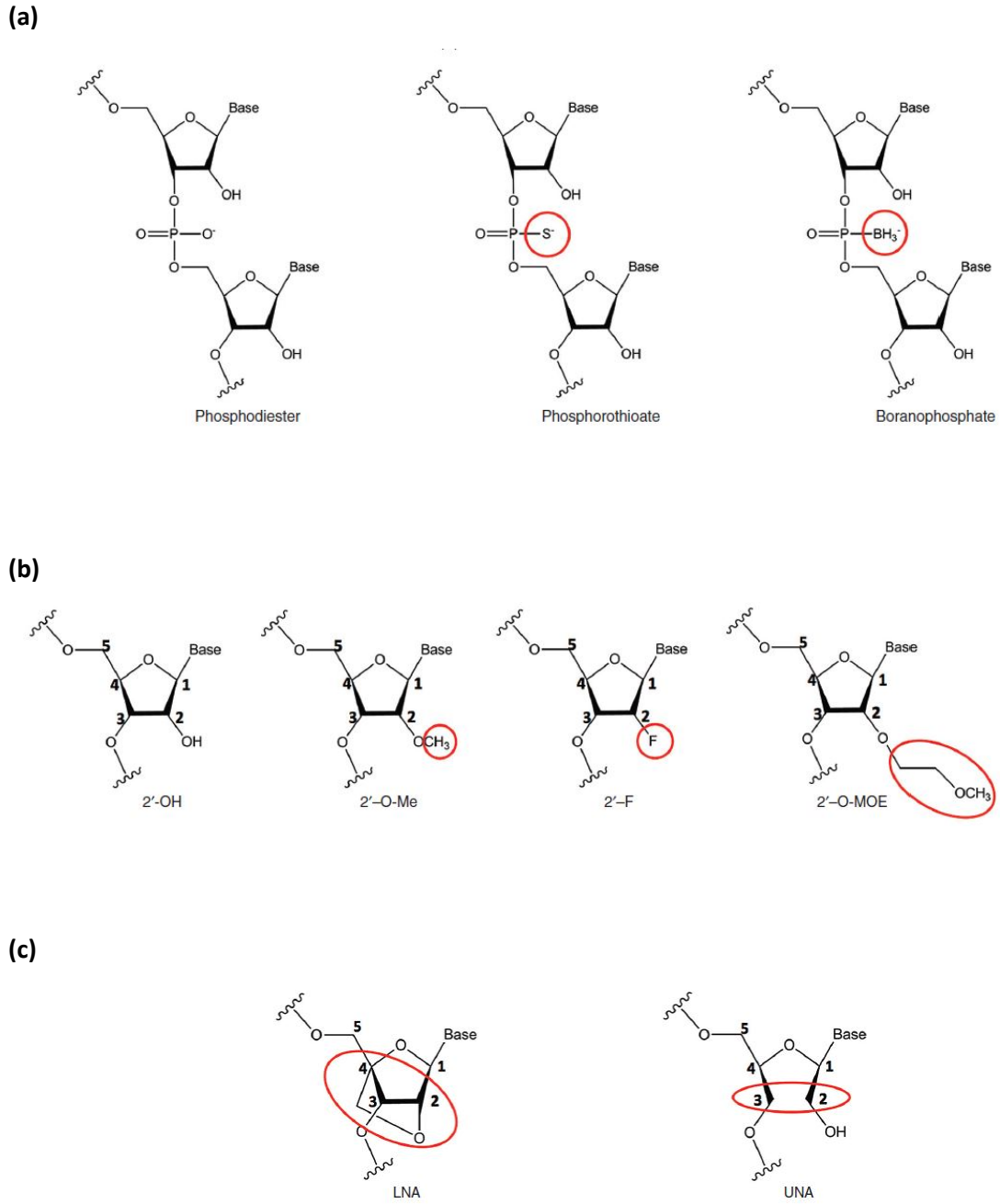

Figure 1.12: Chemical modifications of siRNA.

The chemical modifications shown are (a) Backbone modification where the phosphodiester backbone linkage is substituted**;** (b) Ribose 2'-OH group modifications including 2'-O-methyl (2'-O-Me), 2'-fluoro (2'-F), and 2'-methoxyethyl (2'-O-MOE); and (c) Locked nucleic acid (LNA) and unlocked nucleic acid (UNA) modifications. The images, from a paper by Lam et al. (2015), are used with kind permission from the American Society of Gene and Cell Therapy (Waukesha, WI, USA).

1.5.3 Delivery and delivery systems for siRNA

Naked siRNA is prone to quick degradation by serum nucleases and its uptake by cells is not efficient due to the impermeability of the lipid bilayer cell membrane and the hydrophilic nature and negative charge of siRNA molecules. Naked siRNAs are also rapidly removed by glomerular filtration resulting in short *in vivo* half-lives of below ten minutes (Layzer et al., 2004; Bumcrot et al., 2006; Wang et al., 2010). These issues have led to the development of various delivery systems for siRNA *in vivo* administration (Aigner, 2006), taking into account the important requirements of any such delivery vehicle.

The optimal siRNA delivery system needs to be biocompatible, biodegradable, and non-immunogenic (Lam et al., 2015). It should provide efficient delivery of siRNA into cells or tissues, protect the siRNA from degradation, and avoid being rapidly lost through clearance by the liver or kidneys (Lam et al., 2015). If delivering the siRNA into target cells via endocytosis, the delivery method needs to ensure that the siRNA is released from the endosome to allow the siRNA to interact with RISC to promote gene silencing (Lam et al., 2015). This process can depend on the charge and size of the siRNA and its delivery vehicle (Ozcan et al., 2015; Tai and Gao, 2017). An efficient delivery system can also mean that there is less need for chemical modifications that have the potential to adversely affect the specificity and the gene silencing effect of the siRNA. Two main types of delivery system have been investigated, namely, viral and non-viral and these are discussed in Sections 1.5.3.1 to 1.5.3.4.

In addition to the delivery system itself, efficient siRNA delivery is dependent on the route of administration with local application more effective when compared with systemic application (Wang et al., 2010; Chakraborty et al., 2017). Interestingly, intranasal application of siRNA for respiratory syncytial virus found that naked siRNA and delivery via cationic liposomes were equally effective (Bitko et al., 2005).

1.5.3.1 Viral delivery systems

Viral vectors are very efficient at delivering nucleic acids in to cells. They can be genetically engineered to stop their virulence and their specificity can be manipulated by altering the viral capsid so that specific cell types can be targeted (Lam et al., 2015). Indeed, attenuated adenoviruses and lentiviruses have shown to deliver efficient

knockdown of genes after just a single administration (Bumcrot et al., 2006). Despite the high levels of delivery, there have been concerns about safety that have limited the application of viral vectors. These include the induction of immune responses and the risk of mutagenesis (Lam et al., 2015). Their clinical applications have also been limited by low packaging capacity of the virus and by the high costs involved in production (Lam et al., 2015). To overcome these obstacles, there has been a move towards developing non-viral vectors to deliver siRNA (Deng et al., 2014; Şalva et al., 2016).

1.5.3.2 Lipid-based delivery systems

The most attractive lipid-based vehicles for siRNA delivery have been cationic liposomes because of the simple way in which they form complexes with the negatively charged siRNA by electrostatic interaction (Figure 1.13). The positively charged surface of the liposome then interacts and fuses with negatively charged cell membranes. The transfection complex enters the cell through endocytosis forming a membrane surrounded-intracellular vesicle. Inside the cell, the complex escapes the endosomal pathway and the siRNA is released into the cell cytoplasm. Liposomes allow a high transfection efficiency, enhance pharmacokinetic properties by protecting siRNA from enzymatic degradation, reduce siRNA renal clearance, and have relatively low immunogenic and toxic effects (Oh and Park, 2009). Commercially available cationic liposome reagents that have been used for *in vivo* siRNA delivery include Lipofectamine and Oligofectamine (Giladi et al., 2003; Sun et al., 2014). Interestingly, Lipofectamine has been shown to avoid being entrapped in endosomes, therefore, preventing degradation of the enclosed siRNA (Cardarelli et al., 2016).

It is thought that cationic liposomes can interact with negatively charged serum components, a property that can adversely affect the delivery properties of liposomes (Santel et al., 2006). To overcome this problem, many liposomal reagents have been coated with polyethylene glycol (PEG) to form stable nucleic acid lipid particles (SNALPs) (Figure 1.13). These structures can avoid carrier clearance by serum proteins or the complement system, improve circulation time, and reduce macrophage clearance (Santel et al., 2006). They also incorporate fusogenic lipid bilayers in addition to cationic bilayers and this enhances their cellular uptake and the endosomal release of siRNA (Morrissey et al., 2005; Santel et al., 2006).

The non-specific nature of liposomes and SNALPs can lead to aggregate formation. The aggregates can become trapped in the bed of capillaries or be taken up by the liver and spleen. As a result, most of the siRNA accumulates in these organs rather than being delivered to the target cells (Lee et al., 2016; Şalva et al., 2016). To overcome these disadvantages, more complex lipid-based nanoparticles that carry monoclonal antibodies to target specific cells have also been developed (Figure 1.13) (Li and Huang, 2006; Li et al., 2008; Peer et al., 2008).

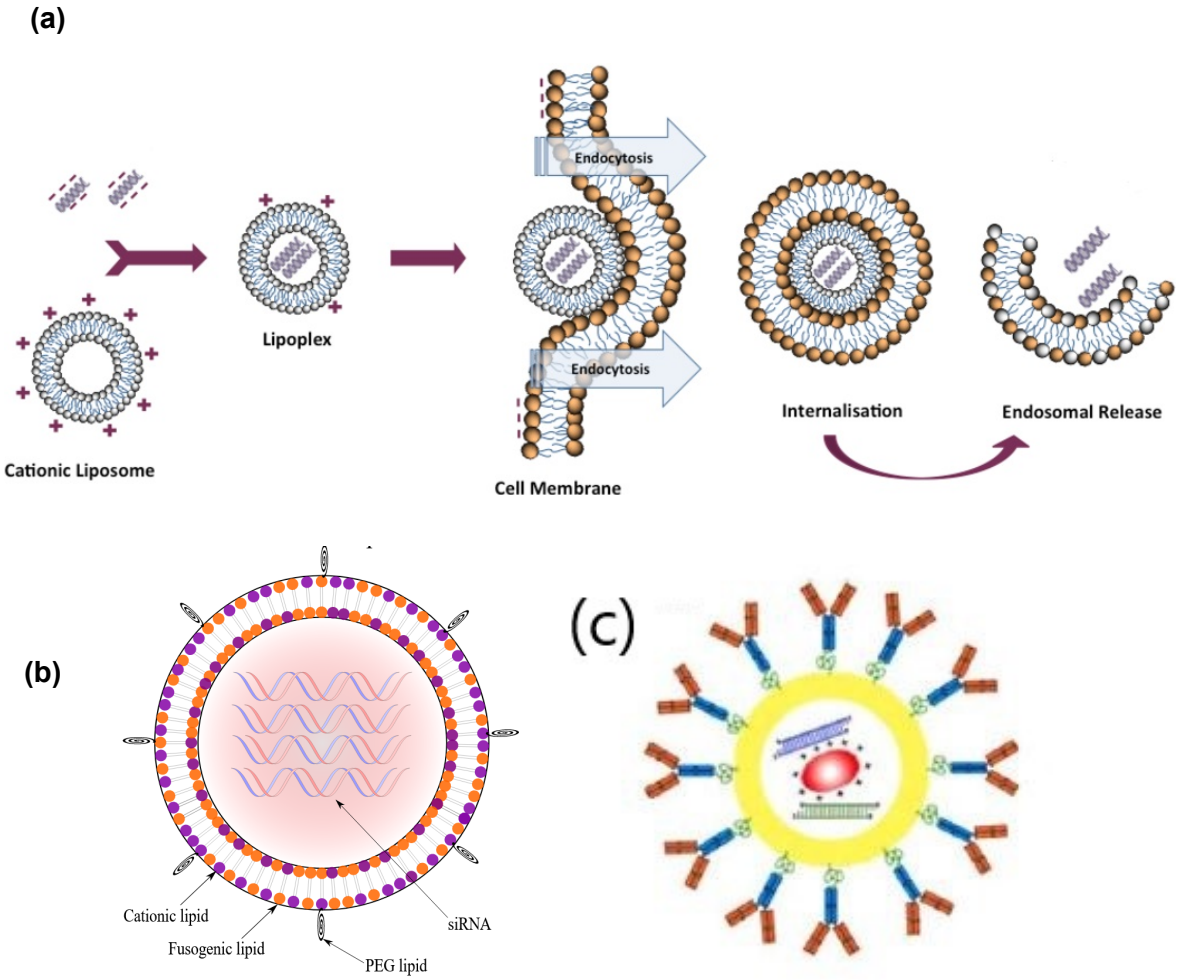

Figure 1.13: The principle of liposome-mediated siRNA delivery.

(a) Cationic lipids consist of a positively charged head group and one or two hydrocarbon chains that are able to form lipid bilayer structures called liposomes. Liposomes can be used to entrap siRNA due its interaction with the positively charged lipid head groups. The positively charged surfaces of liposomes interact with negatively charged cell membranes and fuse with the cell membranes. The transfection complex enters the cell through endocytosis forming a membrane surrounded-intracellular vesicle. Inside the cell, the complex escapes the endosomal pathway and the siRNA is released into the cell cytoplasm. The image, from a thesis by Moghaddam (2013), is used with kind permission from Aston University (Birmingham, UK). (b) A stable nucleic acid lipid particle that incorporates fusogenic lipid bilayers in addition to cationic bilayers as well as being coated with polyethylene glycol (PEG) The image is used with kind permission from commons.wikimedia.org. (c) A lipid-based nanoparticle with an attached monoclonal antibody against the required cellular target. The image, from a paper by Oh and Park (2009), is used with kind permission from Elsevier Limited (Cambridge, UK).

1.5.3.3 Polymer-based delivery systems

Cationic polymer delivery systems are advantageous because of the simplicity involved in their production, which involves mixing the positively-charged polymer with negatively-charged siRNA (Gary et al., 2007; Oh and Park, 2009). Cationic polymers are classed as either naturally occurring or synthetic. Natural polymers are non-toxic, biocompatible, and biodegradable. The most commonly used is chitosan (Oh and Park, 2009). Chitosans describe a family of polymers with differing molecular weights and degrees of deacetylation that have been used to enable nasal absorption of siRNA-carrying nanoparticles (Howard et al., 2006). Synthetic polymers require careful design to prevent cytotoxicity and immunogenicity. Polyethylenimine is extensively used and consists of numerous protonable amino groups that contribute to their high cationic charge density at physiological pH. It has a high transfection capacity compared with other polymers (Boussif et al., 1996). However, they are cytotoxic at higher molecular weights and higher branching (Fischer et al., 2002; Thomas and Klibanov, 2002), so, their working concentrations for in vivo delivery must be carefully monitored (Boeckle et al., 2004, Oh and Park, 2009).

1.5.3.4 siRNA-conjugates as delivery systems

Enhanced delivery of siRNA can be achieved by conjugation of siRNA with various different moieties (Figure 1.14). Lipophilic molecules such as cholesterol have been shown to prolong the half-life of siRNAs when conjugated, although high doses were required for gene silencing (Soutschek et al., 2004; Wolfrum et al., 2007). Cell-penetrating peptides (CPP) such as transportan and penetratin have also been investigated as delivery agents for siRNA. However, although efficient knock down of gene expression was achieved, there remains concern about the cytotoxicity and immunogenicity of such siRNA-CPP conjugates (Moschos et al., 2007). More recently, the amino sugar N-acetyl-D-galactosamine (GalNAc) has been used as a delivery mechanism for siRNA. The molecule binds to the Asialoglycoprotein receptor that is predominantly expressed on liver hepatocytes and so serves as a simple siRNA delivery solution for this cell type (Springer and Dowdy, 2018).

Targeted delivery of siRNA can also be achieved by conjugation with a ligand peptide that recognises a specific cell receptor (Cesarone et al., 2007). In addition, siRNA

molecules can be conjugated directly to monoclonal antibodies that bind to specific receptors on target cells. The complex is then endocytosed via the receptor into the cell to deliver the siRNA (Daka and Peer, 2012; Tam et al., 2017). More recently, siRNA-aptamers have been used as a novel approach for targeted delivery of siRNAs via membrane receptors (McNamara et al., 2006, Li et al., 2014). Aptamer conjugates have the advantage of low immunogenicity. However, the intracellular processing of the potency of aptamers might be different from unmodified siRNA so they need careful design (Oh and Park, 2009).

Having described the potential challenges and solutions for the use of siRNAs as therapeutics, the use of siRNA as drugs to treat human disease are discussed in the next section.

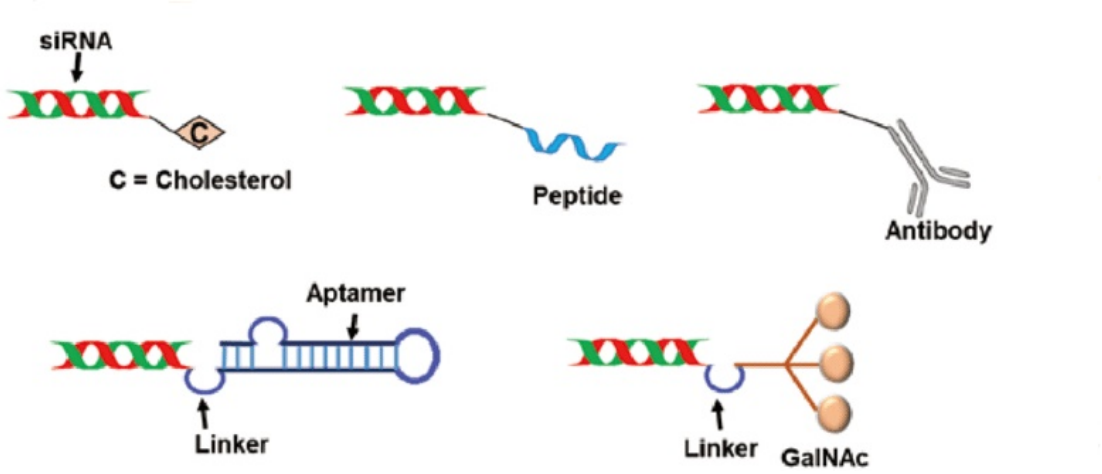

Figure 1.14: siRNA-conjugates as delivery systems.

siRNA conjugates to cholesterol, peptides, antibodies, aptamers and N-acetyl-D-galactosamine (GalNAc) are shown. The image, from a paper by Chandela and Ueno, (2019), is used with kind permission from Elsevier Limited (Cambridge, UK).

1.5.4 Therapeutic uses of siRNA in human disease

Since many diseases result from the expression of undesired or mutated genes, as well as the overexpression of normal genes, the discovery of siRNA opened up a new therapeutic approach for the treatment of diseases by targeting genes that are typically involved in the pathological process (Lam et. al., 2015). A summary of siRNA therapeutics in clinical trials (Table 1.3) (Lam et. al., 2015).

In 2004, Bevasiranib became the first siRNA-based drug to enter clinical trials in patients with age-related macular degeneration (Garba and Mousa, 2010). To date, there are several ongoing clinical trials of potential siRNA candidates in the treatment of a variety of diseases. Other clinical trials of siRNA for age-related macular degeneration, which target the vascular endothelial growth factor (VEGF) signaling pathway and RTP801 gene, have also begun (Nguyen et al., 2012). A phase 1 human safety study was conducted to evaluate an siRNA-based product called NUC B1000 in reducing the malignant effects of chronic HBV infection (Dyawanapelly et al., 2014). The ALNRSV01 by Alnylam Pharmaceuticals, which targets respiratory syncytial virus, is the first siRNA against respiratory viral infection. A second phase II trial of this intranasal drug has commenced in infected adult patients (DeVincenzo et al., 2008).

siRNA-based drugs designed to inhibit the VEGF gene, which is overexpressed by cancer cells, have resulted in anti-cancerous activity with sufficient tolerance to the drug (Fitzgerald et al., 2017). PCSK9-silencing using siRNA resulted in a significant reduction of the level of blood low-density lipoprotein cholesterol in healthy patients (Fitzgerald et al., 2014). Other siRNA-based drugs are undergoing clinical trials in acute kidney injury and neovascularisation (Chandela and Ueno, 2019). QPI-1002 is an siRNA drug tested to alleviate acute renal failure and kidney injury post-cardiac surgery (Demirjian et al., 2017). A milestone was achieved in 2018 with the approval of the first siRNA drug ONPATTRO for the treatment of the polyneuropathy of hereditary transthyretin-mediated amyloidosis in adults (Adams et al., 2018).

Table 1.3: siRNA therapeutics in clinical trials

Name	Indications	siRNA target
Cancer		
ALN-VSP02	Advanced solid tumors with liver involvement	KSP and VEGF
CALAA-01	Solid tumor	RRM2
siRNA-EphA2-DOPC	Advanced cancers	EphA2
Infectious diseases		
ALN-RSV01	RSV infection	RSV nucleocapsid
ARC-520	Chronic HBV infection	Conserved regions of HBV
TKM-100201	Ebola virus infection	Ebola L
Ocular conditions		
AGN211745 (Sirna-027)	CNV, AMD	VEGF receptor 1
PF-04523655 (PF-655)	AMD	RTP801
SYL1001	Ocular pain; dry eye syndrome	Capsaicin receptor TRPV1
Cardiovascular and metabolic diseases		
ALN-PCS02, ALN-PCSsc	Hypercholesterolemia	PCSK9
PRO-040201 (TKM-ApoB)	Hypercholesterolemia	ApoB
Genetic Disorders		
ALN-AT3sc	Hemophilia A and B	AT
Patisiran (ALN-TTR02)	TTR-mediated amyloidosis (FAP)	TTR
TD101	Pachyonychia Congenita	Keratin 6a (N171k mutant)
Other diseases		
ND-L02-s0201	Hepatic fibrosis	HSP47
QPI-1002 (I5NP)	Acute renal failure; injury of kidney	p53

AMD, age-related macular degeneration; ApoB, apolipoprotein B; AT, antithrombin; CNV, chloroidal neovascularization; EphA2, ephrin type-A receptor 2; FAP, familial amyloidotic polyneuropathy; HBV, hepatitis B virus; HSP47, heat-shock protein 47; KSP, kinesin spindle protein; PCSK9, proprotein convertase subtilisin/kexin type 9; RRM2, ribonucleotide reductase subunit M2; RSV, respiratory syncytial virus; TRPV1, transient receptor potential cation channel subfamily V member 1; TTR, transthyretin; VEGF, vascular endothelial growth factor.

1.6 The current project

1.6.1 Justification

The high levels of ACTH that are seen in Cushing's disease result from the up-regulation of *POMC* expression in corticotroph adenomas. Excessive ACTH drives the synthesis of steroid hormones in the adrenal glands resulting in raised levels of blood cortisol with consequent morbidities. Overall, transphenoidal surgery remains the most effective therapy for Cushing's disease, but it is far from ideal as the disease can reoccur. Medical therapies are also often associated with unpleasant side effects and can leave the patient deficient in other pituitary hormones. So, there is a need for a suitable medical therapeutic that can reduce the excessive amounts of ACTH produced in Cushing's disease. Indeed, the 2008 international consensus statement on the treatment of ACTH-dependent Cushing's syndrome, stated that there was "Real need for therapy directed at ACTH" (Biller et al., 2008).

Overall, an ideal therapy for Cushing's disease would be specific and effective by selectively reducing circulating ACTH, having a rapid effect, minimising damage to other pituitary functions, and resolving clinical features. These required effects have led to the investigation of gene-silencing as a possible therapeutic for Cushing's disease.

1.6.2 Gene-silencing as a treatment for Cushing's disease

There have been reports of the employment of antisense oligonucleotides that prevent POMC expression by interacting with POMC mRNA causing the reduction of ACTH production. For example, AtT20 cells, a cell line derived from a mouse ACTH-secreting adenoma (Furth et al, 1953; Schiller, 2000) that constitutively expresses POMC and secretes ACTH, were transfected with anti-POMC oligonucleotides that effectively suppressed the expression of β-endorphin and ACTH (Spampinato et al., 1994). A similar effect was also observed in rats treated with the same oligonucleotides (Spampinato et al., 1994). In addition, human ACTH-secreting adenoma cells were transfected with antisense POMC oligomers that reduced POMC mRNA and ACTH levels by 62%-76% and 48%-58%, respectively (Woloschak et al., 1994). However, these initial studies with antisense oligonucleotides have not progressed further as a potential the treatment for Cushing's disease.

More recently, siRNA molecules were designed against the exonic regions of POMC and were shown to decrease the amount of ACTH secreted from transfected AtT20 cells (Munir, 2012). The details of this previous work with anti-POMC siRNAs are summarised in Chapter 3 (Section 3.1).

1.6.3 Targeted delivery of POMC siRNAs

As discussed previously (Section 1.5.2), the use of any siRNA as a therapeutic is faced with a number of challenges, one being the delivery of the siRNA molecule to the required tissue (Section 1.5.3). Cell membrane receptors that have restricted tissue expression may be effective for delivering siRNAs that have been coupled to either the receptor's peptide ligand or to an antibody against the specific receptor.

For the treatment of Cushing's disease with anti-POMC siRNAs, the CRHR1 is a potential target for their delivery. The receptor is specifically expressed on anterior pituitary corticotroph cells. It is also endocytosed when the extracellular domain interacts and binds to its peptide ligand CRH (dos Santos Claro et al., 2019), indicating that it may internalise any siRNA conjugated to the hormone.

1.6.4 Overall aims of the project

The overall aims of the current project were:

- To further investigate siRNA gene-silencing as a therapy for Cushing's disease.
- To investigate CRHR1 as a possible target for the delivery of siRNA molecules that might be conjugated to CRH or anti-CRHR1 antibodies.

Chapter 2

Materials and Methods

2 Materials and Methods

Unless otherwise stated, all described materials and methods were provided by Dr Helen Kemp (Department of Oncology and Metabolism, University of Sheffield, Sheffield, UK).

2.1 Reagents and plasticware

Most reagents such as buffers, chemicals, solvents, and acids were from Fisher Scientific UK Ltd. (Loughborough, UK), Sigma-Aldrich (Poole, UK) or Melford Laboratories (Ipswich, UK). The reagents were of molecular biology or analytical grade. The suppliers of more specialised reagents are given in the methods text.

Plasticware was obtained from one of the following suppliers: Corning Incorporated (Corning, NY, USA), Starlab (UK) Ltd. (Milton Keynes, UK), Sarstedt Ltd. (Numbrecht, Germany), Nalgene Nunc International (Rochester, NY, USA) or Bibby Sterilin Ltd. (Bargoed, UK). This included: 0.5-ml and 1.5-ml tubes, 6-well plates, 96-well plates, 25-ml universal tubes, pipettes, pipette tips, cell culture flasks, and 50-ml centrifuge tubes.

2.2 Mammalian cell culture methods

2.2.1 Cell lines

The murine corticortroph tumour cell line AtT20/D16vF2 (AtT20) was purchased from the European Collection of Cell Cultures (ECACC) (Salisbury, UK). Originally, the AtT20 cell line was derived from a mouse ACTH-secreting adenoma (Furth et al., 1953). AtT20 cells constitutively express POMC and secrete ACTH making them an ideal model system for analysing altered POMC expression by measuring the downstream effects on ACTH production (Schiller, 2000). The AtT-20/D16v-F2 cell line is an adherent clonal strain derived from the parental AtT-20 line.

Chinese hamster ovary (CHO) Flp-IN cells were obtained from ECACC. They were used for the quick generation of stable cell lines that express the protein of interest from a Flp-IN expression vector.

2.2.2 Cell culture

AtT20 cells were grown in Dulbecco's Modified Eagle Medium (DMEM) high glucose GlutaMAX medium containing 10% fetal calf serum, 100 units/ml penicillin and 100 µg/ml streptomycin (All from Life Technologies, Paisley, UK). CHO Flp-IN and CHO Flp-IN-CRHR1 cells were cultured in Ham's F-12 Nutrient Mixture, 10% fetal calf serum, 100 units/ml of penicillin, 100 µg /ml streptomycin and 2 mM L-glutamine (All from Life Technologies). All cells were cultured in a humidified incubator at 37°C with 5% carbon dioxide.

To culture cells, a 1-ml vial of frozen cells was thawed rapidly from liquid nitrogen in a 37°C water bath. The 1-ml aliquot of cells was added to 10 ml of culture medium and the cells centrifuged for 5 min at 1000 revolutions per minute (rpm) in a Sorvall RT 6000D centrifuge (ThermoFisher Scientific Inc., Waltham, MA, USA). The cell pellet was resuspended in 3 ml of culture medium, and the cells transferred to a T75 flask containing 10 ml of culture medium. The flask was placed in a humidified incubator. Optimal cell culture involved changing the culture medium every two days. Cells were observed routinely under a microscope to assess their growth, and were passaged when at 90% confluence.

For passaging, T75 flasks of cells were taken from the incubator, and the culture medium removed from the cells. The cells were washed with 5 ml of phosphate-buffered saline (pH 7.4) (Sigma-Aldrich). Then, 2 ml of Trypsin/EDTA solution (Life Technologies) were added to the cells to dissociate them from the flask surface. Following incubation for 3 min, 10 ml of culture medium were added to the cells, which were then pipetted from the flask into a 25-ml tube. The cells were pelleted by centrifugation for 5 min at 1000 rpm, resuspended in 5 ml of culture medium, and 1 ml of the cell suspension added to a new T75 flask containing 10 ml of culture medium. Incubation was continued as before. Cells were passaged a minimum of two times before proceeding with experiments.

2.2.3 Cell counting and cell viability

Cells were counted with the aid of a haemocytometer. Initially, cells (50 µl) were diluted in Trypan Blue solution (Sigma-Aldrich) at a ratio of 1:1 and then applied to the haemocytometer. Staining with Trypan Blue allowed for the differentiation of live and

dead cells as only dead cells are stained and this can be visualised under a microscope. Cells were counted in five squares of the counting chamber and this number averaged and then doubled to take account of the dilution factor with the stain. The number of cells/ml was calculated as: cell counted x 10^4. To calculate cell numbers in the original cell suspension volume, the number of cells/ml was multiplied by the appropriate factor. The percentage of viable cells was calculated as 100 x (viable cells/total cells).

2.2.4 Cell freezing and storage

Cells were stored in liquid nitrogen to preserve the cell line as continuous growth can induce genetic changes and alter the cell genotype. Cells were frozen at a low passage number in fetal calf serum freezing medium containing 10% dimethylsulfoxide, which acts as a cryoprotective agent. To freeze, cells were detached from a T75 flask, with Trypsin/EDTA solution or by using a sterile plastic scraper, and collected in 10 ml of culture medium. The cells were centrifuged at 1000 rpm for 5 min Sorvall RT 6000D centrifuge and the cell pellet resuspended in fresh culture medium. The cells were counted and viability determined using Trypan Blue staining. Subsequently, the cells were pelleted by centrifugation and resuspended in 1 or 2 ml of freezing medium or at a density of between 10^6 to 10^7 cells/ml in cryogenic vials. The vials were initially stored at -80°C for at least 48 h before being transferred into liquid nitrogen for final storage.

2.3 DNA and RNA methods

2.3.1 RNA preparation

A Qiagen RNeasy Mini Kit (Qiagen, Manchester, UK) was used for the isolation of total RNA (including mRNA) according to the manufacturer's specifications. Briefly, < 1 x 10^7 of freshly grown cells were harvested and the culture medium removed completely. The cell pellet (or cell pellets stored at -80°C) was resuspended in 350 µl of RLT lysis buffer containing dithiothreitol, and homogenised by passing the lysate five times through a 20G needle using a 1-ml syringe. This was necessary to reduce the viscosity of the cell lysates.

An equal volume of 70% ethanol was added to the lysate and the mixture (up to 700 µl) transferred into a RNeasy Mini spin column with an attached collection tube and

centrifuged for 15 sec at > 8000 x g. The flow through in the collection tube was discarded. To wash the spin column, 700 µl of buffer RW1 were added followed by centrifuging for 15 sec at > 8000 x g. Again, the flow through was discarded.

The column was washed with 500 µl of buffer RPE that contained ethanol. The column was centrifuged for 15 sec at > 8000 x g, followed by addition of 500 µl of buffer RPE and further centrifuging for 2 min at > 8000 x g. Finally, the spin column was centrifuged at full speed for 1 min to dry the membrane, after which the spin column was transferred into a new 1.5 ml collection tube. To elute the RNA from the column membrane, 30–50 µl of RNase-free water was added directly to the column membrane and the column centrifuged for 1 min at > 8000 x g to elute the RNA.

To ensure removal of any DNA contamination from the sample, the eluted RNA was treated with a TURBO DNA-free Kit according to the manufacturer's protocol (Life Technologies). A 0.1 volume of 10X TURBO DNase buffer and 1 µl of TURBO DNase enzyme were added to the RNA sample and mixed gently. The mixture was incubated at 37°C for 20–30 min, after which 0.1 volume of resuspended DNase Inactivation Reagent was added. The reaction was incubated for 5 min at room temperature with occasional mixing. The reaction was centrifuged at 10,000 x g for 1.5 min, and the RNA transferred to a clean 1.5 ml tube. RNA samples were stored at -80°C until needed.

To quantify the concentration of RNA by way of absorbance spectroscopy at 260 nm, a NanoDrop ND-1000 spectrophotometer (Labtech, Wilmington, DE, USA) was used. The read out was in ng/µl. Qualitative analysis of RNA was undertaken using agarose gel electrophoresis (Section 2.4.10).

2.3.2 Reverse transcription

The total RNA extracted from cells, was reverse transcribed to generate complementary DNA (cDNA). This process was carried out by the use of reverse transcriptase (RT), an enzyme which copies mRNA into cDNA for subsequent use as a template in polymerase chain reaction (PCR) amplifications. To make cDNA, a RT reaction involving a mixture of total RNA and random decamers in nuclease-free water was set up as shown in Table 2.1 and according to a RETROscript Kit (Life Technologies). A second identical reaction was set up and referred to as a Minus RT

control (Table 2.1). Both reactions were heated for 3 min at 85°C, centrifuged briefly to remove any condensation, and kept on ice. Further components, including Moloney Murine Leukemia Virus (MMLV) RT, were added to each of the reactions (Table 2.1). The reactions were incubated at 44ºC for 1 h, followed by another incubation period at 92ºC for 10 min to inactivate the RT. The RT reaction and control tubes were taken forward for the PCR reaction or stored at -20ºC until needed.

Table 2.1: Reverse transcription reaction set-up

Component	Amount for RT reaction	Amount for minus RT control
Total RNA[1]	1-2 µg	1-2 µg
Random decamers (50 µM)[2]	2 µl	2 µl
Nuclease-free water[1]	to 12 µl	to 12 µl
Heat reactions for 3 min at 85ºC and then keep on ice. Add the following components to give a final volume of 20 µl		
10X RT buffer (500 mM Tris-hydrochloride, pH 8.3; 750 mM potassium chloride; 30 mM magnesium chloride; 50 mM dithiothreitol)[2]	2 µl	2 µl
dNTP mix (2.5 mM of each dNTP)[2]	4 µl	4 µl
RNase inhibitor (10 units/µl)[3]	1 µl	1 µl
MMLV-RT (100 units/µl)[2]	1 µl	0 µl
Nuclease-free water[2]	0 µl	1 µl
Incubate reactions at 44ºC for 1 h Incubate at 92ºC for 10 min to inactivate the RT Store reactions at -20ºC		

[1]Total RNA from required cells.
[2]Component from the RETROscript Kit (Life Technologies, Paisley, UK).
[3]Component from Promega (Southampton, UK).

2.3.3 Polymerase chain reaction of cDNA

The amplification of cDNA by polymerase chain reaction (PCR) produced in RT reactions was carried out according to a RETROscript Kit. PCR amplifications were carried out in 0.5-ml tubes in 50-µl volumes and assembled on ice as shown in Table 2.2. A reaction without cDNA (minus RT reaction) was included to demonstrate that the template for any PCR product was cDNA and not genomic DNA that might be contaminating the RNA preparations. A no template negative control, where nuclease-free water replaced the cDNA template, was used to verify that none of the PCR components were contaminated with DNA. A positive control using S15-forward and S15-reverse primers (Table 2.3) was also included in experiments to ensure that the components of the PCR were working. The different primers used in PCR amplification reactions are listed in Table 2.3.

The RT reactions were subjected to PCR amplification in a Techne TC-312 thermal cycler (GeneFlow, Lichfield, UK). Unless otherwise stated, the cycling conditions were initial denaturation at 95°C for 10 min, followed by, for 35 cycles, denaturation at 95°C for 30 sec, annealing at 55°C for 30 sec, and extension at 72°C for 1 min. The reactions were completed by a final extension at 72°C for 20 min, followed by a soak at 10°C. When using CRHR1 forward and reverse primers, the annealing temperature was altered to 59°C. Amplification products were analysed by agarose gel electrophoresis (Section 2.4.10).

2.3.4 Primers for PCR amplification and DNA sequencing

Forward and reverse primers for PCR and primers for DNA sequencing are listed in Table 2.3. The majority of primers for PCR and DNA sequencing were synthesised to order by Eurofins Genetic Services Ltd. (London, UK) and were stored at -40°C in sterile nuclease-free water at 100 pmol/µl (100 µM) concentration.

Table 2.2: Reaction components for PCR amplification of cDNA

Component	PCR with RT reaction (cDNA)	PCR with minus RT reaction (no cDNA)	PCR control without any template
RT reaction (cDNA)[1]	1-5 µl	0 µl	0 µl
Minus RT reaction (no cDNA)[1]	0 µl	1-5 µl	0 µl
10x PCR buffer (100 mM Tris-hydrochloride, pH 8.3; 500 mM potassium chloride; 15 mM magnesium chloride)[2]	5 µl	5 µl	5 µl
dNTP mix (2.5 mM of each dNTP)[2]	2.5 µl	2.5 µl	2.5 µl
Nuclease-free water[2]	to 50 µl	to 50 µl	to 50 µl
PCR primers (mixture with 5 uM of each primer)[3]	2.5 µl	2.5 µl	2.5 µl
Go Taq Polymerase (5 units/µl)[4]	1 µl	1 µl	1 µl

[1]Component from RT reactions.
[2]Components from the RETROscript Kit (Life Technologies, Paisley, UK).
[3]Components from the RETROscript Kit or Eurofins (London, UK).
[4]Component from Promega (Southampton, UK).

Table 2.3: Primers for PCR amplification and DNA sequencing

Primer name	Primer sequence	Primer details	Supplier
S15-Forward	5'-TTCCGCAAGTTCACCTACC-3'	Intron-spanning control primers designed to amplify a 361-base pair fragment of the "house-keeping" gene S15, which encodes a small ribosomal subunit protein. The primers work with mouse and human cDNA (Inoue et al., 1987; Kitagawa et al., 1991).	RETROscript Kit (Life Technologies, Paisley, UK)
S15-Reverse	5'-CGGGCCGGCCATGCTTTACG-3'		
POMC-Forward	5'-GAGAGCAACCTGCTGGCTTGC-3'	Intron-spanning POMC primers designed to amplify a 514-base pair fragment of POMC. Figure 3.2.	Eurofins (London, UK)
POMC-Reverse	5'-AGGTCATGAAGCCACCGTAACG-3'		
CRHR1-Forward	5'-CTGCGGCTCAGGAGCATCCG-3'	Intron spanning CRHR1 primers designed to amplify a 199-base pair fragment of CRHR1. The primers work with mouse and human cDNA. Figure 4.3.	Eurofins (London, UK)
CRHR1-Reverse	5'-CGAACATCCAGAAGAAGTTGG-3'		Eurofins (London, UK)

2.3.5 Plasmids

The plasmids used in this study are listed in Table 2.4. They were stored in TE buffer (10 mM Tris-hydrochloride; 1 mM ethylenediaminetetraacetic acid (EDTA); pH 8.0) (Promega) at –20°C.

Table 2.4: Plasmids used in this study

Plasmid	Details	Supplier
pOG44	A 5.79-kb Flp-recombinase vector. CHO Flp-IN cells are co-transfected with pOG44 and the relevant plasmid carrying the cDNA of interest. It carries an ampicillin resistance gene (Figure 5.2).	Life Technologies (Paisley, UK)
pSecTag-Link-CRHR1	pSecTag-Link carrying human CRHR1 cDNA cloned at the *Bam*H1 site. The plasmid was used for CHO Flp-IN-CRHR1 stable cell line isolation. It carries a cytomegalovirus (CMV) promotor region, an ampicillin resistance gene, and a Zeocin™ resistance gene for eukaryotic selection (Figure 5.3).	Dr Helen Kemp (Department of Oncology and Metabolism, University of Sheffield, UK)

2.3.6 Agarose gel electrophoresis

RNA and DNA were analysed in 0.8-1% of agarose gels that were prepared by melting agarose in TAE (40 mM Tris-acetate; 1 mM EDTA; pH 8.3) electrophoresis buffer (Promega). One microlitre of ethidium bromide solution (10 mg/ml) (Promega) was added for every 50 ml of the gel solution. The molten agarose was cooled and poured into the casting deck of a Sub-Cell® Horizontal Electrophoresis System (Bio-Rad Laboratories Ltd., Hemel Hempstead, UK), which had been set up with an appropriate gel comb.

After setting, gel combs were removed and the gel placed into the electrophoresis tank with TAE buffer. Samples of RNA or DNA were mixed with Blue/Orange Loading Dye 6x (0.4% orange G; 0.03% bromphenol blue; 0.03% xylene cyanol FF; 15% Ficoll® 400; 10 mM Tris-hydrochloride, pH 7.5; 50 mM EDTA, pH 8.0) (Promega) at 1/6th of the RNA or DNA volume, and then loaded into the gel slots. A DNA marker lane was included on each gel and contained a 0.5-1.0-µg sample of a 1-kb DNA Ladder (250-10,000-bp DNA fragments) (Promega) or a 100-bp DNA Ladder (100-1,500-bp DNA fragments) (Promega),

Gels were run at 50-70 volts using a PowerPac Basic Power Supply (Bio-Rad Laboratories Ltd.). They were viewed and recorded using a GBOX Gel Documentation System (Syngene, Cambridge, UK) with GeneSnap Image Acquisition Software (Syngene).

2.3.7 Purification of DNA fragments

DNA fragments for sequencing were initially separated by agarose gel electrophoresis (Section 2.4.10). They were then recovered from an agarose gel using a Wizard® PCR Preps DNA Purification Kit (Promega). Briefly, the relevant band of DNA was visualised using an ultra-violet transilluminator. Using a clean scalpel, it was excised from the gel and placed in a 1.5-ml tube. One milliliter DNA Purification Resin Wizard® PCR Preps was used to dissolve the gel slice and the resulting emulsion applied to a Wizard® Minicolumn using a 2-ml syringe. Subsequently, 2 ml of 80% (v/v) isopropanol was used to wash the column, followed by centrifugation in an Eppendorf MiniSpin at 13,000 rpm for 2 min, to remove excess isopropanol. Purified DNA was eluted with 50 µl of nuclease-free water and stored at -20˚C until required. Purified DNA fragments

were analysed by agarose gel electrophoresis (Section 2.4.10) and DNA sequencing (Section 2.4.12), to ensure that the correct fragment had been obtained.

2.3.8 Sequencing of DNA

The Genetics Core Facility at the University of Sheffield (Sheffield, UK) was used for DNA sequencing. DNA was provided to the service at a concentration of 50-100 ng/µl. DNA sequencing primers (Table 2.3) were provided to the service at a concentration 1 pmol/µl. Sequencing reactions were carried out according to an Applied Biosystems BigDye® Terminator v3.1 Cycle Sequencing Kit (Applied Biosystems, Foster City, CA, USA). Subsequently, sequencing reactions were analysed using an ABI 3730 Capillary Sequencer (Applied Biosystems).

2.3.9 Analysis of DNA sequences

DNA sequences were analysed using the Lasergene® Core Suite version 11.0 (DNASTAR, Inc., Madison, WI, USA). The online facilities of the European Bioinformatics Institute-European Molecular Biology Laboratory (EBI-EMBL) (http://www.ebi.ac.uk/) (Cambridge, UK), and the ExPASy Bioformatics Resources Portal (http://web.expasy.org) (SIB Swiss Institute of Bioinformatics, Switzerland) were also used. DNA homology searches were carried out using the GenBank database and the BLAST online facility of the National Center for Biotechnology Information (NCBI) (www.ncbi.nlm.nih.gov) (Bethesda, MD, USA).

2.4 siRNA methods

2.4.1 siRNA molecules

siRNAs targeted against POMC (Table 2.5) were synthesised by Ambion (Glasgow, UK) and delivered at a concentration of 100 µM. Non-POMC-specific siRNAs were obtained from Dharmacon (Cambridge, UK), and included ON-TARGETplus GAPDH control siRNA, ON-TARGETplus Cylophilin B control siRNA, and ON-TARGETplus non-targeting siRNAs.

Table 2.5: siRNA molecules

siRNA	siRNA sequence
POMC siRNA1	Sense (passenger): 5'-GAUGCCGAGAUUCUGCUACUU-3' Antisense (guide): 5'-GUAGCAGAAUCUCGGCAUCUU-3'
POMC siRNA2	Sense (passenger): 5'-GUACGUCAUGGGUCACUUCUU-3' Antisense (guide): 5'-GAAGUGACCCAUGUCGUACUU-3'
POMC siRNA3	Sense (passenger): 5'-GAACGCCAUCAUCAAGAACUU-3' Antisense (guide): 5'-GUUCUUGAUGAUGGCGUUCUU-3'

2.4.2 Transfection of AtT20 cells with siRNAs

All transfections of AtT20 cells were performed in 6-well plates using cells seeded at a density of 2 x 10^5 cells per well in 2 ml of antibiotic-free medium. To achieve this density, cultured AtT20 cells were counted using a haemocytometer and diluted with culture medium to provide a cell suspension at the appropriate density for plating. Plated cells were incubated overnight in a humidified incubator at 37ºC in 5% carbon dioxide. On the day of transfection, the cell culture medium was replaced with 1 ml of fresh antibiotic-free culture medium and 0.5 ml of OptiMEM reduced-serum medium (Life Technologies). Cells were returned to the incubator until the time they were to be transfected.

For transfection, two master mixes were prepared. Master mix 1 was 500 µl of OptiMEM containing the required concentration of siRNA. Master mix 2 was made by adding 20 µl of Lipofectamine 2000 Reagent (Life Technologies) to 480 µl of OptiMEM and gently mixing by pipetting. Both master mixes were incubated at room temperature for 5 min after which they were combined, mixed gently, and incubated at room temperature for 20 min. After the incubation period, 500 µl of the transfection mix were added to duplicate wells of the AtT20 cells in the 6-well plate. Control transfection mixes were siRNA only with no Lipofectamine 2000 Reagent and Lipofectamine 2000 Reagent without siRNA. In addition, 100 nM Block-iT Fluorescent Oligo (Life Technologies), a fluorescein isothiocyanate (FITC)-labelled oligonucleotide, was used routinely in transfection experiments in the place of siRNA to assess transfection efficiency. A further 6-well plate of cells left untreated entirely was included to provide a baseline level of ACTH secretion.

All plates were gently swirled to ensure even dispersal of the transfection mixes and the cells returned to the incubator. After 24 h, 30-µl samples of the culture medium were collected for ACTH assay. Samples were stored at -80ºC. The cells were then returned to the incubator if the experiment was to be continued for a further time period. If required, cells were collected from wells for RNA extraction (Section 2.4.1)

2.4.3 Determination of AtT20 transfection efficiency

To determine transfection efficiency, AtT20 cells that had been transfected with Block-iT Fluorescent Oligo were harvested and counted using fluorescence-activated cell

sorting (FACS) analysis. Initially, cells were washed with 500 µl of phosphate-buffered saline (137 mM sodium chloride; 2.7 mM potassium chloride; 8.1 mM disodium hydrogen phosphate; 1.5 mM potassium dihydrogen phosphate; pH 7.4) (PBS) (Sigma-Aldrich) and then treated with Trypsin/EDTA solution for 3 min at 37°C. The cells were resuspended in 500 µl of antibiotic-free culture medium, transferred into a 1.5-ml Eppendorf tube, and centrifuged for 5 min at 2000 rpm in a SORVALL RT 6000D centrifuge. The culture medium was removed from the cells, which were then resuspended either in 500 µl of PBS or in 500 µl of CellFIX solution (BD Biosciences, San Jose, CA, USA) for same day or later FACS analysis, respectively. For storage, tubes were wrapped in aluminium foil and kept at 4°C.

The cells were sorted based on the basis of their charge and fluorescence using a BD LSR II flow cytometer (BD Biosciences) in the Flow Cytometry Core Facility (University of Sheffield, UK). Initially, the flow cytometer was calibrated by running a sample of untreated AtT20 cells to define the cell size as well as to standardise the intensity of background fluorescence. Gating by the FACS analysis software was set to include only viable single cells and to eliminate debris, dead cells, and cell clumps or doublets. The number of fluorescently-labelled and unlabelled cells in samples was determined in the flow cytometer and thus the proportion of cells that had been transfected successfully could be calculated.

2.4.4 Measurement of ACTH secretion by AtT20 cells

The concentration of ACTH in AtT20 cell culture medium was measured using an Immulite 2000 ACTH immunoassay (Siemens Healthcare, Camberley, UK). The sandwich ELISA employs a mouse monoclonal anti-ACTH (24-39) antibody that is coated around beads as the capture antibody for ACTH. Then, a rabbit polyclonal anti-ACTH (1-24) antibody, that recognises a different part of the ACTH molecule, forms a sandwich. The polyclonal antibody is conjugated to alkaline phosphatase that causes dephosphorylation of the chemiluminescent substrate, adamantyl dioxetane phosphate. The resulting 1,2-dioxetane is unstable and decomposes further emitting light as it does so. The light is detected within the Immulite 2000 XPi Immunoassay System (Siemens Healthcare) and its measurement is converted to pg/ml of ACTH by comparison with known ACTH standards used in the assay concurrently.

The specifications of the immunoassay were: assay range 5-1250 pg/ml; intra-assay precision of 6.7-9.5%; inter-assay precision of 6.1-10%; sensitivity, 5 pg/ml; linearity, 90-109%; and recovery, 89-111%. The specificity of the assay was assessed by lack of reactivity against melanocyte-stimulating hormone (MSH), ACTH (1-18), or ACTH (1-24).

After transfection of AtT20 cells, at 24 h or other required timing, a 30-µl sample of the culture medium was taken from each plate well. The samples were stored immediately at -80°C. When required for immunoassay, samples were thawed quickly and then diluted 1:100 in 100 mM phosphate buffer (pH 4.0). In the majority of samples, this dilution factor enabled a concentration of ACTH that came within the assay range of 5-1250 pg/ml. Then, 150 µl of each sample were assayed using an Immulite 2000 XPi Immunoassay System in the Clinical Chemistry Laboratory at the Sheffield Teaching Hospitals NHS Foundation Trust (Sheffield, UK). Output concentrations of ACTH were in pg/ml.

2.4.5 Measurement of interferon and pro-inflammatory cytokine secretion by AtT20 cells

2.4.5.1 Treatment of AtT20 cells

AtT20 cells were transfected with the required siRNAs (POMC siRNAs or control siRNAs) at 30 nM as per the transfection protocol (Section 2.4.2). In addition, polyinosinic-polycytidylic acid (poly I:C) (Sigma Aldrich), which is a synthetic analog of dsRNA and acts as a stimulant of the immune response, was included as a positive control in transfection experiments. Poly I:C was at a stock concentration of 10 mg/ml and was used in transfections at a final concentration of 7.5 µg/ml. Controls included untreated cells, cells transfected with siRNA or poly-I:C alone, and cells transfected with transfection reagent only. At 24 h post-transfection, 1-ml samples of the culture medium were collected and stored at -80°C ready for interferon and pro-inflammatory cytokine assays. When required, samples were diluted so that concentrations were measured within the assay range.

2.4.5.2 Interferon ELISAs

The concentration of interferons in AtT20 cell culture medium was measured using VeriKine™ Mouse interferon (IFN)-α and Mouse IFN-β ELISA Kits (PBL Assay Science, Piscataway, NJ, USA). Both assays were in a sandwich ELISA format and designed to measure IFN-α or IFN-β in cell culture media. Briefly, IFN-α or IFN-β in samples is bound to a specific anti-IFN-α or anti-IFN-β antibody that is coated on the wells of a 96-well plate. Detection of the binding of IFN-α or IFN-β in samples is then accomplished using a secondary antibody followed by streptavidin conjugated to horse-radish peroxidase (HRP). The binding of the conjugate is detected by the addition of the chromogenic HRP substrate 3,3′,5,5′-tetramethylbenzidine (TMB). Upon oxidation, TMB forms a blue reaction product that, upon acidification, becomes yellow with an absorbance peak at 450 nm. The parameters of the ELISAs are given in Table 2.6.

For the ELISAs, standards of IFN-α (12.5-400 pg/ml) and IFN–β (15.6-1000 pg/ml) made up in culture medium, wash solution, secondary antibody solution, and HRP-streptavidin conjugate solution were all prepared as per the manufacturers' instructions. Samples to be tested were diluted in culture medium, if required, to bring the IFN-α and IFN-β concentrations to within the range of the ELISAs.

To assay IFN-α, 100 µl of standards, samples, and blanks (zero concentration) were added to wells in duplicate followed by 50 µl of the secondary antibody solution. The plate was covered and shaken for 1 h at room temperature, followed by an incubation for 24 h at 4°C without shaking. The next day, wells were washed four times with 300 µl of wash solution before adding 100 µl of HRP-streptavidin conjugate solution to each well. The plate was covered and shaken for 2 h at room temperature. Following this, the wells were washed four times with wash solution and then 100 µl of TMB substrate solution (TMB with < 1% hydrogen peroxide) were added to each well. The plate was incubated in the dark at room temperature for 15 min without shaking, and then 100 µl of stop solution were added to each well. The absorbance at 450 nm was determined using a Labtech LT-4500 Microplate Reader (Labtech International Ltd., Lewes, UK) and its associated data analysis software (Labtech International Ltd.) within 5 min of stopping the reaction.

The protocol was the same for assaying IFN-β, but all incubations and washing stages took place on the same day.

The average of the duplicate wells for the standards, samples, and blanks was calculated. The blank absorbance value was subtracted from the sample and standard values. The $\log_{10}$ values of the IFN-α and IFN-β standard concentrations were plotted against their absorbance values to give a 4-parameter logistic standard curve. The absorbance of the unknown IFN-α and IFN-β concentrations were then interpolated to the standard curve to find the $\log_{10}$ values of the IFN-α or IFN-β concentration at that absorbance. These values were transformed to give an IFN-α or IFN-β concentration in the sample in pg/ml.

2.4.5.3 Pro-inflammatory cytokine ELISAs

The concentration of pro-inflammatory cytokines in AtT20 cell culture medium was measured using Mouse IL-1β, IL-6, or TNF-α Immunoassay Quantikine ELISAs (R&D Systems, Inc., Minneapolis, MN, USA). The assays employ a quantitative sandwich enzyme immunoassay technique. Briefly, IL-1β, IL-6, or TNF-α in samples is bound to a specific anti-IL-1β, anti-IL-6, or anti-TNF-α antibody that is coated on the wells of a 96-well plate. Detection of the binding of IL-1β, IL-6, or TNF-α is then accomplished using a HRP-conjugated secondary antibody. The binding of the conjugate is detected by the addition of HRP substrate TMB. Upon oxidation, TMB forms a blue reaction product that, upon acidification, becomes yellow with an absorbance peak at 450 nm. The parameters of each of the ELISAs are given in Table 2.6.

For the ELISAs, standards of IL-1β (12.5-800 pg/ml), IL-6 (7.8-500 pg/ml), and TNF-α (10.9-700 pg/ml) made up in Calibrator Diluent RD5T, wash solution, and substrate solution were all prepared as per the manufacturers' instructions. Samples to be tested were diluted in culture medium, if required, to bring the IL-1β, IL-6, or TNF-α concentrations to within the range of the ELISAs.

To assay IL-1β, IL-6, or TNF-α, 50 µl of Assay Diluent RD1N was added to each well. Then, 50 µl of standards, samples, and blanks were added to wells in duplicate. The plate was incubated for 2 h at room temperature. The wells were washed four times with 400 µl of wash solution before adding 100 µl of HRP-conjugated secondary antibody to each well. The plate was incubated for 2 h at room temperature. Following

this, the wells were washed four times with wash solution and then 100 µl of TMB substrate solution were added to each well. The plate was incubated in the dark at room temperature for 30 min, and then 100 µl of stop solution were added to each well. The absorbance at 450 nm was determined using a Labtech LT-4500 Microplate Reader and its associated data analysis software within 30 min of stopping the reaction.

The average of the duplicate wells for the standard, samples, and blanks was calculated. The blank absorbance value was subtracted from the sample and standard values. The log10 values of the IL-1β, IL-6, or TNF-α standard concentrations were plotted against their absorbance values to give a 4-parameter logistic standard curve. The absorbance of the unknown IL-1β, IL-6, or TNF-α concentrations were then interpolated to the standard curve to find the log10 values of the IL-1β, IL-6, or TNF-α concentrations at that absorbance. These values were transformed to give an IL-1β, IL-6, or TNF-α concentration in the sample in pg/ml.

Table 2.6: Pro-inflammatory cytokine ELISA details

ELISA	Intra-assay precision (% coefficient of variation)	Inter-assay precision (% coefficient of variation)	Range (pg/ml)	Sensitivity (pg/ml)	Recovery (%)
Mouse IFN-α	≤ 10.0	≤ 10.0	12.5-400	<12.5	≥ 94
Mouse IFN-β	≤ 8.0	≤ 8.0	15.0-1000	<15.6	82-135
Mouse IL-1β	3.0-7.5	5.7-8.4	12.5-800	2.3	95-119
Mouse IL-6	3.5-6.7	6.2-8.8	7.8-500	1.6	86-120
Mouse TNF-α	2.7-3.1	6.2-8.8	10.9-700	1.9	94-111

2.5 FACS analysis

2.5.1 Antibodies

The antibodies used in this study are given in Table 2.7. They were stored at 4°C or -20°C, in accordance with the suppliers' instructions.

2.5.2 Indirect FACS

The required cells were cultured in culture medium and harvested from T75 flasks using 5 ml of cell dissociation buffer (Life Technologies). This is an enzyme-free PBS solution. It is used to dissociate cells while preventing the digestion or cleavage of cell-surface proteins, which can happen when using Trypsin/EDTA solution. The cells were resuspended in culture medium and centrifuged at 1000 rpm for 5 min. The supernatant was discarded and the cell pellet resuspended in 5 ml of 3% bovine serum albumin (BSA) in PBS (pH 7.4) (BSA/PBS). The cells were centrifuged again for 5 min at 1000 rpm and finally resuspended in 3 ml of 3% BSA/PBS.

The cells were counted and diluted to a density of 3.5 x 10^6 cells/ml in cold 3% BSA/PBS. A 30-µl aliquot containing 1x10^5 cells was dispensed into a FACS tube. When using Fc-blocking to minimise non-specific binding, cells were pre-incubated with an anti-mouse CD16/CD32 Fc-blocking antibody (0.25 µg/1 x 10^6 cells) (Table 2.7) on ice for 10 min. The appropriate primary antibody (Table 2.7) was then added (2.5 µg/1 x 10^6 cells) and the appropriate secondary antibody was then added to the required final dilution as recommended by the manufacturer (Table 2.7).

Untreated cells, with 3% BSA/PBS instead of antibodies, provided the unstained control. A secondary antibody only control was also included to identify non-specific binding. An appropriate isotype control antibody (Table 2.7) was also included where relevant, to confirm the specificity of the antigen-specific antibody and to indicate non-specific binding that may result from binding to Fc receptors or other cell components.

The cell suspensions were mixed well and incubated at 4°C for 40 min. The cells were then washed twice with 1-ml aliquots of cold 3% BSA/PBS, before centrifugation at 1000 rpm for 5 min at 4°C. The supernatant was then discarded, and the cells were

resuspended in 500 µl of cold PBS ready for FACS analysis using a BD LSR II flow cytometer.

Table 2.7: Antibodies used in the study

Antibody	Details	Supplier
Mouse anti-CRHR1 antibody	Mouse monoclonal against human CRHR1 (amino acids 24-415). Supplied at 0.5 mg/ml.	Bio-Techne (Minneapolis, MN, USA)
Anti-mouse IgG-Alexa Fluor®488 antibody	Donkey anti-mouse IgG and conjugated to Alexa Fluor®488. Supplied at 2 mg/ml. Used at 2000x dilution.	ThermoFisher Scientific Inc. (Waltham, MA, USA)
Rabbit anti-CRHR1 antibody	Rabbit polyclonal against human CRHR1 (amino acids 55-150). Cross-reactive with mouse CRHR1. Supplied at 1 mg/ml.	Bioss Antibodies (Woburn, MA, USA)
Anti-rabbit IgG-Alexa Fluor®488 antibody	Goat anti-rabbit IgG and conjugated to Alexa Fluor®488. Supplied at 1 mg/ml. Used at 1000x dilution.	ThermoFisher Scientific Inc. (Waltham, MA, USA)
Goat anti-CRHR1 antibody	Goat polyclonal against human CRHR1 (amino acids 107-117). Supplied at 0.5 mg/ml.	ThermoFisher Scientific Inc. (Waltham, MA, USA)
Anti-goat IgG-Alexa Fluor®488 antibody	Rabbit anti-goat IgG and conjugated to Alexa Fluor®488. Supplied as 1 mg/ml. Used at 1000x dilution.	ThermoFisher Scientific Inc. (Waltham, MA, USA)
Rat anti-CD16/CD32 antibody	Rat monoclonal against mouse CD16 (IgG Fc receptor III) and CD32 (IgG Fc receptor II). Fc-blocking antibody. Supplied at 0.5 mg/ml.	BioLegend (San Diego, CA, USA))

2.6 AtT20 cell CRH-stimulation assays with ACTH measurement

AtT20 cells were plated in 6-well plates at 1 x 10^5 cells per well in 2 ml of culture medium. Each plate contained three wells that would receive treatment and three that would remain untreated. After 48 h, the cells were washed three times with culture medium and then incubated for 1 h in 2 ml of culture medium without antibiotics. From each well, 30 µl of the culture medium was collected for ACTH quantification using an Immulite 2000 ACTH immunoassay. Cells were then stimulated with 100 nM CRH (Sigma-Aldrich), 100 nM melanin-concentrating hormone (MCH) (Sigma-Aldrich) or left untreated. At 0.5, 2, 4, 6, 8, and 24 h, 30 µl of the culture medium were removed for analysis using an Immulite 2000 ACTH immunoassay.

2.7 Isolation of stable CHO Flp-IN-CRHR1 cell line

CHO-Flp-IN cells were cultured as described in Section 2.2.2, but with the addition of the antibiotic Zeocin (Life Technologies) to the culture medium at a concentration of 100 µg/ml. This was applied for at least two passages, to ensure that only cells with the Zeocin resistance survived and grew. The CHO Flp-IN cells were then plated in 6-well plates at 1.25 x 10^5 cell/ml in culture medium and incubated overnight at 37°C with 5% carbon dioxide.

For each transfection of the CHO-Flp-IN cells in the well of a 6-well plate, 92.5 µl of serum-free medium and 7.5 µl of FuGENE® 6 transfection reagent (Promega) were added to a 1.5-ml tube and mixed gently. In a separate 1.5-ml tube, 250 ng of plasmid pSecTag-Link-CRHR1 (Table 2.4) and 5 µg of plasmid pOG44 (Table 2.4) were mixed, and then added dropwise to the serum-free medium and FuGENE® 6. After mixing gently, the transfection mixture was left at room temperature for 15 min. The transfection mixture was then gently added dropwise onto the CHO-Flp-IN cells. The cells were then incubated at 37°C and 5% carbon dioxide for 24 to 48 h.

The medium was removed from the transfected CHO-Flp-IN cells and replaced with culture medium containing 600 µg/ml of hygromycin B (Life Technologies). The transfected CHO-Flp-IN cells were incubated at 37°C and when they started growing out as clumps, each clump of cells was transferred to a T25 flask and grown to 60-70% confluence. The transfected CHO-Flp-IN cells were then transferred to a T75 flask and again grown to 60-70% confluence. Candidate CHO-Flp-IN-CRHR1 cell lines

were then stored at -80°C. One candidate CHO-Flp-IN-CRHR1 cell line was tested for the expression of the CRHR1 by RT-PCR, indirect FACS, and its response to CRH-stimulation and was designated CHO Flp-IN-CRHR1.

2.8 CRH-stimulation assays with cAMP measurement

2.8.1 CRH-stimulation of cells

The response of AtT20 cells or the CHO Flp-IN-CRHR1 cell line to CRH stimulation was assessed by measuring intracellular adenosine 3',5'-cyclic monophosphate (cAMP) accumulation. In 96-well cell culture plates, AtT20, CHO Flp-IN-CRHR1 or CHO Flp-IN cells were plated at 1×10^3 cells per well in 100 µl of culture medium (Section 2.2.2). At 48 h, the medium was removed and replaced with 100 µl of serum-free medium. The cells were then incubated for 30 min at 37°C. Subsequently, a 100-µl sample of medium alone was added to control wells. To other wells the following was added, 100 µl of medium containing 200 µM 3-isobutyl-1-methylxanthine (IBMX; non-specific inhibitor of cyclic nucleotide phosphodiesterases) (Sigma-Aldrich) and CRH or MCH at 100 nM or 200 µM IBMX and 10 µM forskolin (an adenylate cyclase activator) (Sigma-Aldrich). The cells incubated at 37°C for 20 min. Culture medium was removed and 200 µl of Lysis Reagent 1B (Amersham cAMP Biotrak Enzyme Immunoassay System, GE Healthcare Life Sciences, Little Chalfont, UK) were added to the wells. Plates were shaken on a plate shaker for 10 min. The concentration of cAMP in 100-µl duplicate samples of the cell extracts was analysed immediately according to an Amersham cAMP Biotrak Enzyme Immunoassay System. Usually, samples were diluted 1:5 so that cAMP concentrations were measured within the range of the assay standard curve (25–6400 fmol/well).

2.8.2 cAMP Enzyme Immunoassay

Intracellular cAMP measurement using an Amersham cAMP Biotrak Enzyme Immunoassay. The assay is based on competition between unlabelled cAMP, present in a standard or in an experimental sample, and horse-radish peroxidase (HRP)-labelled cAMP (cAMP-HRP) for binding sites on a cAMP-specific rabbit antibody. The cAMP-specific rabbit antibody interacts with a donkey anti-rabbit IgG that is bound to the wells of a microtitre plate. The greater the amount of unlabelled cAMP, the less binding of the cAMP-HRP occurs. The resulting reduction in HRP activity is detected

by a decrease in absorbance at 450 nm due to a reduced amount of the substrate TMB that changes colour.

The specifications of the enzyme immunoassay were: assay range 25-6400 fmol/well; intra-assay precision of 4.3-9.2%; inter-assay precision of 8.0-17.4%; sensitivity, 12 fmol/well; The specificity of the assay was assessed by lack of reactivity against several related molecules including cGMP, cCMP, and cTMP.

Before use, all reagents were equilibrated to room temperature and then prepared according to manufacturer's instructions. Reagents were Assay Buffer (0.05 M acetate, pH 5.8; 0.02% bovine serum albumin), Wash Buffer (0.01 M phosphate buffer, pH 7.5; 0.05% Tween 20), Lysis Reagent 1B (Assay Buffer; 0.25% dodecyltrimethylammonium), cAMP Standards (25–6400 fmol in Lysis Reagent 1B), Anti-cAMP Rabbit Antibody (in Lysis Reagent 2B), and cAMP-HRP conjugate (in Assay Buffer).

For the assay, 100-µl of duplicate samples and cAMP standards (0-6400 fmol) were added to wells of the microtitre plate. Then 100 µl of Lysis Reagent 1B and 100 µl of Lysis Reagent 2B were added to wells to measure non-specific binding (NSB). Two wells were designated as blanks. Except for the blanks and NSB wells, 100 µl of Anti-cAMP Rabbit Antibody was added to the wells. The plate was incubated for 2h at 4°C with shaking. Except for the blanks, 50-µl of the cAMP-HRP conjugate were added to the wells. The plate was incubated for 1 h at 4°C with shaking, and then the wells washed four times with 400 µl of Wash Buffer. Afterwards, 150 µl of TMB substrate solution (TMB with < 1% hydrogen peroxide) were added to all wells. The plate was incubated for 1 h at room temperature with shaking. After a change to a blue colour, the 100 µl of 1 M sulphuric acid were added to each well. The absorbance of the wells was measured at 450 nm within 30 min using a Labtech LT-4500 Microplate Reader and its associated data analysis software.

The mean absorbance for each set of replicate wells was calculated. The percentage cAMP-HRP bound for each standard and sample was calculated using the following: %B/B0 = (standard or sample absorbance - NSB absorbance)/(zero standard absorbance - NSB absorbance) x 100. A standard curve was then generated by plotting the %B/B0 as a function of the $\log_{10}$ of the cAMP concentration of the

standards to give a 4-parameter logistic standard curve. The fmol of cAMP per well of the tested samples was then calculated by interpolation of the standard curve.

2.9 Statistical analyses

Data were analysed using GraphPad Prism 7 software (GraphPad Software, San Diego, CA, USA). One-way analysis of variance (ANOVA) was used to determine statistically significant differences between the means of multiple continuous data sets. Unpaired t tests were used to compare two unpaired groups of continuous data. *P* values <0.05 were considered significant, in all statistical analyses.

Chapter 3

Investigation of siRNA targeting of POMC to reduce expression of ACTH by AtT20 cells

3 Investigation of siRNA targeting of POMC to reduce expression of ACTH by AtT20 cells

3.1 Introduction

Previously, three siRNAs were designed in our laboratory that specifically targeted the exonic regions of mouse and human *POMC* (Figure 3.1; Figure 3.2) (Munir, 2012). Homology to other parts of the genome was not apparent in searches of sequence databases employing the BLAST algorithm (NCIB, Bethesda, MD, USA). Using the AtT20 cell line as an *in vitro* model for Cushing's disease, each of the POMC siRNA molecules at 30 nM was shown to decrease secretion of ACTH following transfection of the cells; siRNA1 by 56%, siRNA2 by 63%, and siRNA3 by 30%, compared with cells treated only with transfection reagent (Munir, 2012). In addition, POMC mRNA levels were reduced by 86%, 89%, and 95%, respectively (Munir, 2012).

Further study of siRNA3 indicated that POMC expression was effectively suppressed for up to 10 days following transfection of AtT20 cells with a 30 nM concentration (Munir, 2012). However, 10 nM POMC siRNA3, although initially as effective as 30 nM, did not give such a sustained longer-term reduction in ACTH secretion (Munir, 2012). Initial experiments using siRNA3 *in vivo*, showed that ACTH secretion from AtT20 cell-induced tumours in mice was reduced by 51-64% of that in controls after five days (Munir, 2012). Levels of circulating cortisol were also lowered but were not statistically significantly affected when compared with controls (Munir, 2012).

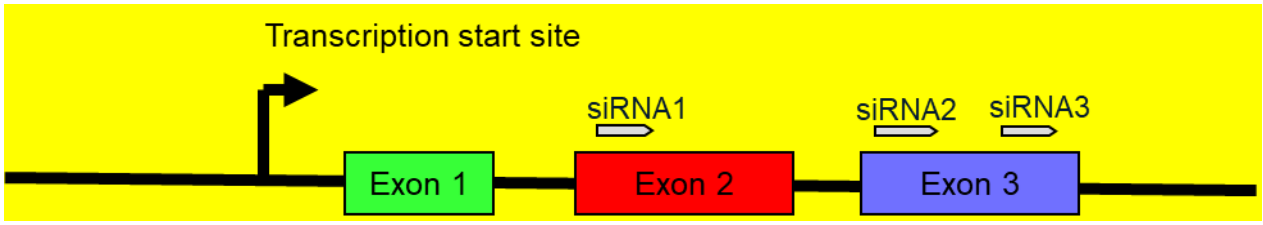

Figure 3.1: Location of POMC-targeted siRNAs.

The location of POMC siRNA1, 2, and 3 are shown relative to the exonic region of *POMC*. All three siRNAs were designed to have sequence homology between mouse, rat and human *POMC*.

TCCCTTTCATCAAACACACACACACACACACACACACACACACACACACACACACACACA
CACACCTTCCATCTTCTGAGCCCCACTCCTGTCCTCAGAAAGCCTTGGGCTGTAAAGGTA
AGAGCTGTTAGTGTTGGCTCAATGTCCTTCCTGGTGACTGGCCAACATTGTTCTGCTCCT
TGCAGGGGTCCCTCCAATCTTGTTTGCCTCTGCAGAGACTAGGCCTGACACGTGGAAGAT
GCCGAGATTCTGCTACAGTCGCTCAGGGGCCCTGTTGCTGGCCCTCCTGCTTCAGACCTC
CATAGATGTGTGGAGCTGGTGCCTGGAGAGCAGCCAGTGCCAGGACCTCACCACGGAGAG
CAACCTGCTGGTATGTGGGCCACGGACACCACCTTGGTTTGGGTGGAAGATGGCATCGGG
GTTAGTACAGAGCAAAGGGAAGAGGGCCGTGGGAAGAGGTGCCGGGGAAATTAATCTTCG
TTCATTGGAGTGGCCCACAGCAGCAATAGAACTTTTTCCATAAGGTTGGAATAAGGGAAA
GGTGAGGAGGGGATGGCTTCAGGGAAAGGGGGCTGGTTCATAATTTCTATCGATTATTCT
CATCCCCTGCTTTGCTTTCTGTGAGGACTCCTCAGCACTACTCAGTTTAAACGATGCTAC
ATTAGCCACGATTGCTCTTAGTTGATCCTATAACTCAGCCCTTTGGCTCCCAAATCAACC
TCCCTTTAAACAGTGAGAACCTACAAACTCATTTCATATTTCTTCCCTCTTTATGTTCTC
TCAGTTACAAAGCCAGTTACTAGTCAGGTATTTCCACACTCCATCTCCAGAGGGCCAGAG
GGAGAAGAAAAGACCAAAACATCCCCCCTCTTCTTCCCCCAAACTGGTGCCAAATATCCC
ATGCTGCTTCTAGAAGACAGGGCTTCAGCCAAGGTCCTTCCCAGTCTTACCTGCGGAAGC
ATGTAAAAGCTCTCTGGGACAGGTTGGGGCCCCTTTCAGGTCACCATGTGCATGCACATG
TGTGCACACAAATGTTGGGTACCCGCTAGTGTCTGCCACAGCATCCTGTTTGTTTTATCA
ATGGACAGTTGAGGGTGAAAGAGACCTCCTCAAGAGCAAGGGTCATATACAGTGTGTTTT
AGTCTTAGAAGGCCCAAGGAATCCTGGGAGATCCAGTTCAGAAAAACCCAAGGCTTCTGA
CTTCCATAGCCTCTCCTGAGATCTCACCAGGAAAGGGGTGGGGGTGGCGGGTAAAGAAGG
TCAGAGGTCATGGGCTCTGTTTCTCTGACACCTCACAATGAGCTGGGGGATCTTAACCAG
ATCCTTCTTTCTTAACGATGCAGCTTATGTGAAAATAACCAGGAATGCAGTTGTGAGTCT
TCTAGGTGTAGCTGCACCAGCAGACCCCTCGCGGAGGATTTATCCTGTGCCTTTTACCCT
CTCTTCCAGTTAGGATAAGGTGGCAGGGAAACTAACCAGTTTGTCTCAAAATTCTGATTG
AGATGATACAAGATCAGTGCACACAGTAAAAGACCTAGTGGGTGCAAGAAAGTTTTGAGA
CAAGAGACCTAGGGATACATGGCTGGAGTAGGCACAAAACTTTGTAGATTACTGGTGCAA
GATTGGATCATTGTTAAAGTCCAGACCCCCAGAAGCCAGAAACCTATTAGCAGGAATATT
CTTTCCCAAATTCCAGGCCCATGCCTGTCCTGGACTTAAATAGTACCATACTTTGACTCC
ATTGACAACACCCCTTTTGGTGCAAGACCTTGCTAGTAAGAGCTAAGAAAGACAAATAAG
CAAGGGGTCGATTGGGCTGCTTACTGCCATCTAGGCAGAATCATGCATGGGCAATAGCTG
CTTGGTGCAGGATGTTGGTGGGACCTCGGGAGTCCACACTGCTAGGTGTGATGGTCTTGA
GGCCCAAACTGGAACCCGAATTAGGGTGCAGAAACGGTGGCCGCAGAGCCAGGCTTGGCT
CACTCGCCTGGCCTCCCTACAGGCTTGCATCCGGGCTTGCAAACTCGACCTCTCGCTGGA
GACGCCCGTGTTTCCTGGCAACGGAGATGAACAGCCCCTGACTGAAAACCCCCGGAAGTA
CGTCATGGGTCACTTCCGCTGGGACCGCTTCGGCCCCAGGAACAGCAGCAGTGCTGGCAG
CGCGGCGCAGAGGCGTGCGGAGGAAGAGGCGGTGTGGGGAGATGGCAGTCCAGAGCCGAG
TCCACGCGAGGGCAAGCGCTCCTACTCCATGGAGCACTTCCGCTGGGGCAAGCCGGTGGG
CAAGAAACGGCGCCCGGTGAAGGTGTACCCCAACGTTGCTGAGAACGAGTCGGCGGAGGC
CTTTCCCCTAGAGTTCAAGAGGGAGCTGGAAGGCGAGCGGCCATTAGGCTTGGAGCAGGT
CCTGGAGTCCGACGCGGAGAAGGACGACGGGCCCTACCGGGTGGAGCACTTCCGCTGGAG
CAACCCGCCCAAGGACAAGCGTTACGGTGGCTTCATGACCTCCGAGAAGAGCCAGACGCC
CCTGGTGACGCTCTTCAAGAACGCCATCATCAAGAACGCGCACAAGAAGGGCCAGTGAGG
GTGCAGGGGTCTTCTCATTCCAAGGCCCCCTCCCTGCATGGGCGAGCTGATGACCTCTAG
CCTCTTAGAGTTACCTGTGTTAGGAAATAAAACCTTTCAGATTTCACAGTCGGCTCTGAT
CTTCAATAAAAACTGCGTAAATAAAGTCAAAACACAACTGTCCAGTTACACTATCACGTG
ACCAGATGCTAGAATGTAAAGAAAACATTTCTCAACCTCCTTGCCCCAGCAAACACTCTT
GGTGGGGGACTAGATAGTTTGGGTGGCCCAGGGTGGTTCTCTGTCCAACTCTTCTAGAAT
GGCTGCTTAATTTGAGCCTGGCCCAAAGCCAAGTCCTACAAGAGTGACTGACCTTAGGGA
CCTGAAGCCAGGTGGCGCTACCAAGACCTATTCCCCACTGGGAATGTCTCTGGGATGTCA
CTCAGGAAGTTACAGGGACACAGGGACACTCTGCAATGTTGAGTCCTTATCTGTGACCCC

Figure 3.2: The mouse *POMC* gene sequence.

The mouse *POMC* gene sequence with exon 2 and exon 3 shaded in orange. The positions of the POMC-Forward and POMC-Reverse intron-skipping PCR amplification primers are underlined. The positions of the siRNAs targeted at *POMC* are highlighted in blue.

3.2 Aims

The aim of this part of the project was to further investigate the effects of the three POMC siRNAs 1, 2, and 3 on ACTH secretion from AtT20 cells. In addition, to determine the effects of the POMC siRNAs on the immune response. The specific objectives were:

- To culture and check AtT20 cells for the expression of POMC mRNA and the secretion of ACTH.
- To set up a AtT20 transfection system.
- To investigate the effects of three POMC siRNAs on ACTH secretion from AtT20 cells.
- To determine the lowest effective concentration of each of the POMC siRNAs.
- To analyse the effectiveness of each of the POMC siRNAs over time.
- To investigate the effects of each POMC siRNA on IFN-α and IFN-β production by AtT20 cells.
- To investigate the effects of each POMC siRNA on pro-inflammatory cytokine (IL1-β, IL-6, and TNF-α) production by AtT20 cells.

3.3 Results

3.3.1 Analysis of *POMC* expression in AtT20 cells

In order to assess the effectiveness of siRNA molecules in silencing *POMC* expression, the expression of the gene in untreated AtT20 cells was initially confirmed by RT-PCR amplification.

3.3.1.1 RNA preparation

AtT20 cells were cultured in a T75 flask, harvested, and total RNA extracted from the cell pellets using a RNAeasy Mini Kit. The RNA was treated with DNase 1 from a TURBO DNA-free Kit to remove any contaminating DNA before the concentration was measured using a NanoDrop 2000 spectrophotometer. All samples of RNA were at a concentration of least 500 ng/ml. In order to assess the RNA qualitatively, samples were analysed by agarose gel electrophoresis in a 1% gel. The results are shown in Figure 3.3. Two separate bands were seen which represented 28S and 18S ribosomal RNAs. The presence of these bands indicated that the RNA preparation was not degraded and was of sufficient quality to proceed with preparing cDNA.

3.3.1.2 cDNA preparation

Total RNA was reversed transcribed into cDNA using the RETROscript Kit protocol with MMLV RT. In addition, a reaction without RT (minus RT) was set up to use as a control in later PCR experiments. The RT reactions (with and minus RT) were then used as templates for PCR amplification using POMC-specific primers POMC-Forward and POMC-Reverse (Table 2.3).

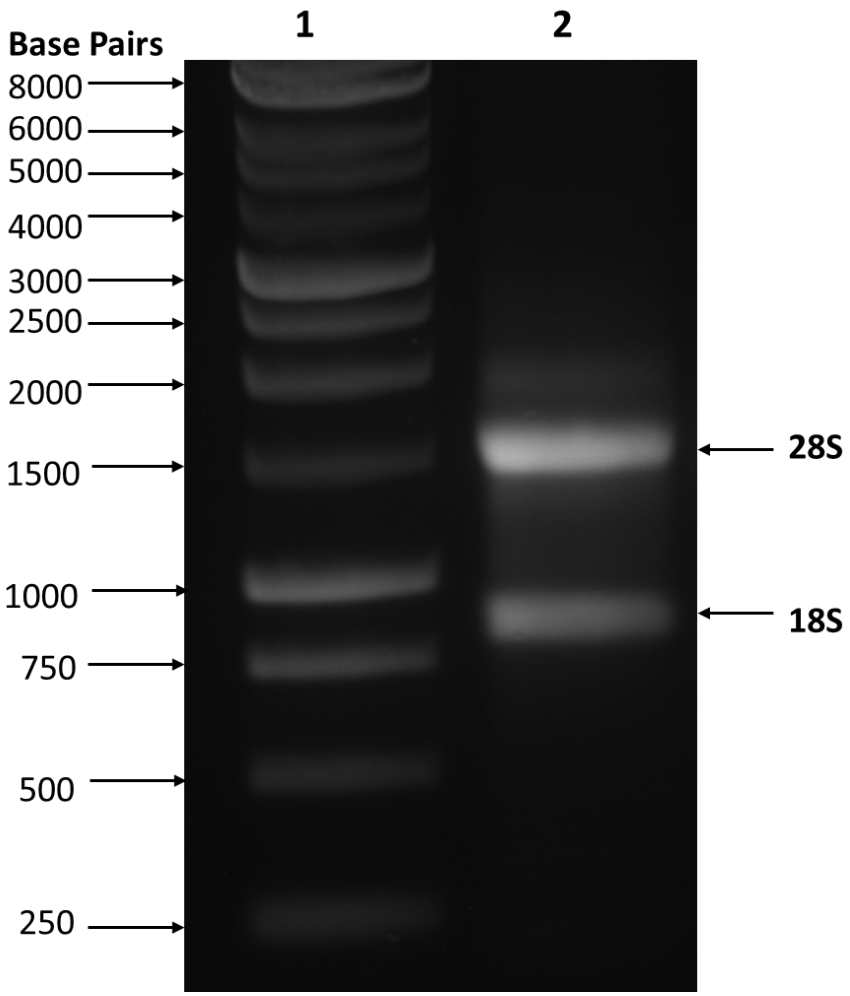

Figure 3.3: Agarose gel electrophoresis of total RNA extracted from AtT20 cells.

Total RNA was extracted from AtT20 cells and a 5-µl sample analysed on a 1% agarose gel. Lane 1, 1-kb DNA ladder; Lane 2, Total RNA sample from AtT20 cells. The bands representing 28S and 18S of ribosomal RNA are indicated.

3.3.1.3 PCR amplification

The POMC-specific primers POMC-Forward and POMC-Reverse (Table 2.3) were designed as intron-skipping primers (Figure 3.2) to avoid the amplification of any genomic DNA that might be contaminating RNA preparations. The primers were also designed to be specific for *POMC* and had no homology to other gene sequences. The expected size of the PCR product was 514 base pairs. Positive control primers were for the “house-keeping gene” rig/S15 which codes for a small ribosomal subunit protein (Table 2.3). The S15 primers were designed to work with human and mouse genes, were intron-skipping, and were anticipated to give a 361-base pair when used in PCR amplification reactions. They were included in PCR experiments to check the integrity of the cDNA samples.

PCR amplification experiments were set up as detailed in the RETROscript Kit protocol (Section 2.4.3) using either POMC-specific or S15-specific primers. Two controls were included in PCR amplification experiments. Firstly, a reaction without any template, but with primers, to verify that none of the PCR reagents were contaminated with DNA. Secondly, a reaction that included a minus RT sample to check for contaminating genomic DNA. Following PCR for 35 cycles, the PCR products were analysed by agarose gel electrophoresis, and the results are shown in Figure 3.4.

DNA fragments of the expected length were seen in the gel lanes corresponding to PCR reactions containing *POMC* primers (514 base pairs) or S15 primers (361 base pairs). No DNA products were visible in gel lanes loaded with PCR reactions containing either no template or a minus RT sample. Both the controls indicated that the amplified products were not a result of contaminated reagents or contaminating genomic DNA, respectively. Overall, the results indicated that the AtT20 cells expressed *POMC* mRNA.

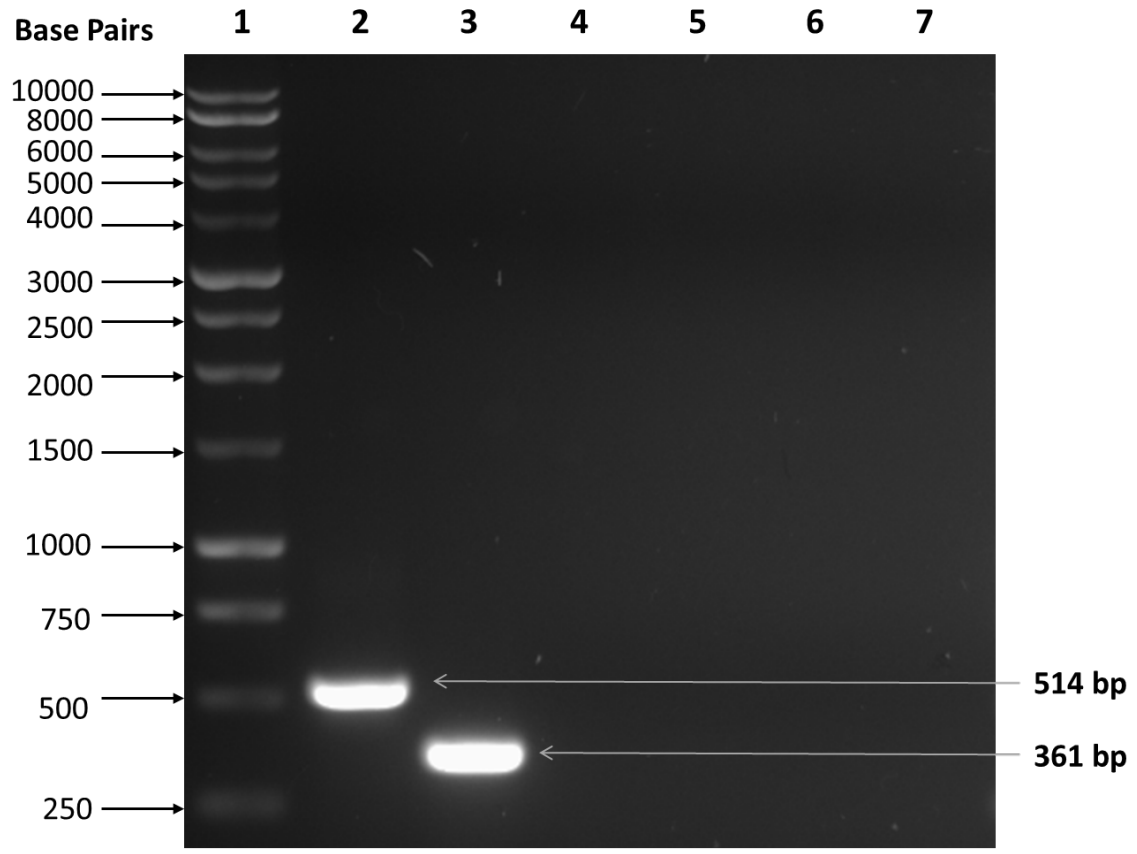

Figure 3.4: Agarose gel electrophoresis of PCR amplification products.

PCR amplification products were electrophoresed in a 1% agarose gel. Lane 1, 1-kb DNA ladder; Lane 2, AtT20 cDNA with POMC primers. The expected size was 514 base pairs (bp); Lane 3, AtT20 cDNA with S15 primers, used as a control to check cDNA integrity. The expected size was 361 base pairs; Lane 4, POMC primers only without any cDNA template; Lane 5, S15 primers only without any cDNA template; Lane 6, minus RT sample with POMC primers; Lane 7, minus RT sample with S15 primers.

3.3.1.4 PCR product sequencing

To confirm that the *POMC* PCR product was correct, the DNA fragment was extracted from an agarose gel and purified according to a Wizard PCR Preps DNA Purification System. The purified PCR product was sequenced using the POMC-Forward and POMC-Reverse primers (Table 2.3; Figure 3.2). The results that are shown in Figure 3.5 confirmed that the sequenced PCR product was the correct one when compared with the expected *POMC* sequence.

```
PCR product      GAGAGCAACCTGCTGGCTTGCATCCGGGCTTGCAAACTCGACCTCTCGCTGGAGACGCCC  60
                 ||||||||||||||||||||||||||||||||||||||||||||||||||||||||||||
POMC sequence    GAGAGCAACCTGCTGGCTTGCATCCGGGCTTGCAAACTCGACCTCTCGCTGGAGACGCCC  60

PCR product      GTGTTTCCTGGCAACGGAGATGAACAGCCCCTGACTGAAAACCCCCGGAAGTACGTCATG  120
                 ||||||||||||||||||||||||||||||||||||||||||||||||||||||||||||
POMC sequence    GTGTTTCCTGGCAACGGAGATGAACAGCCCCTGACTGAAAACCCCCGGAAGTACGTCATG  120

PCR product      GGTCACTTCCGCTGGGACCGCTTCGGCCCCAGGAACAGCAGCAGTGCTGGCAGCGCGGCG  180
                 ||||||||||||||||||||||||||||||||||||||||||||||||||||||||||||
POMC sequence    GGTCACTTCCGCTGGGACCGCTTCGGCCCCAGGAACAGCAGCAGTGCTGGCAGCGCGGCG  180

PCR product      CAGAGGCGTGCGGAGGAAGAGGCGGTGTGGGGAGATGGCAGTCCAGAGCCGAGTCCACGC  240
                 ||||||||||||||||||||||||||||||||||||||||||||||||||||||||||||
POMC sequence    CAGAGGCGTGCGGAGGAAGAGGCGGTGTGGGGAGATGGCAGTCCAGAGCCGAGTCCACGC  240

PCR product      GAGGGCAAGCGCTCCTACTCCATGGAGCACTTCCGCTGGGGCAAGCCGGTGGGCAAGAAA  300
                 ||||||||||||||||||||||||||||||||||||||||||||||||||||||||||||
POMC sequence    GAGGGCAAGCGCTCCTACTCCATGGAGCACTTCCGCTGGGGCAAGCCGGTGGGCAAGAAA  300

PCR product      CGGCGCCCGGTGAAGGTGTACCCCAACGTTGCTGAGAACGAGTCGGCGGAGGCCTTTCCC  360
                 ||||||||||||||||||||||||||||||||||||||||||||||||||||||||||||
POMC sequence    CGGCGCCCGGTGAAGGTGTACCCCAACGTTGCTGAGAACGAGTCGGCGGAGGCCTTTCCC  360

PCR product      CTAGAGTTCAAGAGGGAGCTGGAAGGCGAGCGGCCATTAGGCTTGGAGCAGGTCCTGGAG  420
                 ||||||||||||||||||||||||||||||||||||||||||||||||||||||||||||
POMC sequence    CTAGAGTTCAAGAGGGAGCTGGAAGGCGAGCGGCCATTAGGCTTGGAGCAGGTCCTGGAG  420

PCR product      TCCGACGCGGAGAAGGACGACGGGCCCTACCGGGTGGAGCACTTCCGCTGGAGCAACCCG  480
                 ||||||||||||||||||||||||||||||||||||||||||||||||||||||||||||
POMC sequence    TCCGACGCGGAGAAGGACGACGGGCCCTACCGGGTGGAGCACTTCCGCTGGAGCAACCCG  480

PCR product      CCCAAGGACAAGCGTTACGGTGGCTTCATGACCT  514
                 |||||||||||||||||||||||||||||||||
POMC sequence    CCCAAGGACAAGCGTTACGGTGGCTTCATGACCT  514
```

Figure 3.5: POMC DNA sequence alignments.

Alignment of the *POMC* DNA sequence with the DNA sequence of the purified PCR product from amplification of AtT20 cDNA with *POMC*-specific primers.

3.3.2 Measurement of ACTH secretion levels from AtT20 cells

To determine the baseline levels of ACTH secretion by AtT20 cells, the amount of the hormone secreted by AtT20 cells in culture was analysed over time.

Cells were plated in 6-well plates at a density of 2 x 10^5 cells per well in 2 ml of culture medium and incubated for 24 h. A 30-µl aliquot of the culture medium was removed from four of the wells for ACTH quantification in an Immulite 2000 ACTH immunoassay. Viable cells were counted from two wells at 24 h using Trypan Blue staining. The remaining plates were left for 48, 72, or 96 h, after which the culture medium was sampled and cell counting was undertaken. All culture medium samples were stored at -80°C.

The results of three separate experiments are shown in (Figure 3.6). ACTH was detected in the culture medium at levels of > 24,000 pg/ml after 24 h of incubation. ACTH levels were seen to increase over the four-day time period to 127,000 pg/ml. The increase in ACTH secretion levels correlated with an increase in cell numbers, which reached 1.7 x 10^6 cells at 96 h from an initial base of 2 x 10^5 cells.

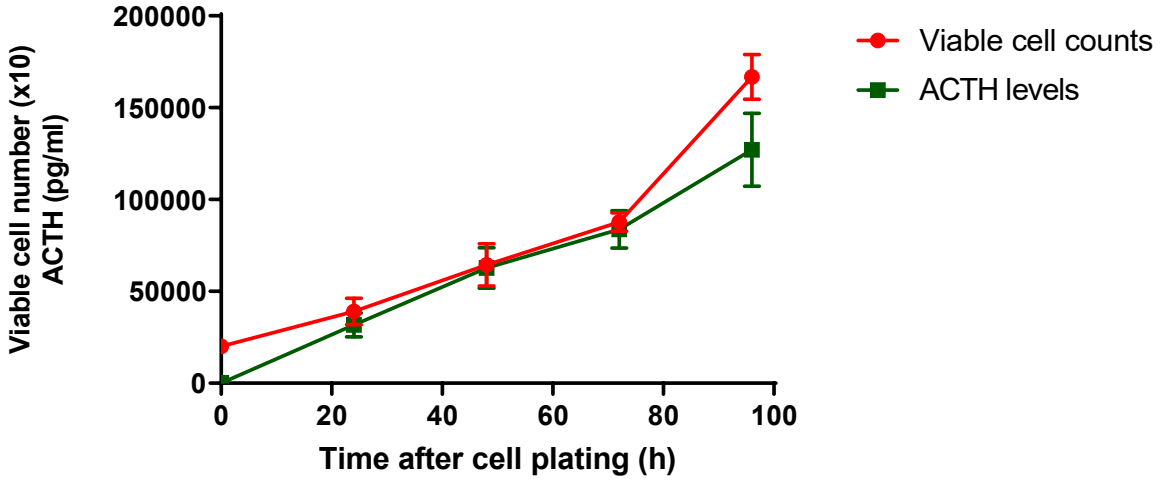

Figure 3.6: ACTH secretion levels by AtT20 cells.

The mean ± SD of three experiments are shown for cell counts and ACTH secretion levels over a four-day period.

3.3.3 Setting-up a transfection protocol of AtT20 cells

Experiments were performed to test the transfection efficiency of AtT20 cells. Cells were plated in 6-well plates at a density of 2 x 10^5 cells per well. After 24 h, the cells were transfected in duplicate with a FITC-labelled oligonucleotide at a final concentration of 100 nM. Control treatments included FITC-labelled oligonucleotide only and transfection reagent only. Untreated cells were also included to set the FACS gate. After 24 h, the cells were washed with PBS, harvested by Trypsin/EDTA treatment, and resuspended in 0.5 ml of PBS in Falcon tubes ready for analysis by FACS. FACS was undertaken in the Flow Cytometry Core Facility (University of Sheffield, Sheffield, UK).

Initially, untreated cells were used to calibrate the FACS machine in terms of standardising the intensity of background fluorescence, and determining the modal cell size. A doublet-discrimination gate was set on the FACS machine in order to exclude non-viable cells or cellular aggregates. Only the fluorescence of AtT20 cells that came within the set gate was recorded so that only single cells were counted. As determined from the control cells, a fluorescence cut-off threshold of 10^3 was on the x-axis. Any cells to the right of this were counted as being transfected successfully. The transfection efficiency was finally defined as the percentage of the total cells that were fluorescent.

The results of duplicate samples of one representative experiment are shown in (Figure 3.7). Cells treated with FITC-oligonucleotide without any transfection reagent showed 0.6% and 0.7% of cells were fluorescently-labelled, indicating that the FITC-oligonucleotide did not bind to the cell surface and only entered in the presence of transfection reagent (Figure 3.7a). Fluorescence was 0% in both samples of cells not treated with FITC-labelled oligonucleotide, indicating that the cells do not show significant auto-fluorescence (Figure 3.7b). Cells treated with the FITC-labelled oligonucleotide and transfection reagent resulted in 83% and 74%. of cells being fluorescently-labelled causing a shift to the right on the FACS histogram (Figure 3.7c).

Of nine separate transfection experiments, a transfection efficiency of between 64.1% and 93.5% was obtained with a mean ± SD of 76.5% ± 11.8% (Table 3.1; Figure 3.8).

The results indicated that the transfection efficiency showed variability, but that AtT20 cells were routinely transfectable using Lipofectamine 2000 reagent. The control using transfection reagent alone gave a transfection efficiency of 1.0% ± 1.4%, with a range 0-3.8% (Table 3.1; Figure 3.8). The control using alone FITC-labelled oligonucleotide gave a transfection efficiency of 3.0% ± 2.8%, with a range 0.6-8.3% (Table 3.1; Figure 3.8).

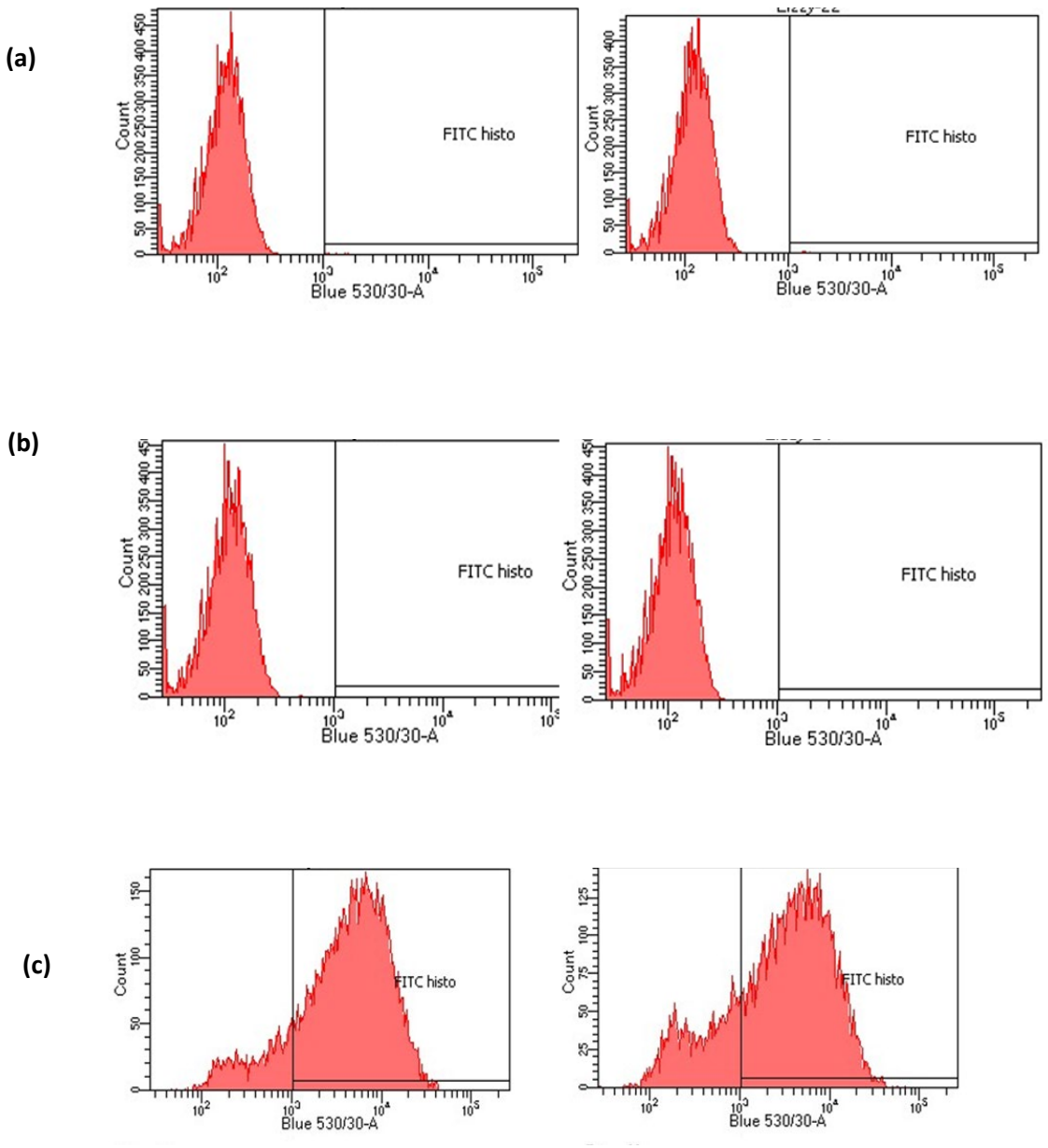

Figure 3.7: FACS analysis of AtT20 cells following transfection with FITC-labelled oligonucleotide.

Duplicate samples showing (a) AtT20 cells treated with FITC-labelled oligonucleotide without transfection reagent (0.7% and 0.6%. fluorescently-labelled cells); (b) AtT20 cells treated with transfection reagent without FITC-labelled oligonucleotide (0% and 0% fluorescently-labelled cells); (c) AtT20 cells treated with FITC-labelled oligonucleotide and transfection reagent (83% and 74% fluorescently-labelled cells).

Table 3.1: Transfection efficiency of AtT-20 cells

Experiment	Transfection efficiency (% of fluorescently-labelled cells out of total cells) with FITC-labelled oligonucleotide only and without transfection reagent	Transfection efficiency (% of fluorescently-labelled cells out of total cells) with transfection reagent only and no FITC-labelled oligonucleotide	Transfection efficiency (% of fluorescently-labelled cells out of total cells) with FITC-labelled oligonucleotide and transfection reagent
1	1.9	0.5	74.9
2	1.2	0.3	71.5
3	8.3	3.0	73.1
4	7.3	3.8	64.1
5	2.6	1.4	57.7
6	2.2	0.0	93.5
7	2.2	0.1	91.4
8	0.6	0.0	83.5
9	0.7	0.0	79.0

[1]Data are the mean of duplicate samples within the same experiment.

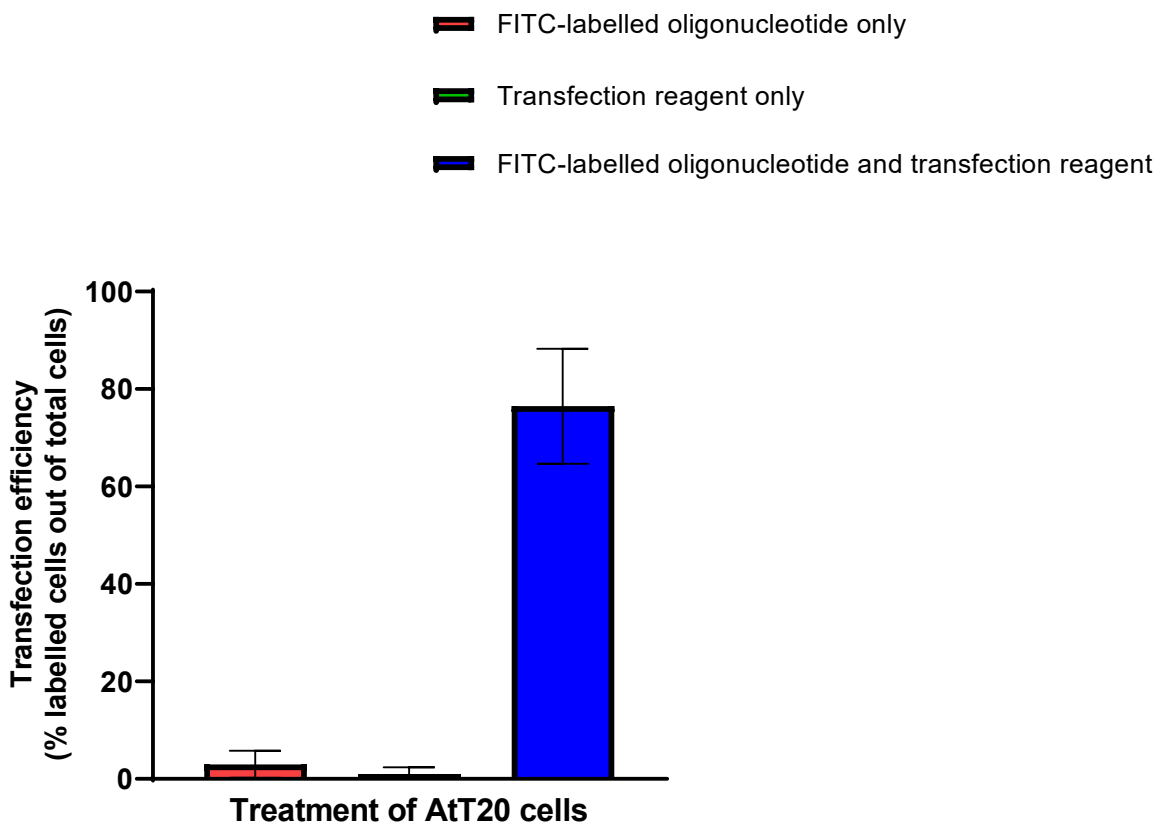

Figure 3.8: AtT-20 cells transfection efficiency using Lipofectamine-2000 and FITC-labelled oligonucleotide.

AtT-20 cells were transfected with 100 nM FITC-labelled oligonucleotide using transfection reagent. Control transfections were cells treated with FITC-labelled oligonucleotide only or with transfection reagent only. The results showed a significant increase in the percentage of fluorescing cells when AtT20 cells were treated with FITC-labelled oligonucleotide and transfection reagent compared to the two control transfection treatments.

3.3.4 Determining the effects of POMC siRNAs on ACTH secretion from AtT20 cells

Initially, the potential effect that siRNAs targeted at POMC might have on ACTH secretion was investigated by transfecting AtT20 cells with POMC siRNA1, 2 or 3 (Table 2.5; Figure 3.1).

AtT20 cells were plated in 6-well plates at 2 x 10^5 cells per well. After 24 h, the cells were transfected in duplicate with siRNA at a final concentration of 30 nM (Munir, 2012). This concentration was determined to be effective previously (Section 3.1.1). Control treatments included siRNA only and transfection reagent only. Cells without any treatment were also included in all experiments to provide an ACTH secretion baseline. After 24 h, 30 µl of the culture medium were collected for ACTH quantification using an Immulite 2000 ACTH immunoassay.

The results of six separate experiments, are shown in Figure 3.9. These indicated that treatment of the cells with POMC siRNA1, 2, and 3 reduced the concentration of ACTH in the culture medium to 15.6% (8,868 pg/ml), 18.1% (10,717 pg/ml), and 10.6% (6,037 pg/ml), respectively, of that secreted from untreated AtT20 cells. All three POMC siRNAs reduced ACTH levels statistically significantly when compared to untreated cells (56,978 pg/ml) (One-way ANOVA, P <0.0001). No significant effect on ACTH secretion was observed when cells were treated with siRNA alone or transfection reagent alone.

The reduction in ACTH levels secreted from AtT20 cells was not significantly different between treatments with the three POMC siRNAs (One-way ANOVA, P = 0.16) (Figure 3.10).

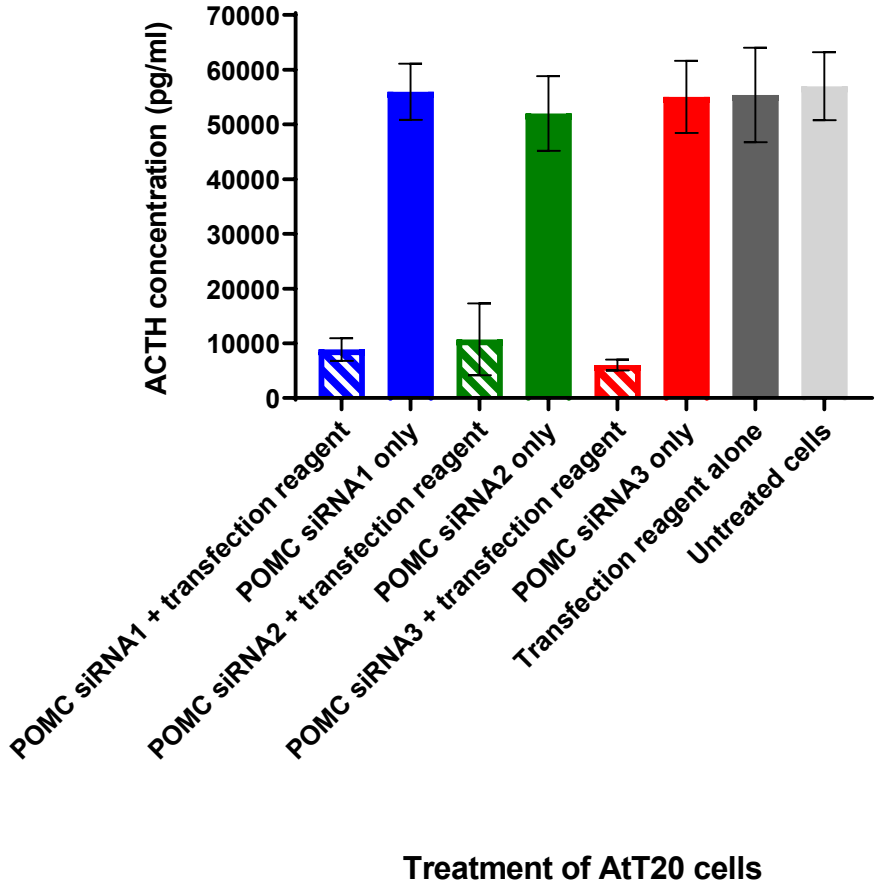

Figure 3.9: Secreted ACTH levels after transfection of AtT20 cells with POMC siRNA1, 2, or 3.

AtT20 cells were transfected with either POMC siRNA1, 2, or 3 at 30 nM, and the levels of ACTH measured in the culture medium after 24 h. Control treatments used were transfection reagent alone and siRNA alone. Untreated cells were also included to produce a baseline level of ACTH secretion. The results show the mean (± SD) ACTH concentrations measured in six separate experiments. All three POMC siRNAs reduced ACTH levels statistically significantly when compared to untreated cells (One-way ANOVA, P <0.0001).

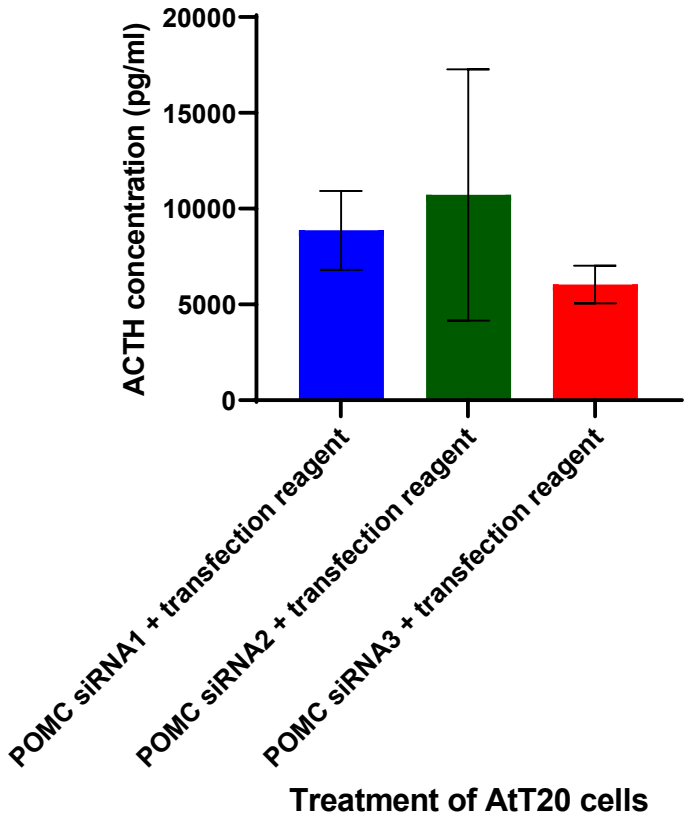

Figure 3.10: Comparison of secreted ACTH levels after transfection of AtT20 cells with POMC siRNA1, 2, or 3.

The reduction in ACTH levels secreted from AtT20 cells was not significantly different between the three POMC siRNAs at 30 nM (One-way ANOVA, *P* = 0.16).

3.3.5 Determining the effects on AtT20 viability of transfection with POMC siRNAs

The initial results of transfection with three POMC siRNAs indicated that they reduced ACTH secretion from AtT20 cells (Figure 3.9). However, it was necessary to investigate whether the viability of the AtT20 cells was affected adversely by treatment with *POMC* siRNAs and that ACTH secretion was reduced as a consequence.

AtT20 cells were plated in 6-well plates at 2 x 10^5 cells per well. After 24 h, the cells were transfected in duplicate with POMC siRNAs at a final concentration of 30 nM. Control treatments included POMC siRNAs only and transfection reagent only. Cells without any treatment were also included in all experiments. After 24 h, 30 µl of the culture medium were collected for ACTH quantification using an Immulite 2000 ACTH immunoassay. The cells were harvested and counted using Trypan Blue staining.

The results of six separate experiments are shown in Figure 3.11. They indicated that treatments with transfection reagent and POMC siRNAs, transfection reagent alone, and POMC siRNAs alone had no significant effect on the number of viable cells 24 h after transfection, when compared with untreated cells (One-way ANOVA, $P = 0.35$). The significant reduction in ACTH concentrations in the cell medium after transfection with *POMC* siRNAs could not be attributed to losses of cell viability during the experiment.

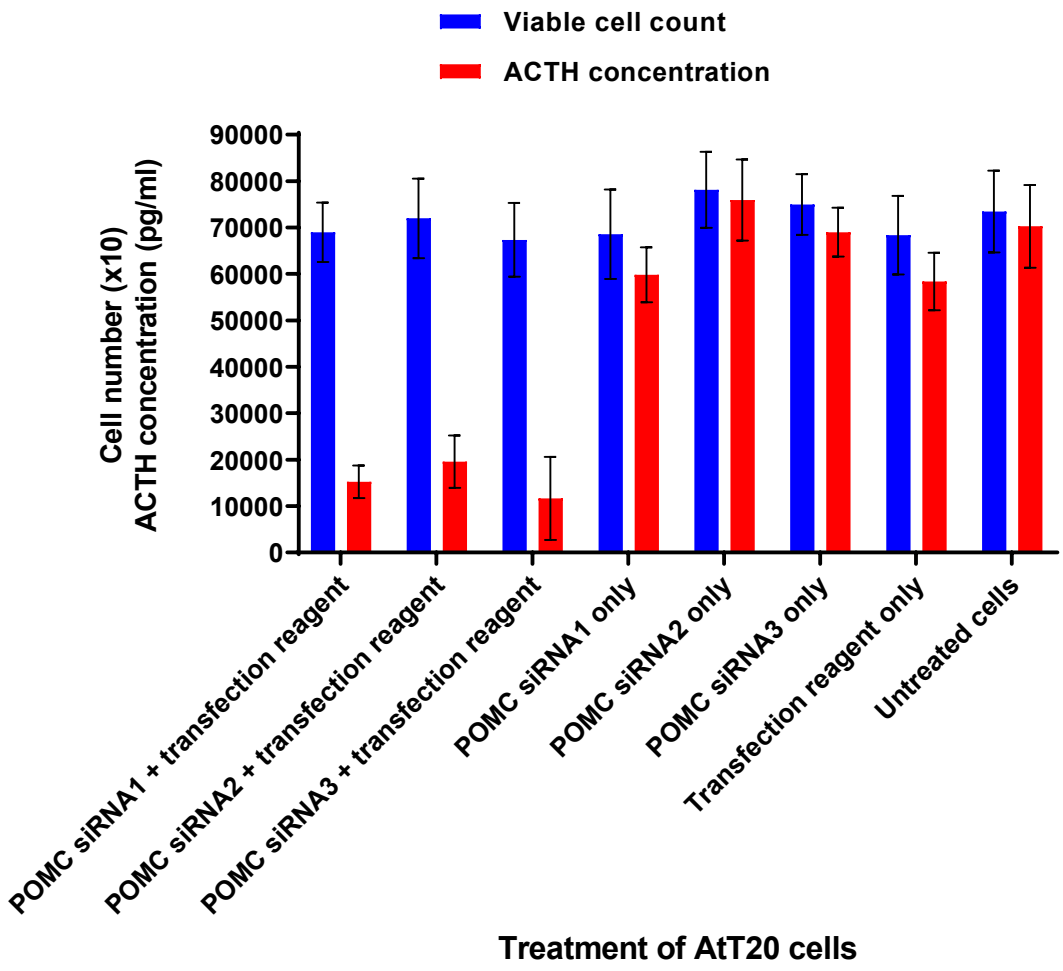

Figure 3.11: Cell counts and secreted ACTH levels after transfection of AtT20 cells with POMC siRNA1, 2, and 3.

AtT20 cells were transfected with POMC siRNAs at 30 nM. The levels of ACTH were measured in the culture medium and the viable cells counted after 24 h. Control treatments used were transfection reagent alone and POMC siRNAs alone. Untreated cells were also included. The results show the mean (± SD) viable cell counts and ACTH concentrations measured in six separate experiments. There was no significant effect on the number of viable cells when treatments were compared with untreated cells (One-way ANOVA, $P = 0.35$).

3.3.6 Determining the effects of non-POMC-specific siRNAs on ACTH secretion from AtT20 cells

To determine if the ACTH-reducing effects of POMC siRNAs were specific and not due to siRNA molecules in general, transfection experiments using two ON-TARGET*plus* non-targeting siRNAs (Section 2.5.1) were undertaken. These were designed by the supplier to have no target in the genome. In addition, the effects of siRNAs against GAPDH, ON-TARGET*plus* GAPDH control siRNA, and cyclophilin B, ON-TARGET*plus* Cyclophilin B control siRNA (Section 2.5.1), on ACTH secretion were analysed.

AtT20 cells were plated in 6-well plates at 2 x 10^5 cells per well. After 24 h, the cells were transfected in duplicate with POMC siRNA3 or non-POMC-specific siRNAs at a final concentration of 30 nM. Control treatments included siRNA only and transfection reagent only. Cells without any treatment were also included in all experiments. After 24 h, 30 µl of the culture medium were collected for ACTH quantification using an Immulite 2000 ACTH immunoassay.

The results of three separate experiments are shown in (Figure 3.12). The results indicated that treatment of AtT20 cells with control siRNAs, that did not specifically target POMC, had no significant effect upon the secretion of ACTH when compared with untreated cells (One-way ANOVA, $P = 0.21$). This confirmed that the knockdown of POMC expression was not due to a non-specific effect of dsRNA.

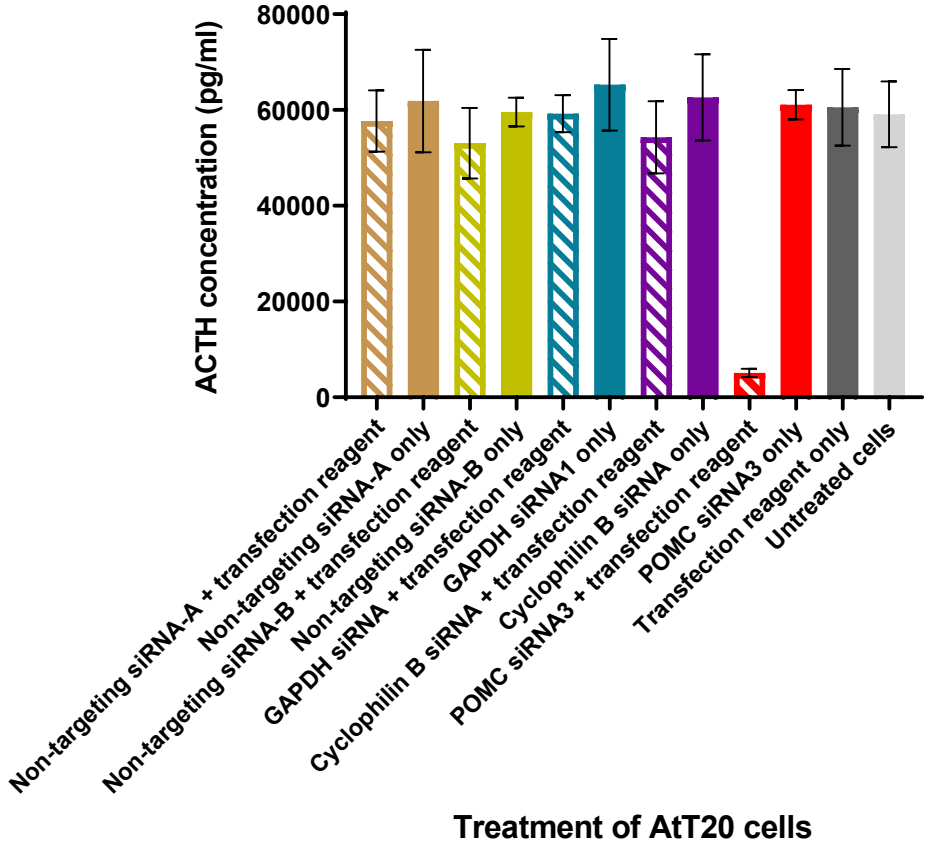

Figure 3.12: Secreted ACTH levels after transfection of AtT20 cells with POMC siRNA3 and non-POMC-specific siRNAs.

AtT20 cells were transfected with *POMC* siRNA3, non-targeting siRNAs, and specific siRNAs against GAPDH or cyclophilin B at 30 nM. The levels of ACTH were measured in the culture medium after 24 h. Control treatments used were transfection reagent alone and siRNA alone. Untreated cells were also included. The results show the mean (± SD) ACTH concentrations measured in three separate experiments. Non-POMC-specific siRNAs had no significant effect upon the secretion of ACTH when compared with untreated cells (One-way ANOVA, $P = 0.21$).

3.3.7 Determining the effects of mismatched and scrambled POMC siRNAs on ACTH secretion from AtT20 cells

To determine if alterations in the POMC siRNAs 1, 2, and 3 were able to adversely affect their POMC gene-silencing ability, changes were made to the siRNA sequences. The siRNA seed region (nucleotides 2-8), the splice site (nucleotides 10-11) and nucleotide 16 are the least tolerant of mismatches (Figure 3.13) because of their active role in gene silencing. The first nucleotide, the nucleotides of the 3'-overhang (nucleotides 20-21), and nucleotides 17-19 are the most tolerant of mismatches (Figure 3.13) because their ability to base pair is at least partially blocked by Ago2. Mismatches are tolerated, but not favoured at nucleotides 9 and 12-15 (Figure 3.13).

Mismatched bases in all three POMC siRNA molecules were created at positions 2, 4, 6, 10, and 19 of the antisense strand (Table 3.2). In addition, scrambled versions of all three POMC siRNAs were designed to ensure that their effects upon ACTH secretion were not due to their specific base composition (Table 3.2).

AtT20 cells were plated in 6-well plates at 2 x 10^5 cells per well. After 24 h, the cells were transfected in duplicate with POMC siRNA1, 2 and 3, and their mismatched versions at a final concentration of 30 nM. Control treatments included siRNA only and transfection reagent only. Cells without any treatment were also included in all experiments. After 24 h, 30 µl of the culture medium were collected for ACTH quantification using an Immulite 2000 ACTH immunoassay.

The results of three separate experiments are given in Figure 3.14. The results indicated that mismatches in all three POMC siRNAs at positions 2, 4, 6, 10, and 19 removed the gene-silencing effects of the original POMC siRNA molecules; POMC expression, and therefore ACTH secretion from AtT20 cells, was no longer suppressed when compared with untreated cells (One-way ANOVA, $P > 0.05$). In addition, scrambled versions of all three POMC siRNA molecules did not affect the levels of ACTH secreted from AtT20 cells (Figures 3.14).

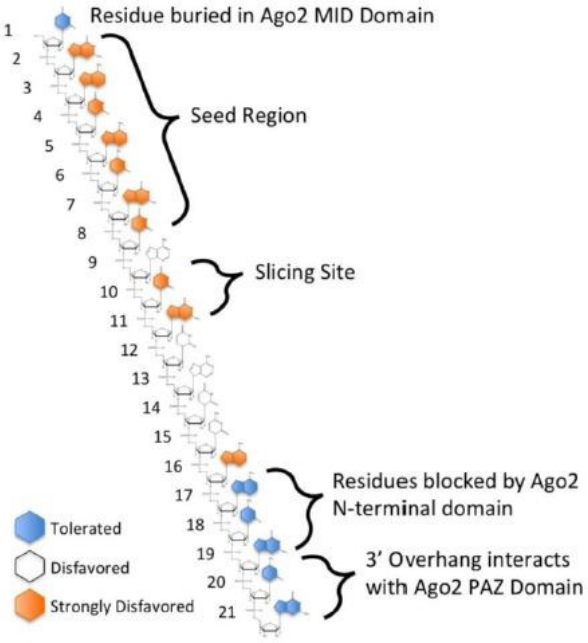

Figure 3.13: Tolerance for mismatches between a siRNA and its target.

The siRNA seed region (nucleotides 2-8), the splice site (nucleotides 10-11) and nucleotide 16 are the least tolerant of mismatches. The first nucleotide, the nucleotides of the 3'-overhang (nucleotides 20-21), and nucleotides 17-19 are the most tolerant of mismatches. Mismatches are tolerated but not favoured at nucleotides 9 and 12-15. The image, from a paper by Angart et al. (2013), is used with kind permission from MDPI (Basel, Switzerland).

Table 3.2: Mismatched siRNA molecules

siRNA	Sequence of antisense (guide) strand	Nucleotide change and position
POMC siRNA1(MM2)	5'-GGAGCAGAAUCUCGGCAUCUU-3'	U → G, at 2
POMC siRNA1(MM4)	5'-GUAUCAGAAUCUCGGCAUCUU-3'	G → U, at 4
POMC siRNA1(MM6)	5'-GUAGCGGAAUCUCGGCAUCUU-3'	A → G, at 6
POMC siRNA1(MM10)	5'-GUAGCAGAAGCUCGGCAUCUU-3'	U → G, at 10
POMC siRNA1(MM19)	5'-GUAGCAGAAUCUCGGCAUUUU-3'	C → U, at 19
POMC siRNA1(scrambled)	5'-CAGAGGUGCUUACAACUGCGUU-3'	-
POMC siRNA2(MM2)	5'-GGAGUGACCCAUGUCGUACUU-3'	A → G, at 2
POMC siRNA2(MM4)	5'-GAAUUGACCCAUGUCGUACUU-3'	G → U, at 4
POMC siRNA2(MM6)	5'-GAAGUAACCCAUGUCGUACUU-3'	G → A, at 6
POMC siRNA2(MM10)	5'-GAAGUGACCAAUGUCGUACUU-3'	C → A, at 10
POMC siRNA2(MM19)	5'-GAAGUGACCCAUGUCGUAUUU-3'	C → U, at 19
POMC siRNA2(scrambled)	5'-UAAGGGCCAACCGAUCAUGUU-3'	-
POMC siRNA3(MM2)	5'-GGUCUUGAUGAUGGCGUUCUU-3'	U → G, at 2
POMC siRNA3(MM4)	5'-GUUUUUGAUGAUGGCGUUCUU-3'	C → U, at 4
POMC siRNA3(MM6)	5'-GUUCUGGAUGAUGGCGUUCUU-3'	U → G, at 6
POMC siRNA3(MM10)	5'-GUUCUUGAUUAUGGCGUUCUU-3'	G → U, at 10
POMC siRNA3(MM19)	5'-GUUCUUGAUGAUGGCGUUUUU-3'	C → U, at 19
POMC siRNA3(scrambled)	5'-UGUUUGCUGAACGCUUUCGUU-3'	-

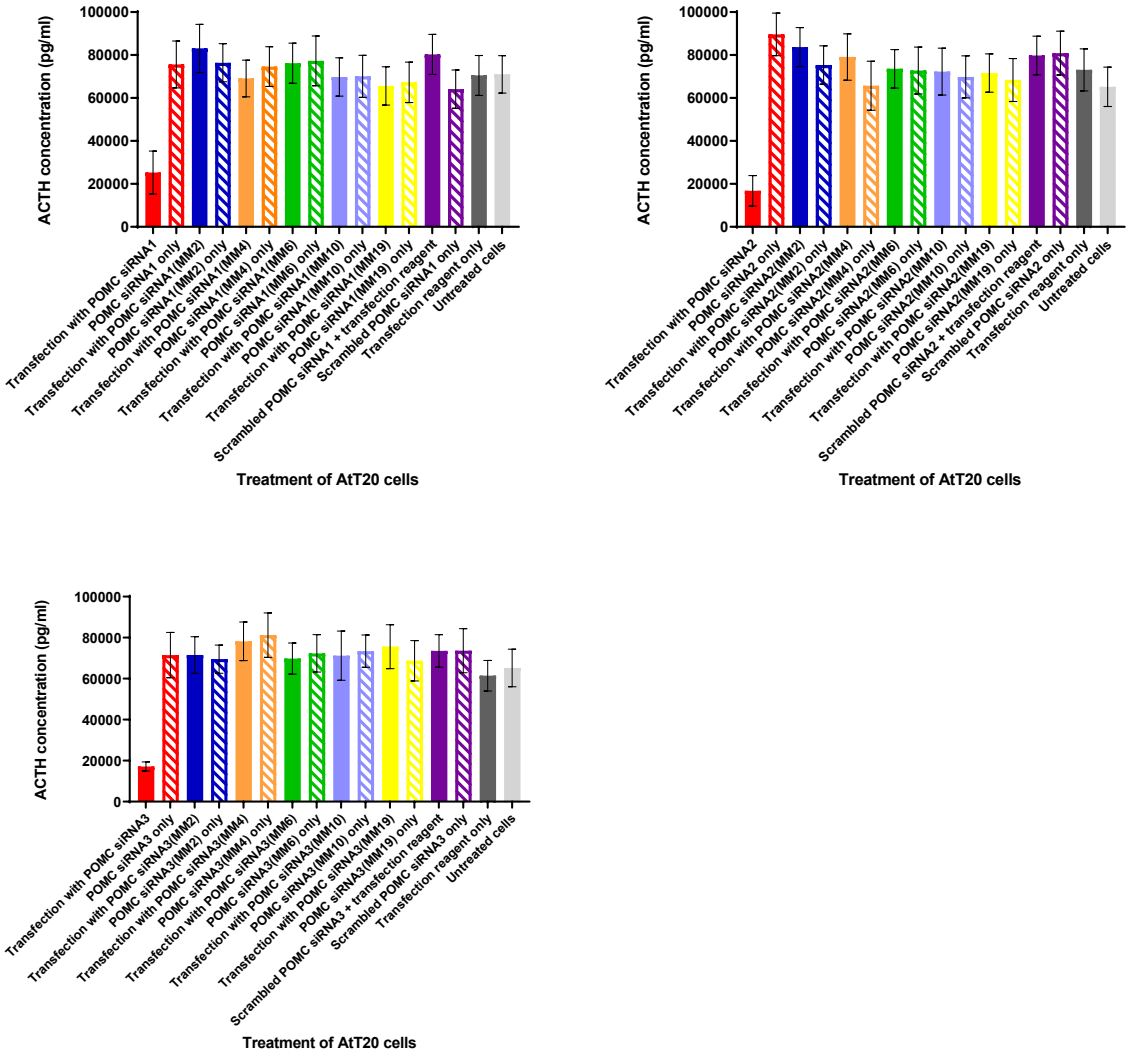

Figure 3.14: Secreted ACTH levels after transfection of AtT20 cells with mismatched and scrambled POMC siRNAs.

AtT20 cells were transfected with POMC siRNAs, mismatched POMC siRNAs and scrambled POMC siRNAs at 30 nM. The levels of ACTH were measured in the culture medium after 24 h. Control treatments used were transfection reagent alone and siRNA alone. Untreated cells were also included. The results show the mean (± SD) ACTH concentrations measured in three separate experiments. Neither the mismatched nor the scrambled siRNA molecules had a significant effect upon the secretion of ACTH when compared with untreated cells (One-way ANOVA, $P = 0.44$, $P = 0.51$, $P = 0.60$ for siRNA1, 2, and 3, respectively).

3.3.8 Determining the effects of POMC siRNA concentration on ACTH secretion from AtT20 cells

Higher doses of siRNA have an increased cost and are more likely to produce off-target effects (Sledz et al., 2003). In order to investigate the effect of siRNA concentration on the secretion of ACTH, AtT20 cells were transfected with a range of concentrations of each siRNA.

AtT20 cells were plated in 6-well plates at 2 x 10^5 cells per well. After 24 h, the cells were transfected with a range of concentrations (30 nM, 10 nM, 1 nM, 100 pM, 10 pM, and 1 pM) of POMC siRNAs. Control treatments included siRNA only and transfection reagent only. Cells without any treatment were also included in all experiments. After 24 h, 30 µl of the culture medium was collected for ACTH quantification using an Immulite 2000 ACTH immunoassay.

The results of three experiments are shown in Figure 3.15. All concentrations of all three POMC siRNAs reduced ACTH levels statistically significantly when compared to untreated cells (One-way ANOVA, $P < 0.0001$).

Table 3.3 summarises and compares using the unpaired t test, the POMC siRNA-effected reduction in ACTH secreted from AtT20 cells. Gene-silencing by concentrations of 30 nM, 10 nM, and 1 nM appeared to reduce ACTH secretion to comparable levels; 12.6-14.9%, 10.7-14.3%, and 10.6-11.6% for POMC siRNAs 1, 2, and 3, respectively. A concentration of 100 pM POMC siRNA3 was also similar, decreasing ACTH secretion to 15.4% of that secreted from untreated cells. By comparison, 100 pM POMC siRNAs 1 and 2 caused less POMC-silencing, reducing ACTH secretion to 23.6% and 32.2%, respectively. Overall, concentrations of 10 pM and 1 pM were less effective at lowering the amount of ACTH secreted from AtT20 cells (Table 3.3).

In Figure 3.16, the reductions in ACTH secretion affected by the three POMC siRNAs at concentrations of 10 nM, 1 nM, 100 pM, 10 pM, and 1 pM are compared. The comparisons showed that reduction in ACTH secreted from AtT20 cells was significantly lowered by POMC siRNA3 at 10 nM, 1 nM, and 100 pM compared with POMC siRNA1 and 2 (Unpaired t test, $P < 0.05$). For 10 pM and 1 pM, both siRNA1

and siRNA3 decreased ACTH secretion significantly compared with POMC siRNA2 (Unpaired t test, $P < 0.05$).

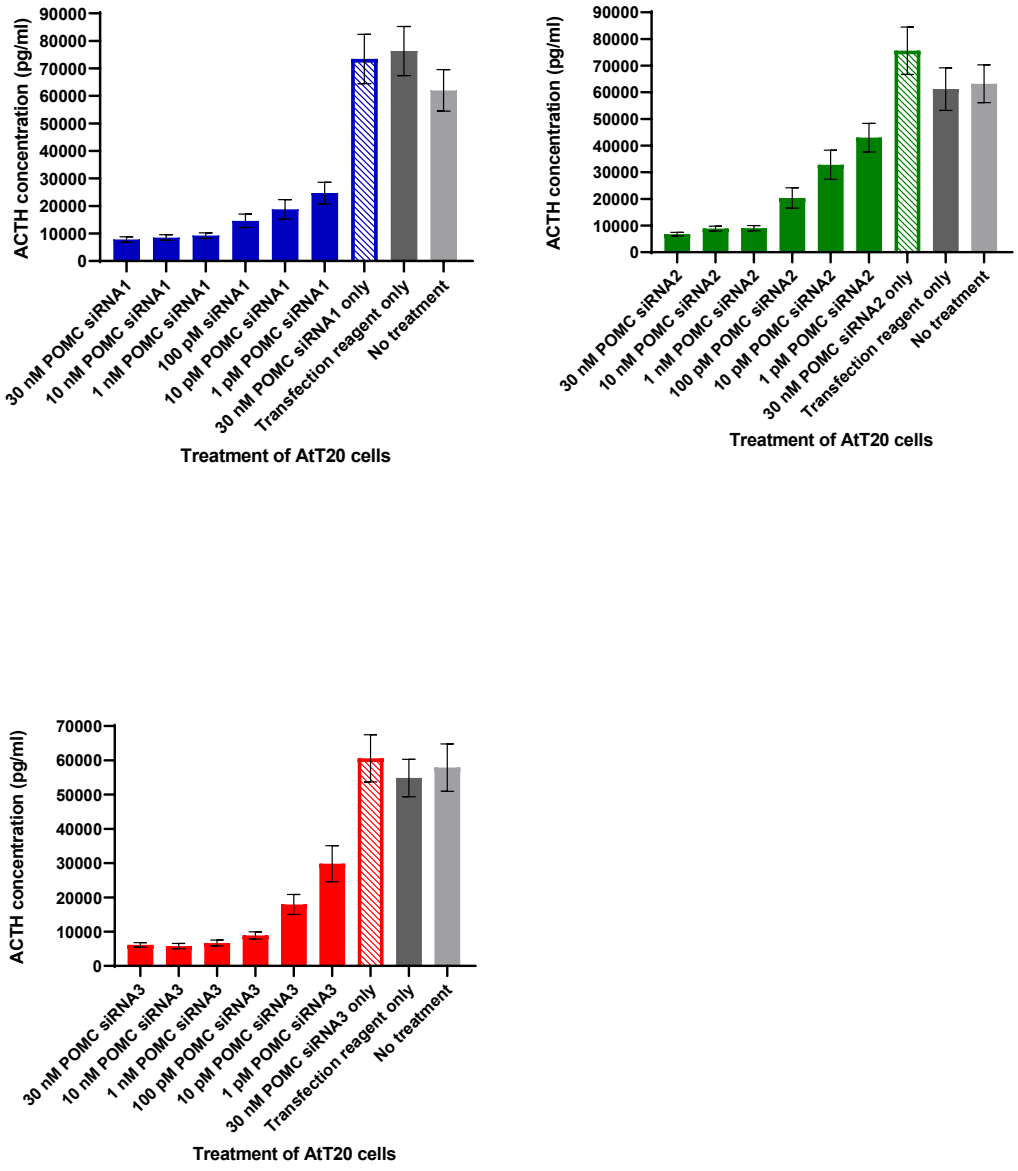

Figure 3.15: Secreted ACTH levels after transfection of AtT20 cells with different concentrations of POMC siRNA1, 2, and 3.

AtT20 cells were transfected with POMC siRNA1, 2, or 3 at concentrations of 30 nM, 10 nM, 1 nM, 100 pM, 10 pM, and 1 pM. The levels of ACTH were measured in the culture medium after 24 h. Control treatments used were transfection reagent alone and siRNA alone. Untreated cells were also included. The results show the mean (± SD) ACTH concentrations measured in three separate experiments. All concentrations significantly decreased the secretion of ACTH when compared with untreated cells (One-way ANOVA, $P < 0.0001$).

Table 3.3: Summary and comparison of effectiveness of different POMC siRNA1, 2, and 3 concentrations

siRNA1 concentration	ACTH concentration as a % of that secreted from untreated AtT20 cells	*P* value (unpaired t test)					
		30 nM	10 nM	1 nM	100 pM	10 pM	1 pM
30 nM	12.6	-	-	-	-	-	-
10 nM	13.8	0.42	-	-	-	-	-
1 nM	14.9	0.16	0.45	-	-	-	-
100 pM	23.6	0.0109	0.0159	0.0239	-	-	-
10 pM	30.3	0.0069	0.0087	0.0112	0.17	-	-
1 pM	39.7	0.0021	0.0025	0.0029	0.0206	0.13	-

siRNA2 concentration	ACTH concentration as a % of that secreted from untreated AtT20 cells	*P* value (unpaired t test)					
		30 nM	10 nM	1 nM	100 pM	10 pM	1 pM
30 nM	10.7	-	-	-	-	-	-
10 nM	14.1	0.0317	-	-	-	-	-
1 nM	14.3	0.0313	0.87	-	-	-	-
100 pM	32.2	0.0037	0.0072	0.0076	-	-	-
10 pM	51.9	0.0012	0.0017	0.0018	0.0319	-	-
1 pM	72.3	0.0003	0.0004	0.0004	0.0040	0.0830	-

siRNA3 concentration	ACTH concentration as a % of that secreted from untreated AtT20 cells	*P* value (unpaired t test)					
		30 nM	10 nM	1 nM	100 pM	10 pM	1 pM
30 nM	10.6	-	-	-	-	-	-
10 nM	10.0	0.55	-	-	-	-	-
1 nM	11.6	0.43	0.24	-	-	-	-
100 pM	15.4	0.0176	0.0139	0.0468	-	-	-
10 pM	31.0	0.0024	0.0022	0.0030	0.0073	-	-
1 pM	51.6	0.0015	0.0014	0.0017	0.0025	0.0264	-

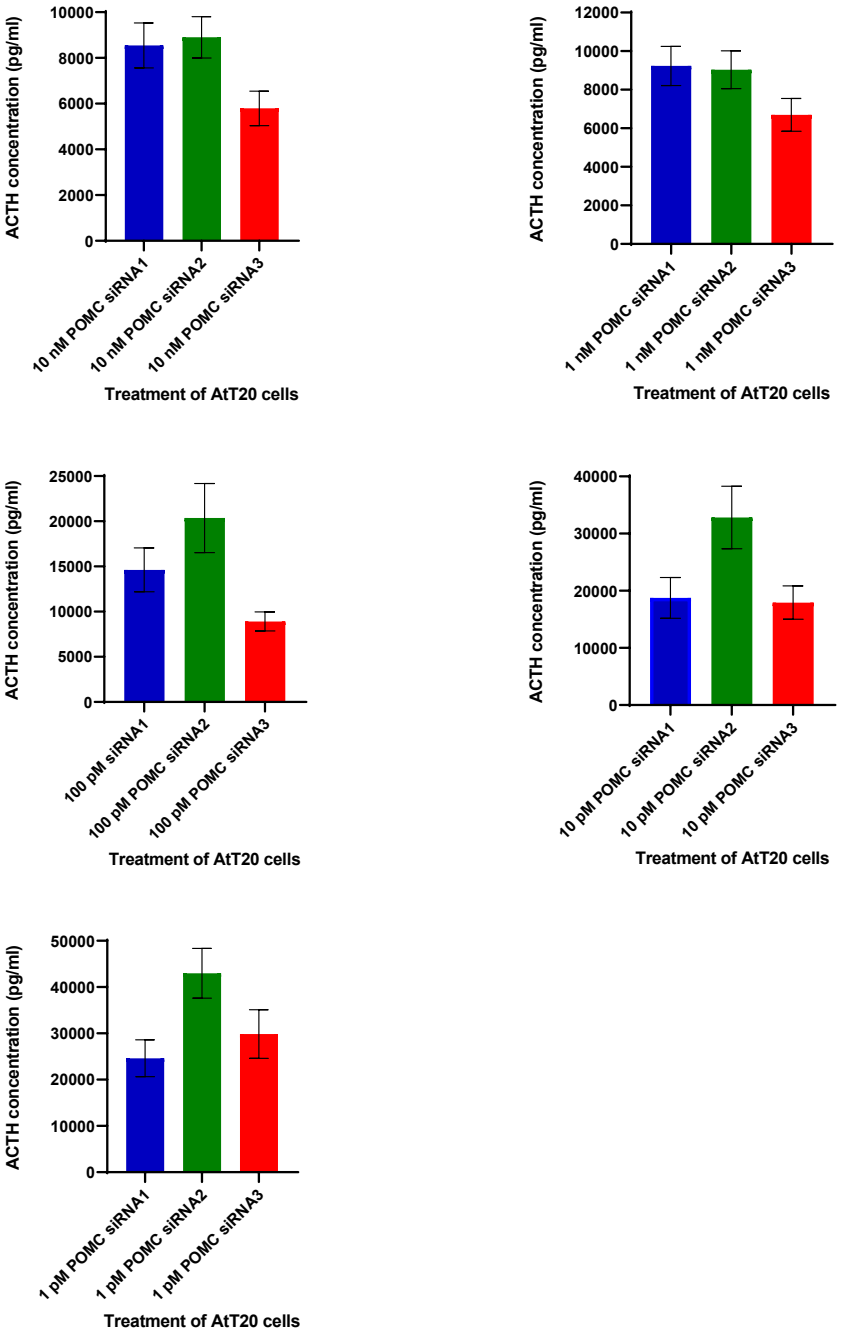

Figure 3.16: Comparison of secreted ACTH levels after transfection of AtT20 cells with different concentrations of POMC siRNA1, 2, and 3.

The reduction in ACTH levels secreted from AtT20 cells was significantly lowered by POMC siRNA3 at 10 nM, 1 nM, and 100 pM compared with POMC siRNA1 and 2 (Unpaired t test, $P < 0.05$). For 10 pM and 1 pM, both siRNA1 and siRNA3 decreased ACTH secretion significantly compared with POMC siRNA2 (Unpaired t test, $P < 0.05$).

3.3.9 Analysing the effectiveness of POMC siRNAs on ACTH secretion from AtT20 cells over time

In order to assess the longevity of action of all three POMC siRNAs, time-course experiments were carried out.

AtT20 cells were plated in 6-well plates at 2 x 10^5 cells per well. After 24 h, the cells were transfected in duplicate with POMC siRNA1, 2 and 3 at final concentrations of 30 nM, 10 nM, and 1 nM. Control treatments included siRNA only and transfection reagent only. Cells without any treatment were also included in all experiments. After 24, 48, 72, and 96 h, 30 µl of the culture medium were collected for ACTH quantification using an Immulite 2000 ACTH immunoassay.

The results of three separate experiments are given in Figure 3.17. They indicated that both 30 nM and 10 nM concentrations gave a prolonged suppression of ACTH secretion of up to 96 h when compared with baseline ACTH secretion from untreated AtT20 cells. For POMC siRNA1 and 3, a 1 nM concentration suppressed ACTH secretion to a similar level up to 48 h post-transfection, but was less effective thereafter (Table 3.4). A concentration of 1 nM siRNA2 lowered ACTH secretion to similar levels as 30 nM and 10 nM up to 96 h (Table 3.4).

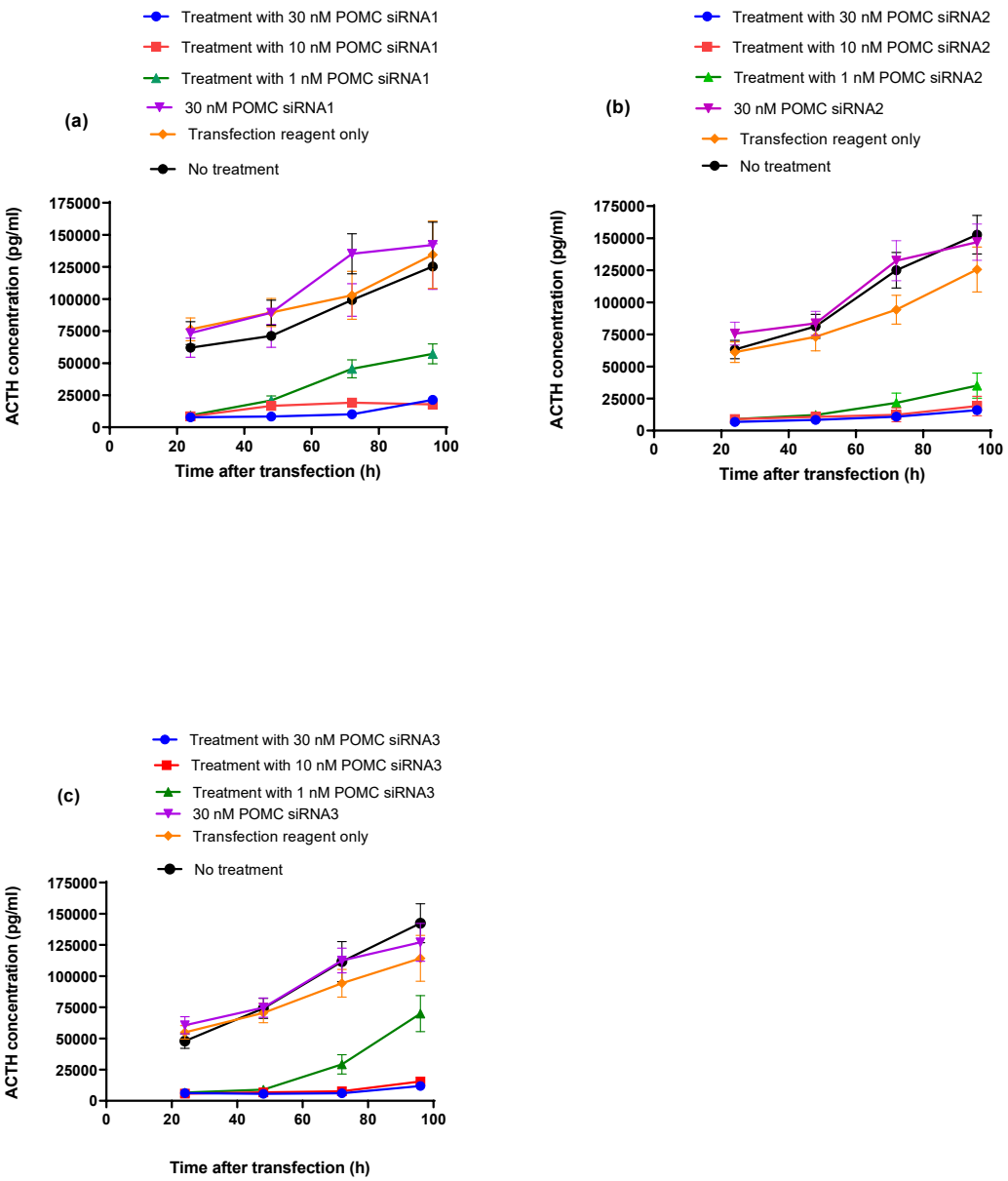

Figure 3.17: Secreted ACTH levels over time after transfection of AtT20 cells with different concentrations of POMC siRNA1, 2, and 3.

AtT20 cells were transfected with POMC siRNA1, 2, or 3 at concentrations of 30 nM, 10 nM, and 1 nM. The levels of ACTH were measured in the culture medium after 24, 48, 72, and 96 h. Control treatments used were transfection reagent alone and siRNA alone. Untreated cells were also included. The results show the mean (± SD) ACTH concentrations measured in three separate experiments.

Table 3.4: Comparison of the reduction of ACTH secretion at 24-hour and 96-hour time points

siRNA		ACTH concentration as a % of that secreted from untreated AtT20 cells	
Name	Concentration	24 h	96 h
POMC siRNA1	30 nM	12.6	17.1
	10 nM	13.8	14.2
	1 nM	14.9	45.7
POMC siRNA2	30 nM	10.7	10.4
	10 nM	14.1	12.6
	1 nM	14.3	23.0
POMC siRNA3	30 nM	12.8	8.3
	10 nM	12.1	10.9
	1 nM	14.0	49.1

3.3.10 Investigation of the effects of POMC siRNAs on the immune response

The innate immune system uses several mechanisms to ensure that dsRNA viruses are detected and responded to robustly (Figure 1.11). For example, cytoplasmic RNA receptors PKR, RIG-1, and MAD5 (Figure 1.11; Figure 3.18), which are present in many mammalian cells, recognise RNA regardless of its sequence and provoke the production of type 1 IFNs, IFN-α and IFN-β (Kawai and Akira, 2008; Kleinman et al., 2008). Toll-like receptor (TLR)-3 can exist both on the cell surface and in the endosomes of several cell types (Matsumoto et al., 2003; Kawai and Akira, 2008; Kawai and Akira, 2010). Its interaction with dsRNA also initiates an immune response that results in the increased production of IFN-α and IFN-β. Expressed specifically in subcellular compartments (endosomes, lysosomes) of immune cells, TLR-7 and TLR-8 recognise single-stranded RNA (ssRNA) with a specific sequence and can activate the production of pro-inflammatory cytokines such as TNF-α, IL-6 and IL-1 (Zarember and Godowski, 2002; Gordon et al., 2005; Robbins et al., 2009), as well as IFN-α and IFN-β (Lee et al., 2003).

Although short in size, it has been reported that siRNA molecules can provoke the above described innate immune responses in some cases by virtue of their sequence (Bridge et al., 2003; Sledz et al., 2003; Judge et al., 2005). Particularly, siRNAs that have many GU-rich motifs tend to stimulate immunoreactivity (Hornung et al., 2005). Delivery vehicles can also influence the immune response to siRNA especially if, on route to the cytoplasm, they traffic via subcellular compartments, for instance, endosomes (Sioud et al., 2005). Such effects can be mitigated to some extent by careful choice of siRNA sequence (Hornung et al., 2005), of siRNA chemical modifications (Broering et al., 2013), and of the mode of delivery (Love et al., 2010).

The aim of this part of the work was to ascertain if any of the POMC siRNAs could elicit an innate immune response in their target cells pituitary corticotrophs, using AtT20 cells as a model system. AtT20 cells express TLR-3 (Iwasaki et al., 2008) and would be expected to express cytoplasmic receptors such as PKR, RIG-1, and MAD5 that could recognise and respond to siRNA molecules. Expression of TLR-3 has also been shown to occur in the rat pituitary adenoma cell line GH3 and in human pituitary adenomas, in addition to the production of several cytokines (Green et al., 1996; Zheng et al., 2016).

For a positive control that could potentially induce IFNs and pro-inflammatory cytokines in AtT20 cells, polyinosinic-polycytidylic acid (poly-I:C) was included in experiments. A synthetic analog of viral dsRNA, poly-I:C induces IFN-β via TLR-3, RIG-1 and MDA5, with the latter two signaling through mitochondrial antiviral-signaling protein (MAVS) and the transcription factor IFN regulatory factor 3 (IRF3) (Figure 3.18) (Raj and Pitha, 1981; Kumagai et al., 2010). Poly I:C can also induce pro-inflammatory cytokines via NF-κB (Dauletbaev et al., 2015; Shi et al., 2015).

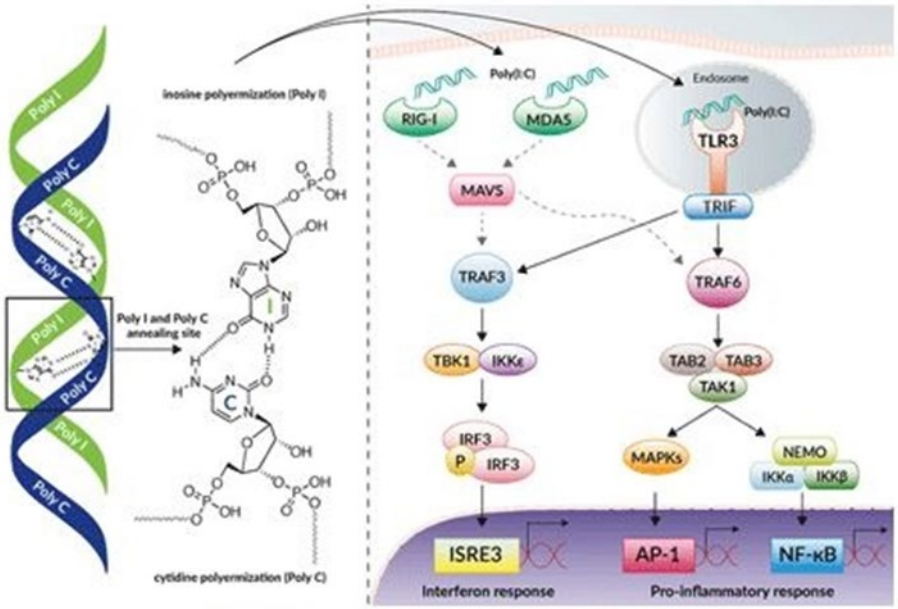

Figure 3.18: Polyinosinic-polycytidylic acid induction of the innate immune response.

A synthetic analog of viral dsRNA, polyinosinic-polycytidylic acid (poly-I:C) induces interferon (IFN)-β via toll-like receptor (TLR)-3, retinoic acid–inducible gene 1 protein (RIG-1) and melanoma differentiation-associated protein 5 (MDA5), with the latter two signaling through mitochondrial antiviral-signaling protein (MAVS) and the transcription factor IFN regulatory factor 3 (IRF3). Poly I:C can also induce pro-inflammatory cytokines via induces nuclear factor kappa light chain enhancer of activated B cells (NF-κB). The image is used with kind permission from InvivoGen Europe, Toulouse, France.

3.3.10.1 Determining the effects of POMC siRNAs on the innate immune response in AtT20 cells

The use of siRNA has been shown to stimulate the immune response (Sledz et al., 2003; Sioud, 2005; Robbins et al., 2009). In order to investigate the potential effect of siRNA on immune activation in AtT20 cells, they were transfected POMC siRNAs and poly-I:C.

AtT20 cells were plated in 6-well plates at 2 x 10^5 cells per well. After 24 h, the cells were transfected in duplicate with POMC siRNAs 1, 2, and 3, at a final concentration of 30 nM or poly-I:C at a final concentration of 7.5 µg/ml. Control treatments included siRNA only and transfection reagent only. Cells without any treatment were also included in all experiments. After 24 h, 1 ml of the culture medium was collected for analysis using the appropriate interferon (IFN-α and IFN-β) ELISAs (Section 2.4.5.2) and pro-inflammatory cytokine (IL-1β, IL-6, and TNF-α) ELISAs (Section 2.4.5.3). In some cases, culture medium samples from AtT20 cells treated with transfection reagent and poly-I:C required a dilution of 10-fold for assay within the range of the ELISAs.

3.3.10.2 Detection of interferons IFN-α and IFN-β

The results of three separate experiments are shown in Figures 3.19a-d. Neither IFN-α nor IFN-β was detected in the culture medium at 24 h after transfection of AtT20 cells with any of the three POMC siRNAs. All concentrations of IFN-α and IFN-β were below 6.3 pg/ml and 10 pg/ml, respectively, including for untreated cells. In contrast, IFN-α and IFN-β were secreted by AtT20 cells transfected with poly-I:C reaching a concentration at 24 h of 975 ± 292 pg/ml and 3580 ± 507 pg/ml, respectively. Transfection of AtT20 cells with poly-I:C alone, siRNAs alone or transfection reagent alone failed to stimulate IFN-α and IFN-β secretion.

(a)

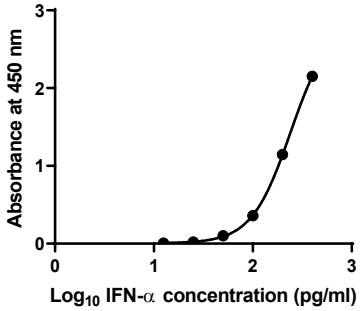

(b)

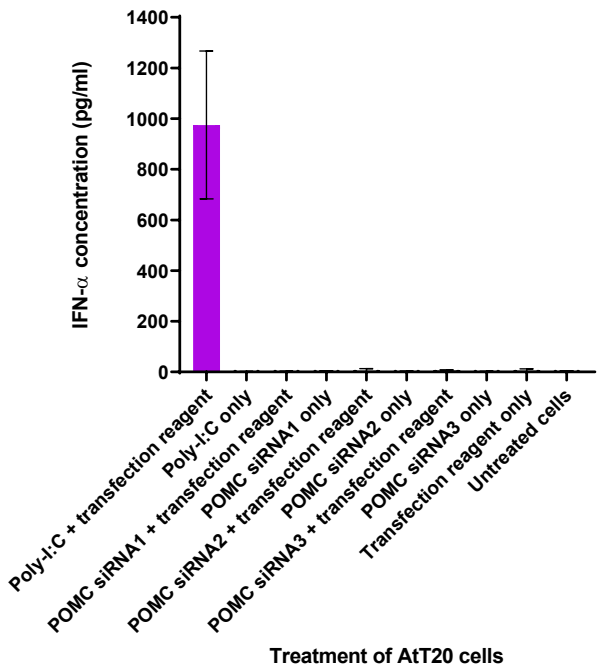

Figure 3.19a-b: Concentrations of IFN-α and IFN-β secreted by AtT20 cells after transfection with POMC siRNAs and poly-I:C.

(a) Example standard curve for IFN-α ELISA. The log10 of the concentration of a panel of standards of IFN-α were plotted against the mean absorbance values at 450 nm. (b) AtT20 cells were transfected with POMC siRNAs at 30 nM or poly-I:C at 7.5 µg/ml. The levels of IFN-α were measured in the culture medium after 24 h. Control treatments used were transfection reagent alone, siRNAs alone, and poly-I:C alone. Untreated cells were also included. The results show the mean (± SD) IFN-α concentrations measured in three separate experiments.

(c)

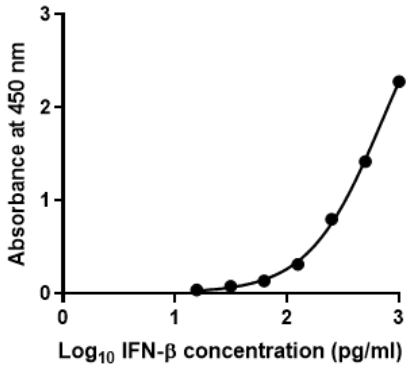

(d)

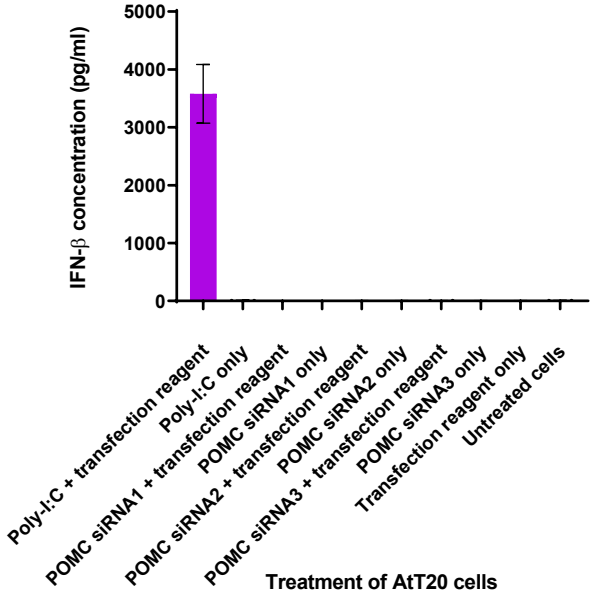

Figure 3.19c-d: Concentrations of IFN-α and IFN-β secreted by AtT20 cells after transfection with POMC siRNAs and poly-I:C.

(c) Example standard curve for IFN-β ELISA. The $\log_{10}$ of the concentration of a panel of standards of IFN-β were plotted against the mean absorbance values at 450 nm. (d) AtT20 cells were transfected with POMC siRNAs at 30 nM or poly-I:C at 7.5 µg/ml. The levels of IFN-β were measured in the culture medium after 24 h. Control treatments used were transfection reagent alone, siRNAs alone, and poly-I:C alone. Untreated cells were also included. The results show the mean (± SD) IFN-β concentrations measured in three separate experiments.

3.3.10.3 Detection of pro-inflammatory cytokines

The results of three separate experiments are shown in Figures 3.20a-f. IL-1β, IL-6 and TNF-α were not detected in the culture medium at 24 after transfection of AtT20 cells with any of the three POMC siRNAs; concentrations of all three cytokines were below the limit of detection in pg/ml, including untreated cells. In contrast, IL-1β, IL-6 and TNF-α were secreted by AtT20 cells transfected with poly-I:C reaching a concentration at 24 h of 571 ± 85 pg/ml, 362 ± 72 pg/ml, and 773 ± 90 pg/ml, respectively. Transfection of AtT20 cells with poly-I:C alone, siRNAs alone or transfection reagent alone failed to stimulate IL-1β, IL-6, and TNF-α secretion.

(a)

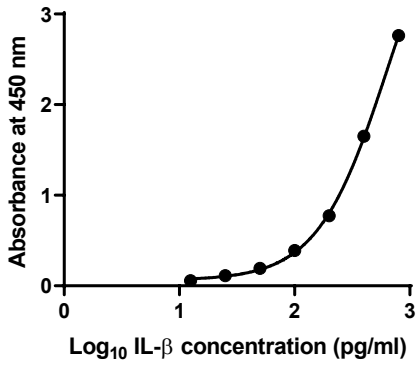

(b)

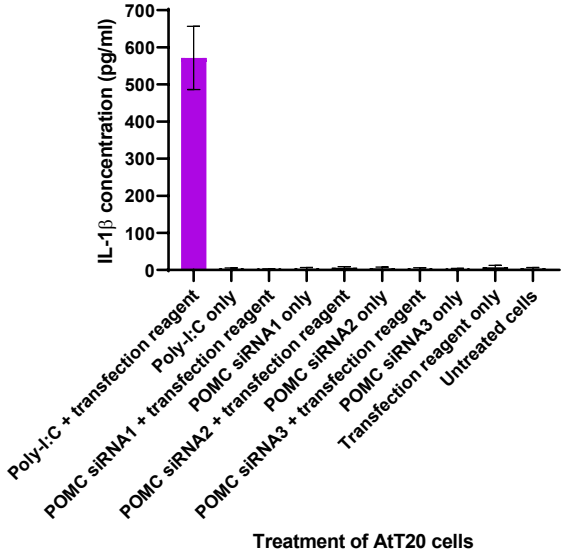

Figure 3.20a-b: Concentrations of IL-1β, IL-6, and TNF-α secreted by AtT20 cells after transfection with POMC siRNAs and poly-I:C.

(a) Example standard curve for IL-1β ELISA. The log10 of the concentration of a panel of standards of IL-1β were plotted against the mean absorbance values at 450 nm. (b) AtT20 cells were transfected with POMC siRNAs at 30 nM or poly-I:C at 7.5 µg/ml. The levels of IL-1β were measured in the culture medium after 24 h. Control treatments used were transfection reagent alone, siRNAs alone, and poly-I:C alone. Untreated cells were also included. The results show the mean (± SD) IL-1β concentrations measured in three separate experiments.

(c)

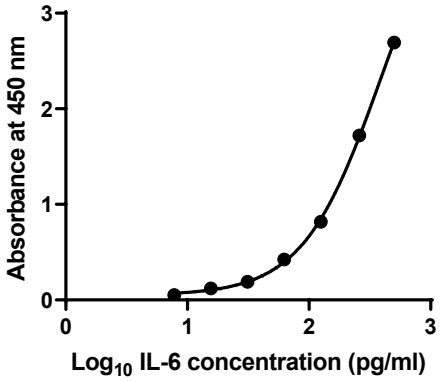

(d)

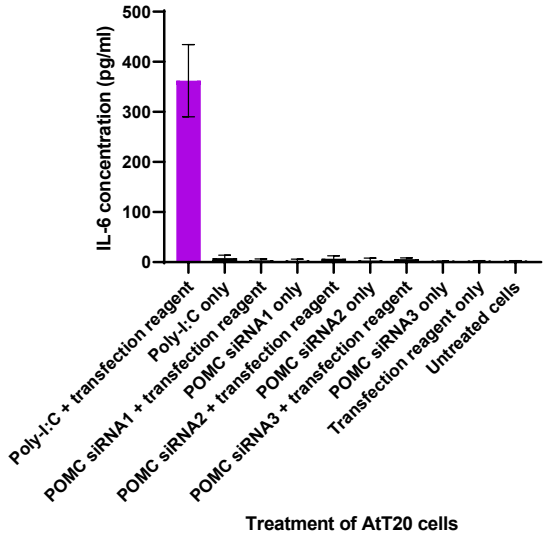

Figure 3.20c-d: Concentrations of IL-1β, IL-6, and TNF-α secreted by AtT20 cells after transfection with POMC siRNAs and poly-I:C.

(c) Example standard curve for IL-6 ELISA. The log10 of the concentration of a panel of standards of IL-6 were plotted against the mean absorbance values at 450 nm. (d) AtT20 cells were transfected with POMC siRNAs at 30 nM or poly-I:C at 7.5 µg/ml. The levels of IL-6 were measured in the culture medium after 24 h. Control treatments used were transfection reagent alone, siRNAs alone, and poly-I:C alone. Untreated cells were also included. The results show the mean (± SD) IL-6 concentrations measured in three separate experiments.

(e)

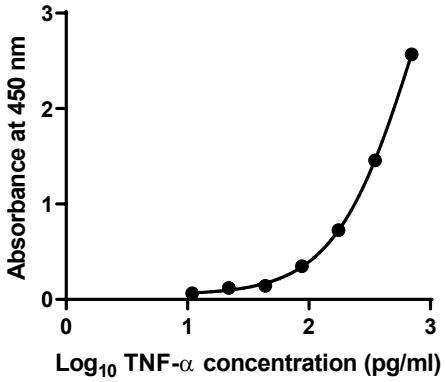

(f)

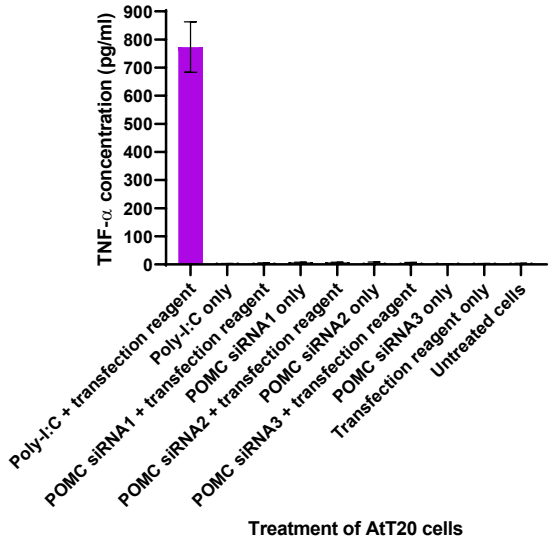

Figure 3.20e-f: Concentrations of IL-1β, IL-6, and TNF-α secreted by AtT20 cells after transfection with POMC siRNAs and poly-I:C.

(e) Example standard curve for TNF-α ELISA. The log10 of the concentration of a panel of standards of TNF-α were plotted against the mean absorbance values at 450 nm. (f) AtT20 cells were transfected with POMC siRNAs at 30 nM or poly-I:C at 7.5 μg/ml. The levels of TNF-α were measured in the culture medium after 24 h. Control treatments used were transfection reagent alone, siRNAs alone, and poly-I:C alone. Untreated cells were also included. The results show the mean (± SD) TNF-α concentrations measured in three separate experiments.

3.4 Discussion

The aim of this part of the project was to determine how effective three POMC siRNAs were at suppressing the secretion of ACTH from AtT20 cells. The latter can be used as an *in vitro* model of Cushing's disease, as they produce ACTH into their culture medium, and the effectiveness of novel treatments that may modulate secretion of the hormone can therefore be assessed. Previously, all three POMC siRNAs had been shown to reduce secretion of ACTH from AtT20 cells (Munir, 2012), and the results here confirmed these initial findings; POMC siRNA1, 2, and 3 reduced the concentration of ACTH in the culture medium of AtT20 cells to 15.6%, 18.1%, and 10.6%, respectively, of that secreted from untreated cells.

Several important controls were used in transfection experiments to ensure that valid conclusions could be made with regard to the specific silencing effects of the POMC siRNAs. A FITC-labelled oligonucleotide was always used to ensure that the AtT20 cells were transfectable; a transfection efficiency of 76.5% ± 11.8% (mean ± SD) was obtained and this seemed to be great enough to make certain that lower concentrations of siRNA were taken up by the cells. The possibility that the Lipofectamine 2000 transfection reagent was cytotoxic and therefore responsible for the reduction in ACTH was also investigated. However, cell counting experiments indicated that there was no statistically significant difference between the number of viable cells in Lipofectamine 2000-treated and untreated groups. Other controls included transfections with siRNAs that were not expected to silence POMC; cyclophilin B, GAPDH, and ON-TARGETplus non-targeting siRNAs. None of these siRNAs knocked-down the expression of ACTH indicating that the effects of the POMC siRNAs were not due to a non-specific consequence of transfecting AtT20 cells with dsRNA.

To determine if alterations in the POMC siRNAs 1, 2, and 3 were able to adversely affect their POMC gene-silencing ability, changes were made to the siRNA sequences. The siRNA seed region (nucleotides 2-8), the splice site (nucleotides 10-11) and nucleotide 16 are the least tolerant of mismatches because of their active role in gene silencing. The first nucleotide, the nucleotides of the 3'-overhang (nucleotides 20-21), and nucleotides 17-19 are the most tolerant of mismatches because their ability to base pair is at least partially blocked by Ago2. Mismatches are tolerated, but not

favoured at nucleotides 9 and 12-15. Mismatched bases in all three POMC siRNA molecules were created at positions 2, 4, 6, 10, and 19 of the antisense strand. In addition, scrambled versions of all three POMC siRNAs were designed to ensure that their effects upon ACTH secretion were not due to their specific base composition.

Neither the scrambled nor the mismatched POMC siRNA variants caused a reduction in ACTH secretion from AtT20 cells in comparison to untreated cells. Thus, it can be concluded that the POMC siRNAs with their particular sequences were having a specific effect upon POMC expression.

Previous observations have been made that siRNAs can cause immune responses and off-target effects (Sledz et al., 2003). Coupled with a high cost of production, it would therefore be prudent to avoid high siRNA concentrations and use the lowest effective dose. The results indicated that 30 nM and 10 nM of all three POMC siRNAs produced a prolonged reduction in the level of ACTH secretion from AtT20 cells. Post-transfection, this effect lasted up to 96 h. For POMC siRNA2, 1 nM also had an effective gene-silencing effect of up to 96 h. For POMC siRNA3, the results are compatible of those found before (Munir, 2012).

In conclusion, the three POMC siRNAs were effective at silencing POMC expression in AtT20 cells. They gave a statistically significant reduction in the amount of ACTH secreted by the cells in culture. The results indicated that siRNAs against POMC could form the basis of an effective therapeutic for Cushing's disease by specifically reducing ACTH expression from pituitary corticotrophs.

To test the ability of the POMC siRNAs to stimulate the innate immune response in AtT-20 cells, samples of culture medium were taken after transfection and assayed using ELISAs for the presence of IFN-α and IFN-β, and pro-inflammatory cytokines IL-1β, IL-6, and TNF-α. An immunostimulatory siRNA-IS (Sioud, 2005) and poly-I:C (Kumagai et al., 2010; Dauletbaev et al., 2015) were also used in experiments as these molecules were expected to stimulate an innate immune response. Other control treatments of AtT20 cells were transfection reagent alone and siRNA or poly-I:C alone. Untreated cells were used to analyse any baseline secretion of interferon or pro-inflammatory cytokines.

The results suggested that treatment of AtT20 cells with POMC siRNAs did not stimulate an innate immune response. However, the cells were able to produce interferon and pro-inflammatory cytokines when treated with poly-I:C indicating that the necessary signaling pathways are present in the AtT20 cell line. Currently, it is not known which RNA receptors are responsible for detecting and responding to poly-I:C in AtT20 cells. They have been shown to express TLR-3 (Iwasaki et al., 2008), which could detect poly-I:C (Figure 3.18). Similar to other cell types (Whitehead et al., 2011), it is also likely that AtT20 cells express cytoplasmic receptors such as PKR, RIG-1, and MAD5 (Figure 3.18) that could recognise and respond to the presence of poly-I:C (Figure 3.18). The TLR-3 signaling pathway could detect endosome-trafficked siRNAs independent of their sequence. However, there was no evidence that the POMC siRNAs used in this study initiated an innate immune response This may be due to their length (21 nucleotides); a previous report has demonstrated that siRNAs of more than 23 base pairs can activate the interferon response via TLR-3 (Reynolds et al., 2006).

Although the preliminary data suggests that POMC siRNAs do not stimulate an innate immune response in their target cells, only one siRNA concentration (30 nM) was tested and the culture medium was only sampled at one time-point (24 h). It may be that increased the sampling time could raise the potential of detecting an immune response. In addition, the results would need to be confirmed in human pituitary corticotrophs in which the expression of TLR-3 has been reported (Green et al., 1996; Zheng et al., 2016) and which may not respond in an identical way to AtT20 cells.

Furthermore, the effect of the POMC siRNAs on immune cells such as monocytes, dendritic cells and macrophages requires study, as they express TLR-7 and TLR-8. These endosome RNA receptors recognise and instigate an innate immune response against siRNA which is sequence-dependent (Whitehead et al., 2011). Indeed, several immunostimulatory motifs 5′-UGU-3′, 5′-UGUGU-3′, 5’-UGGC-3’ and 5’-GUCCUUCAA-3’ have been identified that stimulate the production of interferons and/or TNF-α (Hornung et al., 2005; Judge et al., 2005). The motif 5’-UGU-3’ is present in the sense strand of POMC siRNA1 (5’-GAUGCCGAGAUUCUGCUACUU-3’) and in the anti-sense strand of POMC siRNA2 (5’-GAAGUGACCCAUGUCGUACUU-3’). The motif 5’-UGGC-3’ is part of the anti-sense strand of POMC siRNA3 (5’-

GUUCUUGAUGAUGGCGUUCUU-3'). Analysis of the effects of each POMC siRNA in an *in vivo* setting where immune cells are encountered would therefore be particularly important. Clinically, the results of hyperstimulating an innate immune response in patients can have serious consequences inducing low blood pressure, chills and fever (Michie et al., 1988). The outcome of a cytokine storm can include cardiovascular shock, respiratory distress syndrome, and possibly death (Suntharalingam et al., 2006). Such dangerous side-effects, mean it is critical to research and control any immunostimulatory effects when using siRNA in both animal models and in clinical trials involving human patients.

Chapter 4

Analysis of the expression of corticotrophin-releasing hormone receptor 1 on AtT20 cells

4 Analysis of the expression of corticotrophin-releasing hormone receptor 1 on AtT20 cells

4.1 Introduction

There are several challenges to the delivery of siRNA *in vivo* and these have been discussed previously in Section 1.5.3. One drawback is a lack of cell specificity which can lead to off-target effects occurring if siRNA molecules enter the wrong cell-type (Snove and Holen, 2004). Cell membrane receptors that have restricted tissue expression may be effective for delivering siRNAs that have been coupled to either the receptor's peptide ligand or to an antibody against the specific receptor (Tam et al., 2017).

For the treatment of Cushing's disease with anti-POMC siRNAs, the CRHR1 is a potential target for their delivery. The receptor is mainly expressed on anterior pituitary corticotroph cells (Aguilera et al., 2004). It is also endocytosed when the extracellular domain interacts and binds to its peptide ligand CRH (dos Santos Claro et al., 2019), indicating that it may internalise any siRNA conjugated to the hormone.

The CRHR1 is an important regulator of neuroendocrine, behavioral, and autonomic response to stress, and is essential for the activation of signal transduction pathways that regulate diverse physiological processes including stress, reproduction, immune responses and obesity (Reul and Holsboer, 2002). Dysregulation of CRHR1 and its ligand CRH has been causally linked to stress-related pathologies including mood and anxiety disorders (Holsboer, 2000).

The CRHR1 is a G protein-coupled receptor (GPCR) of the B1 family. It has seven transmembrane domains, an N-terminal extracellular domain, three extracellular domain loops, and an intracellular C-terminal (Figure 4.1). On activation by CRH, the receptor preferentially signals via Gsα resulting in the activation of the adenylyl cyclase/protein kinase A pathway (Figure 4.2) (Hauger et al., 2002; Grammatopoulos et al., 2009). However, depending on its cellular localisation and context, CRHR1 can activate multiple G proteins which can trigger alternative second messengers like cAMP (Grammatopoulos et al., 2002). For example, the coupling of CRHR1 to Gsα can activate the extracellular signal-regulated kinases 1 and 2 (ERK1/2) signaling

pathway which can also be activated by Gqα (Figure 4.2) (Papadopoulou, et al., 2004; Refojo et al., 2005).

The CRHR1 gene contains at least 14 exons spanning 20 kb of genomic DNA. The CRHR1 isoforms appear to originate from the same gene by alternative splicing which results in multiple transcript variants. The isoform with the highest CRH affinity and the ability to transduce the highest cAMP accumulation in response to CRH binding is encoded by 13 exons and excludes exon 6 (Sakai et al., 1998). The gene was mapped the CRHR gene to chromosome 17 and sublocalised to 17q12-q22 (Polymeropoulos et al., 1995).

However, although AtT20 cells, the model system used in the current work, have been reported to respond to simulation by CRH, indicating the presence of CRHR1 (Gagner and Drouin, 1987; Bugarini et al., 2017), there has not been confirmation by other experimental methods that the cell line expresses the receptor to a high level.

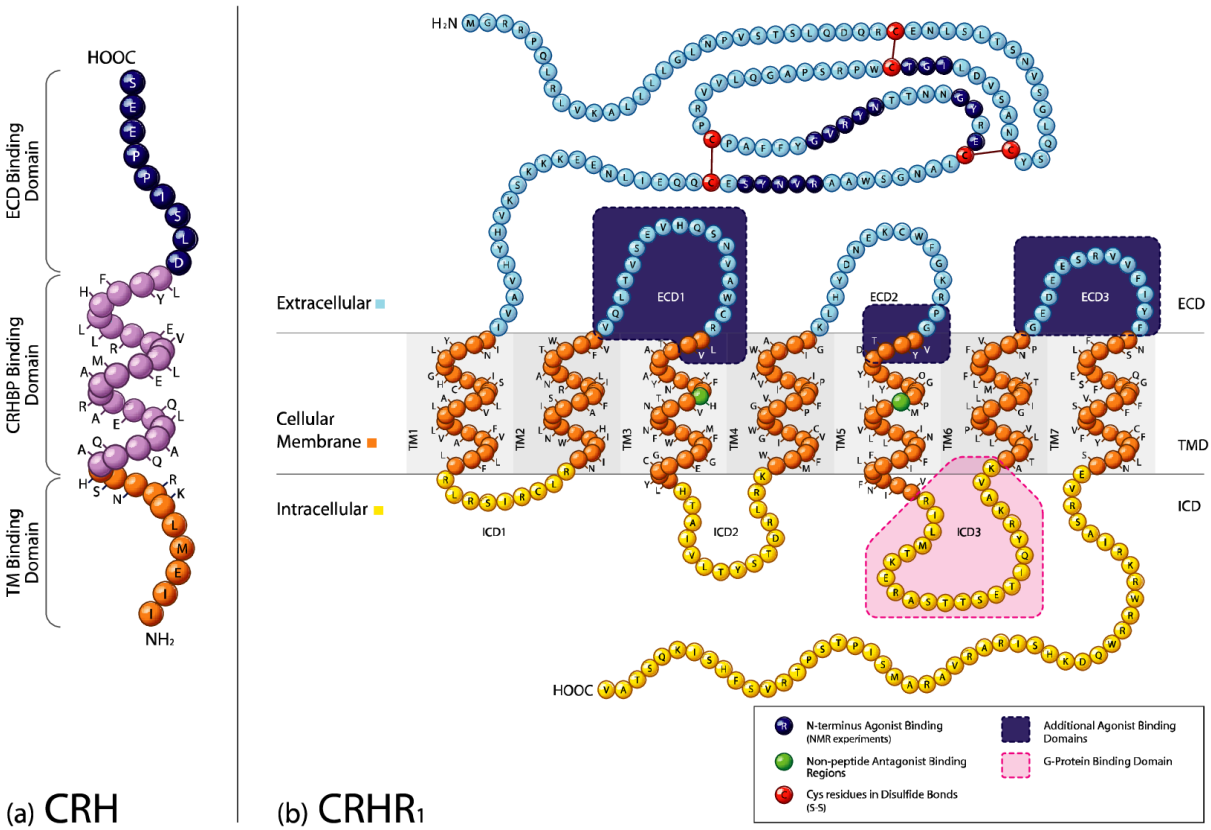

Figure 4.1: Schematic diagram of the corticotropin-releasing hormone receptor type 1.

(a)Structure of the corticotropin-releasing hormone receptor (CRH). (b)The corticotropin-releasing hormone receptor type 1 (CRHR1) is a G protein-coupled receptor (GPCR) of the B1 family that binds ligand CRH. It has seven transmembrane domains, an N-terminal extracellular domain, three extracellular domain loops, and an intracellular C-terminal. The image, from a paper by Hemley et al. (2007), is used with kind permission from Bentham Science Publishers.

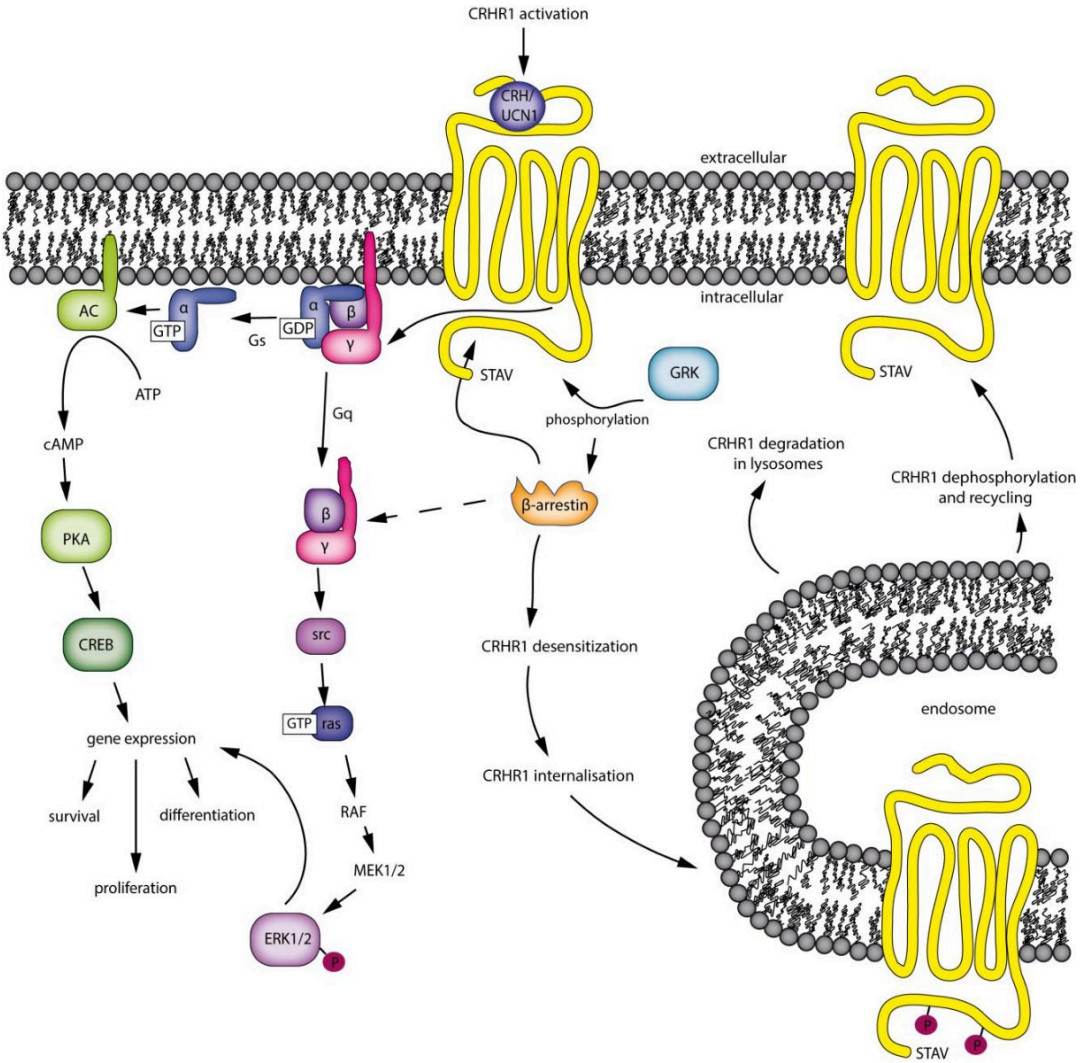

Figure 4.2: Corticotropin-releasing hormone receptor type 1 signalling pathways.

AC, adenylyl cyclase; ATP, adenosine triphosphate; cAMP, cyclic adenosine monophosphate; CREB, cAMP response element-binding protein; CRH, corticotropin-releasing hormone; ERK1/2, extracellular signal-regulated kinase 1/2; GDP, guanosine diphosphate; GRK, G protein-coupled kinases; GTP, guanosine triphosphate; MEK, mitogen-activated protein kinase; PKA, protein kinase A; UCN1, urocortin 1. The image, from a thesis by Bender (2015), is used with kind permission from the University of Munich (Munich, Germany).

4.2 Aims

The aim of this part of the work was to investigate if AtT20 cells express the CRHR1. The specific objectives were:

- To detect CRHR1 mRNA in AtT20 cells.
- To detect the receptor on AtT20 cells using stimulation with CRH.
- To detect the receptor on the surface of AtT20 cells using indirect FACS with different anti-CRHR1 antibodies.

4.3 Results

4.3.1 Detecting CRHR1 mRNA in AtT20 cells

Initially, the presence of CRHR1 mRNA in AtT20 cells was investigated by employing RT-PCR amplification.

4.3.1.1 RNA and cDNA preparation

Both RNA and cDNA were prepared from AtT20 cells as previously detailed in Sections 2.3.1 and 2.3.2, respectively. The RT reactions (with and minus RT) were then used as templates for PCR amplification using CRHR1-specific primers CRHR1-Forward and CRHR1-Reverse (Table 2.3).

4.3.1.2 PCR amplification

The CRHR1-specific primers CRHR1-Forward and CRHR1-Reverse (Table 2.3) were designed as intron-skipping primers (Figure 4.3) to avoid the amplification of any genomic DNA that might be contaminating RNA preparations. The primers were also designed to be specific for mouse and human CRHR1 and had no homology to other gene sequences. The expected size of the PCR product was 199 base pairs. Positive control intron-skipping primers were for S15 (Table 2.3). They gave a 361-base pair when used in PCR amplification reactions (Figure 4.4) and were included in PCR experiments to check the integrity of the cDNA samples.

PCR amplification experiments were set up as detailed in the RETROscript Kit protocol (Section 2.3.3) using either CRHR1-specific or S15-specific primers. Two controls were included in PCR amplification experiments. Firstly, a reaction without any template, but with primers, to verify that none of the PCR reagents were contaminated with DNA. Secondly, a reaction that included a minus RT sample to check for contaminating genomic DNA. Following PCR for 35 cycles, the PCR products were analysed by agarose gel electrophoresis, and the results are shown in Figure 4.4.

DNA fragments of the expected length were seen in the gel lanes corresponding to PCR reactions containing CRHR1 primers (199 base pairs) or S15 primers (361 base pairs). No DNA products were visible in gel lanes loaded with PCR reactions containing either no template or a minus RT sample. Both the controls indicated that

the amplified products were not a result of contaminated reagents or contaminating genomic DNA, respectively. Overall, the results indicated that the AtT20 cells expressed CRHR1 mRNA.

4.3.1.3 PCR product sequencing

To confirm that the CRHR1 PCR product was correct, the DNA fragment was extracted from an agarose gel and purified according to a Wizard PCR Preps DNA Purification System. The purified PCR product was sequenced using the CRHR1-Forward and CRHR1-Reverse primers (Table 2.3; Figure 4.3). The results that are shown in Figure 4.5 confirmed that the sequenced PCR product was the correct one when compared with the expected POMC sequence.

Figure 4.3: Mouse and human CRHR1 sequences indicating the positions of intron-skipping CRHR1 primers.

The positions of the CRHR1-Forward (in exon 6) and CRHR1-Reverse (in exon 7) intron-skipping PCR amplification primers are underlined.

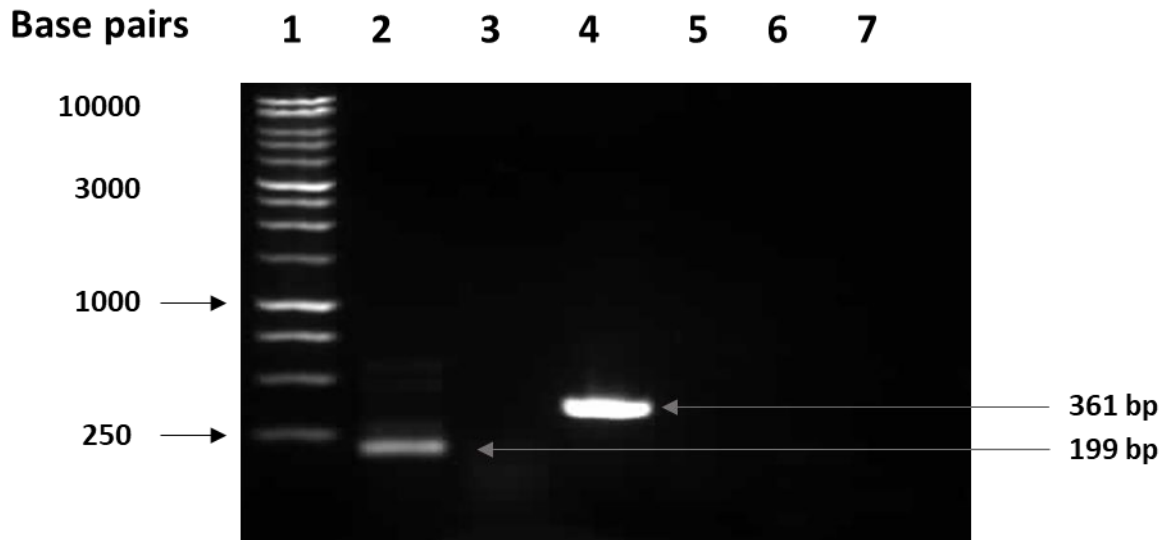

Figure 4.4: Agarose gel electrophoresis of PCR amplification products.

PCR amplification products were electrophoresed in a 1% agarose gel. Lane 1, 1-kb DNA ladder; Lane 2, AtT20 cDNA with CRHR1 primers. The expected size was 199 base pairs (bp); Lane 3, minus RT sample with CRHR1 primers; Lane 4, AtT20 cDNA with S15 primers, used as a control to check cDNA integrity. The expected size was 361 base pairs (bp); Lane 5, minus RT sample with S15 primers; Lane 6, CRHR1 primers only without any cDNA template; Lane 7, S15 primers only without any cDNA template.

Figure 4.5: CRHH1 DNA sequence alignments.

Alignment of the CRHR1 DNA sequence with the DNA sequence of the purified PCR product from amplification of AtT20 cDNA with CRHR1-specific primers.

4.3.2 Detecting the CRHR1 on AtT20 cells using CRH-stimulation and ACTH measurement

The RT-PCR experiment detected mRNA for CRHR1 in the AtT20 cell line. However, although the detected mRNA appeared specific for the receptor, it was necessary to assess if the CRHR1 was itself present on the surface of the AtT20 cells. This assessment was carried out using stimulation with the receptor's ligand CRH which would be expected to lead to an increase in the secretion of ACTH over and above the normal basal level.

AtT20 cells were plated in 6-well plates at 1 x 10^5 cells per well. Each plate contained three wells that would receive treatment and three that would remain untreated. After 48 h, the cells were washed three times with culture medium and then incubated for 1 h in 2 ml of culture medium without antibiotics. From each well, 30 µl of the culture medium was collected for ACTH quantification using an Immulite 2000 ACTH immunoassay. This was to provide a basal level of ACTH secretion. Cells were then stimulated with 100 nM CRH, 100 nM MCH or left untreated. At 0.5, 2, 4, 6, 8, and 24 h, 30 µl of the culture medium were removed for analysis using an Immulite 2000 ACTH immunoassay.

The results of three separate experiments are given in Figure 4.6. They indicated that AtT20 cells responded to CRH-stimulation with a statistically significant increase in ACTH secretion at time points from 4, 6, and 8 h compared with stimulation with MCH or no stimulation at all (One-way ANOVA, P = 0.0013, P = 0.0011, P = 0.0337, respectively). The results demonstrated a correlation between CRH-stimulation and secretion of ACTH, indicating that the functional receptors for CRH were present on AtT20 cells.

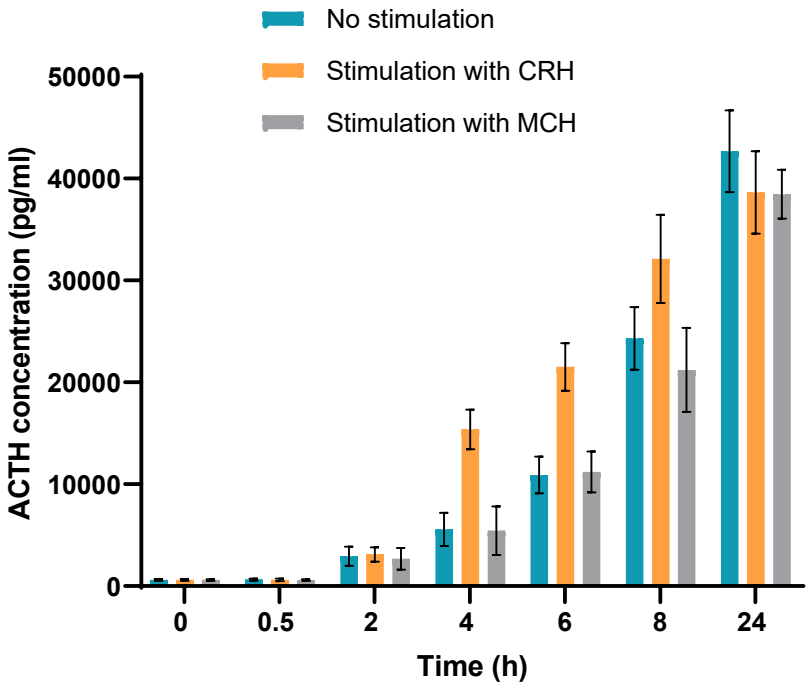

Figure 4.6: Stimulation of AtT20 cells with corticotropin-releasing hormone with ACTH measurement.

AtT20 cells were then stimulated with 100 nM corticotropin-releasing hormone (CRH), 100 nM melanin-concentrating hormone (MCH) or left untreated. At 0.5, 2, 4, 6, 8, and 24 h, 30 µl of the culture medium were removed for analysis using an Immulite 2000 ACTH immunoassay. The results of three separate experiments are shown. They indicated that AtT20 cells responded to CRH-stimulation with a statistically significant increase in ACTH secretion at time points from 4, 6, and 8 h compared with stimulation with MCH or no stimulation at all (One-way ANOVA, $P = 0.0013$, $P = 0.0011$, $P = 0.0337$, respectively).

4.3.3 Detecting the CRHR1 on AtT20 cells using CRH-stimulation and cAMP measurement

AtT20 cells were plated in 96-well plates at 1 x 10^3 cells per well. They were then treated with CRH, MCH or forskolin as detailed in Section 2.8.1. The accumulation of cAMP was then assayed using a cAMP enzyme immunoassay as detailed in Section 2.8.2.

The results in Figure 4.7 showed that AtT20 cells responded to CRH-stimulation as accumulation of cAMP was evident. The cells did not respond to stimulation by MCH peptide which is a ligand for the melanin-concentrating hormone receptor 1. The cells also accumulated cAMP in response to forskolin treatment.

(a)

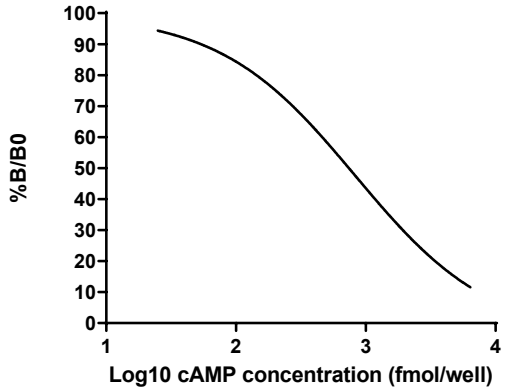

(b)

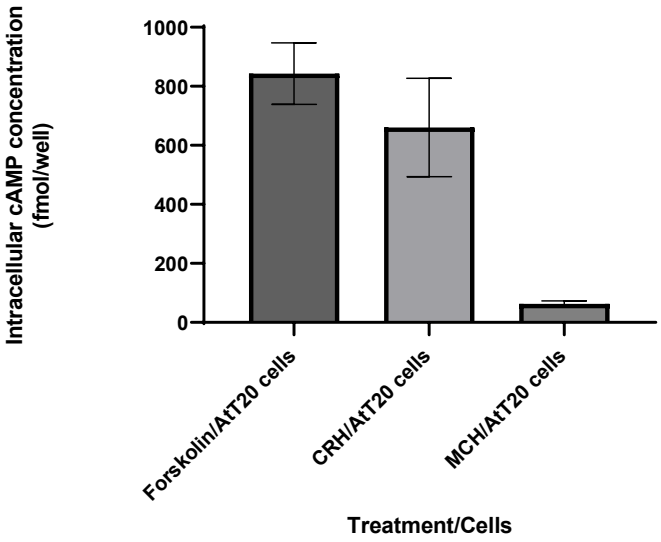

Figure 4.7: Stimulation of AtT20 cells with corticotropin-releasing hormone with cAMP measurement.

In (a) An example of a standard curve for determination of cAMP concentration. Percentage cAMP-HRP bound (%B/B0) in the ELISA plotted against $\log_{10}$ of the cAMP concentration in the standards. (b) AtT20 cells were treated with 3-isobutyl-1-methylxanthine (IBMX) and corticotropin-releasing hormone (CRH), melanin-concentrating hormone (MCH) or forskolin. Intracellular cAMP was measured in a cAMP Enzyme Immunoassay. The results show the mean (± SD) intracellular cAMP concentration in fmol/well from three experiments.

4.3.4 Detecting the CRHR1 on AtT20 cells using indirect FACS

The results of CRH-stimulation confirmed that CRHR1 receptors were present on AtT20 cells. In addition, it was necessary to investigate if the receptor was detectable by FACS, as this would allow the testing of the applicability of anti-CRHR1 antibodies to deliver conjugated POMC siRNA molecules.

Expression of the CRHR1 on AtT20 cells was analysed using an indirect FACS staining method. Indirect labelling requires two incubation steps; the first with a primary antibody followed by a compatible secondary antibody which allows signal amplification. Three primary antibodies were available for use in the FACS experiments to detect surface-expressed CRHR1. Two were polyclonal antibodies against extracellular domain peptides of the human CRHR1 (Table 2,7; Figure 4.8) that were cross-reactive with the mouse receptor, according to the manufacturer's data. The third was a mouse antibody that had been raised against amino acids 24-415 of the human CRHR1 (Table 2,7; Figure 4.8). No data regarding cross-reactivity with the mouse receptor was available from the supplier.

Indirect FACS experiments were undertaken out as described in Section 2.6. with secondary antibodies used at the concentrations given in Table 2.7. As well as the primary and secondary antibody-treated cell samples, experiments included AtT20 cells that were left untreated in order to determine background fluorescence. Cells stained with only secondary antibody were also included to identify any binding that was non-specific. Before the cell samples were treated with primary and/or secondary antibody, they were pre-incubated with a Fc-blocking antibody (Table 2.7) that binds to Fc receptors CD16 and CD32 on the cell surface. The blocking interaction stops the binding of primary and secondary antibodies via their constant regions to the Fc receptors.

4.3.4.1 Indirect FACS with mouse anti-CRHR1 antibody

The results of duplicate samples of one representative indirect FACS experiment are shown in (Figure 4.9). Unstained AtT20 cells showed that 0% of cells were fluorescing (Figure 4.9a). Fluorescence was 2.5% and 8.8% in cell samples stained with only secondary donkey anti-mouse IgG-Alexa Fluor®488 antibody (Figure 4.9b). Cells stained with primary mouse anti-CRHR1 antibody and secondary donkey anti-mouse

IgG-Alexa Fluor®488 antibody resulted in 14.3% and 13.3% of cells being fluorescently-labelled (Figure 4.9c).

A summary of the results of two separate experiments is given in Table 4.1. The results indicated that there was only a small difference in the percentage of fluorescing AtT20 cells when comparing the staining with secondary antibody alone and the staining with both primary and secondary antibodies.

```
Human   1    MGGHPQLRLVKALLLLGLNPVSASLQDQHCESLSLASNISGLQCNASVDLIGTCWPRSPA  60
Mouse   1    MGQRPQLRLVKALLLLGLNPVSTSLQDQQCESLSLASNVSGLQCNASVDLIGTCWPRSPA  60
Human   61   GQLVVRPCPAFFYGVRYNTTNNGYRECLANGSWAARVNYSECQEILNEEKKSKVHYHVAV  120
Mouse   61   GQLVVRPCPAFFYGVRYNTTNNGYRECLANGSWAARVNYSECQEILNEEKKSKVHYHIAV  120
Human   121  IINYLGHCISLVALLVAFVLFLRLRPGCTHWGDQADGALEVGAPWSGAPFQVRRSIRCLR  180
Mouse   121  IINYLGHCISLVALLVAFVLFLRLR----------------------------SIRCLR  151
Human   181  NIIHWNLISAFILRNATWFVVQLTMSPEVHQSNVGWCRLVTAAYNYFHVTNFFWMFGEGC  240
Mouse   152  NIIHWNLISAFILRNATWFVVQLTVSPEVHQSNVAWCRLVTAAYNYFHVTNFFWMFGEGC  211
Human   241  YLHTAIVLTYSTDRLRKWMFICIGWGVPFPIIVAWAIGKLYYDNEKCWFGKRPGVYTDYI  300
Mouse   212  YLHTAIVLTYSTDRLRKWMFVCIGWGVPFPIIVAWAIGKLYYDNEKCWFGKRPGVYTDYI  271
Human   301  YQGPMILVLLINFIFLFNIVRILMTKLRASTTSETIQYRKAVKATLVLLPLLGITYMLFF  360
Mouse   272  YQGPMILVLLINFIFLFNIVRILMTKLRASTTSETIQYRKAVKATLVLLPLLGITYMLFF  331
Human   361  VNPGEDEVSRVVFIYFNSFLESFQGFFVSVFYCFLNSEVRSAIRKRWHRWQDKHSIRARV  420
Mouse   332  VNPGEDEVSRVVFIYFNSFLESFQGFFVSVFYCFLNSEVRSAIRKRWRRWQDKHSIRARV  391
Human   421  ARAMSIPTSPTRVSFHSIKQSTAV  444
Mouse   392  ARAMSIPTSPTRVSFHSIKQSTAV  415
```

Figure 4.8: Target peptide sequences of anti-CRHR1 antibodies.

The sequences against which rabbit anti-CRHR1 antibody (amino acids 55-150) and goat anti-CRHR1 antibody (amino acids 107-117) are highlighted in blue and yellow, respectively. The mouse anti-CRHR1 antibody was raised against a peptide consisting of amino acids 24-415 of the human CRHR1 sequence.

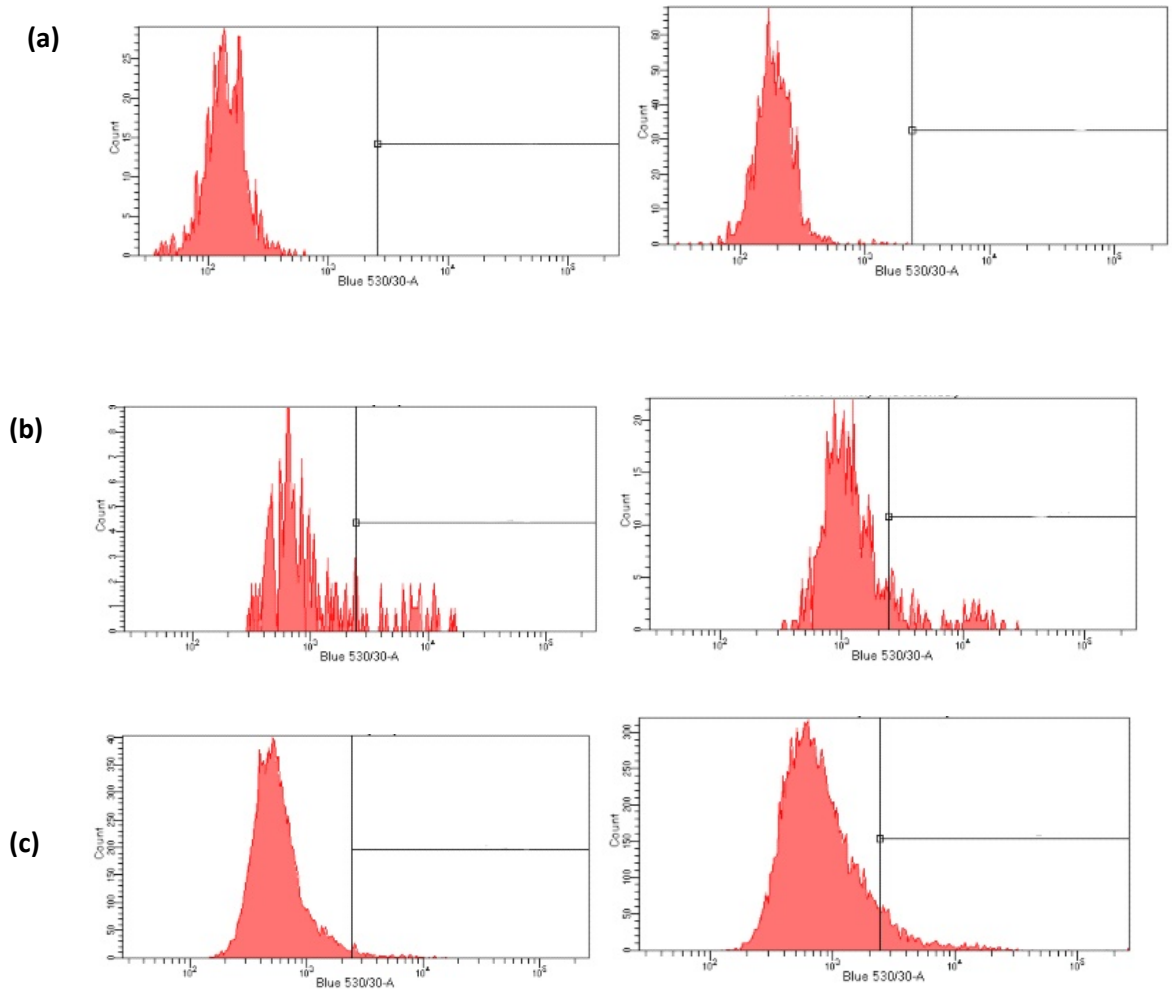

Figure 4.9: Indirect FACS analysis for CRHR1 expression on AtT20 cells using a mouse anti-CRHR1 (amino acids 24-415) antibody.

Duplicate samples showing (a) Unstained AtT20 cells (0% and 0.01%. fluorescently-labelled cells); (b) AtT20 cells stained with secondary donkey anti-mouse IgG-Alexa Fluor®488 antibody (2.5% and 8.8% fluorescently-labelled cells); (c) AtT20 cells stained with mouse anti-CRHR1 (amino acids 24-415) antibody and secondary donkey anti-mouse IgG-Alexa Fluor®488 antibody (14.3% and 13.3% fluorescently-labelled cells).

Table 4.1: Results summary of indirect FACS staining of AtT20 cells with mouse anti-CRHR1 (amino acids 24-415) antibody

	Fluorescing AtT20 cells as a percentage of total cells		
Experiment	Mouse anti-CRHR1 (amino acids 24-415) antibody and secondary donkey anti-mouse IgG-Alexa Fluor®488 antibody	Secondary donkey anti-mouse IgG-Alexa Fluor®488 antibody	Unstained
1	13.8%[1]	5.7%[1]	0.0%[1]
2	13.1%[2]	5.4%[2]	0.0%[2]

[1]Data are the mean of duplicate samples within the same experiment.

[2]Data are for one sample within the same experiment.

4.3.4.2 Indirect FACS with rabbit and goat anti-CRHR1 antibodies

Expression of the CRHR1 on AtT20 cells was further analysed using indirect FACS, with different antibody pairs. The primary antibody used was either a rabbit anti-CRHR1 antibody against amino acids 55-150 of the human CRHR1 (Figure 4.8; Table 2.7) or a goat anti-CRHR1 antibody against human CRHR1 (amino acids 107-117) (Figure 4.8; Table 2.7). Both antibodies were expected to be cross-reactive with the mouse receptor. The secondary antibodies used were goat anti-rabbit IgG conjugated to Alexa Fluor®488 (Table 2.7), and rabbit anti-goat IgG conjugated to Alexa Fluor®488 (Table 2.7), respectively. They were used at a 1:1000 dilution in FACS staining, and indirect FACS experiments were undertaken as described earlier in this section.

The results of duplicate samples of one indirect FACS experiment using the rabbit anti-CRHR1 (amino acids 55-150) antibody are shown in (Figure 4.10). Unstained AtT20 cells showed that 0% of cells were fluorescing (Figure 4.10a). Fluorescence was 5.4% and 3.4% in cell samples stained with only secondary goat anti-rabbit IgG-Alexa Fluor®488 antibody (Figure 4.10b). Cells stained with primary rabbit anti-CRHR1 (amino acids 55-150) antibody and secondary goat anti-rabbit IgG-Alexa Fluor®488 antibody resulted in 4.9% and 3.3% of cells being fluorescently-labelled causing a small shift to the right on the FACS histogram (Figure 4.10c).

The results of duplicate samples of one indirect FACS experiment using the goat anti-CRHR1 (amino acids 107-117) antibody are shown in (Figure 4.11). Unstained AtT20 cells showed that 0% of cells were fluorescing (Figure 4.11a). Fluorescence was 3.3% and 3.5% in cell samples stained with only secondary rabbit anti-goat IgG-Alexa Fluor®488 antibody (Figure 4.11b). Cells stained with primary goat anti-CRHR1 (amino acids 107-117) antibody and secondary rabbit anti-goat IgG-Alexa Fluor®488 antibody resulted in 6.1% and 4.6% of cells being fluorescently-labelled causing a small shift to the right on the FACS histogram (Figure 4.11c).

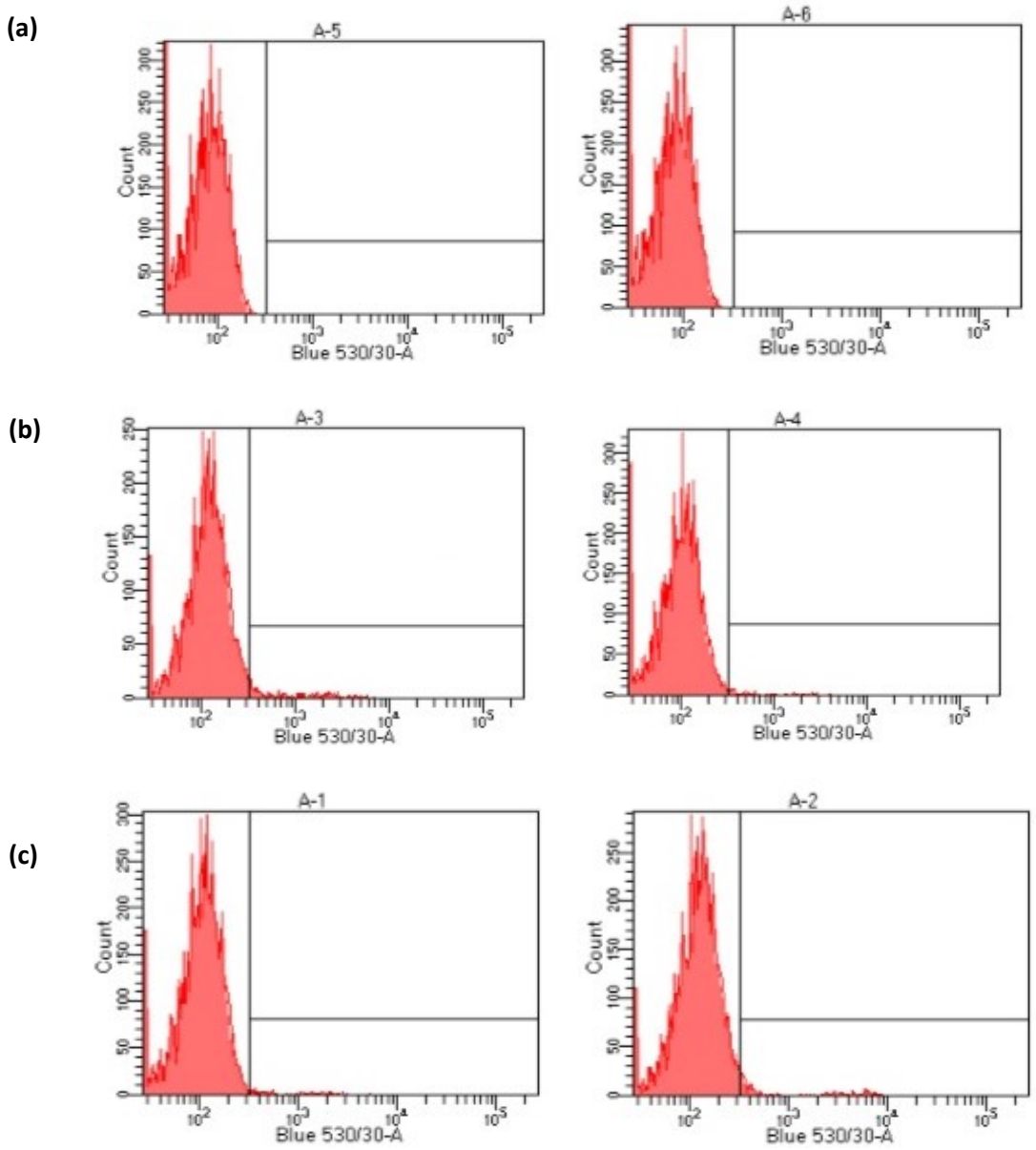

Figure 4.10: Indirect FACS analysis for CRHR1 expression on AtT20 cells using a rabbit anti-CRHR1 (55-150) antibody.

Duplicate samples showing (a) Unstained AtT20 cells (0% and 0% fluorescently-labelled cells); (b) AtT20 cells stained with secondary goat anti-rabbit IgG-Alexa Fluor®488 antibody (5.4% and 3.4% fluorescently-labelled cells); (c) AtT20 cells stained with primary rabbit anti-CRHR1 (55-150) antibody and secondary goat anti-rabbit IgG-Alexa Fluor®488 antibody (3.3% and 4.9% fluorescently-labelled cells).

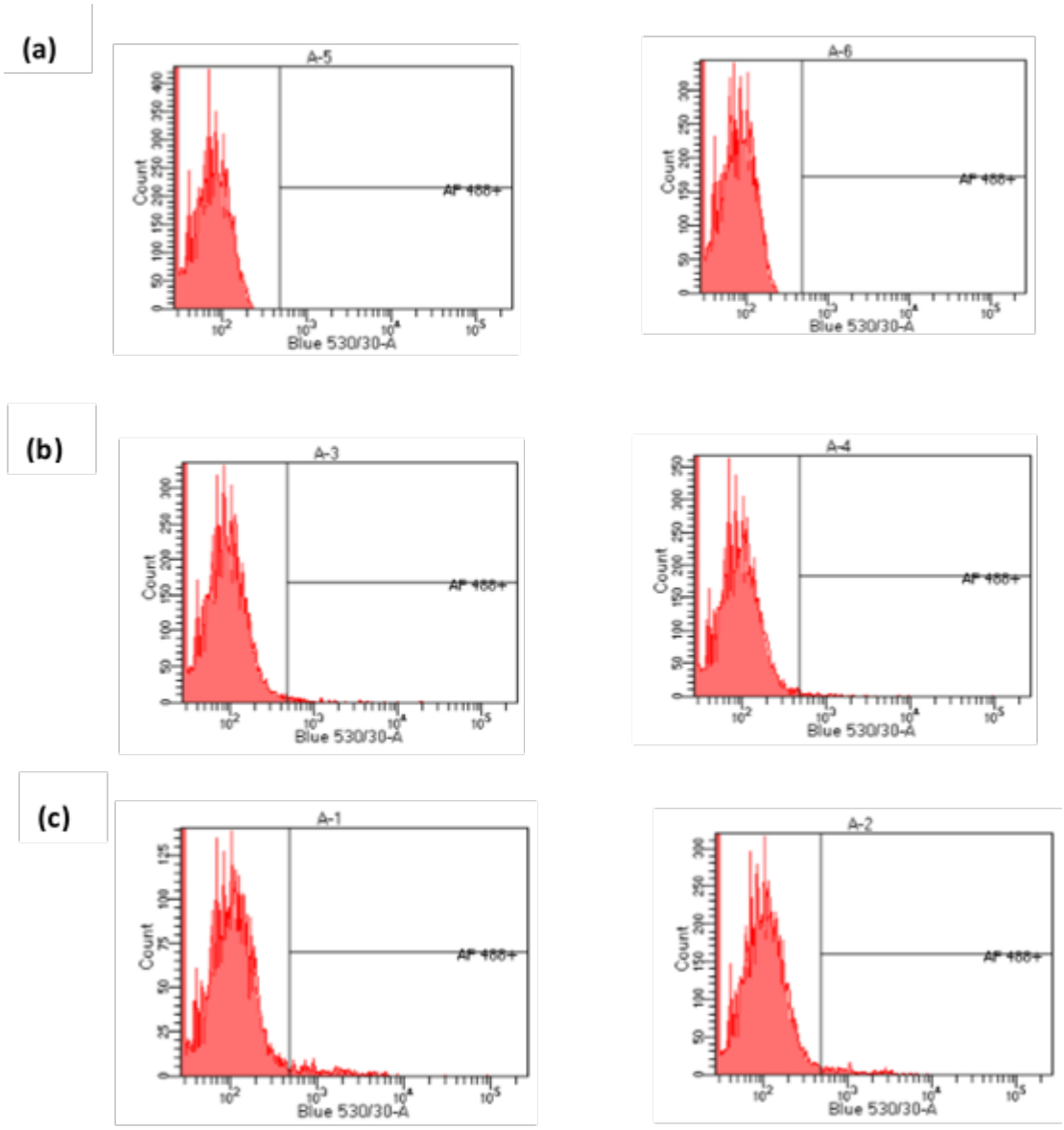

Figure 4.11: Indirect FACS analysis for CRHR1 expression on AtT20 cells using a goat anti-CRHR1 (amino acids 107-117) antibody.

Duplicate samples showing (a) Unstained AtT20 cells (0% and 0%. fluorescently-labelled cells); (b) AtT20 cells stained with secondary rabbit anti-goat IgG-Alexa Fluor®488 antibody (3.3% and 3.5% fluorescently-labelled cells); (c) AtT20 cells stained with primary goat anti-CRHR1 (amino acids 107-117) antibody and secondary rabbit anti-goat IgG-Alexa Fluor®488 antibody (6.1% and 4.6% fluorescently-labelled cells).

4.4 Discussion

In part, the current project aimed to assess the effectiveness of siRNAs in the gene-silencing of POMC expression, ultimately with the view to their as a medical therapy for Cushing's disease. However, the delivery of siRNA to the appropriate cell type is challenging. The CRHR1 is a G protein-coupled receptor that is present on corticotrophs in the anterior pituitary. When the receptor interacts with its ligand CRH, the production of ACTH and ultimately cortisol is stimulated as part of the regulation of glucocorticoid synthesis by the HPA axis. It is possible that conjugating POMC siRNAs to an anti-CRHR1 antibody or to the receptor's ligand CRH could target them to and improve their uptake by pituitary corticotrophs.

As the AtT20 cell line was expected to endogenously express the CRHR1 (Kronsbein et al., 2008), the aim of the work in this chapter was to confirm the presence of CRHR1 mRNA in AtT20 cells, to investigate the presence of CRHR1 on the surface of AtT20 cells, and to determine whether specific antibodies could target the receptor so as to provide the basis for a novel antibody-siRNA conjugate.

Initially, CHRH1 mRNA was detected in AtT20 cells using RT-PCR with CHRH1-specific primers. The functional receptor was then detected on the cell surface using the receptor's response to stimulation by CRH. When AtT20 cells were treated with the hormone ligand, ACTH was released above the basal level and intracellular cAMP was accumulated.

Three different anti-CRHR1-specific antibodies were chosen for use in indirect FACS analysis (Table 2.7). Two of them were targeted at the extracellular domain of the receptor (Figure 4.8) and were reported to be cross-reactive with both the human and mouse protein. The epitope of the third antibody, a mouse monoclonal, was not specifically defined so reactivity against the mouse CRHR1 was uncertain. However, the indirect FACS analysis did not produce a large rightward shift on the FACS histograms when comparing AtT20 cells stained with both anti-CRHR1 primary antibody and secondary antibody compared with cells treated only with secondary antibody.

The results might reflect a naturally low density of receptors on AtT20 cells or there may have been poor expression of CRHR1 on the cells used due to sub-optimum cell

passage number or incubation time, variables that need further investigation. Alternatively, the antibodies may have had less than optimal binding to the receptor when it was expressed on the cell surface in its native form.

In conclusion, AtT20 cells appeared to express the CRHR1, as evidenced by mRNA presence and response to CRH-stimulation. However, this was at too low a level for the cell line to be useful in assessing which anti-CRHR1 antibodies might be amenable as delivery vehicles for siRNA.

Chapter 5

Isolation of a cell line expressing the corticotrophin-releasing hormone receptor 1

5 Isolation of a cell line expressing the corticotrophin-releasing hormone receptor 1

5.1 Introduction

The expression of CRHR1 on AtT20 cells was difficult to interpret using FACS analysis possibly due to less than optimal binding of the primary anti-CRHR1 antibodies or to low expression of the receptor expression. Therefore, using a cell line stably expressing the CRHR1 was considered desirable so that binding of anti-CRHR1 antibodies their target could be better studied.

To generate a cell line that stably expressed CRHR1, the CHO Flp-IN system was used. CHO cells do not endogenously express the receptor (Horlick et al., 1997) so were considered suitable for expression of transfected CRHR1. Figure 5.1 illustrates the CHO Flp-IN system. By this method, both pSecTag-Link plasmid containing the required cDNA, in addition to the site of a Flp recombinase target (FRT), and plasmid pOG44 (Figure 5.2), which encodes Flp recombinase, are transfected into CHO Flp-IN cells. The result is that the pSecTag-Link-cDNA plasmid becomes integrated at the site of a FRT within the DNA of the cell. Homogeneity of the transfected cells, is ensured by such specific targeting. The insertion of the pSecTag-Link-cDNA plasmid at the FRT insertion site of the cell DNA disrupts a Zeocin resistance gene. This causes transfected cells to lose their resistance to Zeocin. The hygromycin B resistance gene on the pSecTag-Link-cDNA plasmid is also inserted into the cell's DNA along with the cDNA of interest. Therefore, transfected cells can be isolated by selecting in culture medium that contains the antibiotic hygromycin B.

Previously, cDNA encoding the human CRHR1 was cloned into pSecTag-Link to give pSecTag-Link-CRHR1 (Figure 5.3) (Kemp and Whatmore, unpublished data). The plasmid that would allow the insertion of the receptor cDNA into the genome of CHO Flp-IN cells and potentially the surface expression of the CRHR1.

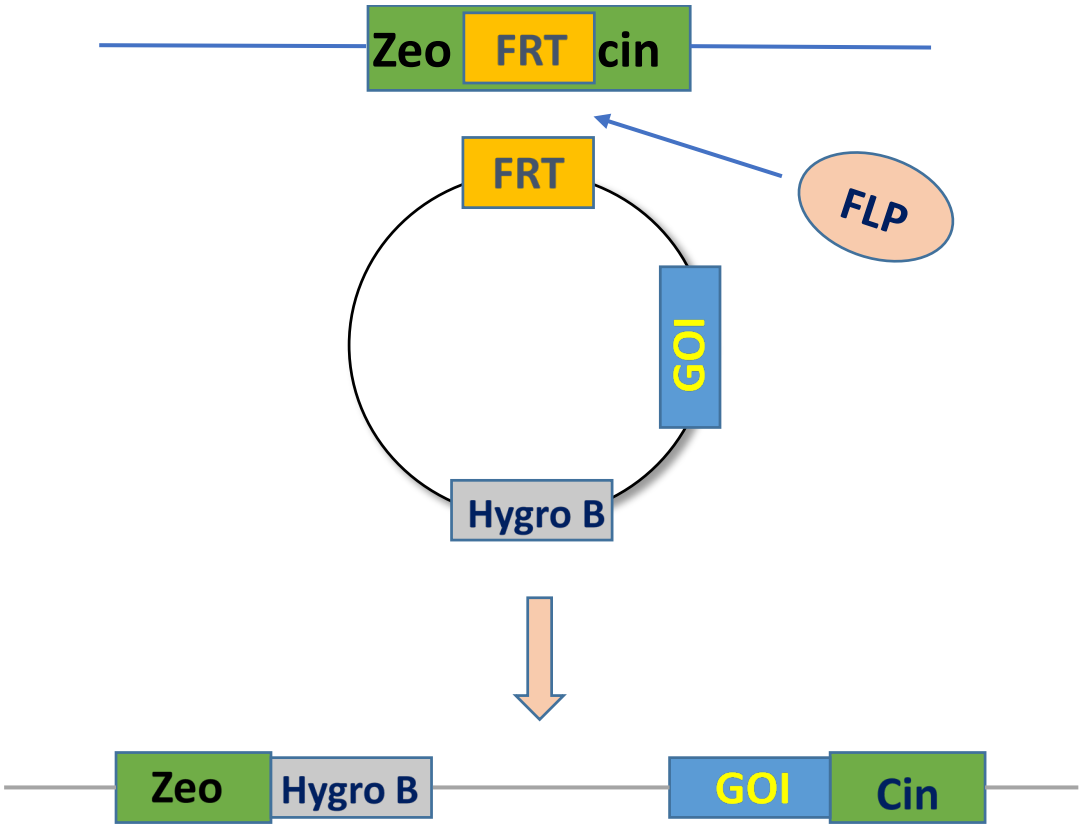

Figure 5.1: A representation of the CHO Flp-IN system.

The Flp recombinase (FLP) enzyme is encoded by plasmid pOG44 (Figure 6.2). It inserts the pSecTag-Link plasmid carrying the gene of interest (GOI) into the Flp-recombinase target (FRT) site that is present in the genome of the recipient cell. The pSecTag-Link carries a hygromycin B (Hygro B) resistance gene, which is also inserted into the cell's DNA. The insertion disrupts the Zeocin resistance gene in the genome of the cell. Therefore, transfected cells lose resistance to Zeocin but become resistant to hygromycin B. The image is adapted from http://2009.igem.org/Team: Heidelberg/stables.

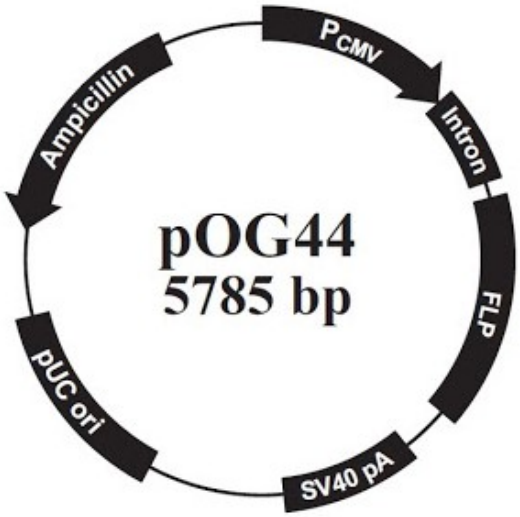

Figure 5.2: Map of plasmid pOG44.

pOG44 is a 5.8-kb Flp recombinase expression vector designed for use with the Flp-IN system. When cotransfected into a Flp-IN mammalian cell line, the Flp recombinase expressed from pOG44 mediates integration of the plasmid containing the cDNA of interest into the genome via Flp recombination target sites. The vector contains the human cytomegalovirus (CMV) promoter for high-level constitutive expression of the Flp recombinase (FLP). It carries an ampicillin resistance gene for selection in bacteria.

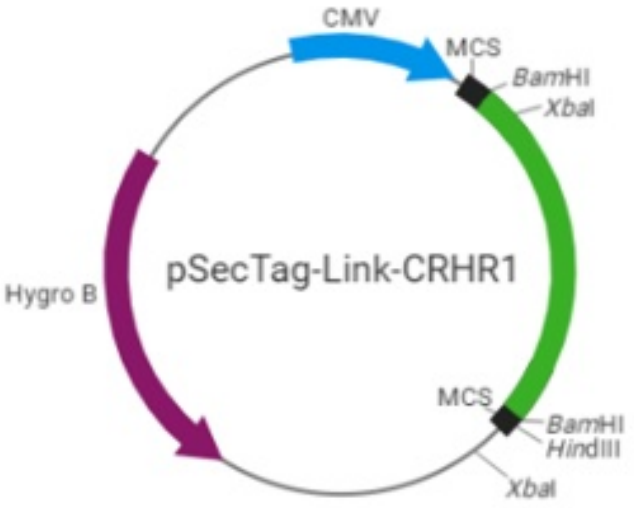

Figure 5.3: A representation of the CRHR1 cDNA cloned into plasmid pSecTag-Link-CRHR1.

The cDNA encoding the human CRHR1 (shown in green) was cloned into the *Bam*H1 site of plasmid pSecTag-Link. The resultant plasmid was designated pSecTag-Link-CRHR1. It carries an ampicillin resistance gene for selection in bacteria, and a hygromycin B resistance gene for selection in eukaryotic cells. Hygro B, hygromycin B resistance gene; CMV, cytomegalovirus promoter; MCS; multiple cloning site.

5.2 Aims

The aim of this part of the work was to isolate a CHO Flp-IN cell line expressing the CRHR1. This would allow for the analysis of a panel of anti-CRHR1 antibodies in terms of their binding to the receptor and their potential usefulness as a conjugation delivery vehicle for POMC siRNAs. The specific objectives were:

- To isolate a CHO Flp-IN cell line expressing the CRHR1 using the CHO Flp-IN system.
- To confirm CRHR1 mRNA expression in the CHO Flp-IN-CRHR1 cell line by RT-PCR.
- To detect the receptor on CHO Flp-IN-CRHR1 using stimulation with CRH.
- To confirm CRHR1 surface expression on the CHO Flp-IN-CRHR1 cell line by indirect FACS analysis.
- To analyse the stability of the CHO Flp-IN-CRHR1 cell line.

5.3 Results

5.3.1 Isolation of a stable CHO Flp-IN cell line expressing the CRHR1

A stable CHO Flp-IN cell line expressing the CRHR1 was isolated as detailed in Section 2.2.2 by transfecting plasmid pSecTag-Link-CRHR1 (Table 2.4; Figure 5.3) and plasmid pOG44 into CHO Flp-IN cells in the wells of 6-well plates. After transfection, 120 different clumps of cells from several different plate wells were transferred to T25 flasks and then to T75 flasks and grown to 60-70% confluence each time. The 120 potential CHO-Flp-IN-CRHR1 cell lines were preserved at -80°C. From the potential cell lines, one was then chosen at random and analysed for expression of the receptor CRHR1, and was eventually designated CHO Flp-IN-CRHR1.

5.3.2 Detection of CRHR1 mRNA in the CHO Flp-IN-CRHR1 cell line

The presence of CRHR1 mRNA in the CHO Flp-IN-CRHR1 cell line was investigated by employing RT-PCR amplification.

5.3.2.1 RNA and cDNA preparation

Both RNA and cDNA were prepared from AtT20 cells (as a control), CHO-Flp-IN cells, and CHO-Flp-IN-CRHR1 cells as previously detailed in 2.3.1 and 2.3.2, respectively. Samples of the total RNA preparations are shown in Figure 5.4. The RT reactions (with and minus RT) were then used as templates for PCR amplification using CHRH1-specific primers CHRH1-Forward and CRHR1-Reverse (Table 2.3).

5.3.2.2 PCR amplification

The CRHR1-specific intron-skipping primers CRHR1-Forward and CRHR1-Reverse (Table 2.3) are shown in Figure 4.3. They gave a PCR product of 199 base pairs in previous experiments (Figure 4.4). Positive control intron-skipping primers were for S15 (Table 2.3). They gave a 361-base pair when used in PCR amplification reactions in previous experiments (Figure 4.4) and were included in PCR experiments to check the integrity of the cDNA samples.

As before, PCR amplification experiments were set up as detailed in the RETROscript Kit protocol (Section 2.3.3) using either CRHR1-specific or S15-specific primers. Two

controls were included in PCR amplification experiments; a reaction without any template, but with primers, to verify that none of the PCR reagents were contaminated with DNA, and a reaction that included a minus RT sample to check for contaminating genomic DNA. Following PCR for 35 cycles, the PCR products were analysed by agarose gel electrophoresis.

DNA fragments of the expected length were seen in the gel lanes corresponding to PCR reactions containing cDNA and S15 primers (361 base pairs) (Figure 5.5) or CRHR1 primers (199 base pairs) (Figure 5.6). No DNA products were visible in gel lanes loaded with PCR reactions containing either no template or a minus RT sample. Both the controls indicated that the amplified products were not a result of contaminated reagents or contaminating genomic DNA, respectively. Overall, the results indicated that the CHO Flp-IN-CRHR1 cells expressed CRHR1 mRNA.

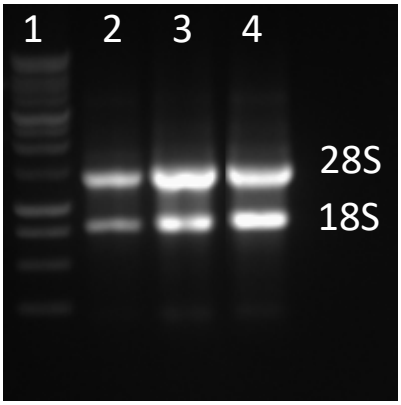

Figure 5.4: Agarose gel electrophoresis of total RNA extracted from AtT20 cells, CHO Flp-IN cells, and CHO Flp-IN-CRHR1 cells.

Total RNA was extracted from AtT20 cells, CHO Flp-IN cells, and CHO Flp-IN-CRHR1 cells. A 5-µl sample was analysed on a 1% agarose gel. Lane 1, 1-kb DNA ladder; Lane 2, Total RNA sample from AtT20 cells; Lane 3, Total RNA sample from CHO Flp-IN cells; Lane 4, Total RNA sample from CHO Flp-IN-CRHR1 cells. The bands representing 28S and 18S of ribosomal RNA are indicated.

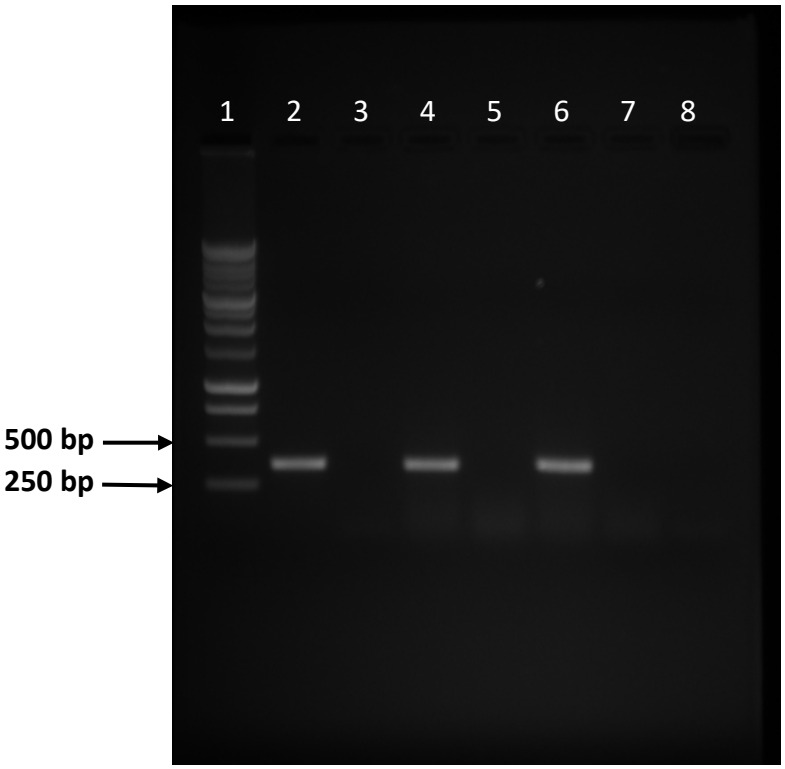

Figure 5.5: Agarose gel electrophoresis of PCR amplification products using S15 primers.

PCR amplification products were electrophoresed in a 1% agarose gel. Lane 1, 1-kb DNA ladder; Lane 2, AtT20 cell cDNA; Lane 3, AtT20 minus RT sample; Lane 4, CHO Flp-IN cell cDNA; Lane 5, CHO Flp-IN cell minus RT sample; Lane 6, CHO Flp-IN-CRHR1 cell cDNA; Lane 7, CHO Flp-IN-CHRH1 cell minus RT sample; Lane 8, No cDNA template control. The expected size of the fragment was 361 base pairs (bp).

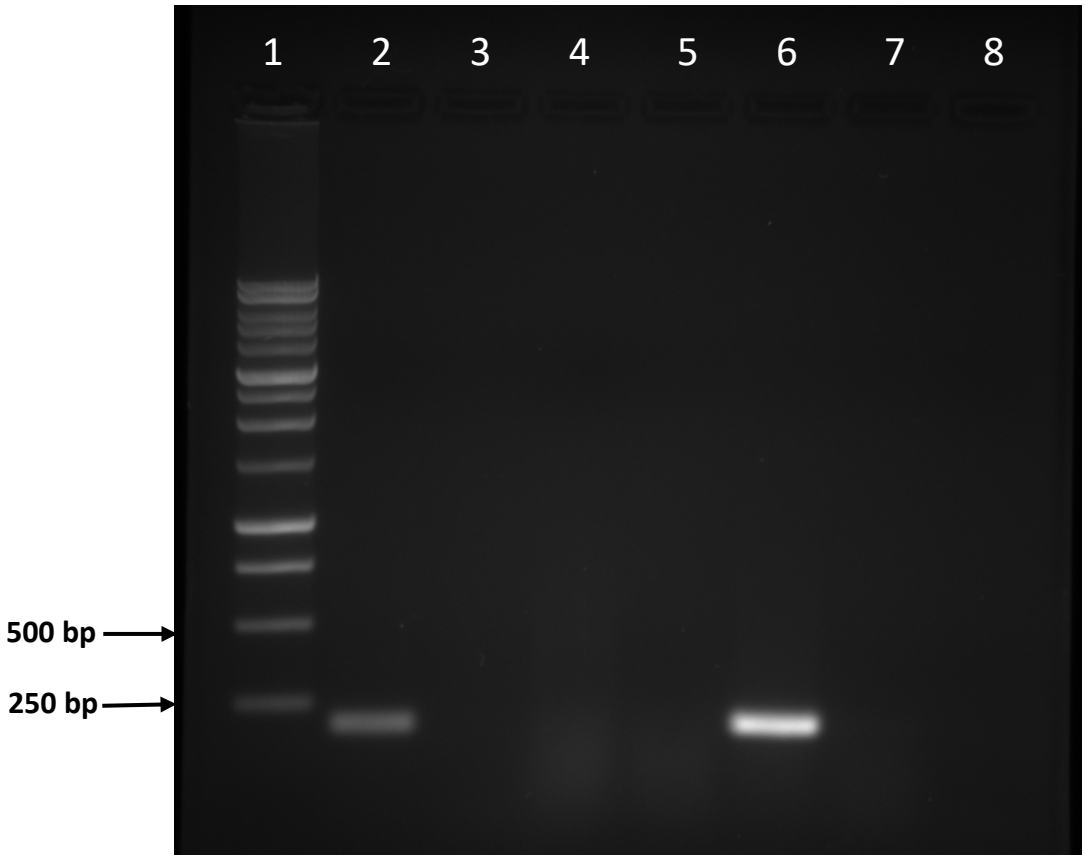

Figure 5.6: Agarose gel electrophoresis of PCR amplification products using CRHR1 primers.

PCR amplification products were electrophoresed in a 1% agarose gel. Lane 1, 1-kb DNA ladder; Lane 2, AtT20 cell cDNA; Lane 3, AtT20 minus RT sample; Lane 4, CHO Flp-IN cell cDNA; Lane 5, CHO Flp-IN cell minus RT sample; Lane 6, CHO Flp-IN-CRHR1 cell cDNA; Lane 7, CHO Flp-IN-CHRH1 cell minus RT sample; Lane 8, No cDNA template control. The expected size of the fragment was 199 base pair (bp).

5.3.3 Detecting the CRHR1 on CHO Flp-IN-CRHR1 cells using CRH-stimulation

The RT-PCR experiment detected mRNA for CRHR1 in the CHO Flp-IN-CRHR1 cell line. However, although the detected mRNA appeared specific for the receptor, it was necessary to assess if the CRHR1 was itself present on the surface of the CHO Flp-IN-CRHR1 cells. This assessment was carried out using stimulation with CRH which would be expected to lead to an increase in intracellular cAMP.

CHO Flp-IN-CRHR1 and CHO Flp-IN cells were plated in 96-well plates at 1 x 10^3 cells per well. They were then treated with CRH or MCH as detailed in Section 2.8, and the results are illustrated in Figure 5.7.

The results indicated a response to CRH-stimulation was only evident in the CHO Flp-IN-CRHR1 cells as these showed accumulation of cAMP. CHO Flp-IN cells did not respond to CRH, and neither cell type was stimulated by the control peptide MCH. In both cell lines, cAMP accumulation was stimulated by forskolin.

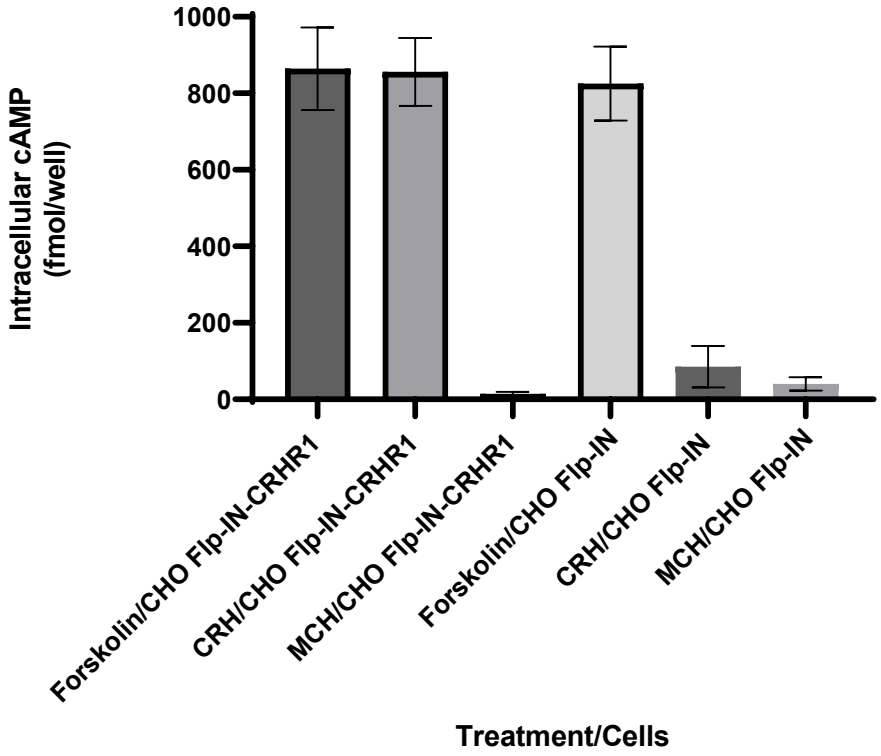

Figure 5.7: Effect of CRH-stimulation on CHO Flp-IN-CRHR1 cells.

CHO Flp-IN-CRHR1 and CHO Flp-IN cells were treated with 3-isobutyl-1-methylxanthine (IBMX) plus CRH, MCH or forskolin. Intracellular cAMP was measured in a cAMP Enzyme Immunoassay. The results show the mean (± SD) intracellular cAMP concentration in fmol/well from four experiments.

5.3.4 Indirect FACS for CRHR1 on CHO Flp-IN-CRHR1 cells with a mouse anti-CRHR1 antibody

Expression of the CRHR1 on CHO Flp-IN-CRHR1 cells was also analysed using an indirect FACS staining method. The primary antibody used was a mouse anti-CRHR1 antibody raised against peptide (amino acids 24–415) of the human CRHR1 (Table 2.7). The secondary antibody used was an anti-mouse IgG raised in donkey and conjugated to Alexa Fluor®488 (Table 2.7). It was used at a 1:2000 dilution in FACS staining.

Indirect FACS experiments were undertaken as described in Section 2.6. As well as the primary and secondary antibody-treated cell samples, experiments included CHO Flp-IN-CRHR1 cells that were left untreated in order to determine background fluorescence. CHO Flp-IN-CRHR1 cells stained with only secondary antibody were also included to identify any binding that was non-specific. In addition, CHO Flp-IN cells were stained with primary and secondary antibody. Before the cell samples were treated with primary or secondary antibody, they were pre-incubated with a Fc-blocking antibody (Table 2.7) that binds to Fc receptors CD16 and CD32 on the cell surface. The blocking interaction stops the binding of primary and secondary antibodies via their constant regions to the Fc receptors.

The results of duplicate samples of one indirect FACS experiment are shown in (Figure 5.8). Unstained CHO Flp-IN-CRHR1 cells showed that 0% of cells were fluorescing (Figure 5.8a). Fluorescence was 0.5% and 0.7% in CHO Flp-IN-CRHR1 cell samples stained with only secondary anti-mouse IgG-Alexa Fluor®488 antibody (Figure 5.8b). For CHO Flp-IN cells stained with mouse anti-CRHR1 antibody and secondary anti-mouse IgG-Alexa Fluor®488 antibody, there were 4.4% and 6.3% fluorescently-labelled cells (Figure 5.8c). CHO Flp-IN-CRHR1 cells stained with mouse anti-CRHR1 antibody and secondary anti-mouse IgG-Alexa Fluor®488 antibody resulted in 57.9% and 54.2% of cells being fluorescently-labelled causing a shift to the right on the FACS histogram (Figure 5.8d).

Overall, the results indicated that the mouse anti-CRHR1 antibody appeared to detect the CRHR1 expressed on the surface of the CHO Flp-IN-CRHR1 cells.

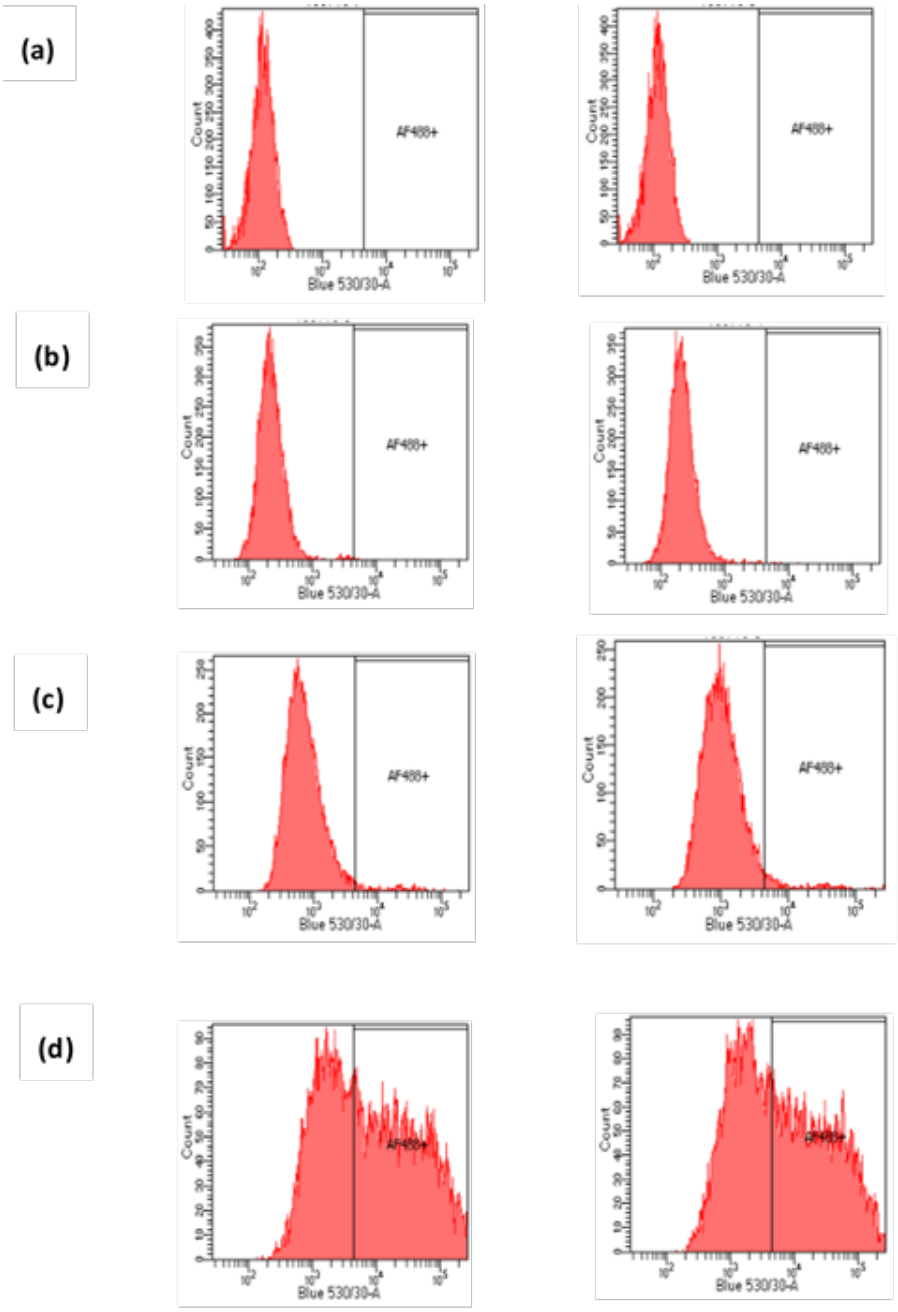

Figure 5.8: Indirect FACS analysis for CRHR1 expression on CHO Flp-IN-CRHR1 cells using a mouse anti-CRHR1 (amino acids 24-415) antibody.

Duplicate samples showing (a) Unstained CHO Flp-IN-CRHR1 cells (0% and 0%. fluorescently-labelled cells); (b) CHO Flp-IN-CRHR1 cells stained with secondary anti-mouse IgG-Alexa Fluor®488 antibody (0.5% and 0.7% fluorescently-labelled cells); (c) CHO Flp-IN cells stained with mouse anti-CRHR1 antibody and secondary anti-mouse IgG-Alexa Fluor®488 antibody (4.4% and 6.3% fluorescently-labelled cells); (d) CHO Flp-IN-CRHR1 cells stained with mouse anti-CRHR1 antibody and secondary anti-mouse IgG-Alexa Fluor®488 antibody (57.9% and 54.2% fluorescently-labelled cells).

5.3.5 Indirect FACS for CRHR1 on CHO Flp-IN-CRHR1 cells with rabbit and goat anti-CRHR1 antibodies

Expression of the CRHR1 on CHO Flp-IN-CRHR1 cells was further analysed using indirect FACS, with different antibody pairs. The primary antibody used was either a rabbit anti-CRHR1 antibody against amino acids 55-150 of the human CRHR1 (Figure 4.8; Table 2.7) or a goat anti-CRHR1 antibody against human CRHR1 (amino acids 107-117) (Figure 4.8; Table 2.7). The secondary antibodies used were goat anti-rabbit IgG conjugated to Alexa Fluor®488 (Table 2.7), and rabbit anti-goat IgG conjugated to Alexa Fluor®488 (Table 2.7), respectively. They were used at a 1:1000 dilution in FACS staining and indirect FACS experiments were undertaken as described earlier in Section 5.3.4.

The results of duplicate samples of one indirect FACS experiment using the rabbit anti-CRHR1 (amino acids 55-150) antibody are shown in (Figure 5.9). Unstained CHO Flp-IN-CRHR1 cells showed that 0% of cells were fluorescing (Figure 5.9a). Fluorescence was 2.3% and 2.2% in CHO Flp-IN-CRHR1 cell samples stained with only secondary anti-rabbit IgG-Alexa Fluor®488 antibody (Figure 5.9b). For CHO Flp-IN cells stained with rabbit anti-CRHR1 antibody and secondary anti-rabbit IgG-Alexa Fluor®488 antibody, there were 1.3% and 1.5% fluorescently-labelled cells (Figure 5.9c). CHO Flp-IN-CRHR1 cells stained with rabbit anti-CRHR1 antibody and secondary anti-rabbit IgG-Alexa Fluor®488 antibody resulted in 4.2% and 4.1% of cells being fluorescently-labelled (Figure 5.9d).

The results of duplicate samples of one indirect FACS experiment using the goat anti-CRHR1 (amino acids 107-117) antibody are shown in (Figure 5.10). Unstained CHO Flp-IN-CRHR1 cells showed that 0% of cells were fluorescing (Figure 5.10a). Fluorescence was 2.9% and 3.3% in CHO Flp-IN-CRHR1 cell samples stained with only secondary anti-goat IgG-Alexa Fluor®488 antibody (Figure 5.10b). For CHO Flp-IN cells stained with goat anti-CRHR1 antibody and secondary anti-goat IgG-Alexa Fluor®488 antibody, there were 3.9% and 3.6% fluorescently-labelled cells (Figure 5.10c). CHO Flp-IN-CRHR1 cells stained with goat anti-CRHR1 antibody and secondary anti-goat IgG-Alexa Fluor®488 antibody resulted in 3.9% and 4.1% of cells being fluorescently-labelled (Figure 5.10d).

Neither antibody appeared to detect the CRHR1 expressed on the surface of the CHO Flp-IN-CRHR1 cells.

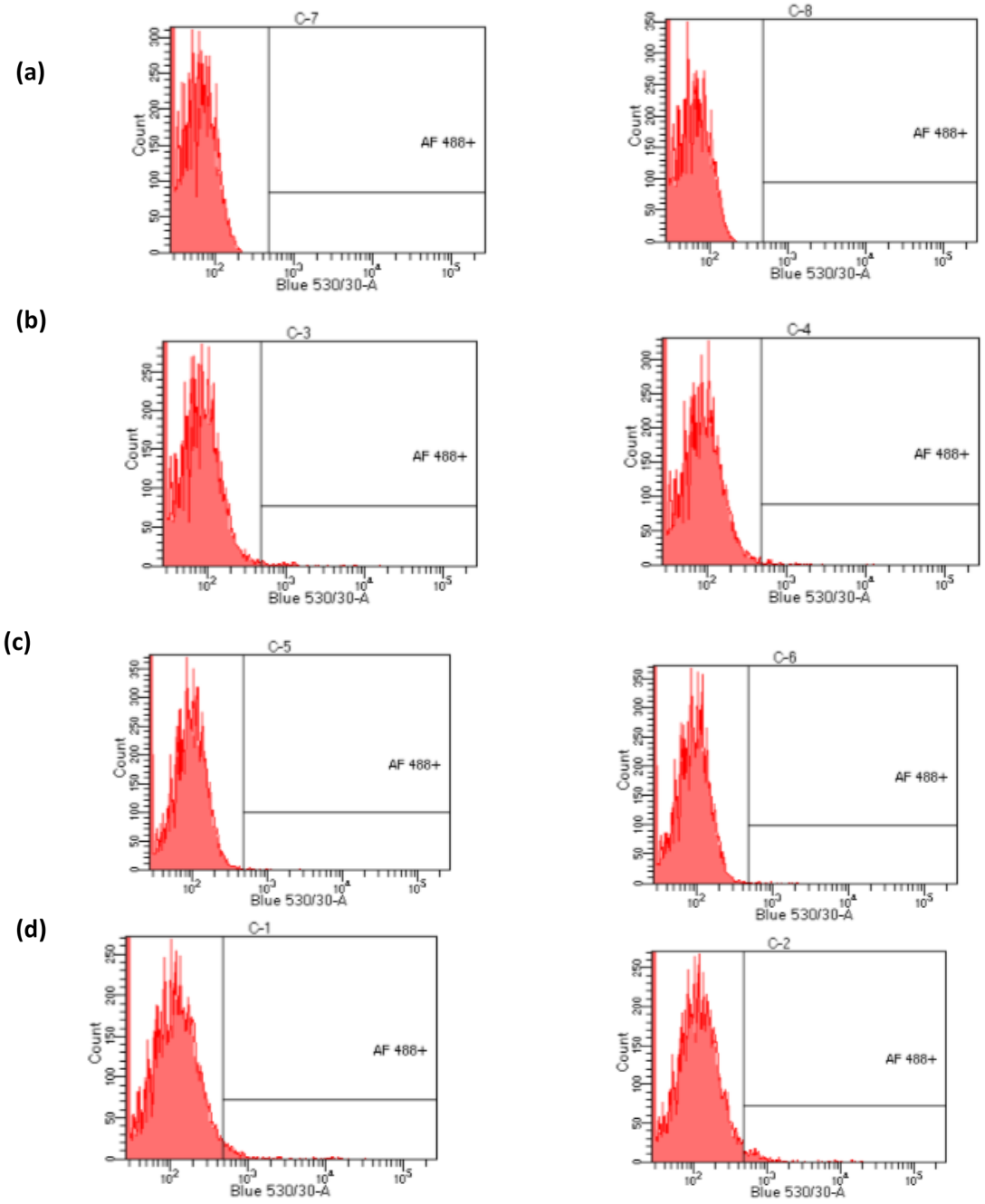

Figure 5.9: Indirect FACS analysis for CRHR1 expression on CHO Flp-IN-CRHR1 cells using a rabbit anti-CRHR1 (amino acids 55-150) antibody.

Duplicate samples showing (a) Unstained CHO Flp-IN-CRHR1 cells (0% and 0%. fluorescently-labelled cells); (b) CHO Flp-IN-CRHR1 cells stained with secondary anti-rabbit IgG-Alexa Fluor®488 antibody (2.3% and 2.2% fluorescently-labelled cells); (c) CHO Flp-IN cells stained with rabbit anti-CRHR1 antibody and secondary anti-rabbit IgG-Alexa Fluor®488 antibody (1.3% and 1.5% fluorescently-labelled cells); (d) CHO Flp-IN-CRHR1 cells stained with rabbit anti-CRHR1 antibody and secondary anti-rabbit IgG-Alexa Fluor®488 antibody (4.2% and 4.1% fluorescently-labelled cells).

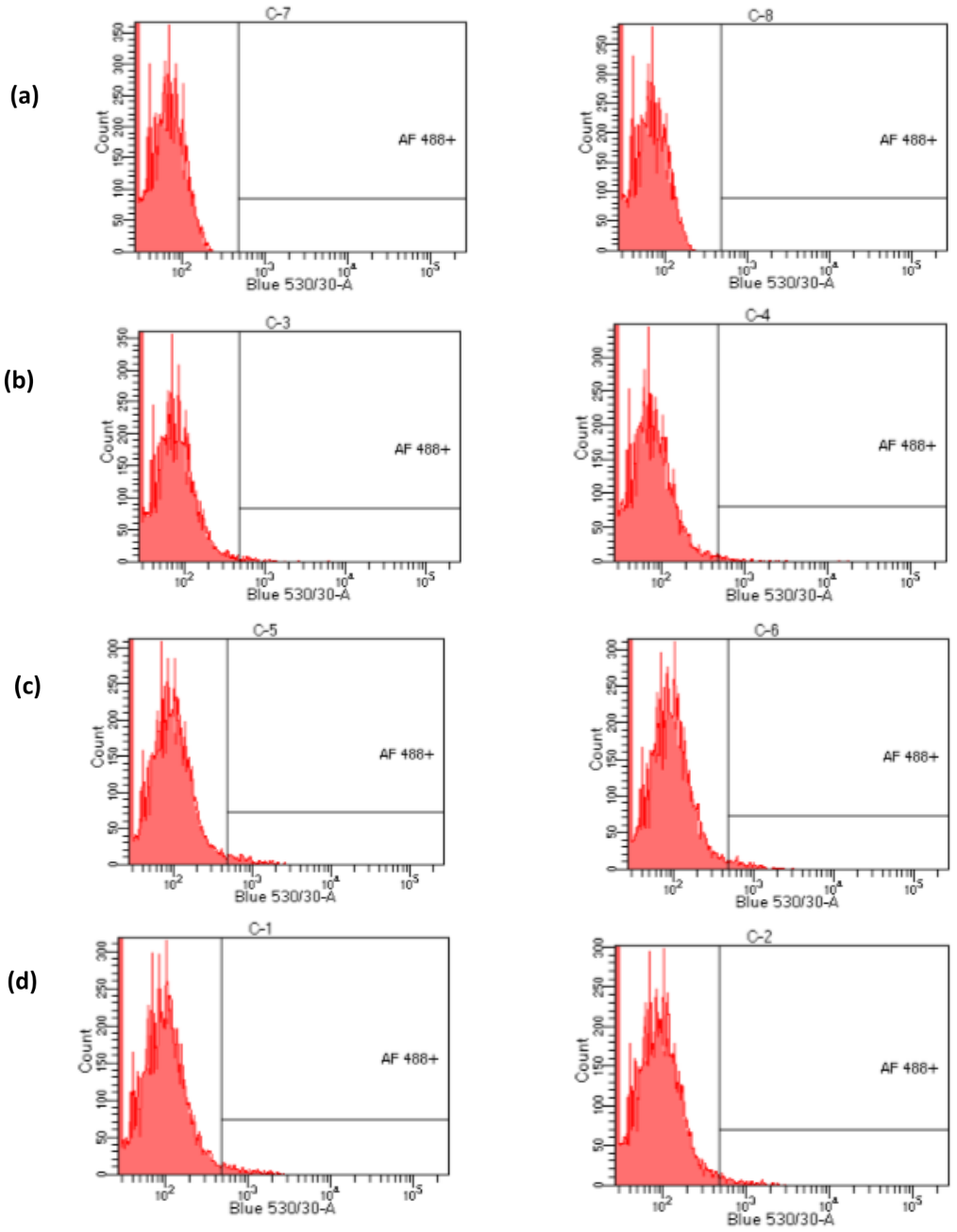

Figure 5.10: Indirect FACS analysis for CRHR1 expression on CHO Flp-IN-CRHR1 cells using a goat anti-CRHR1 (amino acids 107-117) antibody.

Duplicate samples showing (a) Unstained CHO Flp-IN-CRHR1 cells (0% and 0%. fluorescently-labelled cells); (b) CHO Flp-IN-CRHR1 cells stained with secondary anti-goat IgG-Alexa Fluor®488 antibody (2.9% and 3.3% fluorescently-labelled cells); (c) CHO Flp-IN cells stained with goat anti-CRHR1 antibody and secondary anti-goat IgG-Alexa Fluor®488 antibody (3.9% and 3.6% fluorescently-labelled cells); (d) CHO Flp-IN-CRHR1 cells stained with goat anti-CRHR1 antibody and secondary anti-goat IgG-Alexa Fluor®488 antibody (3.9% and 3.3% fluorescently-labelled cells).

5.3.6 Stability of the CHO Flp-IN-CRHR1 cell line

To investigate the stability of the CHO Flp-IN-CRHR1 cell line, cells were cultured and passaged five, 10, 15, and 20 times. At each passage, the expression of the receptor was analysed by RT-PCR and indirect FACS.

5.3.6.1 Detection of CRHR1 mRNA in passaged CHO Flp-IN-CRHR1 cells

CHO Flp-IN-CRHR1 and CHO Flp-IN cells were cultured and passaged five, 10, 15, and 20 times. Both RNA and cDNA were prepared from the CHO-Flp-IN and CHO-Flp-IN-CRHR1 cells as previously detailed in 2.3.1 and 2.3.2, respectively. Samples of the total RNA preparations are shown in Figure 5.11. The RT reactions (with and minus RT) were then used as templates for PCR amplification using CHRH1-specific primers CHRH1-Forward and CRHR1-Reverse (Table 2.3).

The CRHR1-specific intron-skipping primers CRHR1-Forward and CRHR1-Reverse (Table 2.3) are shown in Figure 4.3. They gave a PCR product of 199 base pairs (Figure 4.4). Positive control intron-skipping primers were for S15 (Table 2.3). They gave a 361-base pair when used in PCR amplification reactions (Figure 4.4) and were included in PCR experiments to check the integrity of the cDNA samples.

As before, PCR amplification experiments were set up as detailed in the RETROscript Kit protocol (Section 2.3.3) using either CRHR1-specific or S15-specific primers. Two controls were included in PCR amplification experiments; a reaction without any template, but with primers, to verify that none of the PCR reagents were contaminated with DNA, and a reaction that included a minus RT sample to check for contaminating genomic DNA. Following PCR for 35 cycles, the PCR products were analysed by agarose gel electrophoresis.

DNA fragments of the expected length were seen in the gel lanes corresponding to PCR reactions containing cDNA and S15 primers (361 base pairs) (Figure 5.12). With CRHR1 primers, the correct sized fragment of 199 base pairs was only noted in the gel lanes corresponding to PCR reactions containing CHO Flp-IN-CRHR1 cell cDNA from passages five, 10, 15, and 20 (Figure 5.13). No DNA products were visible in gel lanes loaded with PCR reactions containing either no template or a minus RT sample, which indicated that the amplified products were not a result of contaminated reagents

or contaminating genomic DNA, respectively. In addition, PCR products were not detected in the CHO Flp-IN cell cDNA samples from any of the tested passages. Overall, the results indicated that the CHO Flp-IN-CRHR1 cells expressed CRHR1 mRNA at all the cell passages tested.

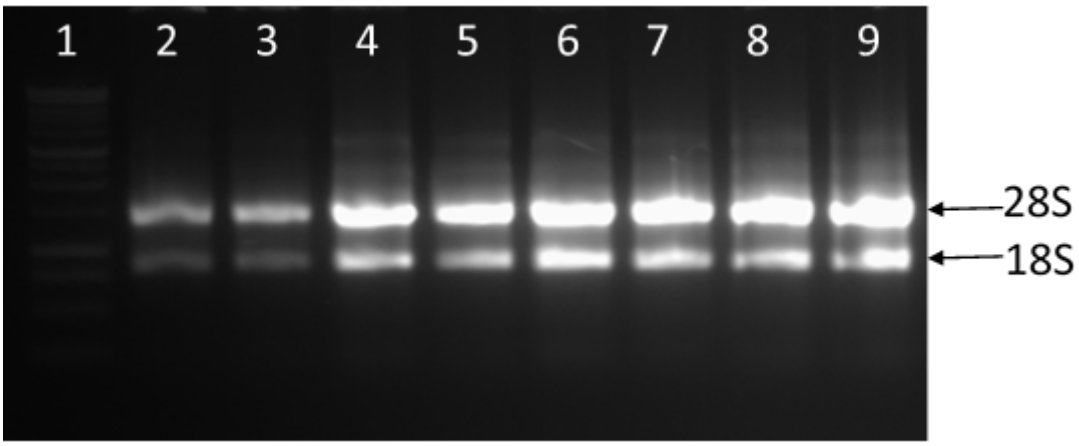

Figure 5.11: Agarose gel electrophoresis of total RNA extracted from CHO Flp-IN and CHO Flp-IN-CRHR1 cells.

RNA was extracted from CHO Flp-IN and CHO Flp-IN-CRHR1 cells from the different passages. A 5-µl sample was analysed on a 1% agarose gel. Lane 1, 1-kb DNA Ladder; Lane 2, Total RNA sample from CHO Flp-IN cells (passage 5); Lane 3, Total RNA sample from CHO Flp-IN cells (passage 10); Lane 4, Total RNA sample from CHO Flp-IN cells (passage 15); Lane 5, Total RNA sample from CHO-Flp-IN cells (passage 20); Lane 6, Total RNA sample from CHO Flp-IN-CRHR1 cells (passage 5); Lane 7, Total RNA sample from CHO Flp-IN-CRHR1 cells (passage 10); Lane 8, Total RNA sample from CHO Flp-IN-CRHR1 cells (passage 15); Lane 9, Total RNA sample from CHO Flp-IN-CRHR1 cells (passage 20). The bands representing 28S and 18S of ribosomal RNA are indicated.

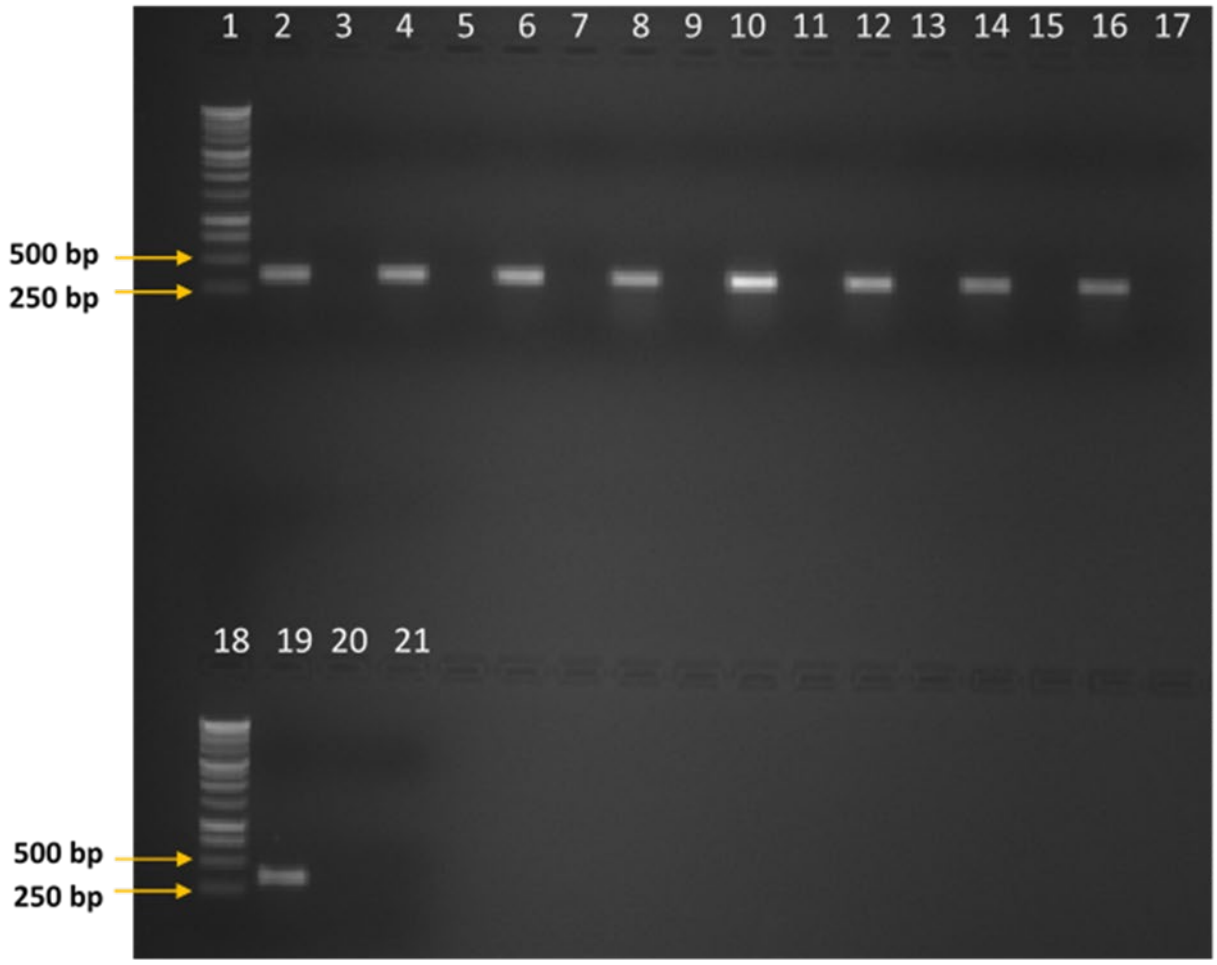

Figure 5.12: Agarose gel electrophoresis of PCR amplification products using S15 primers.

PCR amplification products were electrophoresed in a 1% agarose gel. Lane 1, 1-kb DNA Ladder; Passage 5: Lane 2, CHO Flp-IN cDNA; Lane 3, CHO-Flp-IN cells (-RT sample); Lane 4, CHO Flp-IN-CRHR1 cDNA; Lane 5, CHO Flp-IN-CRHR1 (-RT sample); Passage 10: Lane 6, CHO Flp-IN cDNA; Lane 7, CHO Flp-IN (-RT sample); Lane 8, CHO Flp-IN-CRHR1 cDNA; Lane 9, CHO Flp-IN-CRHR1 (-RT sample); Passage 15: Lane 10, CHO Flp-In cDNA; Lane 11, CHO Flp-IN (-RT sample); Lane 12, CHO Flp-IN-CRHR1 cDNA; Lane 13, CHO Flp-IN-CRHR1 (-RT sample); Passage 20: Lane 14, CHO Flp-IN cDNA; Lane 15, CHO Flp-IN (-RT sample); Lane 16, CHO-Flp-IN-CRHR1 cDNA; Lane 17, CHO Flp-IN-CRHR1 (-RT sample); Lane 18, 1-kb DNA Ladder; Lane 19, AtT20 cDNA; Lane 20, AtT20 (-RT sample), Lane 21, S15 primers only without any cDNA template. The expected size of the fragment was 361 base pairs (bp).

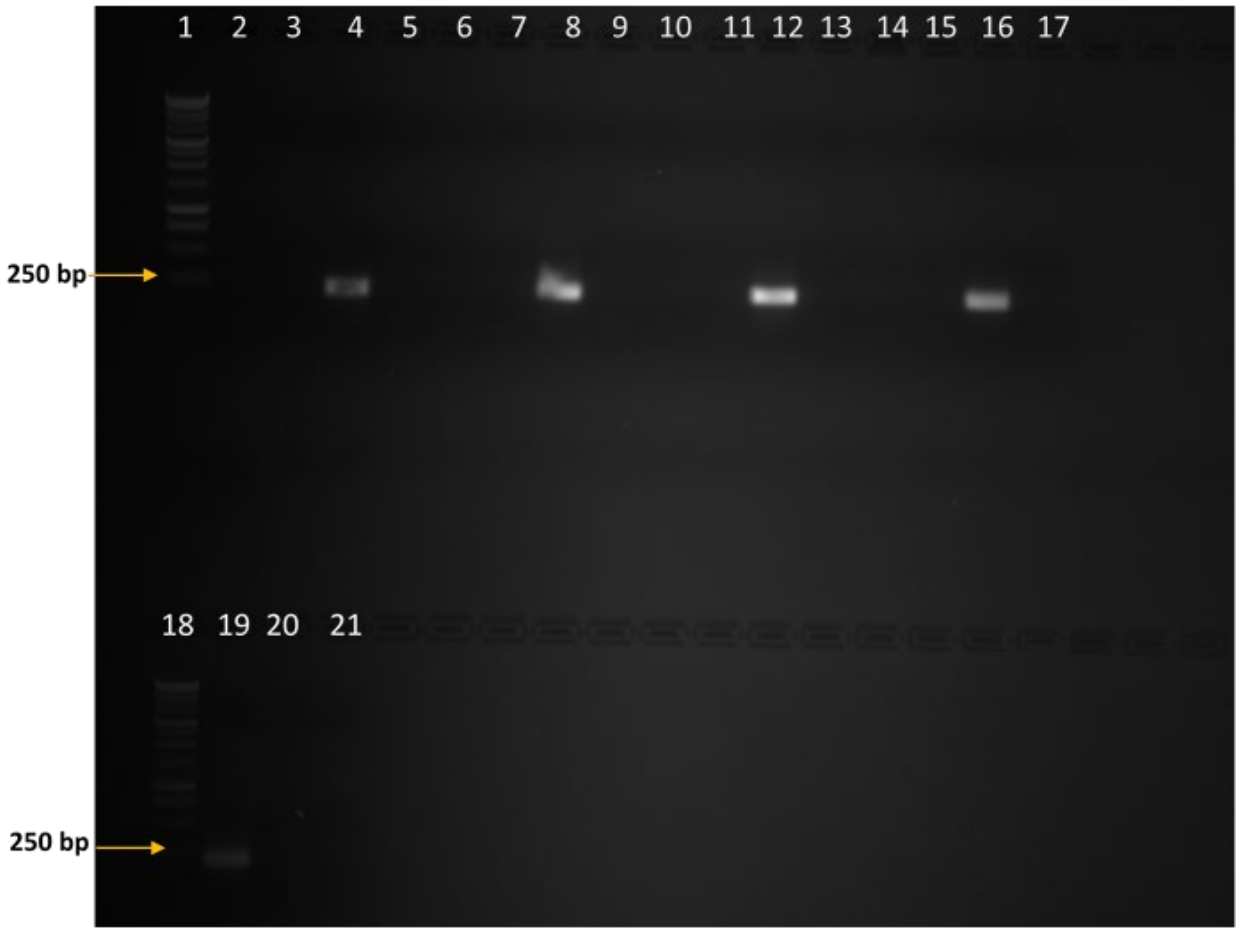

Figure 5.13: Agarose gel electrophoresis of PCR amplification products using CRHR1 primers.

PCR amplification products were electrophoresed in a 1% agarose gel. Lane 1, 1-kb DNA Ladder; Passage 5: Lane 2, CHO Flp-IN cDNA; Lane 3, CHO-Flp-IN cells (-RT sample); Lane 4, CHO Flp-IN-CRHR1 cDNA; Lane 5, CHO Flp-IN-CRHR1 (-RT sample); Passage 10: Lane 6, CHO Flp-IN cDNA; Lane 7, CHO Flp-IN (-RT sample); Lane 8, CHO Flp-IN-CRHR1 cDNA; Lane 9, CHO Flp-IN-CRHR1 (-RT sample); Passage 15: Lane 10, CHO Flp-In cDNA; Lane 11, CHO Flp-IN (-RT sample); Lane 12, CHO Flp-IN-CRHR1 cDNA; Lane 13, CHO Flp-IN-CRHR1 (-RT sample); Passage 20: Lane 14, CHO Flp-IN cDNA; Lane 15, CHO Flp-IN (-RT sample); Lane 16, CHO-Flp-IN-CRHR1 cDNA; Lane 17, CHO Flp-IN-CRHR1 (-RT sample); Lane 18, 1-kb DNA Ladder; Lane 19, AtT20 cDNA; Lane 20, AtT20 (-RT sample), Lane 21, CRHR1 primers only without any cDNA template. The expected size of the fragment was 199 base pairs (bp).

5.3.6.2 Indirect FACS for CRHR1 on CHO Flp-IN-CRHR1 cells at passages 5, 10, 15, and 20 with a mouse anti-CRHR1 antibody

Expression of the CRHR1 on CHO Flp-IN-CRHR1 cells at passages five, 10, 15, and 20 was analysed using indirect FACS staining. The primary antibody used was a mouse anti-CRHR1 antibody raised against peptide (amino acids 24–415) of the human CRHR1 (Table 2.7). The secondary antibody used was an anti-mouse IgG raised in donkey and conjugated to Alexa Fluor®488 (Table 2.7). It was used at a 1:2000 dilution in FACS staining.

Indirect FACS experiments were undertaken as described in Section 2.6. As well as the primary and secondary antibody-treated cell samples, experiments included CHO Flp-IN-CRHR1 cells that were left untreated in order to determine background fluorescence. CHO Flp-IN-CRHR1 cells stained with only secondary antibody were also included to identify any binding that was non-specific. In addition, CHO Flp-IN cells were stained with primary and secondary antibody. Before the cell samples were treated with primary or secondary antibody, they were pre-incubated with a Fc-blocking antibody (Table 2.7) that binds to Fc receptors CD16 and CD32 on the cell surface. The blocking interaction stops the binding of primary and secondary antibodies via their constant regions to the Fc receptors.

The results of duplicate samples of indirect FACS experiments are shown in (Figures 5.14-5.17). In all passages, unstained CHO Flp-IN-CRHR1 cells showed that 0% of cells were fluorescing (Figures 5.14a, 5.15a, 5.16a, and 5.17a).

Fluorescence was 4.2% and 2.7% (passage five), 1.1% and 1.5% (passage 10), 0.1% and 0.5% (passage 15), and 0.5% and 3.3% (passage 20) in CHO Flp-IN-CRHR1 cell samples stained with only secondary anti-mouse IgG-Alexa Fluor®488 antibody (Figures 5.14b, 5.15b, 5.16b, and 5.17b).

For CHO Flp-IN cells stained with mouse anti-CRHR1 antibody and secondary anti-mouse IgG-Alexa Fluor®488 antibody, there were 3.0% and 2.5% (passage five), 4.3% and 3.6% (passage 10), 0% and 4.9% (passage 15), and 5.3% and 3.1% (passage 20) fluorescently-labelled cells (Figures 5.14c, 5.15c, 5.16c, and 5.17c).

CHO Flp-IN-CRHR1 cells stained with mouse anti-CRHR1 antibody and secondary anti-mouse IgG-Alexa Fluor®488 antibody resulted in 78.3% and 91.8% (passage five), 86.3% and 88.3% (passage 10), 95.3% and 96.2% (passage 15), and 97.5% and 94.4% (passage 20) of cells being fluorescently-labelled causing a shift to the right on the FACS histogram (Figures 5.14d, 5.15d, 5.16d, and 5.17d).

Overall, the results indicated that the CHO Flp-IN-CRHR1 cells expressed CRHR1 on their surface at all the cell passages tested.

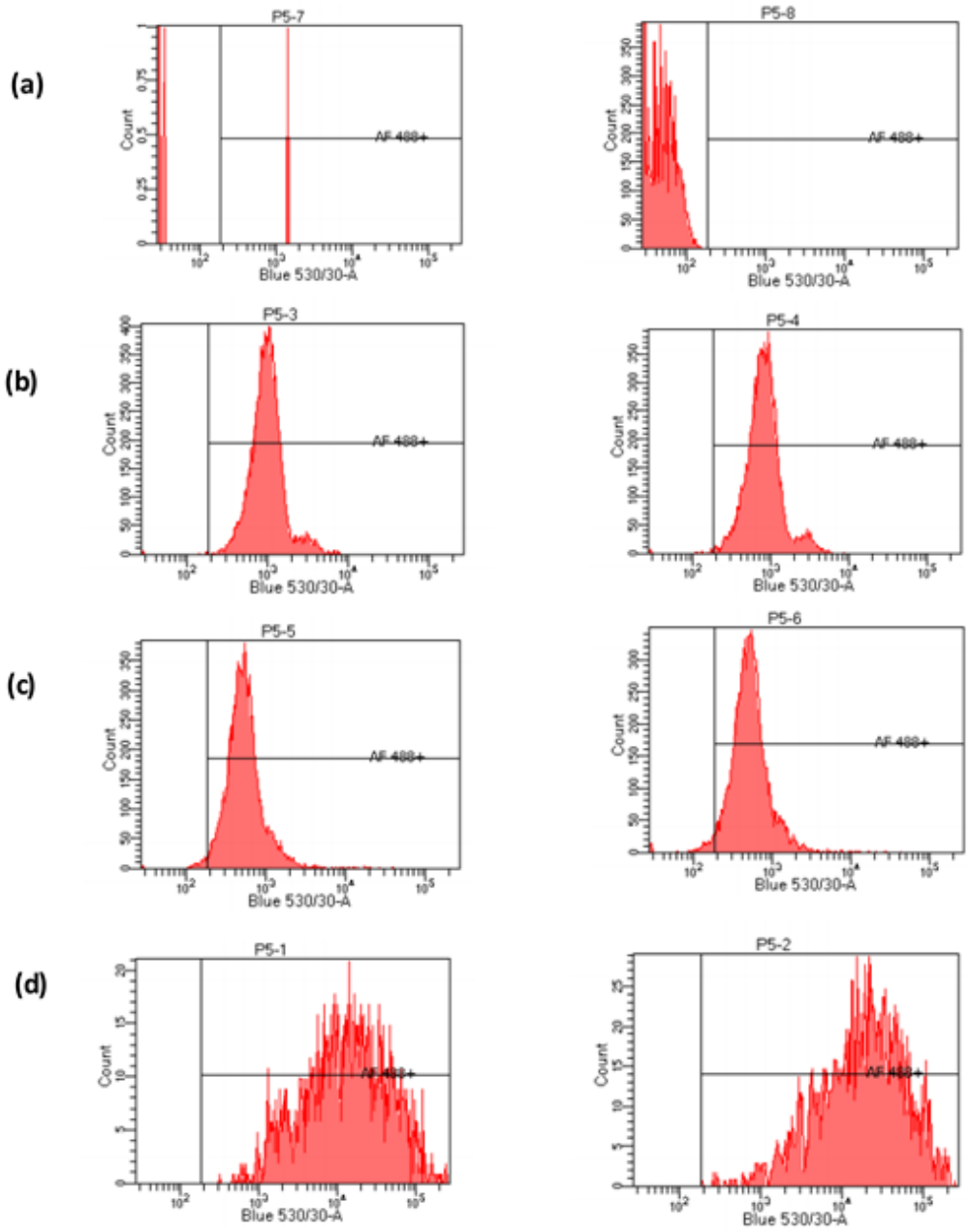

Figure 5.14: Indirect FACS analysis for CRHR1 expression on passage five CHO Flp-IN-CRHR1 cells using a mouse anti-CRHR1 (amino acids 24-415) antibody.

Duplicate samples showing (a) Unstained CHO Flp-IN-CRHR1 cells (0% and 0%. fluorescently-labelled cells); (b) CHO Flp-IN-CRHR1 cells stained with secondary anti-mouse IgG-Alexa Fluor®488 antibody (4.2% and 2.7% fluorescently-labelled cells); (c) CHO Flp-IN cells stained with mouse anti-CRHR1 antibody and secondary anti-mouse IgG-Alexa Fluor®488 antibody (3.0% and 2.5% fluorescently-labelled cells); (d) CHO Flp-IN-CRHR1 cells stained with mouse anti-CRHR1 antibody and secondary anti-mouse IgG-Alexa Fluor®488 antibody (78.3% and 91.8% fluorescently-labelled cells).

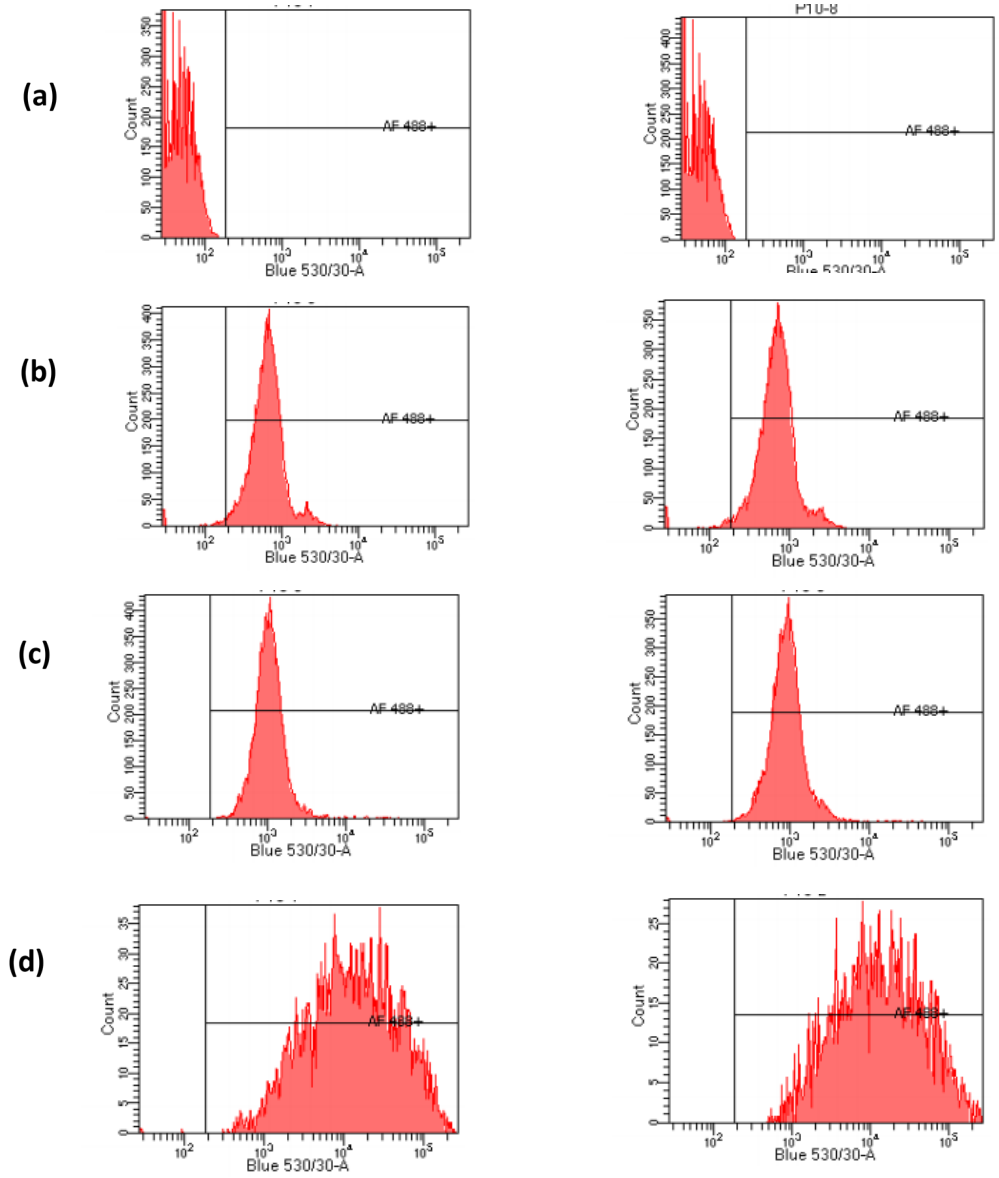

Figure 5.15: Indirect FACS analysis for CRHR1 expression on passage 10 CHO Flp-IN-CRHR1 cells using a mouse anti-CRHR1 (amino acids 24-415) antibody.

Duplicate samples showing (a) Unstained CHO Flp-IN-CRHR1 cells (0% and 0%. fluorescently-labelled cells); (b) CHO Flp-IN-CRHR1 cells stained with secondary anti-mouse IgG-Alexa Fluor®488 antibody (1.1% and 1.5% fluorescently-labelled cells); (c) CHO Flp-IN cells stained with mouse anti-CRHR1 antibody and secondary anti-mouse IgG-Alexa Fluor®488 antibody (4.3% and 3.6% fluorescently-labelled cells); (d) CHO Flp-IN-CRHR1 cells stained with mouse anti-CRHR1 antibody and secondary anti-mouse IgG-Alexa Fluor®488 antibody (86.3% and 88.3% fluorescently-labelled cells).

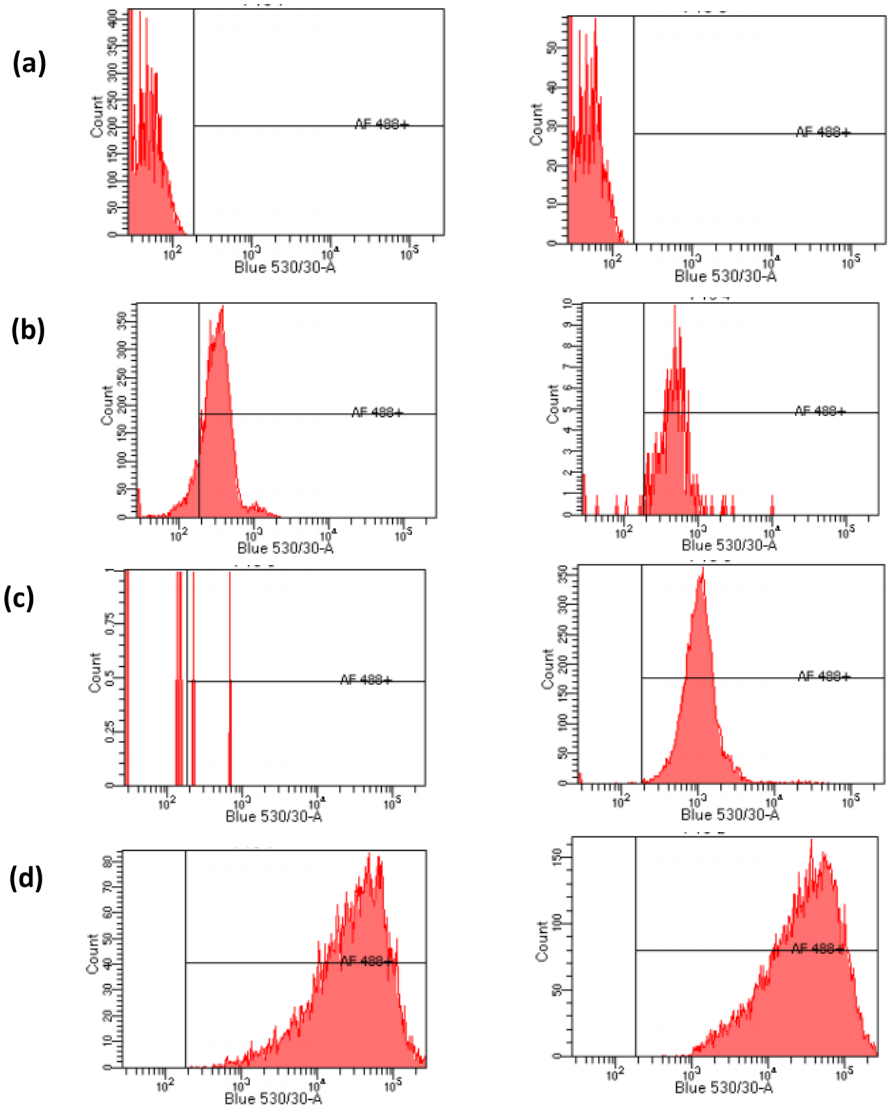

Figure 5.16: Indirect FACS analysis for CRHR1 expression on passage 15 CHO Flp-IN-CRHR1 cells using a mouse anti-CRHR1 (amino acids 24-415) antibody.

Duplicate samples showing (a) Unstained CHO Flp-IN-CRHR1 cells (0% and 0%. fluorescently-labelled cells); (b) CHO Flp-IN-CRHR1 cells stained with secondary anti-mouse IgG-Alexa Fluor®488 antibody (0.1% and 0.5% fluorescently-labelled cells); (c) CHO Flp-IN cells stained with mouse anti-CRHR1 antibody and secondary anti-mouse IgG-Alexa Fluor®488 antibody (0.0% and 4.9% fluorescently-labelled cells); (d) CHO Flp-IN-CRHR1 cells stained with mouse anti-CRHR1 antibody and secondary anti-mouse IgG-Alexa Fluor®488 antibody (95.3% and 96.2% fluorescently-labelled cells).

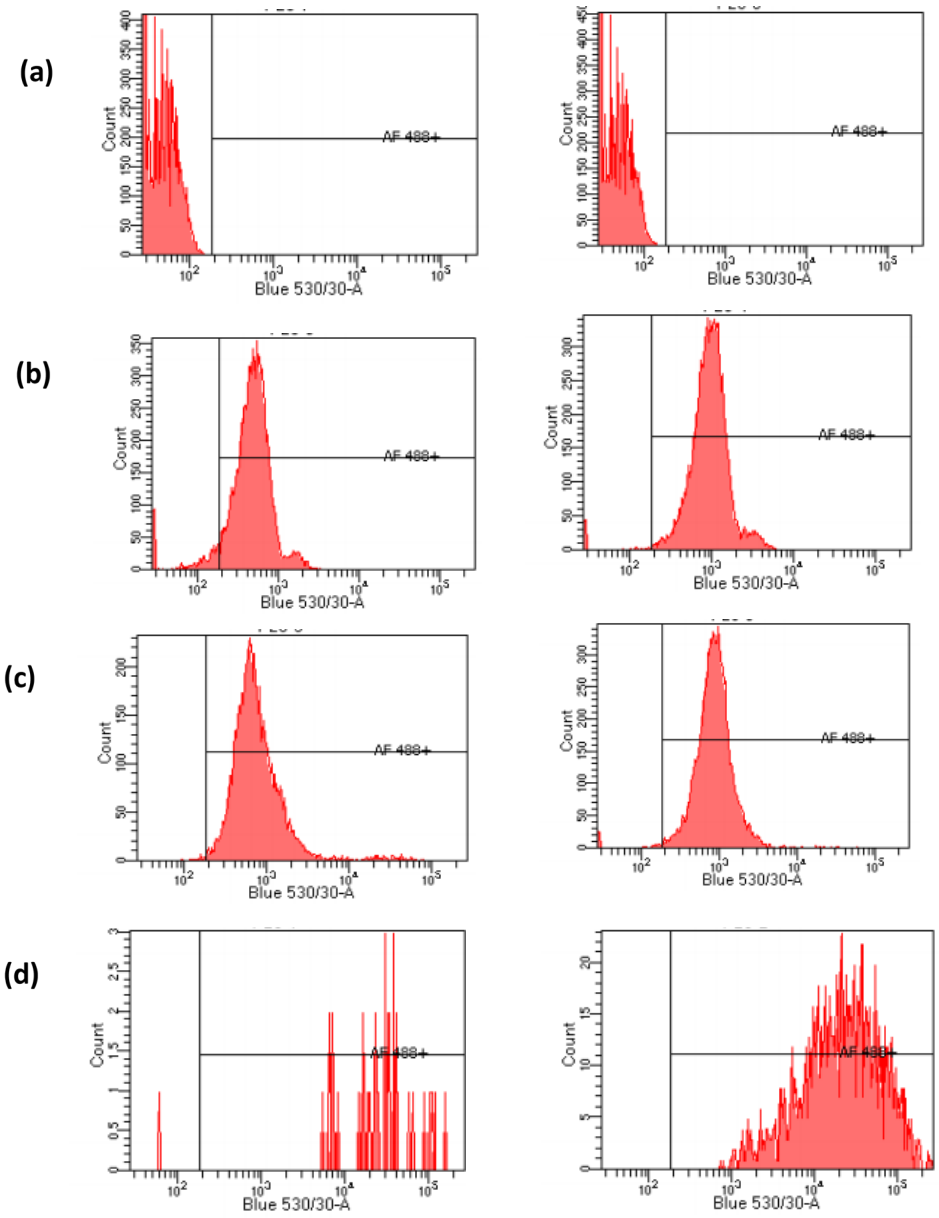

Figure 5.17: Indirect FACS analysis for CRHR1 expression on passage 20 CHO Flp-IN-CRHR1 cells using a mouse anti-CRHR1 (amino acids 24-415) antibody.

Duplicate samples showing (a) Unstained CHO Flp-IN-CRHR1 cells (0% and 0%. fluorescently-labelled cells); (b) CHO Flp-IN-CRHR1 cells stained with secondary anti-mouse IgG-Alexa Fluor®488 antibody (0.5% and 3.3% fluorescently-labelled cells); (c) CHO Flp-IN cells stained with mouse anti-CRHR1 antibody and secondary anti-mouse IgG-Alexa Fluor®488 antibody (5.3% and 3.1% fluorescently-labelled cells); (d) CHO Flp-IN-CRHR1 cells stained with mouse anti-CRHR1 antibody and secondary anti-mouse IgG-Alexa Fluor®488 antibody (97.5% and 94.4% fluorescently-labelled cells).

5.4 Discussion

Part of the research carried out in this thesis investigated whether siRNAs could silence POMC expression. The data obtained suggested that POMC siRNAs could indeed target the POMC gene and reduce ACTH secretion from AtT20 cells. Such activity could form the basis of a medical therapy in the treatment of Cushing's disease. However, the delivery of siRNAs to their target cells has often proven to be a major challenge (Layzer et al., 2004; Bumcrot et al., 2006; Wang et al., 2010). Conjugation of siRNAs to a ligand or antibody specific for a cell surface receptor has therefore been suggested as a way to improve siRNA uptake by their target cells (Cesarone et al., 2007; Daka and Peer, 2012; Tam et al., 2017). In the case of pituitary corticotroph cells, targeting of the CRHR1 with POMC siRNAs attached to CRH or to an anti-CRHR1 antibody could allow cell-specific delivery.

The work in Chapter 5 of this thesis indicated that AtT20 cells were not suitable for testing which anti-CRHR1 antibody interacted with the receptor with a high degree of specificity. This may have been due to a low receptor density or that the AtT20 cells were not under optimum conditions for maximum CRHR1 expression. The main aim of this part of the project was to isolate a cell line that stably expressed the CRHR1. This would allow for the analysis of a panel of anti-CRHR1 antibodies in terms of their binding to the receptor and their potential usefulness as a conjugation delivery vehicle for POMC siRNAs.

Several cell lines that stably express the CRHR1 have been reported, including those derived from Chinese hamster ovary (CHO), human embryonic kidney 293 (HEK293), and neuronal hippocampal cells (Horlick et al., 1997; Chunheng et al., 2015; Inda et al., 2016; Purusothaman et al., 2019). In particular, CHO cells do not endogenously express the CRHR1 (Horlick et al., 1997), so have been considered a suitable cell type for the isolation of cell lines that express the receptor. Here, the CHO Flp-IN system was used to isolate a cell line stably expressing CRHR1. This technology enables the rapid isolation of cell lines that reliably and constitutively express the required protein (O'Gorman et al., 1991; Schlake and Bode, 1994; Turan et al., 2010). In addition, all cells are isogenic and so express the transfected cDNA to a similar level. Furthermore, the expression of exogenous cDNA is controlled at levels akin to endogenous genes,

thereby reducing the risk of artifacts caused by transcription-factor and processing-factor competition.

Initially, a stable CHO Flp-IN cell line expressing the CRHR1 was obtained by transfecting plasmid pSecTag-Link-CRHR1 and plasmid pOG44 into CHO Flp-IN cells. Several methods were then used to investigate CRHR1 expression on the CHO Flp-IN-CRHR1 cell line. The RT-PCR analysis detected CRHR1 mRNA in the CHO Flp-IN-CRHR1 cell line, but not in CHO Flp-IN parent cells. The elevation in the level of intracellular cAMP following stimulation with CRH also indicated the presence of functional CRHR1 on the surface of the CHO Flp-IN-CRHR1 cells. In contrast, CHO Flp-IN cells did not respond, and neither cell type was stimulated by the control peptide MCH.

Expression of the CRHR1 on CHO Flp-IN-CRHR1 cells was also analysed using an indirect FACS staining method with a mouse anti-CRHR1 antibody and an Alexa Fluor®488-labelled secondary antibody. Over 50% of CHO Flp-IN-CRHR1 cells were fluorescently-labelled in the FACS experiments. CHO Flp-IN cells showed a far lower level of staining of < 7%. The results suggested that the CRHR1 was expressed on the surface of the CHO Flp-IN-CRHR1 cells. In contrast, neither rabbit nor goat anti-CRHR1 antibodies detected the receptor on the CRHR1-expressing cell line. This might be due to a lack of access to their respective epitopes on the receptor or that they do not recognise their epitope in the context of the CRHR1 in its native conformation.

To study the stability of the CHO Flp-IN-CRHR1 cell line, the cells were cultured and passaged five, 10, 15, and 20 times. The expression of the receptor was then analysed by RT-PCR and by indirect FACS. The results indicated that the CHO Flp-IN-CRHR1 cells expressed CRHR1 mRNA and protein at all the cell passages tested.

In conclusion, the work carried out successfully isolated a cell line stably expressing the CRHR1, although further study of the mouse anti-CRHR1 antibody’s interaction with and its specificity for the receptor is required.

Chapter 6

General Discussion

6 General Discussion

Cushing's disease is a rare condition that results from sustained secretion of cortisol from the adrenal glands, which in turn is caused by hypersecretion of ACTH from a pituitary adenoma (Cushing, 1912; Cushing, 1932). Clinical manifestations include obesity, diabetes, hypertension, osteoporosis, and depression. If left untreated, the disease has a five-year 50% mortality rate (Steffensen et al., 2010; Castinetti et al., 2012). The present first-line treatment is transsphenoidal surgery, but this is characterised by high rates of recurrence (Newell-Price et al., 2006; Biller et al., 2008; Pivonello et al., 2008). Medical therapies are considered a second-line treatment, but these often produce detrimental side-effects (Vieira et al., 2014). Due to the unsatisfactory outcomes of current treatments, an international consensus identified the need for a medical therapy for Cushing's diseases that would lower circulating ACTH levels (Biller et al., 2008). Such a therapy has to be rapid in effect, specific, and produce a minimal effect on other pituitary functions. In this project, it was hypothesised that by efficiently silencing the expression of the ACTH-encoding POMC gene using specific siRNAs, ACTH production from pituitary adenoma cells might be minimised, thus lowering cortisol levels and relieving disease characteristics.

Delivery of siRNAs to their target cells is a challenge to their use as therapeutics. One mechanism by which this problem can be overcome, potentially, is the attachment of the siRNA molecule to an antibody or a peptide ligand that can interact with a cell surface receptor. The CRHR1, which is a G protein-coupled receptor expressed specifically on the surface of pituitary corticotrophs, could be the target for POMC siRNAs that are conjugated to CRH or an antibody that recognises the receptor exclusively. In this project, the expression of CRHR1 on AtT20 cells was investigated and a CRHR1 cell line was isolated that could be used to analyse the specificities of a panel of anti-CRHR1 antibodies. Both AtT20 cells and the cell line could then be used to test the delivery of siRNA conjugates via the receptor.

6.1 Use of POMC siRNAs to decrease ACTH production in AtT20 cells

6.1.1 Results summary

In this study, three siRNAs against POMC exon regions proved to be efficient in decreasing the ACTH secretion from cultured AtT20 cells that served as an *in vitro*

model for Cushing's disease. The use of appropriate controls indicated that the effect of the POMC siRNAs was specific. Indeed, when sufficient controls are absent, a non-specific effect could explain the gene-silencing effects that are ascribed to a precise siRNA (Echeverri et al., 2006). The decrease in ACTH could not be attributed mainly to the negative impacts of the Lipofectamine 2000 transfection reagent (Nguyen et al., 2007). Viable cell counts were by and large equal in experiments that used siRNA plus transfection reagent or left cells untreated. In addition, siRNAs unrelated to POMC, including commercial "non-targeting negative-control" siRNAs and siRNAs that specifically targeted GAPDH or cyclophilin B, had no effect upon ACTH secretion from AtT20 cells. Furthermore, the study of scrambled and mismatched versions of the POMC siRNAs demonstrated that there was no major impact on ACTH secretion from AtT20 cells, indicating that the specific sequences of the siRNAs were essential for POMC gene-silencing.

High doses of siRNA can produce off-target effects and cellular toxicity and optimal concentrations have been reported to be around 1 nM (Frantz, 2003). In this study, it was observed that a 10 nM concentration of POMC siRNAs seemed to be as efficient at reducing ACTH secretion as the higher 30 nM. Both concentrations were efficient for up to 96 h post-transfection. Additionally, 1 nM POMC siRNA also had an effective gene-silencing effect of up to 96 h. The use of low concentrations of siRNA that are still effective also has the advantage of reduced costs (Fedorov et al., 2006).

Activation of the innate immune system is an off-target, non-specific effect of siRNAs that can occur upon their entry into mammalian cells (Whitehead et al., 2011). The production of interferon and pro-inflammatory cytokines can result from detection of siRNAs by the components of cytoplasmic or endosomal signalling pathways such as PKR, TLR-3, TLR-7 and TLR-8. Although the exact effect is dependent upon cell type, it is prudent to investigate whether or not the proposed target cells could mount an immune reaction in response to transfected siRNA.

The analysis carried out using AtT20 cells indicated that none of the POMC siRNAs induced an immune response that resulted in the production of IFN-α, IFN-β, IL-1β, IL-6 or TNF-α. In contrast, the synthetic dsRNA poly-I:C stimulated all the aforementioned interferons and cytokines from the AtT20 cell line, providing

confidence that the cells were capable of producing IFN-α, IFN-β, IL-1β, IL-6 and TNF-α, and that the results for the POMC siRNAs were not just false-negatives.

6.1.2 Future work

The subject of off-target effects of the POMC siRNAs needs to be evaluated. Although siRNA molecules are designed to silence the expression of specific genes, off-target effects can potentially limit the utility of them as a therapeutic. Such off-target effects can result in the silencing of genes which the siRNA is not designed to target, with four-fold changes in expression of being reported (Jackson et al., 2006; Birmingham et al., 2007). This can occur if siRNAs bind to mRNAs even though slight mismatches are present in the target (Snove and Holen, 2004; Ozcan et al., 2015). In addition, off-target silencing can occur if there are similarities between the seed region of the antisense strand of the siRNA and the 3'-untranslated region of a mRNA (Jackson et al., 2006; Birmingham et al., 2007). Although sequence alignment tools such as BLAST can be used to identify sequences that share high base pair homology when designing siRNAs, it has been documented that they do not always pinpoint sequences that can cause the targeting of other mRNAs (Birmingham et al., 2007). As an alternative, microarrays enable the expression of several thousand genes to be investigated in relation to the effects of specific siRNAs (Jackson et al., 2006; Jackson et al., 2010).

The immune activation of the POMC siRNAs needs to be further investigated in relation to immune cells such as monocytes, dendritic cells, and macrophages (Whitehead et al., 2011), as ultimately the siRNAs will be used *in vivo*. Initially, this can be analysed using cells *in vitro* and transfection protocols to deliver siRNAs. Clinically, the results of hyperstimulating an innate immune response in patients can have serious consequences inducing low blood pressure, chills and fever (Michie et al., 1988). The outcome of a cytokine storm can include cardiovascular shock, respiratory distress syndrome, and possibly death (Suntharalingam et al., 2006). Such side-effects, mean it is critical to identify and control any immunostimulatory effects when using siRNA in both animal models and in clinical trials involving human patients.

Further work will progress the development of *ex vivo* and *in vivo* models to test the effectiveness of POMC siRNAs. Pituitary adenoma cells obtained from patients with

Cushing's disease would provide an *ex vivo* model where the effect of POMC siRNAs on ACTH secretion could be measured. This could be complemented by examining how POMC siRNA may or may not affect the production of other pituitary hormones.

Previously, *in vivo* work has been undertaken using nude mice that are deficient in T cells due to the absence of a thymus gland (Munir, 2012). As a model of Cushing's disease, the mice were inoculated subcutaneously with AtT20 cells which caused an ACTH-secreting tumour to form under the skin. Treatment of the mice, using POMC siRNA3, showed that ACTH secretion from AtT20 cell-induced tumours was reduced by 51-64% of that in controls after five days (Munir, 2012). Levels of circulating cortisol were also lowered but were not statistically significantly affected when compared with controls (Munir, 2012). Future work using this *in vivo* model will include testing POMC siRNA1 and siRNA2 to ascertain their effects upon ACTH secretion and the levels of other hormones.

6.2 Corticotropin-releasing hormone receptor 1 as a siRNA delivery target

6.2.1 Results summary

The expression of CRHR1 in ATt20 cells was confirmed by RT-PCR. In addition, the functional receptor was detected on the cells by measuring the secretion of ACTH and accumulation of cAMP in response to stimulation with CRH. This result was in agreement with previous findings that had demonstrated the AtT20 cell line responds to CRH by secreting ACTH (Gagner and Drouin, 1987; Bugarini et al., 2017). Though AtT20 cells express the CRHR1, FACS analysis utilising primary anti-CRHR1 antibodies directed at extracellular epitopes and fluorescently-labelled secondary antibodies did not yield a decisive result with only low proportions of the cells fluorescing. This could be attributed to the poor receptor expression in the cell population, to a low density of the receptors on AtT20 cells, or to poor recognition and binding by the anti-CRHR1 primary antibodies.

In order to ensure that commercially available anti-CRHR1 antibodies bound to the receptor specifically, a CHO FlpIN cell line expressing the CRHR1 at a high level was isolated. CRHR1 expression was confirmed by several methods. RT-PCR analysis detected CRHR1 mRNA in the CHO Flp-IN-CRHR1 cell line, but not in the original CHO Flp-IN cells. The accumulation of cAMP in response to CRH-stimulation was also

investigated. A response to CRH was only evident in the CHO Flp-IN-CRHR1 cells. CHO Flp-IN cells did not respond to CRH, even though cAMP accumulated in response to forskolin, a cell-permeable activator of adenylyl cyclase.

FACS analysis utilising a mouse monoclonal anti-CRHR1 antibody demonstrated a high percentage (over 50%) of fluorescing cells compared with CHO Flp-IN cells (7%), indicating the existence of the receptor on the CHO-FlpIN-CRHR1 cells. The apparent, though low level, expression of the CRHR1 on CHO Flp-IN cells is likely due to cross-reactivity of the antibody with other cell surface-expressed proteins, as the cells did not respond to CRH and did not express CRHR1 mRNA. In contrast, two other anti-CRHR1 antibodies raised in either goat or rabbit did not appear to detect the receptor. This might be due to a lack of access to their respective epitopes on the receptor or that they do not recognise their epitope in the context of the CRHR1 in its native conformation.

The stability of the CHO Flp-IN-CRHR1 cell line was studied by culturing the cells and passaging them five, 10, 15, and 20 times. Analysis of the expression of the receptor by RT-PCR and by indirect FACS indicated that the CHO Flp-IN-CRHR1 cells expressed the protein of CRHR1 mRNA at all test results of the cell passages.

6.2.2 Future work

Further analysis of the mouse anti-CRHR1 antibody specificity is required to ensure that there is minimal cross-reactivity with other cell surface receptors. If the antibody proves inadequate for siRNA targeting purposes, an alternative strategy would be to isolate a new antibody using established methods (Huang et al., 2013; Smith and Crowe, 2015; Trier et al., 2019). A CHO Flp-IN cell line expressing a different receptor as a control for antibody binding would also be useful to isolate or to obtain from other researchers, if available. Finally, the methods of conjugation of antibodies to the POMC siRNA molecules warrants investigation so that the project can progress.

6.3 Conclusions

The project has demonstrated the effectiveness of POMC siRNAs at lowering the secretion of ACTH from AtT20 cells. As such, it provides the basis for further research into the use of siRNAs as a possible treatment for Cushing's disease for which there

is an unmet need for a medical therapy that is specific and effective. Furthermore, the study has provided the basis for future study of the CRHR1 as a means of delivering POMC siRNAs to their target cells.

References

References

Adams, D., Gonzalez-Duarte, A., O'Riordan, W. D., Yang, C. C., Ueda, M., Kristen, A. V., Tournev, I., Schmidt, H. H., Coelho, T., Berk, J. L. (2018). Patisiran, an RNAi therapeutic, for hereditary transthyretin amyloidosis*. The New England Journal of Medicine*. 379, 11-21.

Agrawal, N., Dasaradhi, P. V. N., Mohmmed, A., Malhotra, P., Bhatnagar, R. K., Mukherjee, S. K. (2003). RNA interference: biology, mechanism, and applications. *Microbiology and Molecular Biology Reviews.* 67, 657-685.

Allerson, C. R., Sioufi, N., Jarres, R., Prakash, T. P., Naik, N., Berdeja, A. (2005). Fully 2′-modified oligonucleotide duplexes with improved in vitro potency and stability compared to unmodified small interfering RNA. *Journal of Medicinal Chemistry*. 48, 901-904.

Aguilera, A., Zimmermann, F. K. (1986). Isolation and molecular analysis of the phosphoglucose isomerase structural gene of saccharomyces cerevisiae. *Molecular and General Genetics*. 202, 83-89.

Aguilera, G., Nikodemova, M., Wynn, P.C., and Catt, K.J. (2004). Corticotropin releasing hormone receptors: two decades later. *Peptides. 25*, 319-329.

Aigner, A. (2006). Gene silencing through RNA interference (RNAi) in vivo: strategies based on the direct application of siRNAs. *Journal of Biotechnology.* 124, 12-25.

Albani, A., Perez-rivas, L. G., Reincke, M., Theodoropoulou, M. (2018). Pathogenesis of cushing disease: an update on the genetics of corticotropinomas. *Endocrine Practice*. 24, 907-914.

Allen, R. G., Hatfield, J. M., Stack, J. (1988). Post-translational processing of pro-opiomelanocortin (POMC)-derived peptides during fetal monkey pituitary development: I. adrenocorticotropin (ACTH) and alpha-melanotropins (alpha-MSHs). *Developmental Biology.* 126, 156-163.

Alwani, R. A., De Herder, W. W., De Jong, F. H., Lamberts, S. W. J., Van Der Lely, A. J., Feelders, R. A. (2011). Rapid decrease in adrenal responsiveness to ACTH stimulation after successful pituitary surgery in patients with Cushing's disease. *Clinical Endocrinology.* 75, 602-607.

Amar, A. P., Weiss, M. H. (2003). Pituitary anatomy and physiology. *Neurosurgery Clinics of North America*. 14, 11-23.

Angart, P., Vocelle, D., Chan, C., Walton, S. P. (2013). Design of siRNA Therapeutics from the Molecular Scale. *Pharmaceuticals*. 6, 440-468.

Autelitano, D. J., Lundblud, J. R., Blum, M., Roberts, J. L. (1989). Hormonal regulation of POMC gene expression. *Annual Review of Physiology.* 51, 715-726.

Bansal, V., El Asmar, N., Selman, R. W., Arafah, B. M. (2015). Pitfalls in the diagnosis and management of Cushing's syndrome. *Neurosurgical Focus.* 38, 4.

Bartel, D. P. (2009). MicroRNAs: target recognition and regulatory functions. *Cell*. 136, 215-233.

Bender, J. (2015). Characterization of the interaction of CRHR1 with MAGUKs via the PDZ binding motif. In *PhD Thesis*. University of Munich, Munich Germany.

Bernstein, E., Caudy, A. A., Hammond, S. M., Hannon, G. J. (2001). Role for a bidentate ribonuclease in the initiation step of RNA interference. *Nature*. 409, 363-366.

Bertagna, X., Guignat, L., Groussin, L., Bertherat, J. (2009). Cushing's disease. *Best Practice and Research Clinical Endocrinology and Metabolism*. 23, 607-623.

Bicknell, A. (2008). The tissue-specific processing of pro-opiomelanocortin. *Journal of Neuroendocrinology*. 20, 692-699.

Biller, B., Grossman, A. B., Stewart, P., Melmed, S., Bertagna, X., Bertherat, J., Buchfelder, M., Colao, A., Hermus, A., Hofland, L. (2008). Treatment of adrenocorticotropin-dependent Cushing's syndrome: a consensus statement. *Journal of Clinical Endocrinology and Metabolism*. 93, 2454-2462.

Birmingham, A., Anderson, E., Sullivan, K., Reynolds, A., Boese, Q., Leake, D., Karpilow, J., Khvorova, A. (2007). A protocol for designing siRNAs with high functionality and specificity. *Nature Protocols.* 2, 2068-2078.

Bitko, V., Musiyenko, A., Shulyayeva, O., Barik, S. (2005). Inhibition of respiratory viruses by nasally administered siRNA. *Nature Medicine.* 11, 50-55.

Boeckle, S., von Gersdorff, K., van der Piepen, S., Culmsee, C., Wagner, E. Ogris, M. (2004). Purification of polyethylenimine polyplexes highlights the role of free polycations in gene transfer. *The Journal of Gene Medicine.* 6, 1102-1111.

Boronat, M., Carrillo, A., Ojeda, A., Estrada, J., Ezquieta, B., Marín, F., Nóvoa, F. J. (2004). Clinical manifestations and hormonal profile of two women with Cushing's disease and mild deficiency of 21-hydroxylase. *Journal of Endocrinological Investigation*. 27, 583-590.

Bosher, J. M., Labouesse, M. (2000). RNA Interference: genetic wand and genetic watchdog. *Nature Cell Biology.* 2, 31-36.

Boussif, O., Zanta, M., Behr, J. (1996). Optimized galenics improve *in vitro* gene transfer with cationic molecules up to 1000-fold. *Gene Therapy.* 3, 1074-1080.

Braasch, D. A., Paroo, Z., Constantinescu, A., Ren, G., Oz, O. K., Mason, R. P. (2004). Biodistribution of phosphodiester and phosphorothioate siRNA. *Bioorganic and Medicinal Chemistry Letters.* 14, 1139-1143.

Bramsen, J. B., Laursen, M. B., Nielsen, A. F., Hansen, T. B., Bus, C., Langkjær, N., Babu, B. R., Højland, T., Abramov, M., Van Aerschot, A. (2009). A large-scale chemical modification screen identifies design rules to generate siRNAs with high activity, high stability and low toxicity. *Nucleic Acids Research.* 37, 2867-2881.

Bramsen, J. B., Kjems, J. (2013). Engineering small interfering RNAs by strategic chemical modification. In: *siRNA Design. Methods in Molecular Biology*. 942, 87-109. Taxman, D. (editor). Humana Press, Totowa, New Jersey, USA.

Bridge, A. J., Pebernard, S., Ducraux, A., Nicoulaz, A-L., Iggo, R. (2003). Induction of an interferon response by RNAi vectors in mammalian cells. *Nature Genetics*. 34, 263–264.

Broering, R., Real, C. I., John, M. J., Jahn-Hofmann, K., Ickenstein, L. M., Kleinehr, K., Paul, A., Gibbert, K., Dittmer, U., Gerken, G., Schlaak, J. F. (2013). Chemical modifications on siRNAs avoid Toll-like receptor-mediated activation of the hepatic immune system in vivo and in vitro. *International Immunology*. 26, 35-46.

Bugarini, A., Chatain, G., Lu, J., Montgomery, B., Walbridge, S., Zhang, Q., RayChaudhury, A., Lonser, R., and Chittiboina, P. (2017). Corticotropin releasing hormone can selectively stimulate glucose uptake in corticotropinoma via glucose transporter 1. *Neuro-Oncology*. *19*, 33-33.

Bumcrot, D., Manoharan, M., Koteliansky, V., Sah, D. W. (2006). RNAi therapeutics: a potential new class of pharmaceutical drugs. *Nature Chemical Biology*. 2, 711-719.

Cappabianca, P., De Divitiis, E. (2004). Endoscopy and transsphenoidal surgery. *Neurosurgery*. 54, 1043-1050.

Campbell, J. M., Bacon, T. A., Wickstrom, E. (1990) Oligodeoxynucleoside phosphorothioate stability in subcellular extracts, culture media, sera and cerebrospinal fluid. *The Journal of Biochemical and Biophysical Methods*. 20, 259–267

Cardarelli, F., Digiacomo, L., Marchini, C., Amici, A., Salomone, F., Fiume, G., Rossetta, A., Gratton, E., Pozzi, D., and Caracciolo, G. (2016). The intracellular trafficking mechanism of Lipofectamine-based transfection reagents and its implication for gene delivery. *Scientific Reports. 6*, 8.

Castillo, V., Giacomini, D., Páez-Pereda, M., Stalla, J., Labeur, M., Theodoropoulou, M., Holsboer, F., Grossman, A. B., Stalla, G. N. K., Arzt, E. (2006). Retinoic acid as a novel medical therapy for Cushing's disease in dogs. *Endocrinology*. 147, 4438-4444.

Castinetti, F., Fassnacht, M., Johanssen, S., Terzolo, M., Bouchard, P., Chanson, P., Do Cao, C., Morange, I., Pico, A., Ouzounian, S. (2009). Merits and pitfalls of mifepristone in Cushing's syndrome. *European Journal of Endocrinology*. 160, 1003-1010.

Castinetti, F., Morange, I., Conte-devolx, B., Brue, T. (2012). Cushing's disease. *Orphanet Journal of Rare Diseases.* 7, 41.

Catto, J. W., Alcaraz, A., Bjartell, A. S., White, R. D. V., Evans, C. P., Fussel, S., Hamdy, F. C., Kallioniemi, O., Mengual, L., Schlomm, T. (2011). MicroRNA in prostate, bladder, and kidney cancer: a systematic review. *European Urology.* 59, 671-681.

Cekaite, L., Furset, G., Hovig, E., Sioud, M. (2007). Gene expression analysis in blood cells in response to unmodified and 2′-modified siRNAs reveals TLR-dependent and independent effects. *Journal of Molecular Biology*. 365, 90-108.

Cesarone, G., Edupuganti O. P., Chen, C. P., Wickstrom, E. (2007). Insulin receptor substrate 1 knockdown in human MCF7 ER+ breast cancer cells by nuclease-resistant IRS1 siRNA conjugated to a disulfide-bridged D-peptide analogue of insulin-like growth factor 1. *Bioconjugate Chemistry*. 18, 1831-1840.

Chakraborty, C., Sharma, A. R., Sharma, G., Doss, C. G. P., Lee, S. S. (2017). Therapeutic miRNA and siRNA: Moving from bench to clinic as next generation medicine. *Molecular Therapy - Nucleic Acids.* 8, 132-143

Chandela, A., Ueno, Y., (2019). Systemic delivery of small interfering RNA therapeutics: obstacles and advances. *Reviews in Agricultural Science*. 7,10-28.

Chang, C. C., Lauwerys, R., Bernard, A., Roels, H., Buchet, J. P., Garvey, J. S. (1980) Metallothionein in cadmium-exposed workers. *Environmental Research. 23*, 422-428.

Chart, J., Sheppard, H. (1958). Pharmacology and biochemistry of some amphenone analogues and other adrenal cortical inhibitors. *Journal of Medicinal Chemistry*. 1, 407-441.

Choung, S., Kim, Y. J., Kim, S., Park, H. O., Choi, Y. C. (2006). Chemical modification of siRNAs to improve serum stability without loss of efficacy. *Biochemical and Biophysical Research Communications.* 342, 919-927.

Chunheng, M., Guoqing, C., Long, H., Qiuyang, Deng., Dongliang, Lin., Lin, Cui., Yajun, Wang., Juan, Li. (2015). Corticotropin-releasing hormone (CRH) stimulates cocaine- and amphetamine-regulated transcript gene (CART1) expression through CRH type 1 receptor (CRHR1) in chicken anterior pituitary. *Molecular and Cellular Endocrinology*. 417,166-177.

Cool, D. R., Normant, E., Shen, F. S., Chen, H. C., Pannell, L., Zhang, Y., Loh, Y. P. (1997). Carboxypeptidase E is a regulated secretory pathway sorting receptor: genetic obliteration leads to endocrine disorders in Cpefat mice. *Cell*. 88, 73-83.

Coote, J. (2005). A role for the paraventricular nucleus of the hypothalamus in the autonomic control of heart and kidney. *Experimental Physiology*. 90, 169-173.

Cowley, M. A., Smart, J. L., Rubinstein, M., Cerdan, M. G., Diano, S., Horvath, T. L., Cone, R. D., Low, M. J. (2001). Leptin activates anorexigenic POMC neurons through a neural network in the arcuate nucleus. *Nature*, 411, 480-484.

Cushing, H. (1912). The pituitary body and its disorders: clinical states produced by disorders of the hypophysis cerebri. J.B. Lippincott Company, Philadelphia, Pennsylvania, USA.

Cushing, H. (1932). The basophil adenomas of the pituitary body and their clinical manifestations (pituitary basophilism). *Bulletin of the Johns Hopkins Hospital*. 50, 137-195.

Daka, A., Peer, D. (2012). RNAi-based nanomedicines for targeted personalized therapy. *Advanced Drug Delivery Reviews*. 64, 1508-1521.

Dalayeun, J. F., Norès, J. M., Bergal, S. (1993). Physiology of β-endorphins. A close-up view and a review of the literature. *Biomedicine and Pharmacotherapy*. 47, 311-320.

Deng, Y., Wang, C. C., Choy, K. W., Du, Q., Chen, J., Wang, Q., Li, L., Chung, T. K. H., Tang, T. (2014). Therapeutic potentials of gene silencing by RNA interference: Principles, challenges, and new strategies. *Gene. 538*, 217-227.

Daniel, E., Newell-Price, J. (2017). Cushing's syndrome. *Medicine*. 45, 475-479.

Dauletbaev, N., Cammisano, M., Herscovitch, K., Lands, L. C. (2015). Stimulation of the RIG-I/MAVS pathway by polyinosinic:polycytidylic acid upregulates IFN-β in airway epithelial cells with minimal costimulation of IL-8. *Journal of Immunology*. 195, 2829-2841.

Davies, M. U. H., Hardman, J. (2005). Anaesthesia and adrenocortical disease. *Continuing Education in Anaesthesia Critical Care and Pain*. 5, 122-126.

De Menis, E., Roncaroli, F., Calvari, V., Chiarini, V., Pauletto, P., Camerino, G., Cremonini, N. (2005). Corticotroph adenoma of the pituitary in a patient with X-linked adrenal hypoplasia congenita due to a novel mutation of the DAX-1 gene. *European Journal of Endocrinology*. 153, 211-215.

De Paula, D., Bentley, M. V. L., Mahato, R. I. (2007). Hydrophobization and bioconjugation for enhanced siRNA delivery and targeting. *RNA. 13*, 431-456.

Demirjian, S., Ailawadi, G., Polinsky, M., Bitran, D., Silberman, S., Shernan, S. K., Burnier, M., Hamilton, M., Squiers, E., Erlich, S., et al. (2017). Safety and tolerability study of an intravenously administered small interfering ribonucleic acid (siRNA) post On-Pump cardiothoracic surgery in patients at risk of acute kidney Injury. *Kidney International Reports*. 2, 836-843.

De Souza, F. S., Bumaschny, V. F., Low, M. J., Rubinstein, M. (2005). Subfunctionalization of expression and peptide domains following the ancient duplication of the proopiomelanocortin gene in teleost fishes. *Molecular Biology and Evolution*. 22, 2417-2427.

Deipolyi, A., Karaosmanoglu, A., Habito, C., Brannan, S., Wicky, S., Hirsch, J., Oklu, R. (2012). The role of bilateral inferior petrosal sinus sampling in the diagnostic evaluation of Cushing syndrome. *Diagnostic and Interventional Radiology*. 18, 132-138.

DeVincenzo, J., Cehelsky, J. E., Alvarez, R., Elbashir, S., Harborth, J., Toudjarska, I., Nechev, L., Murugaiah, V., Van, A., Vliet., Vaishnaw, A. K., Meyers, R. (2008). Evaluation of the safety, tolerability and pharmacokinetics of ALN-RSV01, a novel RNAi antiviral therapeutic directed against respiratory syncytial virus (RSV). *Antiviral Research*. 77, 225-231.

Ding, D., Starke, R. M., Sheehan, J. P. (2014). Treatment paradigms for pituitary adenomas: defining the roles of radiosurgery and radiation therapy. *Journal of Neuro-Oncology.* 117, 445-457.

dos Santos Claro, P. A., Inda, C., Armando, N. G., Piazza, V. G., Attorresi, A., Silberstein, S., Shukla, A. K. (2019). Assessing real-time signaling and agonist-induced CRHR1 internalization by optical methods. *Methods in Cell Biology.* 149, 239-257.

Doench, J.G., Petersen, C.P., and Sharp, P.A. (2003). siRNAs can function as miRNAs. *Genes and Development*. 17, 438-442.

Drouin, J., Nemer, M., Charron, J., Gagner, J. P., Jeannotte, L., Sun, Y. L., Therrien, M., Tremblay, Y. (1989). Tissue-specific activity of the pro-opiomelanocortin (POMC) gene and repression by glucocorticoids. *Genome*. 31, 510-519

Dyawanapelly, S., Ghodke, S. B., Vishwanathan, R., Dandekar, P., Jain, R. (2014). RNA interference-based therapeutics: molecular platforms for infectious diseases. *Journal of Biomedical Nanotechnology.* 10, 1-40.

Echeverri, C. J., Beachy, P. A., Baum, B., Boutros, M., Buchholz, F., Chanda, S. K., Downward, J., Ellenberg, J., Fraser, A. G., Hacohen, N. (2006). Minimizing the risk of reporting false positives in large-scale RNAi screens. *Nature Methods.* 3, 777-779.

Eckstein, F. (2014). Phosphorothioates, essential components of therapeutic oligonucleotides. *Nucleic Acid Therapeutics*. 24, 374-387.

Elamin, M. B., Murad, M. H., Mullan, R., Erickson, D., Harris, K., Nadeem, S., Ennis, R., Erwin, P. J., Montori, V. M. (2008). Accuracy of diagnostic tests for Cushing's syndrome: a systematic review and metaanalyses. *Journal of Clinical Endocrinology and Metabolism*. 93, 1553-1562.

Elbashir, S. M., Harborth, J., Lendeckel, W., Yalcin, A., Weber, K., Tuschl, T. (2001). Duplexes of 21-nucleotide RNAs mediate RNA interference in cultured mammalian cells. *Nature*. 411, 494-498.

Elias, L. L., Clark, A. J. (2000). The expression of the ACTH receptor. *Brazilian Journal of Medical and Biological Research. 33,* 1245-1248

Elkayam, E., Kuhn, C. D., Tocilj, A., Haase, A. D., Greene, E. M., Hannon, G. J. (2012). The structure of human argonaute-2 in complex with miR-20a. *Cell*. 150, 100–110.

Elmén, J., Thonberg, H., Ljungberg, K., Frieden, M., Westergaard, M., Xu, Y. (2005). Locked nucleic acid (LNA) mediated improvements in siRNA stability and functionality. *Nucleic Acids Research*. 33, 439-447.

Evans, V. R., Manning, A., Bernard, L. H., Chronwall, B. M., Millington, W. R. (1994). Alpha-melanocyte-stimulating hormone and N-acetyl-beta-endorphin immunoreactivities are localized in the human pituitary but are not restricted to the zona intermedia. *Endocrinology*. 134, 97-106.

Fedorov, Y., Anderson, E. M., Birmingham, A., Reynolds, A., Karpilow, J., Robinson, K., Leake, D., Marshall, W. S., Khvorova, A. (2006). Off-target effects by siRNA can induce toxic phenotype. *RNA.* 12, 1188-1196.

Feelders, R. A., De Bruin, C., Pereira, A. M., Romijn, J. A., Netea-Maier, R. T., Hermus, A. R., Zelissen, P. M., Van Heerebeek, R., De Jong, F. H., Van Der Lely, A. J. (2010). Pasireotide alone or with cabergoline and ketoconazole in Cushing's disease. *The New England Journal of Medicine.* 362,1846-1848.

Feelders, R. A., Pulgar, S. J., Kempel, A., Pereira, A. M. (2012). The burden of Cushing's disease: clinical and health-related quality of life aspects. *European Journal of Endocrinology.* 167, 311-326.

Fire, A. (1999). RNA-triggered gene silencing. *Trends in Genetics*. 15, 358-363.

Fire, A., Xu, S., Montgomery, M. K., Kostas, S. A., Driver, S. E. Mello., C. C. (1998). Potent and specific genetic interference by double-stranded RNA in *Caenorhabditis elegans*. *Nature*. 391, 806-811.

Fischer, D., von Harpe, A., Kunath, K., Petersen, H., Li, Y., Kissel, T. (2002). Copolymers of ethylene imine and N-(2-hydroxyethyl)-ethylene imine as tools to study effects of polymer structure on physicochemical and biological properties of DNA complexes. *Bioconjugate Chemistry.* 13, 1124-1133.

Fitzgerald, K., Frank-Kamenetsky, M., Shulga-Morskaya, S., Liebow, A., Bettencourt, B. R., Sutherland, J. E., Hutabarat, R. M., Clausen, V. A., Karsten, V., Cehelsky, J. (2014). Effect of an RNA interference drug on the synthesis of proprotein convertase subtilisin/kexin type 9 (PCSK9) and the concentration of serum LDL cholesterol in healthy volunteers: A randomised, singleblind, placebo controlled, phase 1 trial. *Lancet*. 383, 60-68.

Fitzgerald, K., White, S., Borodovsky, A., Bettencourt, B. R., Strahs, A., Clausen, V., Wijngaard, P., Horton, J. D., Taubel, J., Brooks, A., et al. (2017). A highly durable RNAi therapeutic inhibitor of PCSK9. *The New England Journal of Medicine*. 376, 41-51.

Fleseriu, M. (2012). Medical management of persistent and recurrent Cushing's disease. *Neurosurgery Clinics of North America.* 23, 653-668.

Fleseriu, M. (2014). Recent advances in the medical treatment of Cushing's disease. *F1000 Prime Reports*. 10, 6-18.

Fougerolles, A. D., Vornlocher, H. P., Maraganore, J., Lieberman, J. (2007). Interfering with disease: a progress report on siRNA-based therapeutics. *Nature Reviews Drug Discovery.* 6, 443-453.

Frantz, S. (2003). Studies reveal potential pitfalls of RNAi. *Nature Reviews Drug Discovery*. 2, 763-764.

Furth, J., Gadsen, E. L. Upton, A. C. (1953). ACTH secreting transplantable pituitary tumors. *Proceedings of the Society for Experimental Biology and Medicine. 84*(1), 253-4.

Fukuoka, M., Wu, Y. L., Thongprasert, S., Sunpaweravong, P., Leong, S. S., Sriuranpong, V., Chao, T. Y., Nakagawa, K., Chu, D. T., Saijo, N., Duffield, E. L., Rukazenkov, Y., Speake, G., Jiang, H., Armour, A. A., To, K. F., Yang, J. C,. Mok, T. S. (2011). Biomarker analyses and final overall survival results from a phase III, randomized, open-label, first-line study of gefitinib versus carboplatin/paclitaxel in clinically selected patients with advanced non-small-cell lung cancer in Asia (IPASS). *Journal of Clinical Oncology*. 29, 2866-2874.

Gallo-Payet, N. (2016). 60 years of POMC: adrenal and extra-adrenal functions of ACTH. *Journal of Molecular Endocrinology*. 56, 135-156.

Gagner, J. P., Drouin, J. (1987). Tissue-specific regulation of pituitary proopiomelanocortin gene-transcription by corticotropin-releasing hormone, 3',5'-cyclic adenosine-monophosphate, and glucocorticoids. *Molecular Endocrinology*. 1, 677-682.

Gantier, M. P., Williams, B. R. (2007). The response of mammalian cells to double-stranded RNA. *Cytokine & Growth Factor Reviews*. 18, 363-371.

Garba, A. O., Mousa, S. A. (2010). Bevasiranib for the treatment of wet, age-related macular degeneration. *Ophthalmology and Eye Diseases*. 2, 75-83.

Garren, L. D., Gill, G. N., Walton, G. M. (1971). The isolation of a receptor for adenosine 3′, 5′-cyclic monophosphate (cAMP) from the adrenal cortex: the role of the receptor in the mechanism of action of cAMP. *Annals of the New York Academy of Sciences*. 185, 210-226.

Gary, D. J., Puri, N., Won, Y. Y. (2007). Polymer-based siRNA delivery: perspectives on the fundamental and phenomenological distinctions from polymer-based DNA delivery. *Journal of Controlled Release.* 121, 64-73.

Georgitsi, M., Raitila, A., Karhu, A., Tuppurainen, K., Mäkinen, M. J., Vierimaa, O., Paschke, R., Saeger, W., van der Luijt, R. B., Sane, T. (2007). Molecular diagnosis of pituitary adenoma predisposition caused by aryl hydrocarbon receptor-interacting protein gene mutations. *Proceedings of the National Academy of Sciences USA*. 104, 4101-4105.

Ghaddhab, C., Vuissoz, J. M., Deladoëy, J. (2017). From bioinactive ACTH to ACTH antagonist: the clinical perspective. *Frontiers in Endocrinology*. 8, 8-17.

Gicquel, C., Le Bouc, Y., Luton, J. P., Girard, F., Bertagna, X. (1992). Monoclonality of corticotroph macroadenomas in Cushing's disease. *Journal of Clinical Endocrinology and Metabolism*. 75, 472-475.

Giladi H. (2003). Small interfering RNA inhibits hepatitis B virus replication in mice. *Molecular Therapy.* 8, 769-776.

Gill, G. N. (1972). Mechanism of ACTH action. *Metabolism*. 21, 571-588.

Goldfarb, A. H., Hatfield, B. D., Potts, J., Armstrong, D. (1991). Beta-endorphin time course response to intensity of exercise: effect of training status. *International Journal of Sports Medicine*. 12, 264-268.

Goodchild, A., Nopper, N., Craddock, A., Law, T., King, A., Fanning, G., Rivory, L., Passioura, T. (2009). Primary leukocyte screens for innate immune agonists. *Journal of Biomolecular Screening*. 14, 723-30.

Gorden, K. B., Gorski, K. S., Gibson, S. J., Kedl, R. M., Kieper, W. C., Qiu, X., Tomai, M. A., Alkan, S. S., Vasilakos, J. P. (2005). Synthetic TLR agonists reveal functional differences between human TLR7 and TLR8. *Journal of Immunology*. 174, 1259–1268.

Grammatopoulos, D.K., and Chrousos, G.P. (2002). Functional characteristics of CRH receptors and potential clinical applications of CRH-receptor antagonists. *Trends in Endocrinology and Metabolism*. *13*, 436-444.

Grammatopoulos., Markovic, D., Dimitris, K. (2009). Focus on the splicing of secretin GPCRs transmembrane-domain 7. *Trend in Biochemical Science.* 34, 443-452.

Green, V. L., Atkin, S. L., Speirs, V., Jeffreys, R. V., Landolt, A. M., Mathew, B., Hipkin, L., White, M. C. (1996). Cytokine expression in human anterior pituitary adenomas. *Clinical Endocrinology*. 45, 179-185.

Grimm, D., Streetz, K. L., Jopling, C. L., Storm, T. A., Pandey, K., Davis, C. R., Marion, P., Salazar, F., Kay, M. A. (2006). Fatality in mice due to oversaturation of cellular microRNA/short hairpin RNA pathways. *Nature.* 441, 537-541.

Grishok, A., Pasquinelli, A. E., Conte, D., Li, N., Parrish, S., Ha, I., Baillie, D. L., Fire, A., Ruvkun, G., Mello, C. C. (2001). Genes and mechanisms related to RNA interference regulate expression of the small temporal RNAs that control C. elegans developmental timing. *Cell*. 106, 23-34.

Grunweller, A., Wyszko, E., Bieber, B., Jahnel, R., Erdmann, V. A., Kurreck, J. (2003) Comparison of different antisense strategies in mammalian cells using locked nucleic acids, 2'-O methyl RNA, phosphorothioates and small interfering RNA. *Nucleic Acids Research.* 31, 3185-93.

Haase, M., Schott, M., Kaminsky, E., Lüdecke, D. K., Saeger, W., Fritzen, R., Schinner, S., Scherbaum, W. A., Willenberg, H. S. (2011). Cushing's disease in a patient with steroid 21-hydroxylase deficiency. *Endocrine Journal*. 58: 699-706.

Hall, A. H., Wan, J., Shaughnessy, E. E., Ramsay Shaw, B., Alexander, K. A. (2004). RNA interference using boranophosphate siRNAs: structure-activity relationships. *Nucleic Acids Research*. 32, 5991-6000.

Hamm, S., Latz, E., Hangel, D., Müller, T., Yu, P., Golenbock, D., Sparwasser, T., Wagner, H., Bauer, S. (2010). Alternating 2'-O-ribose methylation is a universal approach for generating non-stimulatory siRNA by acting as TLR7 antagonist. *Immunobiology*. 215, 559-569.

Hammond, S. M., Bernstein, E., Beach, D., Hannon, G. J. (2000). An RNA-directed nuclease mediates post-transcriptional gene silencing in Drosophila cells. *Nature*. 404, 293-296.

Hammond, S. M., Boettcher, S., Caudy, A. A., Kobayashi, R., Hannon, G. J. (2001). Argonaute2, a link between genetic and biochemical analyses of RNAi. *Science*. 293, 1146-1150.

Hannon, G. J. (2002). RNA interference. *Nature*. 418, 244-251.

Hannon, G. J., Rossi, J. J. (2004). Unlocking the potential of the human genome with RNA interference. *Nature*. 431, 371-378.

Hauger, R. L., Shelat, S. G., Redei, E. E. (2002). Decreased corticotropin-releasing factor receptor expression and adrenocorticotropic hormone responsiveness in anterior pituitary cells of Wistar-Kyoto rats. *Journal of Neuroendocrinology*.14, 126-134

Hayashi, K., Inoshita, N., Kawaguchi, K., Ibrahim Ardisasmita, A., Suzuki, H., Fukuhara, N., Okada, M., Nishioka, H., Takeuchi, Y., Komada, M., Takeshita, A., Yamada, S. (2016). The USP8 mutational status may predict drug susceptibility in corticotroph adenomas of Cushing's disease. *European Journal of Endocrinology.* 174, 213-226.

Heil, F., Hemmi, H., Hochrein, H., Ampenberger, F., Kirschning, C., Akira, S., Lipford, G., Wagner, H., Bauer, S. (2004). Species-specific recognition of single-stranded RNA via toll-like receptor 7 and 8. *Science*. 303, 1526-1529.

Hemley, C., McCluskey, A., Keller, P. A. (2007). Corticotropin releasing hormone-a GPCR drug target. *Current Drug Targets*. 8, 105-115.

Hilbert, M., Karow, A. R., Klostermeier, D. (2009). The mechanism of ATP-dependent RNA unwinding by DEAD box proteins. *Biological Chemistry*. 390, 1237-1250.

Hillhouse, E. W., Grammatopoulos, D. K. (2006). The molecular mechanisms underlying the regulation of the biological activity of corticotropin-releasing hormone receptors: implications for physiology and pathophysiology. *Endocrine Reviews.* 27, 260-286.

Hirsch, D., Shimon, I., Manisterski, Y., Aviran-Barak, N., Amitai, O., Nadler, V., Alboim, S., Kopel, V., Tsvetov, G. (2018). Cushing's syndrome: comparison between Cushing's disease and adrenal Cushing's. *Endocrine*. 62, 712-720.

Holen, T., Amarzguioui, M., Wiiger, M. T., Babaie, E., Prydz, H. (2002). Positional effects of short interfering RNAs targeting the human coagulation trigger tissue factor. *Nucleic Acids. Research*. *30*, 1757-1766.

Holsboer, F. (2000). The corticosteroid receptor hypothesis of depression. *Neuropsychopharmacology*. 23, 477-501.

Horlick, R. A., Sperle, K., Breth, L.A., Reid, C. C., Shen, E. S., Robbins, A. K., Cooke G. M., Largent, B. L. (1997). Rapid generation of stable cell lines expressing

corticotropin-releasing hormone receptor for drug discovery. *Protein Expression and Purification.* 9, 301-308.

Hornung, V., Guenthner-Biller, M., Bourquin, C., Ablasser, A., Schlee, M., Uematsu, S. (2005). Sequence-specific potent induction of IFN-alpha by short interfering RNA in plasmacytoid dendritic cells through TLR7. *Nature Medicine.* 11, 263–270.

Howlett, T., Drury, P., Perry, L., Doniach, I., Rees, L. H., Besser, G. (1986). Diagnosis and management of ACTH-dependent Cushing's syndrome: comparison of the features in ectopic and pituitary ACTH production. *Clinical Endocrinology.* 24, 699-713.

Howard, K. A., Rahbek, U. L., Liu, X., Damgaard, C. K., Glud, S. Z., Andersen, M. Ø., Hovgaard, M. B., Schmitz, A., Nyengaard, J. R., Besenbacher, F. (2006). RNA interference *in vitro* and *in vivo* using a chitosan/siRNA nanoparticle system. *Molecular Therapy.* 14, 476-484.

Hruby, V. J., Sharma, S. D., Toth, K., Jaw, J. Y., Al-Obeidi, F., Sawyer, T. K., Hadley, M. E. (1993). Design, synthesis, and conformation of superpotent and prolonged acting melanotropins. *Annals of the New York Academy of Sciences*. 680, 51-63.

Huang, J., Doria-Rose, N. A., Longo, N. S., Laub, L., Lin, C. L., Turk, E., Kang, B. H., Migueles, S. A., Bailer, R. T., Mascola, J. R., Connors, M. (2013). Isolation of human monoclonal antibodies from peripheral blood B cells. *Nature Protocols.* 8, 1907–1915.

Hutvágner, G., Zamore, P. D. (2002). A microRNA in a multiple-turnover RNAi enzyme complex. *Science*. 297, 2056-2060.

Inda, C., José Bonfiglio, J., Paula A. dos Santos, C., Sergio, A., Senin, Natalia, G., Armando, Jan, M., Deussing, Silberstein, S. (2016). cAMP-dependent cell differentiation triggered by activated CRHR1 in hippocampal neuronal cells. *Scientific Reports*. 7, 1944.

Inoue, C., Shiga, K., Takasawa, S., Kitagawa, M., Yamamoto, H., Okamoto, H. (1987). Evolutionary conservation of the insulinoma gene rig and its possible function. *Proceedings of the National Academy of Sciences USA*. 84, 6659-6662.

Ishizuka, A., Siomi, M. C. Siomi, H. (2002). A Drosophila fragile X protein interacts with components of RNAi and ribosomal proteins. *Genes and Development.* 16, 2497-2508.

Iwasaki, Y., Taguchi, T., Nishiyama, M., Asai, M., Yoshida, M., Kambayashi, M., Takao, T., Hashimoto, K. (2008). Lipopolysaccharide stimulates proopiomelanocortin gene expression in AtT20 corticotroph cells. *Endocrine Journal*. 55, 285-298.

Jackson, A. L., Burchard, J., Schelter, J., Chau, B. N., Cleary, M., Lim, L., Linsley, P. S. (2006). Widespread siRNA “off-target” transcript silencing mediated by seed region sequence complementarity. *RNA.* 12, 1179-1187.

Jackson, A. L., Linsley, P. S. (2010). Recognizing and avoiding siRNA off-target effects for target identification and therapeutic application. *Nature Reviews Drug Discovery*. 9, 57-67.

Jahns, H., Roos, M., Imig, J., Baumann, F., Wang, Y., Gilmour, R. (2015). Stereochemical bias introduced during RNA synthesis modulates the activity of phosphorothioate siRNAs. *Nature Communications.* 6, 6317.

Jenks, B. G. (2009). Regulation of proopiomelanocortin gene expression: An overview of the signaling cascades, transcription factors, and responsive elements involved. *Annals of the New York Academy of Sciences*. 1163, 17-30.

Johannsen, S., Allolio, B. (2007). Mifepristone (RU 486) in Cushing's Syndrome. *European Journal of Endocrinology*. 157, 561-569.

Judge, A. D., Sood, V., Shaw, J. R., Fang, D., Mcclintock, K., MacLachlan, I. (2005). Sequence-dependent stimulation of the mammalian innate immune response by synthetic siRNA. *Nature Biotechnology*. 23, 457-462.

Judge, A. D., Bola, G., Lee, A. C., Maclachlan, I. (2006). Design of noninfl ammatory synthetic siRNA mediating potent gene silencing in vivo. *Molecular Therapy*. 13, 494-505.

Juszczak, A., Ertorer, M., Grossman, A. (2013). The therapy of Cushing’s disease in adults and children: an update. *Hormone and Metabolic Research*. 45, 109-117.

Kamenický, P., droumaguet, C., Salenave, S., Blanchard, A., Jublanc, C., Gautier, J. F., Brailly-Tabard, S., Leboulleux, S., Schlumberger, M., Baudin, E. (2011). Mitotane, metyrapone, and ketoconazole combination therapy as an alternative to rescue adrenalectomy for severe ACTH-dependent Cushing's syndrome. *Journal of Clinical Endocrinology and Metabolism*. 96, 2796-2804.

Karl, M., Lamberts, S. W., Koper, J. W., Katz, D. A., Huizenga, N. E., Kino, T., Haddad, B. R., Hughes, M. R., Chrousos, G. P. (1996). Cushing's disease preceded by generalized

glucocorticoid resistance: Clinical consequences of a novel, dominant-negative glucocorticoid receptor mutation. *Proceedings of the Association of American Physicians.* 108, 296-307.

Kawai T., Akira, S. (2008). Toll-like receptor and RIG-1-like receptor signaling. *Annals of the New York Academy of Science*. 1143, 1–20.

Kawai, T., Akira, S. (2010). The role of pattern-recognition receptors in innate immunity: update on Toll-like receptors. *Nature Immunology*. 11, 373–384.

Kawashima, S. T., Usui, T., Sano, T., Iogawa, H., Hagiwara, H., Tamanaha, T., Tagami, T., Naruse, M., Hojo, M., Takahashi, J. A. (2009). P53 gene mutation in an atypical corticotroph adenoma with Cushing's disease. *Clinical Endocrinology*. 70, 656-657.

Khvorova, A., Reynolds, A., Jayasena, S. (2003). Functional siRNAs and miRNAs exhibit strand bias. *Cell.* 115, 209-216.

Kirk, L., Hash, R. B., Katner, H. P., Jones, T. (2000). Cushing's disease: clinical manifestations and diagnostic evaluation. *American Family Physician*. 62, 1119-1127.

Kitagawa, M., Takasawa, S., Kikuchi, N., Itoh, T., Teraoka, H., Yamamoto, H. Okamoto, H. (1991). Rig encodes ribosomal protein S15 the primary structure of mammalian ribosomal protein S15. *FEBS Letters. 283*, 210-214.

Kleinman, M. E., Yamada, K., Takeda, A., Chandrasekaran, V., Nozaki, M., Baffi, J. Z., Albuquerque, R. J., Yamasaki, S., Itaya, M., Pan, Y. (2008). Sequence-and target-independent angiogenesis suppression by siRNA via TLR3. *Nature.* 452, 591-597.

Kozomara, A., Griffiths-Jones, S. (2011). miRBase: integrating microRNA annotation and deepsequencing data. *Nucleic Acids Research*. 39, 152-157.

Kronsbein, H. C. (2008). CRHR1-dependent effects on protein expression and posttranslational modification in AtT-20 cells. *Molecular and Cellular. Endocrinology.* 292, 1-10.

Kumagai, Y., Akira, S. (2010). Identification and functions of pattern-recognition receptors. *Journal of Allergy and Clinical Immunology*. 125, 985-992.

Lacroix, A., Feelders, R. A., Stratakis, C. A., Nieman, L. K. (2015). Cushing's syndrome. *Lancet.* 386, 913-927.

Lam, J. K., Chow, M. Y., Zhang, Y., Leung, S. W. (2015). siRNA versus miRNA as therapeutics for gene silencing. *Molecular Therapy Nucleic Acids*. 4, e252.

Lamolet, B., Pulichino, A. M., Lamonerie, T., Gauthier, Y., Brue, T., Enjalbert, A., Drouin, J. (2001). A pituitary cell-restricted T box factor, Tpit, activates POMC transcription in cooperation with Pitx homeoproteins. *Cell*. 104, 849-859.

Lamonerie, T., Tremblay, J. J., Lanctôt, C., Therrien, M., Gauthier, Y. Drouin, J. (1996). Ptx1, a bicoid-related homeo box transcription factor involved in transcription of the pro-opiomelanocortin gene. *Genes and Development.* 10, 1284-1295.

Layzer, J. M., McCaffrey, A. P., Tanner, A. K., Huang, Z., Kay, M. A., Sullenger, B. A. (2004). In vivo activity of nuclease-resistant siRNAs. *RNA*. 10, 766-771.

Laursen, M. B., Pakula, M. M., Gao, S., Fluiter, K., Mook, O. R., Baas, F. (2010). Utilization of unlocked nucleic acid (UNA) to enhance siRNA performance in vitro and in vivo. *Molecular BioSystems.* 6, 862-870.

Lee, J., Chuang, T-H., Redecke, V., She, L., Pitha, P. M., Carson, D. A., Raz, E., Cottam, H. B. (2003). Molecular basis for the immunostimulatory activity of guanine nucleoside analogs: activation of Toll-like receptor 7. *Proceedings of the National Academy of Sciences USA*. 100:6646–6651.

Lee, S. H., Kang, Y. Y., Jang, H. E., Mok, H. (2016). Current preclinical small interfering RNA (siRNA) based conjugate systems for RNA therapeutics. *Advanced Drug Delivery Reviews*. *104*, 78-92.

Li, L., Hou, J., Liu, X., Guo, Y., Wu, Y., Zhang, L., and Yang, Z. (2014). Nucleolin-targeting liposomes guided by aptamer AS1411 for the delivery of siRNA for the treatment of malignant melanomas. *Biomaterials*. 35, 3840-3850.

Li, S. D., Huang, L. (2006). Targeted delivery of antisense oligodeoxynucleotide and small interference RNA into lung cancer cells (2006). *Molecular Pharmaceutics*. 3, 579-588

Li, W. A., Aravind; Wu., Zhijian. (2008) Engineering and selection of shuffled AAV genomes: a new strategy for producing targeted biological nanoparticles. *Molecular Therapy*. 16, 1252-1260

Lima, W. F., Wu, H., Nichols, J. G., Sun, H., Murray, H. M., Crooke, S. T. (2009). Binding and cleavage specificities of human Argonaute2. *Journal of Biological Chemistry*. 284, 26017-26028.

Lin, X., Ruan, X., Anderson, M. G., McDowell, J. A., Kroeger, P. E., Fesik, S. W., Shen, Y. (2005). siRNA-mediated off-target gene silencing triggered by a 7 nt complementation. *Nucleic Acids Research*. 33, 4527-4535.

Lindholm, J., Hagen, C., Kosteljanetz, M., Led, K., Laurberg, P., Weeke, J. (2004). Relation between pre-and post-dexamethasone test cortisol values in Cushing's disease. *International Journal of Endocrinology and Metabolism*. 2, 74-77.

Loeffler, J. S., Shih, H. A. (2011). Radiation therapy in the management of pituitary adenomas. *Journal of Clinical Endocrinology and Metabolism.* 96, 1992-2003.

López-Fraga, M., Martínez, T., Jiménez, A. (2009). RNA Interference technologies and therapeutics. *BioDrugs*. 23, 305-332.

Loriaux, D., Roy, A. (1986). Responses to corticotropin-releasing-hormone in the hypercortisolism of depression and Cushing's disease. *The New England Journal of Medicine.* 314, 1329-1335.

Losa, M., Mortini, P., Pagnano, A., Detomas, M., Cassarino, M. F., Pecori Giraldi, F. (2019). Clinical characteristics and surgical outcome in USP8-mutated human adrenocorticotropic hormone-secreting pituitary adenomas. *Endocrine*. 63, 240-246.

Love, K. T., Mahon, K. P., Levins, C. G., Whitehead, K. A., Querbes, W., Dorkin, J. R., Qin, J., Cantley, W., Qin, L. L., Racie, T., Frank-Kamenetsky, M., Yip, K. N., Alvarez, R., Sah, D. W. Y., de Fougerolles, A., Fitzgerald, K., Koteliansky, V., Akinc, A., Langer, R., Anderson, D. G. (2010). Lipid-like materials for low-dose, in vivo gene silencing. *Proceedings of the National Academy of Sciences USA*. 107, 1864-1869.

Lund, E., Güttinger, S., Calado, A., Dahlberg, J. E., Kutay, U. (2004). Nuclear export of microRNA precursors. *Science*. 303, 95-98.

Ma, Z. Y., Song, Z. J., Chen, J. H., Wang, Y. F., Li, S. Q., Zhou, L. F., Mao, Y., Li, Y. M., Hu, R. G., Zhang, Z. Y., Ye, H. Y., Shen, M., Shou, X. F., Li, Z. Q., Peng, H., Wang, Q. Z., Zhou, D. Z., Qin, X. L., Ji, J., Zheng, J., Chen, H., Wang, Y., Geng, D. Y., Tang, W. J., Fu, C. W., Shi, Z. F., Zhang, Y. C., Ye, Z., He, W. Q., Zhang, Q. L., Tang, Q. S., Xie, R., Shen, J. W., Wen, Z. J., Zhou, J., Wang, T., Huang, S., Qiu, H. J., Qiao, N. D., Zhang, Y., Pan, L., Bao, W.

M., Liu, Y. C., Huang, C. X., Shi, Y. Y. Zhao, Y. (2015). Recurrent gain-of-function USP8 mutations in Cushing's disease. *Cell Research*. 25, 306-317.

Matsumoto, M., Funami, K., Tanabe, M., Oshiumi, H., Shingai, M., Seto, Y., Yamamoto, A., Seya, T. (2003). Subcellular localization of Toll-like receptor 3 in human dendritic cells. *Journal of Immunology*. 171, 3154–3162.

Matsuzaki, L. N., Canto-Costa, M. H., Hauache, O.M. (2004). Cushing's disease as the first clinical manifestation of multiple endocrine neoplasia type 1 (MEN1) associated with an R460X mutation of the MEN1 gene. *Clinical Endocrinology*. 60, 142-143.

McNamara, j. O., Andrechek, E. R., Wang, Y., Viles, K. D., Rempel, E., Gilboa, B. A. Sullenger, P.H. Giangrande. (2006). Cell type-specific delivery of siRNAs with aptamer siRNA chimeras. *Nature Biotechnology.* 24, 1005-1015.

Meister, G., Tuschl, T. (2004). Mechanisms of gene silencing by double-stranded RNA. *Nature*. 431, 343-349.

Michie, H. R., Manogue, K. R., Spriggs, D. R., Revhaug, A., O'Dwyer, S., Dinarello, C. A., Cerami, A., Wolff, S. M., Wilmore, D. W. (1988). Detection of circulating tumor necrosis factor after endotoxin administration. *The New England Journal of Medicine*. 318, 1481–1486.

Miller, D. B., O'Callaghan, J. P. (2002). Neuroendocrine aspects of the response to stress. *Metabolism Clinical and Experimental*. 51, 5-10.

Miller, J. W., Crapo, L. (1993). The medical treatment of Cushing's syndrome. *Endocrine Reviews*. 14, 443-458.

Millington, G. W. (2007). The role of proopiomelanocortin (POMC) neurones in feeding behaviour. *Nutrition and Metabolism*. 4, 18.

Minniti, G., Brada, M. (2007). Radiotherapy and radiosurgery for Cushing's disease. *Arquivos Brasileiros de Endocrinologia and Metabologia.* 51, 1373-1380.

Moghaddam, B. (2013). Design and development of cationic liposomes as DNA vaccine adjuvants. In *PhD Thesis*. Aston University, Birmingham, UK.

Morrissey, D. V., Lockridge, J. A., Shaw, L., Blanchard, K., Jensen, K., Breen, W., Hartsough, K., Machemer, L., Radka, S., Jadhav, V. (2005). Potent and persistent *in vivo* anti-HBV activity of chemically modified siRNAs. *Nature Biotechnology. 23*, 1002-1007.

Moschos, S.A., Jones, S. W., Perry, M. M., Williams, A.E., Erjefalt, J. S., Turner, J. J., Barnes, P.J., Sproat, P. S., Gait, M. J., LindsayM. A. (2007). Lung delivery studies using siRNA conjugated to TAT (48–60) and penetratin reveal peptide induced reduction in gene expression and induction of innate immunity. *Bioconjugate Chemistry*. 18, 1450–1459.

Munir, A. (2012). RNA interference as therapy in a model of Cushing's Disease. In *PhD Thesis.* University of Sheffield, Sheffield, UK.

Murchison, E. P., Partridge, J. F., Tam, O. H., Cheloufi, S., Hannon, G. J. (2005). Characterization of Dicer-deficient murine embryonic stem cells. *Proceedings of The National Academy of Sciences USA.* 102 ,12135-12140.

Naito, Y., Ui-Tei, K. (2013). Designing functional siRNA with reduced off-target effects. *Methods in Molecular Biology.* 2942, 57-68.

Newell-Price, J. (2003). Proopiomelanocortin gene expression and DNA methylation: implications for Cushing's syndrome and beyond. *Journal of Endocrinology.* 177, 365-372.

Newell-price, J., Bertagna, X., Grossman, A. B., Nieman, L. K. (2006). Cushing's syndrome. *The Lancet.* 367, 1605-1617.

Ney, R. L., Dexter, R. N., Davis, W. W., Garren, L. D. (1967). A study of the mechanisms by which adrenocorticotropic hormone maintains adrenal steroidogenic responsiveness. *Journal of Clinical Investigation*. 46, 1916-1924.

Nguyen, Q. D., Schachar, R. A., Nduaka, C. I., Sperling, M., Basile, A.S., Klamerus, K. J., Chi-Burris, K., Yan, E., Paggiarino, D. A., Rosenblatt, I. (2012). Phase 1 dose-escalation study of a siRNA targeting the RTP801 gene in age-related macular degeneration patients. *Eye.* 26, 1099-1105.

Nieman, L. K., Biller, B. M., Findling, J. W., Newell-Price, J., Savage, M. O., Stewart, P. M., Montori, V. M. (2008). The diagnosis of Cushing's syndrome: an endocrine society clinical practice guideline. *Journal of Clinical Endocrinology and Metabolism.* 93, 1526-1540.

Oh, Y., Park, T. (2009). siRNA delivery systems for cancer treatment. *Advanced Drug Delivery Reviews.* 10, 850-862.

Ohmori, N., Nomura, K., Ohmori, K., Kato, Y., Itoh, T., Takano, K. (2003). Osteoporosis is more prevalent in adrenal than in pituitary Cushing's syndrome. *Endocrine Journal*. 50, 1-7.

O'Gorman S, Fox, D. T., Wahl, G. M. (1991). Recombinase-mediated gene activation and sitespecific integration in mammalian cells. *Science*. 251, 1351-1355.

Olejniczak, M., Galka, P., Wlodzimierz., Krzyzosiak, J. (2010). Sequence-non-specific effects of RNA interference triggers and microRNA regulators. *Nucleic Acids Research.* 38, 1-16.

Ozcan, G., Ozpolat, B., Coleman, R. L., Sood, A. K., Lopez-Berestein, G. (2015). Preclinical and clinical development of siRNA-based therapeutics. *Advanced Drug Delivery Reviews*. 87, 108-119.

Páez-pereda, M., Kovalovsky, D., Hopfner, U., Theodoropoulou, M., Pagotto, U., Uhl, E., Losa, M., Stalla, J., Grübler, Y., Missale, C. (2001). Retinoic acid prevents experimental Cushing syndrome. *Journal of Clinical Investigation*. 108, 1123-1131.

Paquet, L., Zhou, A., Chang, E. Y., Mains, R. E. (1996). Peptide biosynthetic processing: distinguishing prohormone convertases PC1 and PC2. *Molecular and Cellular Endocrinology*. 120, 161-168.

Papadopoulou, N., Chen, J., Harpal., Randeva, S., Michael, A., Edward L. W., Hillhouse., Dimitris, K. (2004). Protein kinase A-induced negative regulation of the corticotropin-releasing hormone R1α receptor-extracellularly regulated kinase signal transduction pathway: the critical role of Ser 301 for signaling switch and selectivity. *Molecular Endocrinology*. 18, 624-639.

Peer, D., Park, E. J., Morishita, Y., Carman, C. V., Shimaoka, M. (2008). Systemic leukocytedirected siRNA delivery revealing cyclin D1 as an anti-inflammatory target. *Science*. 319, 627-630.

Pecot, C. V., Calin, G. A., Coleman, R. L., Lopez-berestein, G., Sood, A. K. (2011). RNA interference in the clinic: challenges and future directions. *Nature Reviews Cancer.* 11, 59-67.

Perez-Rivas, L. G., Theodoropoulou, M., Ferraù, F., Nusser, C., Kawaguchi, K., Stratakis, C. A., Faucz, F. R., Wildemberg, L. E., Assié, G., Beschorner, R. (2015). The gene of the ubiquitin-specific protease 8 is frequently mutated in adenomas causing Cushing's disease. *The Journal of Clinical Endocrinology and Metabolism*. 100, 997-1004.

Petri, S., Meister, G. (2013). siRNA design principles and off-target effects. *Methods in Molecular Biology.* 986, 59-71.

Phillips, S. M., Tipton, K. D., Aarsland, A., Wolf, S. E., Wolfe, R. R. (1997). Mixed muscle protein synthesis and breakdown after resistance exercise in humans. *American Journal of Physiology*. 273, 99-107.

Pivonello, R., De Leo, M., Cozzolino, A., Colao, A. (2015). The treatment of Cushing's disease. *Endocrine Reviews*. 36, 385-486.

Pivonello, R., De Martino, M. C., De Leo, M., Lombardi, G., Colao, A. (2008). Cushing's syndrome. *Endocrinology and Metabolism Clinics of North America*. 37, 135-149.

Prakash, T. P., Allerson, C. R., Dande, P., Vickers, T. A., Sioufi, N., Jarres, R., Baker, B. F., Swayze, E. E., Griffey, R. H., Bhat, B. (2005). Positional effect of chemical modifi cations on short interference RNA activity in mammalian cells. *Journal of Medicinal Chemistry*. 48, 4247-4253.

Pratt, W. (1993). The role of heat shock proteins in regulating the function, folding, and trafficking of the glucocorticoid receptor. *Journal of Biological Chemistry.* 268, 21455-21455.

Polymeropoulos, Mihael H. Luna, R. I. O. D., Susan, E., Ide., Torres, R., Rubenstein, J., Clair, A., Francomano. (1995). The gene for pycnodysostosis maps to human chromosome 1cen-q21. *Nature Genetics*.10, 238-239.

Purusothaman, D., Murugan, S., Bethapudi, B., D'souza, P., Mundkinajeddu, D. (2019). Adaptogenic/Antistress Activity of a Polyherbal Formulation (PhytoceeTM): Mechanism to Combat Stress Adaptogenic/Antistress Activity of Polyherbal Formulation. *International Journal of Innovative Science and Research Technology*. 4, 2456-2165.

Raffin-Sanson, M., De Keyzer, Y., Bertagna, X. (2003). Proopiomelanocortin, a polypeptide precursor with multiple functions: from physiology to pathological conditions. *European Journal of Endocrinology.* 149, 79-90.

Raj, N. B., Pitha, P. M. (1981). Analysis of interferon mRNA in human fibroblast cells induced to produce interferon. *Proceedings of the National Academy of Sciences USA*. 78, 7426–7430.

Reeder, D. M., Kosteczko, N. S., Kunz, T. H., Widmaier, E. P. (2004). Changes in baseline and stress-induced glucocorticoid levels during the active period in free-ranging male and female little brown myotis, Myotis lucifugus (Chiroptera: Vespertilionidae). *General and Comparative Endocrinology.* 136, 260-269.

Refojo, D., Echenique, C., Müller, M. B., Reul, J. M., Deussing, J. M., Wurst, W., Sillaber, I., Paez-Pereda, M., Holsboer, F., Arzt, E. (2005). Corticotropin-releasing hormone activates ERK1/2 MAPK in specific brain areas. *Proceedings of The National Academy of Sciences.* 102, 6183-6188.

Reimondo, G., Paccotti, P., Minetto, M., Termine, A., Stura, G., Bergui, M., Angeli, A., Terzolo, M. (2003). The corticotrophin-releasing hormone test is the most reliable noninvasive method to differentiate pituitary from ectopic ACTH secretion in Cushing's syndrome. *Clinical Endocrinology.* 58, 718-724.

Reincke, M., Sbiera, S., Hayakawa, A., Theodoropoulou, M., Osswald, A., Beuschlein, F., Meitinger, T., Mizuno-Yamasaki, E., Kawaguchi, K., Saeki, Y., Tanaka, K., Wieland, T., Graf, E., Saeger, W., Ronchi, C. L., Allolio, B., Buchfelder, M., Strom, T. M., Fassnacht, M., Komada, M. (2015). Mutations in the deubiquitinase gene USP8 cause Cushing's disease. *Nature Genetics.* 47, 31-38.

Reul, J. M. H. M., Holsboer, F. (2002). Corticotropin-releasing factor receptors 1 and 2 in anxiety and depression. *Current Opinion in Pharmacology*. 2, 23–33.

Reynolds A., Anderson, E. M., Vermeulen, A., Fedorov, Y., Robinson, K., Leake, D., Karpilow, J., Marshall, W. S., Khvorova, A. (2006). Induction of the interferon response by siRNA iscell type- and duplex length-dependent. *RNA*. 12, 988-993.

Richardt-Pargmann, D., Vollmer, J. (2008). Stimulation of the immune system by therapeutic antisense oligodeoxynucleotides and small interfering RNAs via nucleic acid receptors. *Annals of The New York Academy of Sciences.* 1175, 40-54.

Riminucci, M., Collins, M. T., Lala, R., Corsi, A., Matarazzo, P., Gehron., Robey, P., Bianco, P. (2002). An R201H activating mutation of the GNAS1 (Gsalpha) gene in a corticotroph pituitary adenoma. *Molecular Pathology.* 55, 58-60.

Robbins, M., Judge, A., MacLachlan, I. (2009). siRNA and innate immunity. *Oligonucleotides*. 19, 89-102.

Ross, E. J., Linch, D. C. (1982). Cushing's syndrome--killing disease: discriminatory value of signs and symptoms aiding early diagnosis. *Lancet.* 2, 646-649.

Sahakitrungruang, T., Srichomthong, C., Pornkunwilai, S., AmornfaJ, Shuangshoti, S., Kulawonganunchai, S., Suphapeetiporn, K., Shotelersuk, V. (2014). Germline and somatic

DICER1 mutations in a pituitary blastoma causing infantile-onset Cushing's disease. *The Journal of Clinical Endocrinology and Metabolism.* 99, 1487-1492.

Şalva, E., Ekentok, C., Özbaş Turan, S., and Akbuğa, J. I. (2016). Non-viral siRNA and shRNA delivery systems in cancer therapy. In *RNA Interference* (editor Abdurakhmonov, I. Y). IntechOpen Ltd., London, UK. 201-222.

Sakai, H., Hua, J., Qianhong, G., Chen., Chang, C., Leonard, J., Medrano., Anthony, B., Bleecker, Elliot, M., Meyerowitz. (1998). ETR2 is an ETR1-like gene involved in ethylene signaling in Arabidopsis. *Proceedings of The National Academy of Sciences*.12, 5812-5817.

Santel, A., Aleku, M., Keil, O., Endruschat, J., Esche, V., Fisch, G., Dames, S., Löffler, K., Fechtner, M., Arnold, W. (2006). A novel siRNA-lipoplex technology for RNA interference in the mouse vascular endothelium. *Gene Therapy.* 13, 1222-1234.

Sapolsky, R. M., Romero, L. M., Munck, A. U. (2000). How do glucocorticoids influence stress responses? Integrating permissive, suppressive, stimulatory, and preparative actions. *Endocrine Reviews.* 21, 55-89.

Sartor, O., Cutler, G. B. (1996). Mifepristone: treatment of Cushing's syndrome. *Clinical Obstetrics and Gynecology*. 39, 506-510.

Saxena, S., Jonsson, Z. O., Dutta, A. (2003). Small RNAs with imperfect match to endogenous mRNA repress translation: implications for off-target activity of siRNA in mammalian cells. *Journal of Biological Chemistry*. 278, 44312-44319.

Scacheri, P. C., Rozenblatt-Rosen, O., Caplen, N. J., Wolfsberg, T. G., Umayam, L., Lee, J. C., Hughes, C. M., Shanmugam, K. S., Bhattacharjee, A., Meyerson, M. (2004). Short interfering RNAs can induce unexpected and divergent changes in the levels of untargeted proteins in mammalian cells. *Proceedings of the National Academy of Sciences. 101*, 1892-1897.

Schiller, M. R. (2000). Genes expressed in the mouse pituitary corticotrope AtT-20/D-16v tumor cell line. *Pituitary.* 3, 141-152.

Schirle, N. T., Macrae, I. J. (2012). The crystal structure of human Argonaute2. *Science*. 336, 1037-1040.

Schlake, T., Bode, J. (1994). Use of mutated FLP recognition target (FRT) sites for the exchange of expression cassettes at defined chromosomal. *Biochemistry*. 33, 12746-12751.

Schwarz, D. S., Hutvágner, G., Haley, B., Zamore, P. D. (2002). Evidence that siRNAs function as guides, not primers, in the Drosophila and human RNAi pathways. *Molecular Cell*. 10, 537-548.

Schwarz, D. S., Hutvagner, G., Du, T., Xu, Z., Aronin, N., Zamore, P. D. (2003). Unexpected asymmetry in the assembly of the RNAi enzyme complex. *Cell*. 115, 199-208.

Schwyzer, R., Eberle, A. (1977). On the molecular mechanism of alpha-MSH receptor interactions. *Frontiers of Hormone Research*. 4, 18-25.

Scott, L. V., Medbak, S., Dinan, T. G. (1999). ACTH and cortisol release following intravenous desmopressin: a dose–response study. *Clinical Endocrinology.* 51, 653-658.

Seidah, N., Day, R., Benjannet, S., Rondeau, N., Boudreault, A., Reudelhuber, T., Schafer, M., Watson, S., Chretien, M. (1992). The prohormone and proprotein processing enzymes PC1 and PC2: structure, selective cleavage of mouse POMC and human renin at pairs of basic residues, cellular expression, tissue distribution, and mRNA regulation. *NIDA Research Monograph.* 126, 132-150.

Shi, Z., Zhang, Z., Zhang, Z., Wang, Y., Li, C., Wang, X., He, F., Sun, L.,Jiao, S., Weiyang Shi, W., Zhou, Z. (2015). Structural insights into mitochondrial antiviral signaling protein (MAVS)-tumor necrosis factor receptor-associated factor 6 (TRAF6) signaling. *Journal of Biological Chemistry*. 290, 26811-26820.

Siebert, M., Robert, Y., Didier, R., Minster, A., M'sallaoui, W., Bellier, A., Chaffanjon, P. C. (2017). Anatomical variations of the venous drainage from the left adrenal gland: an anatomical study. *World Journal of Surgery.* 41, 991-996.

Simpson, E. R., Waterman, M. R., (1988). Regulation of the synthesis of steroidogenic enzymes in adrenal cortical cells by ACTH. *Annual Review of Physiology*. 50, 427-440.

Sioud, M. (2005). Induction of inflammatory cytokines and interferon responses by double-stranded and single-stranded siRNAs is sequence-dependent and requires endosomal localization. *Journal of Molecular Biology*. 348, 1079-1090.

Sledz, C. A., Holko, M., De Veer, M. J., Silverman, R. H., Williams, B. R. (2003). Activation of the interferon system by short-interfering RNAs. *Nature Cell Biology.* 5, 834-839.

Smith, S., Vale, Ww. (2006). The role of the hypothalamic-pituitary-adrenal axis in neuroendocrine responses to stress. *Dialogues in Clinical Neuroscience.* 8, 383-395.

Smith, S. A., Crowe, J. E. (2015). Use of human hybridoma technology to isolate human monoclonal antibodies. In: *Antibodies for Infectious Diseases*. Crowe, J., Boraschi, D., Rappuoli, R. (editors). ASM Press, Washington DC, USA. 141-156.

Snove, O., Holen, T. (2004). Many commonly used siRNAs risk off-target activity. *Biochemical and Biophysical Research Communications.* 319, 256-263.

Soutschek, J., Akinc, A., Bramlage, B., Charisse, K., Constien, R., Donoghue, M., Elbashir, S., Geick, A., Hadwiger, P., Harborth, J. (2004). Therapeutic silencing of an endogenous gene by systemic administration of modified siRNAs. *Nature. 432*, 173-178.

Spampinato, S., Canossa, M., Carboni, L., Campana, G., Leanza, G., Ferri, S. (1994). Inhibition of proopiomelanocortin expression by an oligodeoxynucleotide complementary to beta-endorphin mRNA. *Proceedings of The National Academy of Sciences.* 91, 8072-8076.

Spiga, F., Lightman, S. L. (2015). Dynamics of adrenal glucocorticoid steroidogenesis in health and disease. *Molecular and Cellular Endocrinology.* 408, 227-234.

Springer, A. D., Dowdy, S. F. (2018) GalNAc–siRNA conjugates: leading the way for delivery of RNAi therapeutics. *Nucleic Acid Therapeutics*. 28, 109-118.

Starke, R. M., Williams, B. J., Vance, M. L., Sheehan, J. P. (2010). Radiation therapy and stereotactic radiosurgery for the treatment of Cushing's disease: an evidence-based review. *Current Opinion in Endocrinology, Diabetes and Obesity.* 17, 356-364.

Steffensen, C., Bak, A. M., Rubeck, K. Z., Jørgensen, J. O. L. (2010). Epidemiology of Cushing’s syndrome. *Neuroendocrinology.* 92, 1-5.

Stratakis C. A., Tichomirowa, M. A., Boikos, S., Azevedo, M.F., Lodish, M., Martari, M., Verma, S., Daly, A. F., Raygada, M., Keil, M. F., (2010). The role of germline AIP, MEN1, PRKAR1A, CDKN1B and CDKN2C mutations in causing pituitary adenomas in a large cohort of children, adolescents, and patients with genetic syndromes. *Clinical Genetics.* 78, 457-463.

Suda, T., Tozawa, F., Mouri, T., Sasaki, A., Shibasaki, T., Demura, H., Shizume, K. (1983). Effects of cyproheptadine, reserpine, and synthetic corticotropin-releasing factor on pituitary glands from patients with Cushing's disease. *Journal of Clinical Endocrinology and Metabolism.* 56, 1094-1099.

Sun, X., Marque, L. O., Jennifer, Z. C., Pruitt, L., Bhat, P., Li, P. P., Kannan, G., Ladenheim, E., Moran, T. H., Margolis, R. L., Rudnicki. D. D. (2014). Phosphorodiamidate morpholino

oligomers suppress mutant huntingtin expression and attenuate neurotoxicity. *Human Molecular Genetics*. 23, 6302-6317.

Suntharalingam, G., Perry, M. R., Ward, S., Brett, S. J., Castello-Cortes, A., Brunner, M. D., Panoskaltsis, N. (2006). Cytokine storm in a phase 1 trial of the anti-CD28 monoclonal antibody TGN1412. *The New England Journal of Medicine*. 355, 1018-1028.

Svoboda, O., Stachura, D. L., Machonova, O., Pajer, P., Brynda, J., Zon, L. I., Traver, D., Bartunek, P. (2014). Dissection of vertebrate hematopoiesis using zebrafish thrombopoietin. *Blood.* 124, 220-228.

Svoboda, P. (2014). Renaissance of mammalian endogenous RNAi. *FEBS Letters*. 588, 2550-2556.

Tabara, H., Grishok, A., Mello, C. C. (1998). RNAi in C. elegans: soaking in the genome sequence. *Science.* 282, 430-431.

Tai, W., Gao, X. (2017). Functional peptides for siRNA delivery. *Advanced Drug Delivery Reviews*. 110, 157-68.

Tam, C., Wong, J. H., Cheung, R. C. F., Zuo, T., Ng, T. B. (2017). Therapeutic potentials of short interfering RNAs. *Applied Microbiology and Biotechnology*. 101, 7091-7111.

Thomas, M., Klibanov, A. M. (2002). Enhancing polyethylenimine's delivery of plasmid DNA into mammalian cells. *Proceedings of The National Academy of Sciences.* 99, 14640-14645.

Thoren, M., Adamson, U., Sjöberg, H. (1985). Aminoglutethimide and metyrapone in the management of Cushing's syndrome. *Acta Endocrinologica.* 109, 451-457.

Trier, T., Hansen, P., Houen, H. (2019). Peptides, antibodies, peptide antibodies and more. *International Journal of Molecular Sciences*. 20, 6289-6310.

Trifanescu, R. A., Stoicescu, A., Caragheorgheopol, A., Hortopan, D., Coculescu, M. (2011). Hyponatremic coma with seizures as onset of isolated ACTH deficiency. *Endocrine Abstracts*. 26, 638.

Tritos, N. A., Biller, B. M. (2014). Medical management of Cushing’s disease. *Journal of Neuro-Oncology.* 117, 407-414.

Turan, S., Kuehle, J., Schambach, A., Baum, C., Bode, J. (2010). Multiplexing RMCE: versatile extensions of the Flp-recombinase-mediated cassette-exchange technology. *Journal of Molecular Biology*. 402, 52-69.

Uhler, M., Herbert, E., D'eustachio, P., Ruddle, F. D. (1983). The mouse genome contains two nonallelic pro-opiomelanocortin genes. *Journal of Biological Chemistry.* 258*,* 9444-9453.

Ui-Tei, K., Naito, Y., Nishi, K., Juni, A., and Saigo, K. (2008). Thermodynamic stability and WatsonCrick base pairing in the seed duplex are major determinants of the efficiency of the siRNA-based offtarget effect. *Nucleic Acids Research*. 36, 7100–7109.

Vaish, N., Chen, F., Seth, S., Fosnaugh, K., Liu, Y., Adami, R. (2011). Improved specificity of gene silencing by siRNAs containing unlocked nucleobase analogs. *Nucleic Acids Research.* 39, 1823-1832.

Van der Neut 1, R., Bär, P. R., Sodaar, P. Gispen, W .H. (1988). Trophic influences of alpha-MSH and ACTH4-10 on neuronal outgrowth in vitro. *Peptides*. 9, 1015-1020.

Van Der Pas, R., De Bruin, C., Leebeek, F., De Maat, M., Rijken, D., Pereira, A., Romijn, J., Netea-Maier, R., Hermus, A., Zelissen, P. (2012). The hypercoagulable state in Cushing's disease is associated with increased levels of procoagulant factors and impaired fibrinolysis, but is not reversible after short-term biochemical remission induced by medical therapy. *Journal of Clinical Endocrinology and Metabolism.* 97, 1303-1310.

Veedu, R. N., Wengel, J. (2010). Locked nucleic acids: promising nucleic acid analogs for therapeutic applications. *Chemistry & Biodiversity*. 7, 536-542.

Vieira, L. N., Gadelha, M. R. (2014). Efficacy of medical treatment in Cushing's disease: a systematic review. *Clinical Endocrinology.* 80, 1-12.

Wang, J., Ze Lu, M., Guillaume Wientjes., Jessie, L. S., Au. (2010). Delivery of siRNA Therapeutics: Barriers and Carriers. *American Association of Pharmaceutical Scientists*. 12, 492–503.

Wang, Y., Sheng, G., Juranek, S., Tuschl, T., and Patel, D.J. (2008). Structureof the guide-strand-containing argonaute silencing complex. *Nature*. 456, 209-213.

Wanichi, I. Q., De Paula Mariani, B. M., Frassetto, F. P., Siqueira, S. A. C., DE Castro Musolino, N. R., Cunha-neto, M. B. C., Ochman, G., Cescato, V. A. S., Machado, M. C.,

Trarbach, E. B., Bronstein, M. D. Fragoso, M. (2019). Cushing's disease due to somatic USP8 mutations: a systematic review and meta-analysis. *Pituitary.* 22, 435-442.

Watson, J. M., Fusaro, A. F., Wang, M., Waterhouse, P. M. (2005). RNA silencing platforms in plants. *FEBS Letters.* 579, 5982-5987.

Watts, J.K., Deleavey, G.F., and Damha, M.J. (2008). Chemically modifiedsiRNA: tools and applications. *Drug Discovery*. 13, 842-855.

Wengander, S., Trimpou, P., Papakokkinou, E., Ragnarsson, O. (2019). The incidence of endogenous Cushing's syndrome in the modern era. *Clinical Endocrinology.* 91, 263-270.

Wessells, H., Levine, N., Hadley, M., Dorr, R., Hruby, V. (2000). Melanocortin receptor agonists, penile erection, and sexual motivation: human studies with Melanotan II. *International Journal of Impotence Research.* 12, 74-79.

Whitehead, K. A., Dahlman, J. E., Langer, R. S., Anderson, D. G. (2011). Silencing or stimulation? siRNA delivery and the immune system. *Annual Review of Chemical and Biomolecular Engineering*. 2, 77-96.

Williamson, E. A., Ince, P. G., Harrison, D., Kendall-Taylor, P., Harris, P. E. (1995). G-protein mutations in human pituitary adrenocorticotrophic hormone-secreting adenomas. *Journal of Endocrinological Investigation*. 25, 128-131.

Willkomm, S., Restle, T. (2015). Conformational dynamics of Ago-mediated silencing processes. *International Journal of Molecular Sciences*. 16, 14769-14785.

Wind, J. J., Lonser, R. R., Nieman, L. K., Devroom, H. L., Chang, R., Oldfield, E. H. (2013). The lateralization accuracy of inferior petrosal sinus sampling in 501 patients with Cushing's disease. *Journal of Clinical Endocrinology and Metabolism.* 98, 2285-2293.

Wolfrum, S., Shi, K. N. Jayaprakash, M. Jayaraman, G. Wang, R.K. Pandey, K.G. Rajeev, T. Nakayama, K. Charrise, E.M. Ndungo, T. Zimmermann, V. Koteliansky, M. Manoharan, M. Stoffel. (2007). E4Q2Mechanisms and optimization of in vivo delivery of lipophilic siRNAs. *Nature Biotechnology*. 25, 1149-1157.

Woloschak, M., Post, K., Roberts, J. (1994). Effects of antisense DNA on POMC mRNA and ACTH levels in cultured human corticotroph adenoma cells. *Journal of Endocrinological Investigation.* 17, 817-819.

Woo, Y. S., Isidori, A. M., Wat, W. Z., Kaltsas, G. A., Afshar, F., Sabin, I., Jenkins, P. J., Monson, J. P., Besser, G. M., Grossman, A. B. (2005). Clinical and biochemical characteristics of adrenocorticotropin-secreting macroadenomas. *Journal of Clinical Endocrinology and Metabolism.* 90, 4963-4969.

Younis, A., Siddique, M. I., Kim, C. K., Lim, K. B. (2014). RNA interference (RNAi) induced gene silencing: a promising approach of hi-tech plant breeding. *International Journal of Biological Sciences.* 10, 1150-1158.

Zarember, K. A., Godowski, P. J. (2002). Tissue expression of human Toll-like receptors and differential regulation of Toll-like receptor mRNAs in leukocytes in response to microbes, their products, and cytokines. *Journal of Immunology*. 168, 554–561.

Zheng X., Li, S., Zang, Z., Hu, J., An, J., Pei, X., Zhu, F., Zhang, W., Yang, H. (2016). Evidence for possible role of toll-like receptor 3 mediating virus-induced progression of pituitary adenomas. *Molecular and Cellular Endocrinology*. 426, 22-32.

Zhang, D., Du, L., Heaney, A. (2016). Testicular receptor-4: novel regulator of glucocorticoid resistance. *Journal of Clinical Endocrinology and Metabolism*. 101, 3123-3133.

Zhou, A., Bloomquist, B. T., Mains, R. E. (1993). The prohormone convertases PC1 and PC2 mediate distinct endoproteolytic cleavages in a strict temporal order during proopiomelanocortin biosynthetic processing. *Journal of Biological Chemistry.* 268, 1763-1769.

Zorrilla, E. P., Valdez, G. R., Nozulak, J., Koob, G. F., Markou, A. (2002). Effects of antalarmin, a CRF type 1 receptor antagonist, on anxiety-like behavior and motor activation in the rat. *Brain Research*. 952, 188-199.